Universität Rostock

Traditio et Innovatio

catalysis LIKAT
Leibniz-Institut für Katalyse e.V.

Sustainable synthesis of amines using molecularly defined and nanoparticles-based catalysts

Dissertation

In Kumulativer Form

zur Erlangung des akademischen Grades

Doctor rerum naturalium (Dr. rer. nat.)

der Mathematisch-Naturwissenschaftlichen Fakultät

der Universität Rostock

vorgelegt von

Thirusangumurugan Senthamarai

geb. am 05. 02. 1986 in India

Rostock, 15.05.2020

Die vorliegende Arbeit entstand in der Zeit von Feb 2017 bis Mai 2020 am Leibniz-Institut für Katalyse e.V.

This thesis has been performed in Leibniz-Institute for Catalysis in the period from Feb 2017 to May 2020 and was supervised by

Prof. Dr. Matthias Beller and Dr. Jagadeesh Rajenahally

1. Gutachter:

Prof. Dr. Matthias Beller

Leibniz-Institut für Katalyse e. V. an der Universität Rostock

Albert-Einstein-Str. 29a, 18059 Rostock, Deutschland

2. Gutachter:

Prof. Dr. Angelika Brückner

Leibniz-Institut für Katalyse e.V. an der Universität Rostock

Tag der Einreichung: 2020

Tag der Verteidigung: 2020

Acknowledgement

Abstract

Sustainable synthesis of amines using molecularly defined and nanoparticles-based catalysts

Thirusangumurugan Senthamarai

Leibniz-Institut für Katalyse e.V. an der Universität Rostock

This dissertation describes the sustainable synthesis and functionalization of amines by catalytic reductive amination of carbonyl compounds and ammonia or amines in presence of molecular hydrogen or formic acid. For these reactions, molecularly defined Ru- and nanoparticles-based catalysts were developed, which enabled the preparation of simple, functionalized and structurally diverse primary, secondary and tertiary amines including N-methyl amines and more complex drug targets. Applying $RuCl_2(PPh_3)_3$ as simple and commercially available catalyst, the synthesis of benzylic, heterocyclic and aliphatic linear and branched primary amines from carbonyl compounds and ammonia is reported. Next, *in situ* generation of reusable ultra-small cobalt nanoparticles from molecularly defined cobalt-salen complexes and their catalytic applications for the reductive aminations to prepare primary amines from carbonyl compounds and ammonia in presence of molecular hydrogen is demonstrated. In addition to *in situ* generated nanoparticles, the catalytic application of isolated cobalt nanoparticles for the preparation of secondary and tertiary amines as well as N-methyl amines is showcased. Finally, the synthesis of secondary and tertiary amines as well as N-methylamines and selected drug molecules from carbonyl compounds and nitroarenes or amines has been performed using N-doped graphene surfaces activated cobalt-based nanoparticles in presence of formic acid as hydrogen donor. The detailed characterization of cobalt nanoparticles by TEM, XPS, XRD is presented here, too. In order to design suitable catalysts and to accomplish reductive amination reactions, several optimization and control experiments including kinetic and mechanistic investigations have been performed.

Nachhaltige Synthese von Aminen mittels molekular definierten und Nanopartikel-basierten Katalysatoren

Thirusangumurugan Senthamarai

Leibniz-Institut für Katalyse e.V. an der Universität Rostock.

Diese Dissertation befasst sich mit der nachhaltigen Synthese und Funktionalisierung von Aminen mittels katalytischer, reduktiver Aminierung von Carbonylverbindungen zusammen mit Ammoniak oder Aminen in der Gegenwart von Wasserstoff oder Ameisensäuren. Für diese Reaktionen wurden sowohl molekular definierte Ruthenium als auch Nanopartikel-basierte Katalysatoren entwickelt, welche die Synthese von strukturell diversen primären, sekundären und tertiären Aminen ermöglichen, inklusive N-Methyl Aminen und pharmakologischen Wirkstoffen. $RuCl_2(PPh_3)_3$, ein einfacher und kommerziell verfügbarer Katalysator, ermöglichte die Synthese von benzylischen, heterocyclischen wie auch linearen und verzweigten aliphatischen primären Aminen, ausgehend von Carbonylverbindungen und Ammoniak. Des Weiteren wurde eine Methode zur *in situ* Herstellung von ultra-kleinen Cobalt-Nanopartikeln aus Cobalt-Salen Komplexen entwickelt, welche mehrfach in der reduktiven Aminierung zur Synthese von primären Aminen eingesetzt werden konnten. Neben der Verwendung von *in situ* hergestellten Nanopartikeln wurde auch die katalytische Aktivität von isolierten Cobalt-Nanopartikeln in der Synthese von sekundären, tertiären und N-Methyl Aminen untersucht. Zuletzt wurden Cobalt-basierte Nanopartikel mit Stickstoff dotierten Graphen Oberflächen hergestellt, welche als Katalysator in der Synthese von sekundären, tertiären und N-Methyl Aminen fungierten, ausgehend von Carbonylverbindungen, Nitroarenen oder Aminen, und Ameisensäure als Wasserstoff Donor. Die beschriebenen Nanopartikel wurden zudem mit Hilfe von TEM, XPS und XRD charakterisiert und im Zuge der Entwicklung der katalytischen Reaktionen wurden unterschiedliche Optimierungen, Kontrollversuche wie auch kinetische und mechanistische Studien durchgeführt.

List of Abbreviations

AMF	5-(Aminomethyl)-2-furanmethanol
Ar	Argon
BDC	Benzene-1,4-dicarboxylic acid
BAF	2,5-Bis(aminomethyl)furan
COD	Cycloocta-1,5-diene
CTAB	Cetyl trimethyl ammonium bromide
CTH	Catalytic Transfer Hydrogenations
DABCO	1,4-Diazabicyclo[2.2.2]octane
DFT	Density Functional Theory
dppe	1,2-Bis(diphenylphosphino)ethane
dppb	1,2-Bis(diphenylphosphino)butane
ee	Enantiomeric excess
EELS	Electron Energy Loss Spectroscopy
EDXS	Energy Dispersive X-Ray Spectroscopy
EPR	Electron Paramagnetic Resonance
et al.	*Et alia*
HAADF	High Angle Annular Dark-Field imaging
HMF	5-Hydroxymethylfurfural
h	Hour
HCOOH	Formic acid
HF	Hydrofluoric acid
L	Ligand
MeOH	Methanol
mL	Milliliter
mmol	Millimole
MOF	Metal organic framework
NMR	Nuclear Magnetic Resonance

NPs	Nanoparticles
PCy$_3$	Tricyclohexylphosphine
PPh$_3$	Triphenylphosphine
PZ	Piperazine
STEM	Scanning Transmission Electron Microscopy
SAED	Selected area electron diffraction
TA	Tartaric acid
t-amyl alcohol	2-Methylbutan-2-ol
t-BuOH	tertiary butanol
TEM	Transmission Electron Microscopy
THF	Tetrahydrofuran
THFAA	5-(Aminomethyl)-2-tetrahydrofurylmethanol
Tripod triphos	1,1,1-Tris(diphenylphosphinomethyl)ethane
TPA	Terephthalic acid
TPPTS	3,3′,3″-Phosphanetriyltris(benzenesulfonicacid) trisodium salt
XRD	X-ray Powder Diffraction
XPS	X-ray Photoelectron Spectroscopy

Table of Contents

List of schemes

List of Figures

List of Tables

1. Introduction

1.1 Synthesis of amines

The development of sustainable processes for the synthesis of essential fine and bulk chemicals as well as molecules related to life science applications continues to be an important goal of chemical research. In order to achieve such sustainable synthesis, catalysis plays a crucial role, which constitutes a key technology in the chemical, pharmaceutical and material industries. As a result, >80% of all chemical products are made via catalytic resections. In this regard, the development of cost-effective and durable catalysts is of central importance to produce all kinds of chemicals at present and in the future. In particular, the development of selective and sustainable catalytic processes for the synthesis of amines, which represent privileged compounds, is highly desired. In general, amines are extensively used in different science areas such as chemistry, biology, medicine, energy, materials and environment.[1-16] These compounds serve as fine and bulk chemicals as well as key precursors and central intermediates for the synthesis of advanced chemicals, pharmaceuticals, biomolecules, agrochemicals and polymers.[1-16]
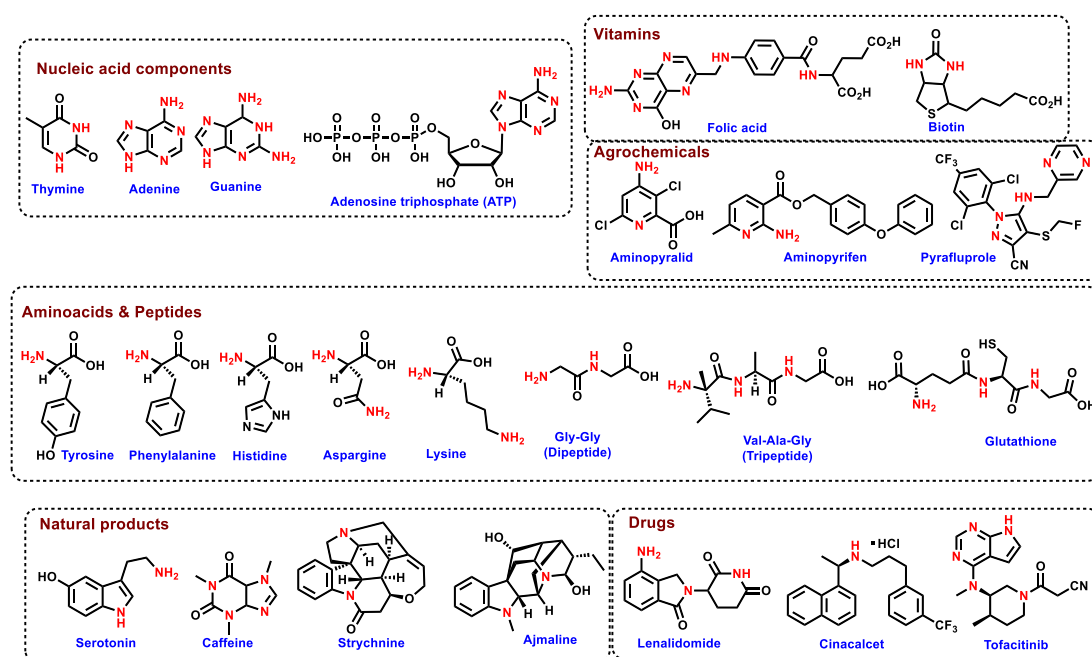
Figure 1. Selected life science molecules containing amine/nitrogen moiety(s).

Notably, amine functionalities constitute integral parts of the majority of drugs and biomolecules (Fig. 1).[1-6] In fact, >75% of the top selling drugs contain amine and/or nitrogen moieties, which play significant roles in their activities.[3] Moreover, amines are involved in the formation of proteins, enzymes, nucleic acids and hormones in living beings (Fig. 1).[1-6] For the synthesis of amines, reductive aminations, [7-37] amination of alcohols, [38-39] nucleophile substitution reactions [40] and C-H amination reactions [40-41] are commonly applied.

1.2 Catalytic reductive aminations

Catalytic reductive aminations are an essential class of reactions widely applied in research laboratories and industries for the cost-efficient and convenient synthesis of different kinds of amines and their functionalization. [7-16] In these reactions, carbonyl compounds (aldehydes and ketones) react with ammonia or amines using suitable catalysts in presence of molecular hydrogen or stoichiometric amounts of reducing agents.[7-16] Regarding potential reducing agents, molecular hydrogen is highly preferred because it is abundant, inexpensive, and atom-economical as well as produces only water as the by-product.[34-37] In addition, catalytic transfer hydrogenations (CTH) [42-50] using formic acid or isopropanol are complementary to reductions with molecular hydrogen. Advantageously, CTH reactions do not require any special experimental setup or the use of high-pressure equipment compared to hydrogenation methods. Notably, formic acid or formate [47-50] as hydrogen donors are abundant, comparably inexpensive and easy to handle. Thus, the reductive aminations using molecular hydrogen and formic acid are attractive and offer significant advantages for the cost-effective production of amines.

1.3 General mechanisms of reductive aminations

Catalytic reductive amination reactions are often non-selective and suffer from side reaction such as over-alkylation and reduction of carbonyl compounds to the corresponding alcohols.[7,13-16] Particularly, the synthesis of primary amines

from carbonyl compounds and ammonia is more challenging. In addition, the catalyst deactivation by ammonia and drastic conditions required for the activation of ammonia constitute additional problems.[7,13-16] The general reaction pathways for catalytic reductive aminations to prepare primary, secondary and tertiary amines is presented in Scheme 1. In the preparation of primary amines, first carbonyl compound condenses with ammonia and generates corresponding primary imine as intermediate, which is then reduced to desired primary amines in the presence of a suitable catalyst (Scheme 1a).[7,15,16] Similarly, carbonyl compound reacts with primary amines and generate secondary imines and these intermediates in presence of catalyst are reduced to give desired secondary amine (Scheme 1b).[7,15,16] Instead of anilines, directly nitroarenes can also be used to prepare secondary N-alkylated amines. Here, first nitro compound is reduced to the corresponding aniline. The *in situ* generated aniline undergoes reductive amination to produce corresponding N-alkylated amine. In general, anilines are produced by the catalytic hydrogenation of nitroarenes. Nobly, the direct one pot reductive amination of carbonyl compounds and nitroarenes is advantageous with respect to step economy and cost of starting materials. In the synthesis of tertiary amines, first the reaction of carbonyl compound and secondary amine proceeds *via* the formation of the corresponding enamine and iminium ion as intermediates in case of benzylic aldehydes and ketones, or enamine in case of aliphatic aldehydes and ketones. These intermediates are finally hydrogenated in presence of catalyst to produce the corresponding tertiary amines (Scheme 1c).[7]
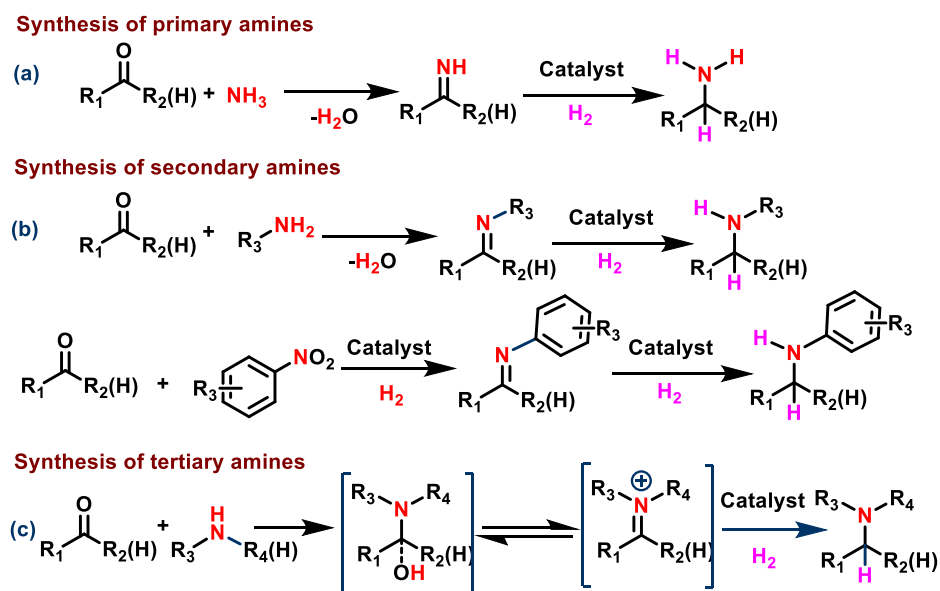
Scheme 1. Reaction pathways of catalytic reductive amination reactions to produce different kinds of amines.

In the reductive amination of carbonyl compound **1** with ammonia, in addition to the desired product primary amine **2,** the formation of other side products such as corresponding alcohol **3**, secondary imine **4**, secondary amine **5**, tertiary amine **6** and imidazoline-based compound **7** (scheme 2) might occur under different reaction conditions.[15,16] The carbonyl compound **1** condenses with ammonia and generates primary imine **8** as unstable intermediate. In presence of catalyst, **8** undergoes reduction and yields the desired primary amine **2**. If a catalyst is less selective towards the reduction of **8**, then the direct reduction of carbonyl compound can also occur to give the corresponding alcohol **3**. The secondary imine **4** forms *via* condensation of the primary amine **2** with either carbonyl compound **1** (releasing water) or imine **8** (releasing NH_3). When the catalyst is sufficiently active and selective, due to the rapid hydrogenation, the stationary concentration of **8,** becomes low, which prevents side reactions. When the hydrogenation does not proceed quickly, this leads to the accumulation of **8** and side reactions involving **8** likely occur. The formation of secondary amine **5** occurs by the reduction of secondary imine **4**. Further, **5** can also react with carbonyl compound **1** to produce tertiary amine **6**. In case of (substituted)

benzaldehyde, the primary imine, **8** can also trimerizes to form **9**, which subsequently undergoes thermal cyclization to give **7**.
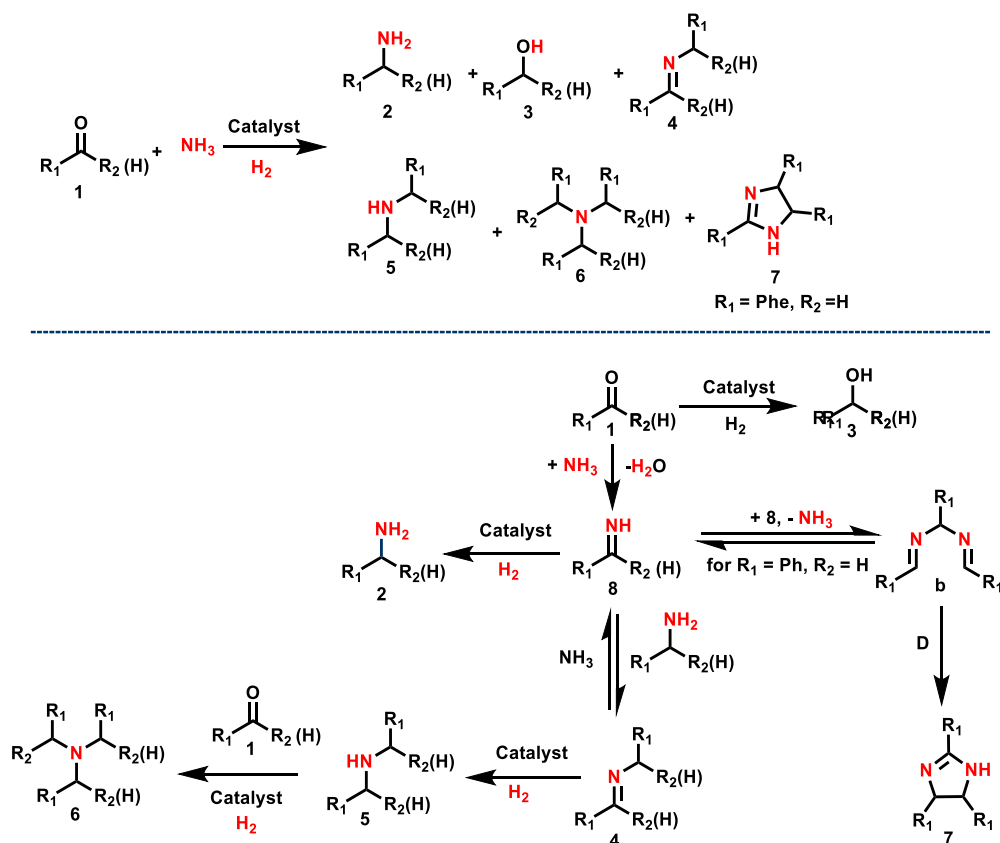
Scheme 2. Catalytic reductive amination of carbonyl compounds with ammonia: Reaction mechanism and the formation of desired and side products.[7,15,16]

In order to synthesize primary amines in a highly selective manner, the development of suitable catalysts is crucial and continues to be important in both research laboratories and industries.

Below we discuss the previous reports on catalytic reductive amination for the synthesis of primary amines using base metal heterogeneous materials (Section 1 and schemes 3 to 7) and homogeneous catalysts (Section 1 and schemes 8 to 13). Next, the synthesis of secondary and tertiary amines using non-noble heterogeneous catalysts in presence of molecular hydrogen (Section 1 and schemes 14 to 15) and formic acid (Section 1 and schemes 16 to 18) is discussed. These reports are

presented as a cumulative collection of publications which have been already published in international journals.

1.4 Reductive aminations for the synthesis of primary amines using base metal heterogeneous catalysts

The majority of the catalysts known for reductive aminations, especially in industry is based on heterogeneous materials. Both noble and non-noble metal based heterogeneous catalysts have been developed to prepare linear and branched primary amines. In this chapter the applications of non-noble metal-based heterogeneous materials for the synthesis of primary amines from carbonyl compounds and ammonia using molecular hydrogen is discussed. Among reductive amination catalysts, Ni-based materials represent the first known systems used for the preparation of primary amines.[51-53] This was initially achieved by Mignonac in 1921 for the preparation of primary amines from simple aldehydes and ketones with liquid ammonia and molecular hydrogen using heterogeneous Ni-catalyst (scheme 3).[51] After his invention, this reaction is named as Mignonac reaction.[51] Followed by these investigations, Winans[52] and Haskelberg[53] have applied Raney nickel for the preparation of primary amines.
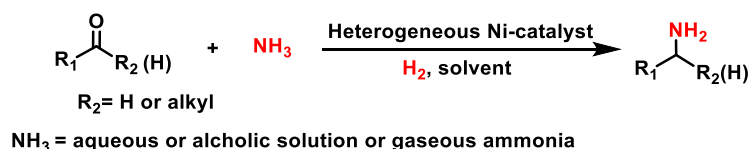
Scheme 3. Ni-based catalyst for amine synthesis (Mignonac reaction)**.**

Unfortunately, these traditional Ni-based catalysts work well only for the reductive amination of simple and non-functionalized molecules. Hence, they cannot be applied to the synthesis of functionalized and structurally diverse amines. Nevertheless, no significant efforts were made on the development of base metal heterogeneous catalysts until 2017. After that time, few catalysts

based on Co,[13] Ni,[14,16,37-39,56-60], and Fe,[59] were developed, which constitute nowadays excellent reductive amination catalysts for the preparation of broad range of primary amines.

More specifically in 2017, Beller and co-workers[13] reported MOFs-derived cobalt nanoparticles and supported Co single atoms as general reductive amination catalysts to prepare different kinds of amines. These cobalt-based catalysts (Co-DABCO-TPA@C-800; DABCO= 1,4-diazabicyclo[2.2.2]octane; TPA=terephthalic acid) were prepared by the immobilization of an *in situ* generated cobalt nitrate-DABCO-terephthalic acid MOF template on carbon and subsequent pyrolysis at 800 °C under argon (fig. 2).
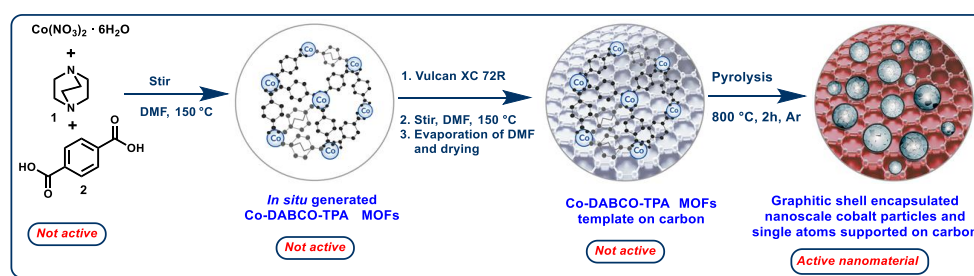
Figure 2. Preparation of Co-DABCO-TPA@C-800.

The optimal Co-DBCO-TPA@C-800 catalyst allowed for the reductive amination of 39 aldehydes and 34 ketones in presence of gaseous ammonia and molecular hydrogen to produce functionalized benzylic, heterocyclic and aliphatic linear as well as branched primary amines in up to 92% yield (scheme 4). Interestingly, applying this catalyst, –NH2 moiety has been introduced in structurally complex life science molecules and steroid derivatives. In addition to primary amines, this Co-DBCO-TPA@C-800 was applied for the synthesis of secondary and tertiary amines including N-methyl amines and existing drug molecules.
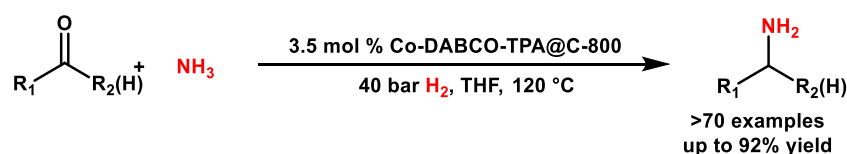
Scheme 4. Co-DABCO-TPA@C-800 catalyzed primary amine synthesis.

After this report, Kempe and coworkers [14] disclosed Ni/Al$_2$O$_3$ catalyst for reductive amination of carbonyl compounds using aqueous ammonia and molecular hydrogen to synthesis both linear and branched primary amines. Their Ni-catalyst was prepared by the immobilization of a Ni-salen complex on Al$_2$O$_3$ and subsequent pyrolysis under N$_2$ atmosphere at 700°C followed by reduction under hydrogen at 550°C. Applying the Ni/Al$_2$O$_3$ catalyst, reductive amination of all kinds of aldehydes and ketones was performed under mild reaction conditions (10 bar H$_2$, 80 $^{\circ}$C) and the corresponding primary amines were obtained in up to 99 % yield (scheme 5).
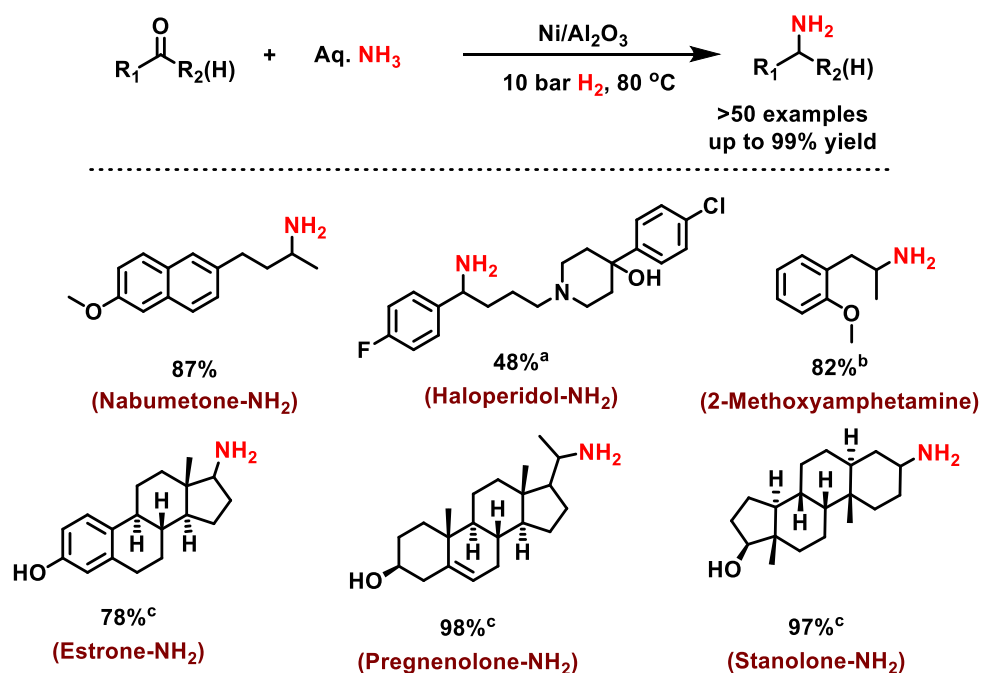
Scheme 5. Ni/Al$_2$O$_3$-catalyzed synthesis of primary amines under mild conditions.

Later, Beller and Jagadeesh et al.[16] prepared Ni-nanoparticles by the immobilization of an *in situ* generated Ni-tartaric acid complex (Ni-TA) on silica and subsequent pyrolysis to produce a novel reductive amination catalyst (Ni-tartaric acid@SiO$_2$-800). The schematic mechanism for this Ni-tartaric acid@SiO$_2$-800 catalyzed reductive amination protocol using ammonia and molecular hydrogen is presented in scheme 6.
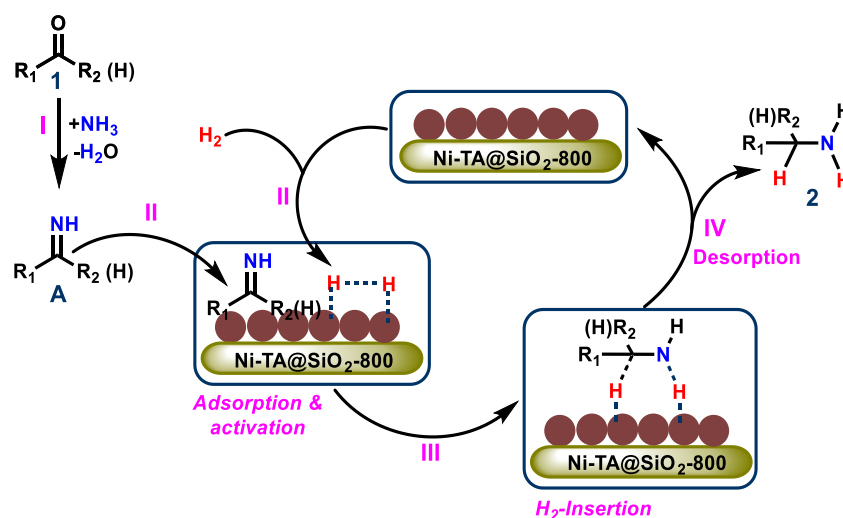
Scheme 6. Proposed mechanism for the Ni-tartaric acid@SiO$_2$-800

The preparation of 5-(aminomethyl)-2-furanmethanol (AMF) is possible by Ni/SBA-15 catalyzed reductive amination of HMF (5-hydroxymethylfurfural) with aqueous ammonia.[54] In addition to Ni/SBA-15, Lei and coworkers also used Raney Ni. Both Ni/SBA-15 (89.9%) and Ni-Raney (90%) gave AMF in up to 90%. Furthermore, Colacino and Varma et al.[55] reported magnetically separable Ni NPs supported on SiO$_2$-Fe$_3$O$_4$ (Fe$_3$O$_4$@SiO$_2$-Ni) for reductive amination to prepare primary amines under unconventional micro-wave irradiation. Yang and Zhang et al[56] reported carbon supported nickel nanoparticles (MC/Ni)-catalyzed reductive amination of aldehydes with aqueous ammonia under comparably mild conditions (80 °C, 1 bar H$_2$, 200 µL NH$_3$·H$_2$O (26.5 wt % and 12 h). Notably, Pera-Titus and Shi et al.[57] performed Ni$_6$AlO$_x$-catalyzed reductive amination of biomass derived ketones and aldehydes. Shi and co-workers[58] developed bi-functional CuNiAlOx catalysts for one pot transformation of 5-(hydroxymethyl) furfural (5-HMF) into 2,5-bis(aminomethyl)furan (BAF) by two-step reductive amination of -CHO group and amination of -OH group.

Very recently, Kempe and coworkers[59] reported the first iron catalyst for reductive amination of carbonyl compounds with ammonia and hydrogen. Here, the key was the use of a specific Fe complex for the catalyst synthesis and a N-doped SiC material as catalyst support. The catalyst showed broad scope and

a very good tolerance of functional groups, the yield of amines were up to 99% (scheme 7).
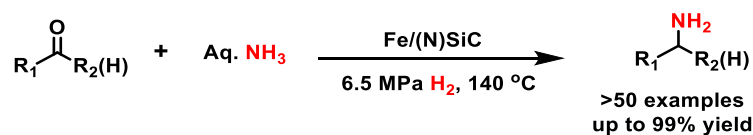
Scheme 7. Fe/(N)SiC-catalyzed selective synthesis of amines.

1.5 Reductive aminations for the synthesis of primary amines using homogeneous catalysts

Compared to heterogeneous catalysts, the development of homogeneous complexes for the reductive amination of carbonyl compounds with ammonia has been less studied. In general, transition metal complexes catalyzed reactions involving ammonia encounter difficulties due to the deactivation of homogeneous catalysts by the formation of stable Werner-type amine complexes. In addition, the common problems of reductive aminations such as over-alkylation and reduction to the corresponding alcohols, also affect catalytic activities and selectivities. In order overcome these problems and to perform reductive amination with ammonia aminations in selective manner, the development of efficient homogeneous catalysts, are highly desired. In recent decades, Rh[60-61], Ir[62] and Ru[15,63] as well as Co[64] and Ni[65] complexes were developed and successfully applied for the synthesis primary amines from carbonyl compounds and NH_3/H_2. In this section, homogeneous metal complexes catalyzed reductive amination for the synthesis of primary amines is discussed.

In 2002 Beller and coworkers [60] introduced a first homogeneous catalyst based on [Rh(COD)Cl]$_2$-TPPTS complex for the reductive amination aldehydes to prepare primary amines (scheme 8). Unfortunately, this catalyst has not been applied for the reductive amination of ketones to prepare branched primary amines.
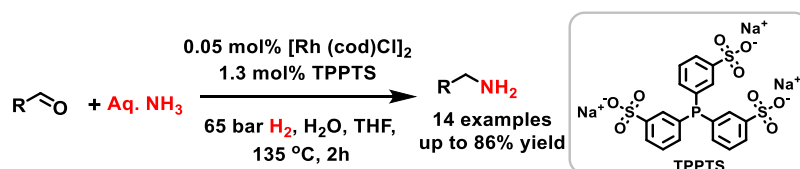
Scheme 8. [Rh(COD)Cl]$_2$-TPPTS catalyzed reductive amination

In addition to simple aldehydes, the Rh-TPPTS system was also able to aminate renewable terpenoid aldehyde such as citronellal to give citronellylamine.[61] Apart from Rh-TPPTS, other Rh-based catalysts such as Rh[(dppb)(COD)]BF$_4$ and [Rh(COD) Cl]$_2$-BINAS were used for the preparation of primary amines. Also, [Ir(COD)Cl]$_2$-BINAS catalyst was applied to prepare branched amines from ketones.[62]

Regarding Ru-based homogeneous catalysts, Schaub and co-workers[63] reported a Ru(CO)ClH(PPh$_3$)$_3$-dppe catalyst system for the synthesis of branched primary amines from ketones (scheme 9).
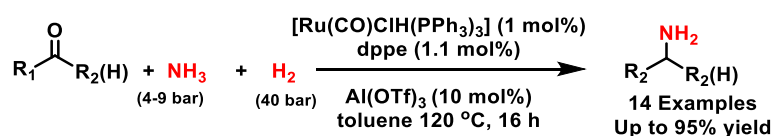
Scheme 9. Ru-dppe catalyzed synthesis of primary amines.

With respect to asymmetric reductive aminations to prepare chiral primary amines, Schaub and co-workers[66] and Zhang and Co-workers[67] reported Ru(CO)ClH(PPh$_3$)$_3$-(S,S)-f-binaphane (scheme 10A) and Ru/C$_3$-Tunephos (scheme 10B) systems, respectively.
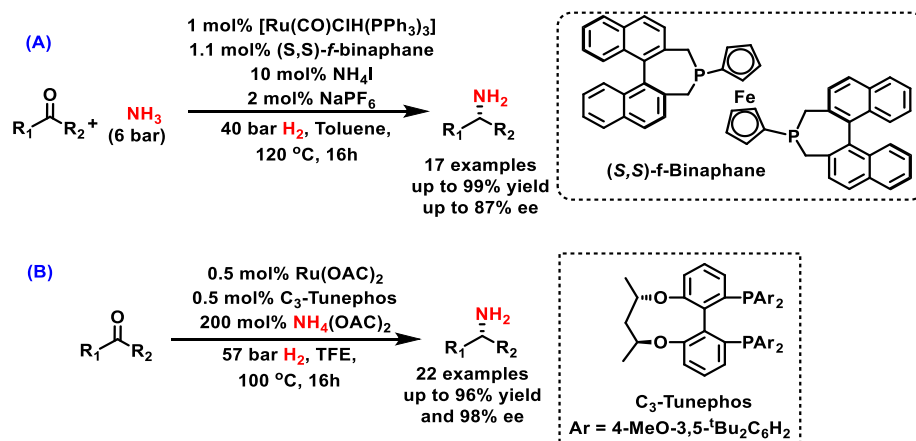
Scheme 10. Ru-catalyzed asymmetric reductive amination for the preparation of chiral primary amines.

In 2019, Beller and Jagadeesh et al[64] reported Co-triphos as the first homogeneous base metal catalyst for the reductive amination of carbonyl compounds with ammonia to prepare primary amines. Using this complex, benzylic, heterocyclic and aliphatic primary amines were prepared in good to excellent yields (scheme 11). In addition to the synthetic investigations, the authors also made DFT studies, and proposed a plausible mechanism (scheme 12).
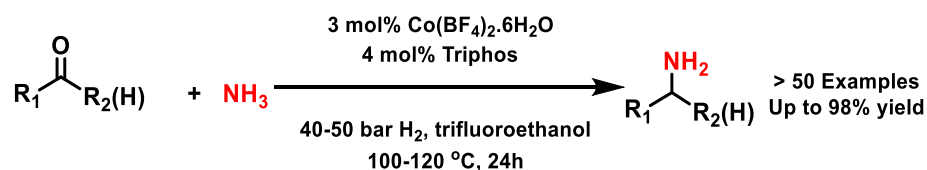
Scheme 11. Co-triphos catalyzed reductive amination for the synthesis of primary amines.

Scheme 12. Proposed mechanism (A) and Gibbs free energy surface (B) for Co-triphos catalyzed reductive amination with NH_3 and H_2.
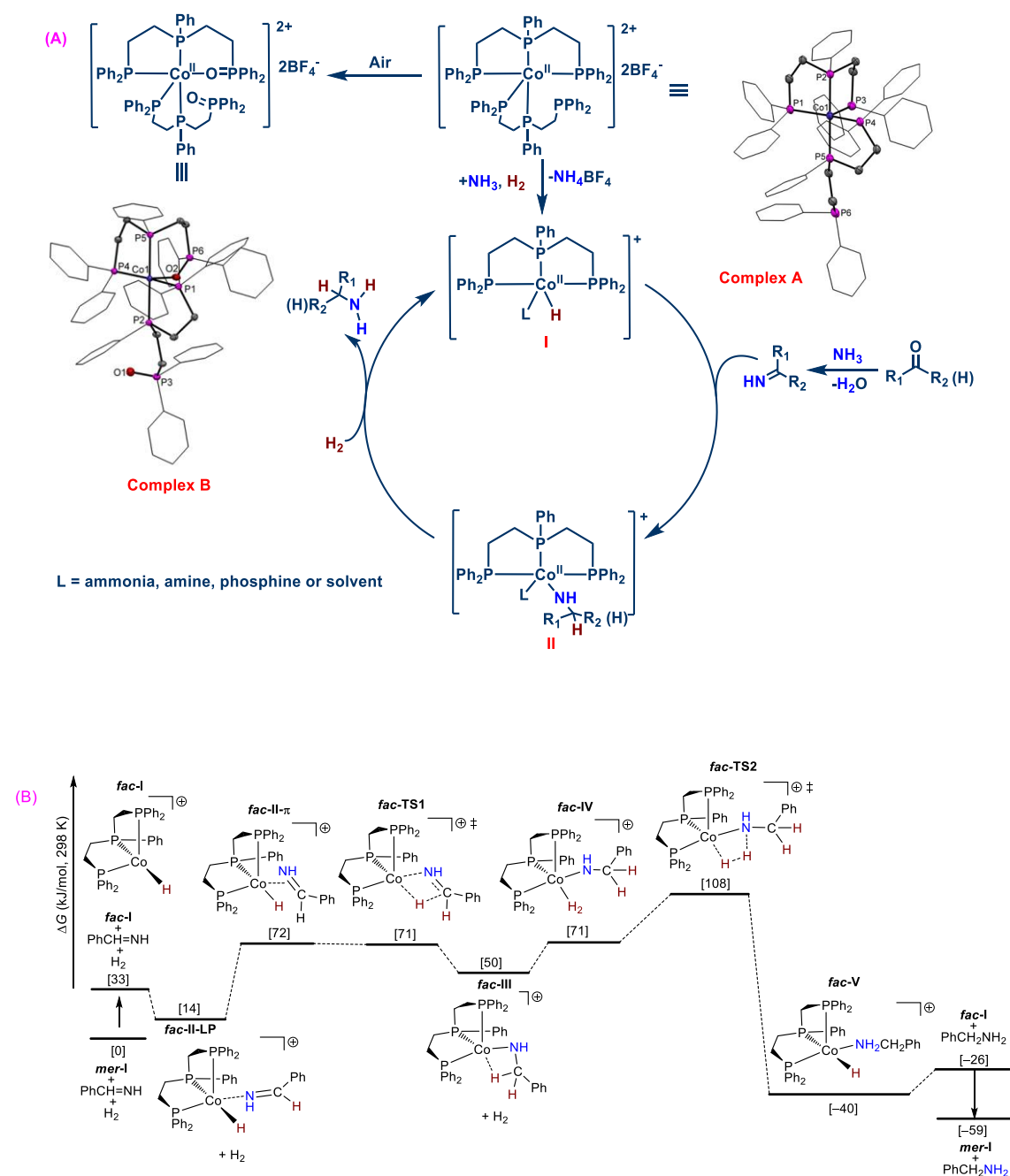
Subsequently, the same authors[65] showed that a related Ni-triphos complex also acts as an efficient catalyst for the reductive amination of carbonyl compounds with ammonia to access functionalized and structurally divers primary amines (scheme 13). In addition, this Ni-triphos complex was used for the hydrogenation of nitroarenes to produce anilines.
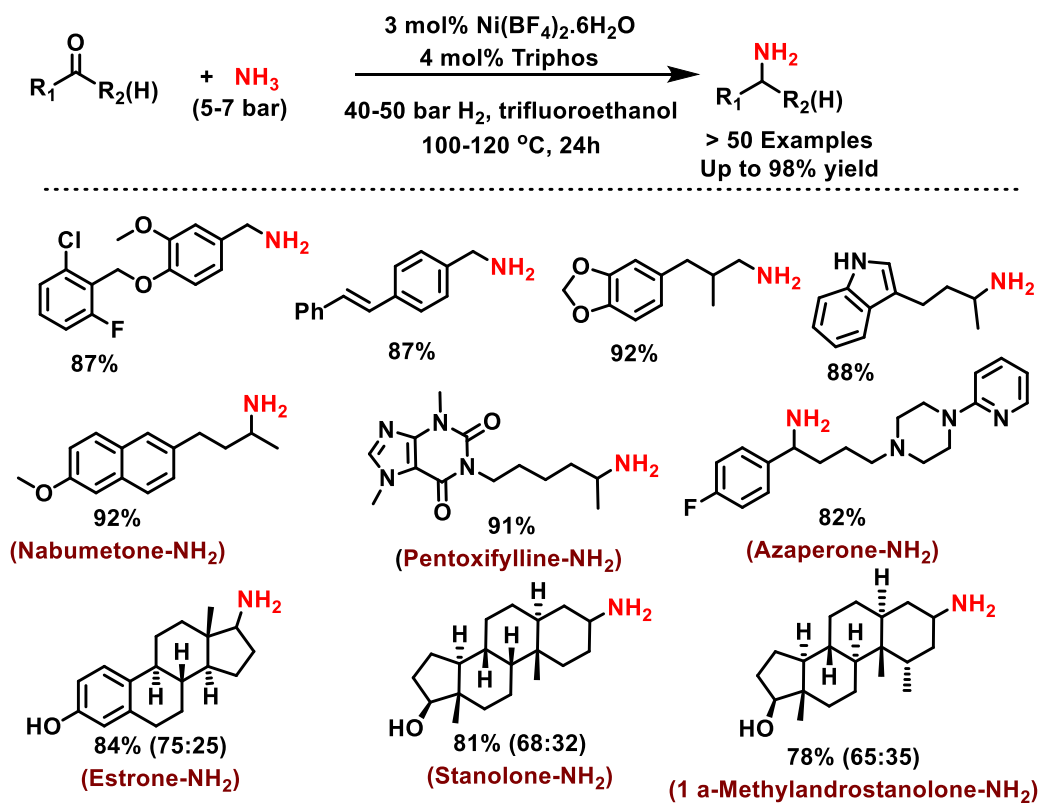
Scheme 13. Homogeneous Ni-catalyzed synthesis of primary amines.

1.6 Synthesis of secondary and tertiary amines by base-metal heterogeneous catalyzed reductive aminations using molecular hydrogen.

In this section, the catalytic reductive amination for the synthesis of secondary and tertiary amines using molecular hydrogen in the presence of base metal heterogeneous materials is discussed.

Beller and coworkers developed nitrogen doped graphene activated Fe_2O_3-(Fe_2O_3/NGr@C)[68,69] and Co_3O_4-(Co_3O_4/NGr@C)[70,71] based catalysts for one pot reductive amination of carbonyl compounds and nitro compounds to access various N-alkylamines. These supported nano-metal oxide catalysts were prepared by the immobilization of *in situ* generated phenanthroline ligated Fe- or Co-complexes on carbon and subsequent pyrolysis under argon at 800 °C for 2h (Fig. 3). Compared to Fe_2O_3/NGr@C, Co_3O_4/NGr@C catalyst worked under mild conditions and exhibited more activity and selectivity (scheme 14).
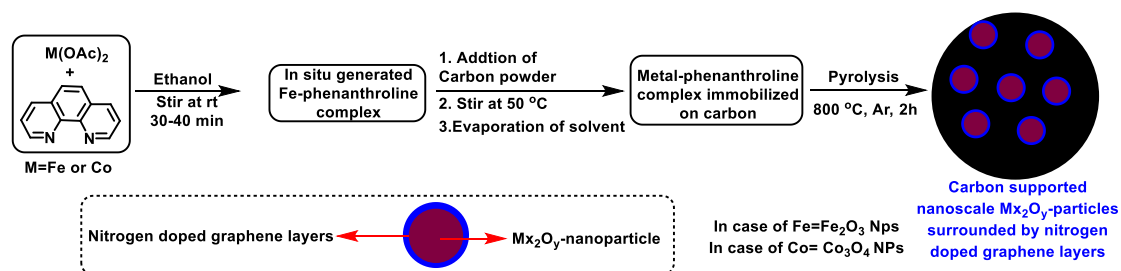
Figure 3. Preparation of carbon supported Fe- and Co-oxide nanoparticles
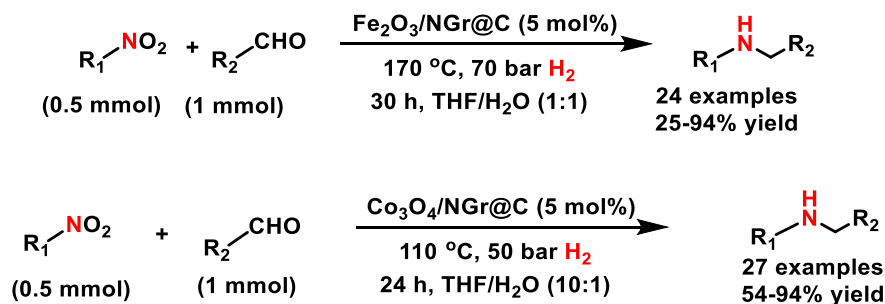
Scheme 14. Fe_2O_3/NGr@C and Co_3O_4(Co_3O_4/NGr@C catalyzed one-pot reductive amination

In 2017, again Beller and co-workers[13] reported a cobalt-nanoparticles- and single atoms-based catalyst (Co-DABCO-TPA) for the preparation of secondary and tertiary amines. Both nitroarenes and amines reacted with aldehydes and produced the corresponding secondary and tertiary amines selectively in up to 92% yield. Applying the optimal Co-DABCO-TPA@C-800 catalyst 10 existing drug molecules have been prepared in good the excellent yields. (scheme 15).
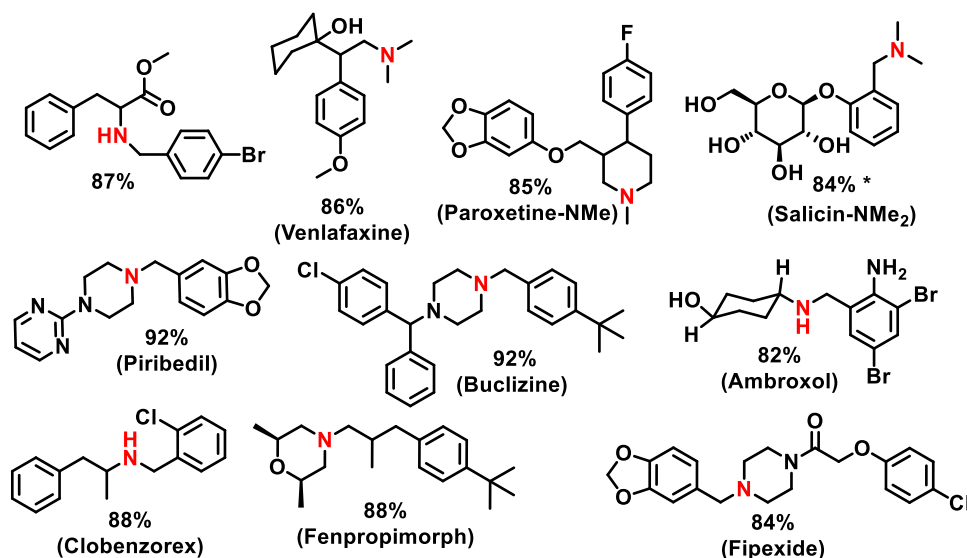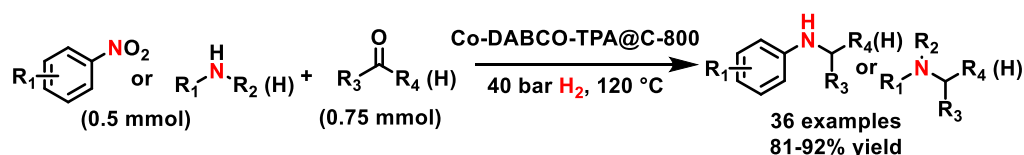
Scheme 15. Co-DABCO-TPA@C-800 catalyzed synthesis amines.

In addition, Jin et al.[72] Huang et al.[73] and Chi et al.[74] developed cobalt-based heterogeneous catalysts for the synthesis of both secondary and tertiary amines. Regarding Ni-catalysis, Pera-Titus and Shi et al.[59] reported Ni_6AlO_x catalyzed reductive amination of HMF with primary amines to obtain bio-base secondary amines.

1.7 Base metal heterogeneous catalyzed reductive amination for synthesis of secondary and tertiary amines using formic acid

In this section, the catalytic reductive amination for the synthesis of secondary and tertiary amines in the presence of base metal heterogeneous catalyst using formic acid is discussed.

In 2017, the Wang group[47] reported Co nanoparticles supported on mesoporous nitrogen-doped carbon (abbreviated as Co@CN-800) for the one pot reductive

amination of aldehydes and nitro compounds for the synthesis of different N-alklyated amines using formic acid as the reducing agent (scheme 16).

$$R^1NO_2 \quad + \quad R^2\text{-CHO} \xrightarrow[\substack{170\ ^\circ\text{C, HCOOH} \\ 10\text{-}20\ \text{h, THF}}]{\text{Co@CN-800 (5 mol\%)}} R^1\text{-}\underset{\text{H}}{N}\text{-}R^2$$

(1 mmol)   (2 mmol)   32 examples
88-95% yield
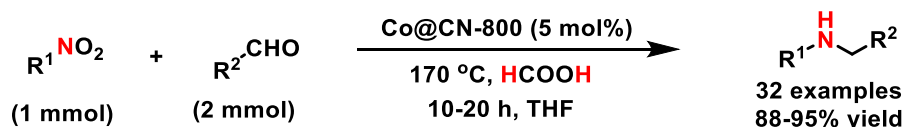
Scheme 16. Co@CN-800 catalyzed reductive amination for the synthesis of N-alkylamines.

Next, Chi et Al.[48] reported nitrogen-doped carbon embedded Co catalysts (abbreviated as Co@CN-800-AT, in which T represents the pyrolysis temperature, AT represents the acid-leaching process) prepared by the simple pyrolysis of graphene oxide-supported cobalt-based zeolitic imidazolate-frameworks, followed by an acid-leaching process for the reductive amination for the synthesis of N-alkylated amines using formic acid (scheme 17).

$$R^1NO_2 \quad + \quad R^2\text{-CHO} \xrightarrow[\substack{190\ ^\circ\text{C, HCOOH} \\ 10\ \text{bar N}_2, 15\text{h, THF}}]{\text{Co@CN-600-AT}} R^1\text{-}\underset{\text{H}}{N}\text{-}R^2$$

(1 mmol)   (2 mmol)   33 examples
32-95% yield
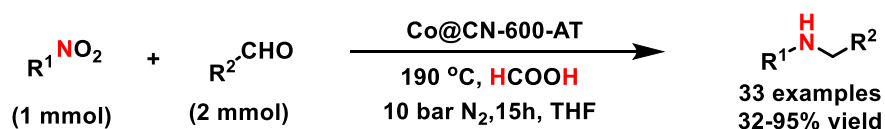
Scheme 17. Co@CN-800-AT catalyzed synthesis of N-alkylated amines using formic acid.

Further, Zhang et al.[49] prepared nitrogen-doped carbon based Co–Nx/C-800-AT catalyst by the pyrolysis of cobalt phthalocyanine/silica composite at 800°C under a N_2 atmosphere and subsequent etching by HF. The resulting materials were applied for the one-pot reductive amination of aldehydes and nitro compounds to obtain different secondary amines using formic acid as the hydrogen donor (scheme 18).

$$R^1NO_2 \quad + \quad R^2\text{-CHO} \xrightarrow[\substack{150\ ^\circ\text{C, HCOOH,} \\ 15\text{h, EA}}]{\text{Co-Nx/-800-AT}} R^1\text{-}\underset{\text{H}}{N}\text{-}R^2$$

(1 mmol)   (2 mmol)   33 examples
32-95% yield
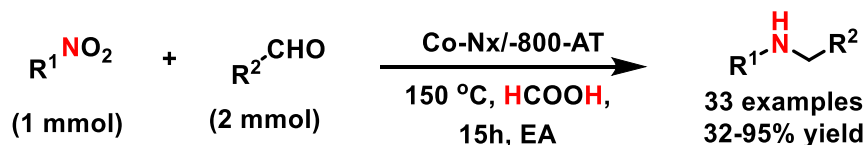
Scheme 18. Co–catalyzed reductive amination reactions.

2. Objectives of this work

The development of novel catalysts for the synthesis of amines continues to be important topic both in academic research and the chemical industry. In particular, the design of simple and easily accessible catalysts for reductive aminations for the expedient synthesis of amines is desired and attracts scientific interest. Known homogeneous catalysts applied for the reductive amination to prepare primary amines are based on sophisticated or synthetically demanding metal complexes and ligands. In this regard our aim was to introduce more simple and commercially available and/or easily accessible catalysts for the preparation of structurally diverse and functionalized primary amines from carbonyl compounds and ammonia using molecular hydrogen. Before this work, the majority of the nanoparticles-based heterogeneous catalysts, especially non noble metal-based ones, required special techniques and instruments for their preparation. However, the design of more convenient methods is highly desired for the practical synthesis of nanoparticles-based catalysts. In this regard, our objective was to introduce a straightforward approach for the generation of cobalt-based NPs *in situ* from molecularly-defined metal complexes and their application to prepare different kinds of amines. Finally, it was intended to demonstrate reductive aminations for the preparation different N-(methyl)alkylated amines using formic acid as suitable reducing agent, which avoids the use of pressurized equipment.

3. Summary of this work

Following the objectives, we describe the development of homogeneous ruthenium complex and heterogeneous cobalt based catalyst and their applications in reductive amination reactions.

3.1 Simple ruthenium-catalyzed reductive amination enables the synthesis of a broad range of primary amines (*Nature Communications*, 2018, *9*, 4123.)

The majority of the known homogeneous catalysts applied for challenging synthetic reactions and advanced organic synthesis are based on sophisticated metal complexes and/or ligands. However, to achieve a convenient and practical chemical synthesis, the catalyst must be simple, effective and commercially available and/or easily accessible. In this regard, triphenylphosphine (PPh_3)-based metal complexes are found to be expedient and advantageous for catalysis applications, since PPh_3 is a stable and comparatively cheap ligand.[75-79] Among PPh_3-based Ru complexes, $RuCl_2(PPh_3)_3$ is the simplest and least expensive one and is also commercially available.[80-86] Noteworthy, this simple complex was used as catalyst for number of synthetic transformation.[76-79] Here, we demonstrate that $RuCl_2(PPh_3)_3$ is an efficient and highly selective homogeneous pre-catalyst for reductive amination that empowers the preparation of a variety of primary amines of industrial importance and pharmaceutically relevance. In order to design a practical homogeneous catalyst system, different metal precursors with PPh_3 were tested for the reductive amination of benzaldehyde **1** to benzylamine **2** with ammonia using molecular hydrogen. As shown in Table 1, the *in situ* generated Fe-, Co-, Mn-, Ni- and Cu-PPh_3 complexes were not active for the formation of benzylamine. However, *in situ* generated Ru(II)-PPh_3 complexes showed some activity and produced benzylamine in up to 40 % yield. After observing this reactivity, *in situ* generated Ru-complexes with differently substituted

19

PPh$_3$-type ligands as well as simple nitrogen ligands (L1-L10) have been tested. Among these, Ru-catalysts containing either PPh$_3$ or derivatives with electron donating groups in *para*-position showed the highest activity (Table 1; entries 1,4,5). However, none of the tested nitrogen ligands (L7-L10) produced the desired product (Table 1, entries 7-10).
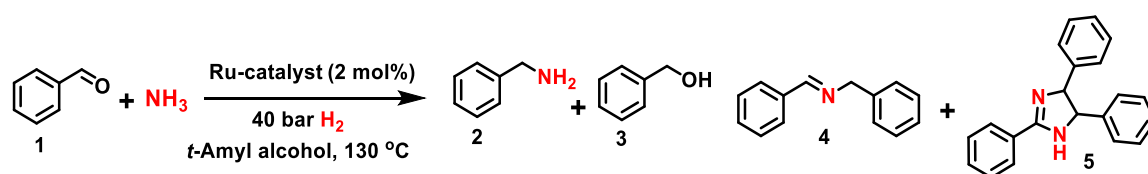
Entry	Ru-precursor/ Defined Ru-catalyst	Ligand	Yield (%)			
			2	3	4	5
1 [a]	[RuCl$_2$(p-cymene)]$_2$	L1	40	2	40	17
2 [a]	[RuCl$_2$(p-cymene)]$_2$	L2	5	-	60	33
3 [a]	[RuCl$_2$(p-cymene)]$_2$	L3	2	-	25	70
4 [a]	[RuCl$_2$(p-cymene)]$_2$	L4	50	5	20	24
5 [a]	[RuCl$_2$(p-cymene)]$_2$	L5	53	4	16	25
6 [a]	[RuCl$_2$(p-cymene)]$_2$	L6	10	2	42	44
7 [a]	[RuCl$_2$(p-cymene)]$_2$	L7	-	-	20	76
8 [a]	[RuCl$_2$(p-cymene)]$_2$	L8	-	-	18	79
9 [a]	[RuCl$_2$(p-cymene)]$_2$	L9	-	-	25	74
10 [a]	[RuCl$_2$(p-cymene)]$_2$	L10	-	-	30	68
11 [b]	RuCl$_2$(PPh$_3$)$_3$	-	95	4	-	-
12 [b]	RuCl$_2$(PPh$_3$)$_4$	-	92	7	-	-
13	RuCl$_2$(tris(4-methoxyphenyl) phosphine)$_3$	-	95	4	-	-
14	RuCl$_2$(tris(4-chlorophenyl) phosphine)$_3$	-	50	-	49	-
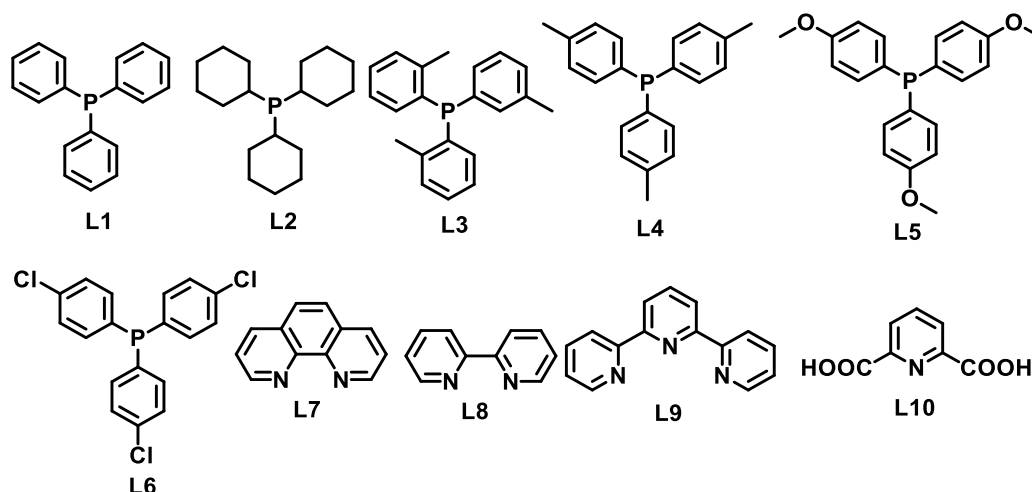
Reaction conditions: [a]0.5 mmol benzaldehyde, 1 mol% [RuCl$_2$(p-cymene)]$_2$ (2 mol% corresponds to monomer), 6 mol% ligand, 5-7 bar NH$_3$, 40 bar H$_2$, 1.5 mL *t*-amyl alcohol, 130 °C, 24 h, GC yields using n-hexadecane as standard. [b]Same as 'a' but using 2 mol% defined catalyst.

Table 1. Reductive amination of benzaldehyde using *in situ* generated and molecularly defined ruthenium catalysts.

After having identified RuCl$_2$(PPh$_3$)$_3$ to be among the most active pre-catalysts, kinetic investigations to examine the effect of reaction time, catalyst concentration and hydrogen pressure on the model reaction have been made. Based on these results, it was concluded that in order to get maximum yield of **2** without the formation of **4** and **5**, 40 bar of hydrogen, a reaction time of 24 h, a catalyst loading of 2 mol% and temperature of 130 °C are required to obtain best results. In addition, these results confirmed the formation of side products such as alcohols **3**, secondary imine **4** and the imidzole-based product **5** in addition to the desired product, primary amine **2**.
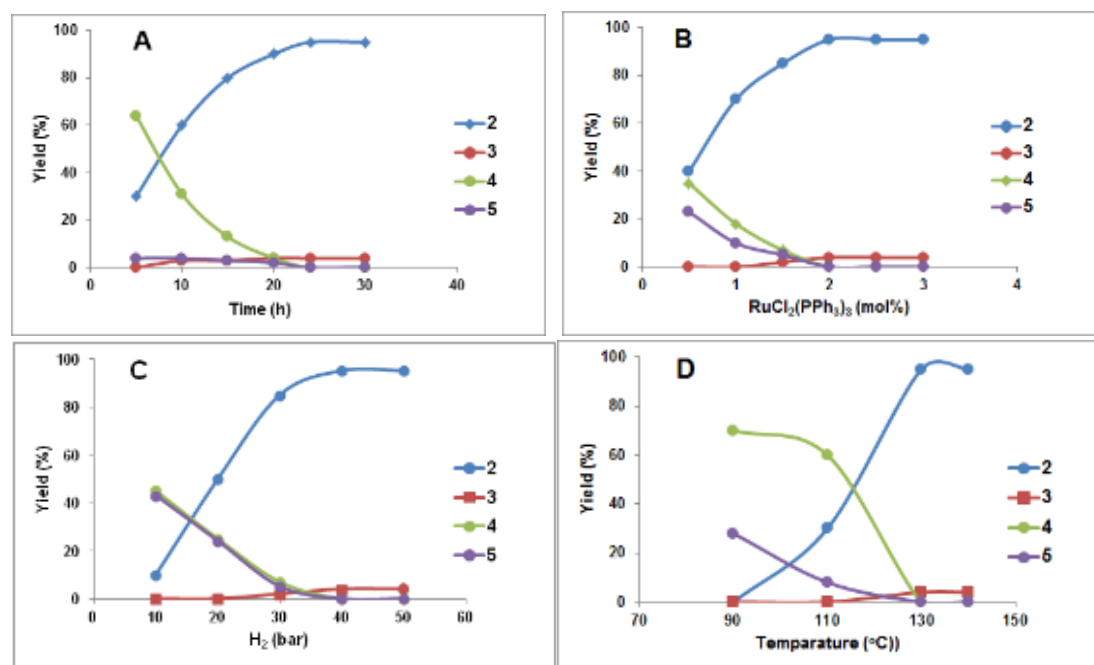
Figure 4. Effect of reaction time, Ru-concentration and pressure of H_2 on reductive amination of benzaldehyde with NH_3 and H_2.

Reaction condition: A=yield *vs* reaction time; B=yield *vs* concentration of $RuCl_2(PPh_3)_3$; C=yield *vs* pressure of H_2; D=yield *vs* temperature. 2=Yield of benzylamine; 3=yield of benzyl alcohol; 4=yield of *N*-benzylidenebenzylamine; 5=yield of 2,4,5-triphenyl-4,5-dihydro-1H-imidazole. Reaction conditions: For Fig. A: 0.5 mmol benzaldehyde, 2 mol% $RuCl_2(PPh_3)_3$, 5-7 bar NH_3, 40 bar H_2 1.5 mL t-amyl alcohol, 130 °C, 5-30 h; for Fig. B: 0.5 mmol benzaldehyde, 0.5-3 mol% $RuCl_2(PPh_3)_3$, 5-7 bar NH_3, 40 bar H_2 1.5 mL t-amyl alcohol, 130 °C, 24 h; for Fig. C=: 0.5 mmol benzaldehyde, 2 mol% $RuCl_2(PPh_3)_3$, 5-7 bar NH_3, 10-50 bar H_2 1.5 mL t-amyl alcohol, 130 °C, 24 h. for Fig. D: 0.5 mmol benzaldehyde, 2 mol% $RuCl_2(PPh_3)_3$, 5-7 bar NH_3, 40 bar H_2 1.5 mL t-amyl alcohol, 90-140 °C 130 °C, 24h. Yields were determined by GC using n-hexadecane as standard.

Under optimized reaction conditions, $RuCl_2(PPh_3)_3$ catalyst allowed for the preparation of >90 functionalized and structurally diverse linear and branched primary amines starting from inexpensive and easily accessible aldehydes and ketones and ammonia in presence of molecular hydrogen (scheme 19). The application of this Ru-based reductive amination process has been applied for the synthesis and amination of various drug molecules and steroid derivatives. In addition, the possibility of upscaling up this amination protocol up to 10 g scale was demonstrated (scheme 20).

Primary linear amines

$$R\text{—CHO} + NH_3 + H_2 \xrightarrow[\text{(5-7 bar)(40 bar)}]{\begin{array}{c}\textbf{RuCl}_2\textbf{(PPh}_3\textbf{)}_3\textbf{ (3 mol\%)}\\ \textit{t}\text{-amyl alcohol, 130 °C}\end{array}} R\text{—CH}_2\text{—NH}_2$$

89%

88%

95%

87%

72%

82%

87%

82%

81%

87%

71%

92%

85%

89%

89%

83%

80%
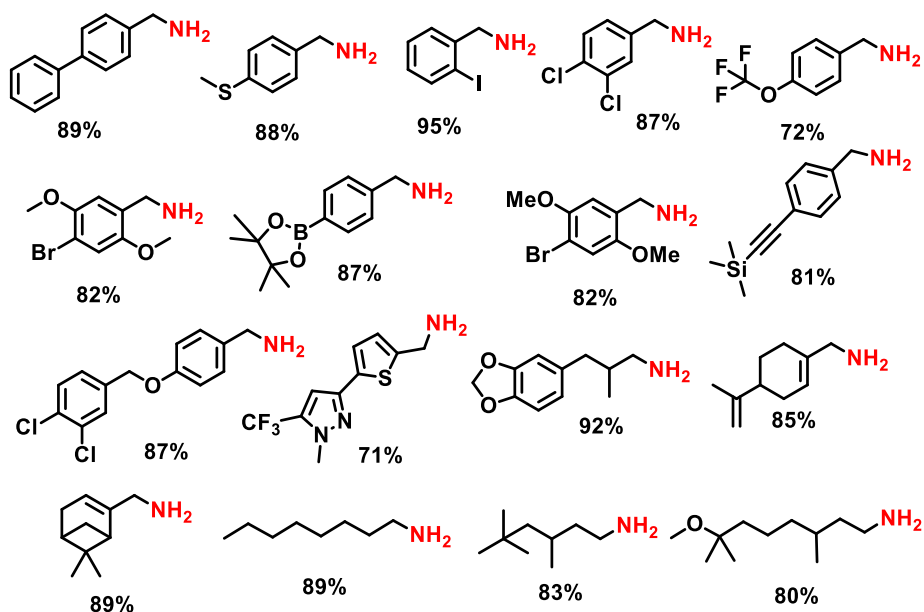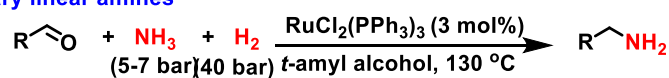
Primary branched amines

$$R_1\text{—CO—}R_2 + NH_3 + H_2 \xrightarrow[\text{(5-7 bar)(40 bar)}]{\begin{array}{c}\textbf{RuCl}_2\textbf{(PPh}_3\textbf{)}_3\textbf{ (3 mol\%)}\\ \textit{t}\text{-amyl alcohol, 130 °C}\end{array}} R_1\text{—CH(NH}_2\text{)—}R_2$$

63: 93%

69: 82% [d]

72: 82% [d]

77: 82% [d]

93%

80%

85: 85%

80%

Biologically active molecules

90%
(**Nabumetone-NH₂**)

76%
(**Pentoxifylline-NH₂**)

80%
(**Azaperone-NH₂**)

93% (92:8)
(**Androstanolone-NH₂**)

79%
(**Estrone-NH₂**)

92%
(**Testosterone propionate-NH₂**)
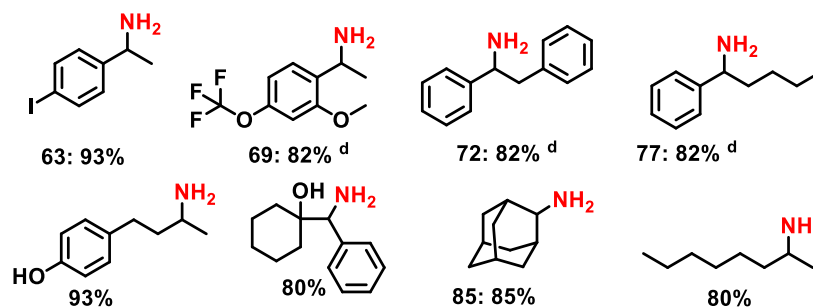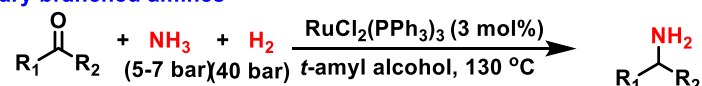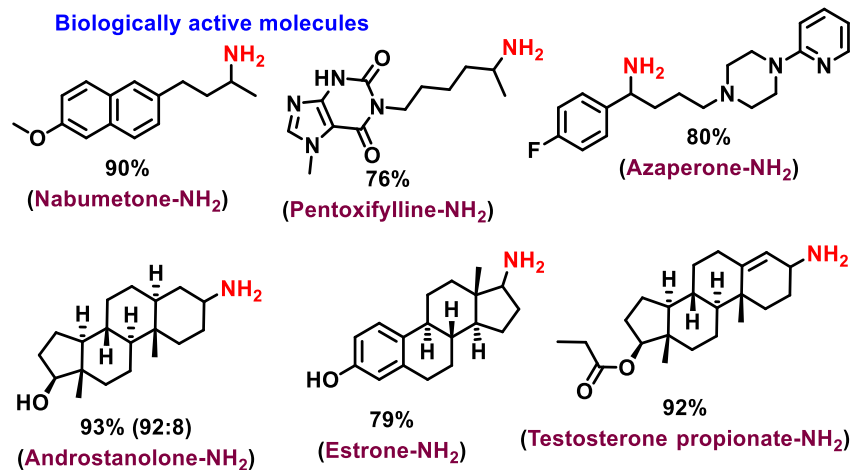
Scheme 19. RuCl₂(PPh₃)₃ catalyst reductive amination for the synthesis of primary amine.

17: 92%
(2.5g scale)

12: 90%
(10g scale)

30: 92%
(5g scale)

2: 93%
(3g scale)

89: 90%
(20g scale)

66: 91%
(2.5g scale)

80: 90%
(5g scale)
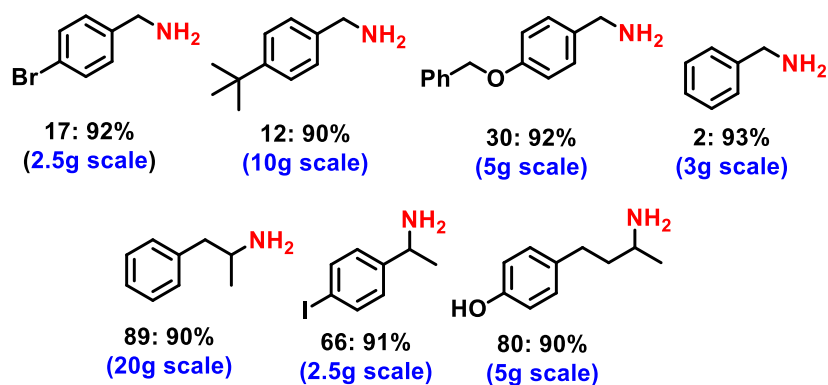
Scheme 20. Demonstrating the synthetic utility for gram-scale reactions.

Reaction conditions: 2-20 g carbonyl compound, 2-3 mol% of $RuCl_2(PPh_3)_3$ (2 mol% in case of aldehyde, 3 mol% in case of ketone), 5-7 bar NH_3, 40 bar H_2, 25-150 mL t-amyl alcohol, 130 ^oC, 24-30 h. Isolated as free amines and converted to hydrochloride salts. Corresponding hydrochloride salts were subjected to NMR analysis.

In addition to synthetic applications, *in-situ* NMR studies have been made to identify catalytic species and reaction intermediates (Fig. 5). Based on these NMR studies and kinetic investigations (Fig. 4), the plausible mechanism for the $RuCl_2(PPh_3)_3$-catalyzed reductive amination in presence ammonia and molecular hydrogen is proposed in scheme 21. The pre-catalyst $RuCl_2(PPh_3)_3$ is activated by H_2 and forms the active catalyst species $[RuHX(PPh_3)_3]$ (X = H^- or Cl^-). This active species selectively reacts with the primary imine, which is formed by the condensation of carbonyl compound with ammonia, to initially form a substrate complex (**I**). Next, the substrate coordination is followed by hydride insertion (**II**), generating a Ru-amide complex. Finally, coordination of H_2 (**III**) followed by hydrogenolysis releases the primary amine as the final product with the regeneration of the catalytic species (**IV**) hydrogenolysis releases the primary amine as the final product with regeneration of the catalytic species (**IV**). The formation of side products **4** and **5** is already explained in section 1.3 and scheme 21.
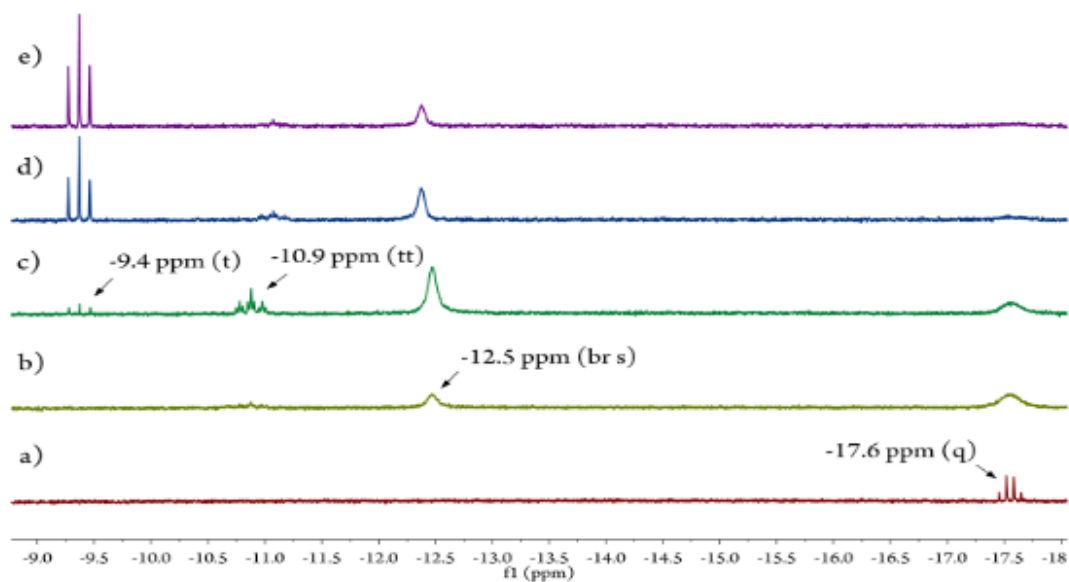
Reaction condition: a) RT, argon atmosphere; b) RT, H_2 atmosphere (1.5 bar), 10 min; c) RT, H_2 atmosphere (1.5 bar), 2.5h; d) 60°C, H_2 atmosphere (1.5 bar), 30 min; e) 60°C, H_2 atmosphere (1.5 bar), 1.5h.
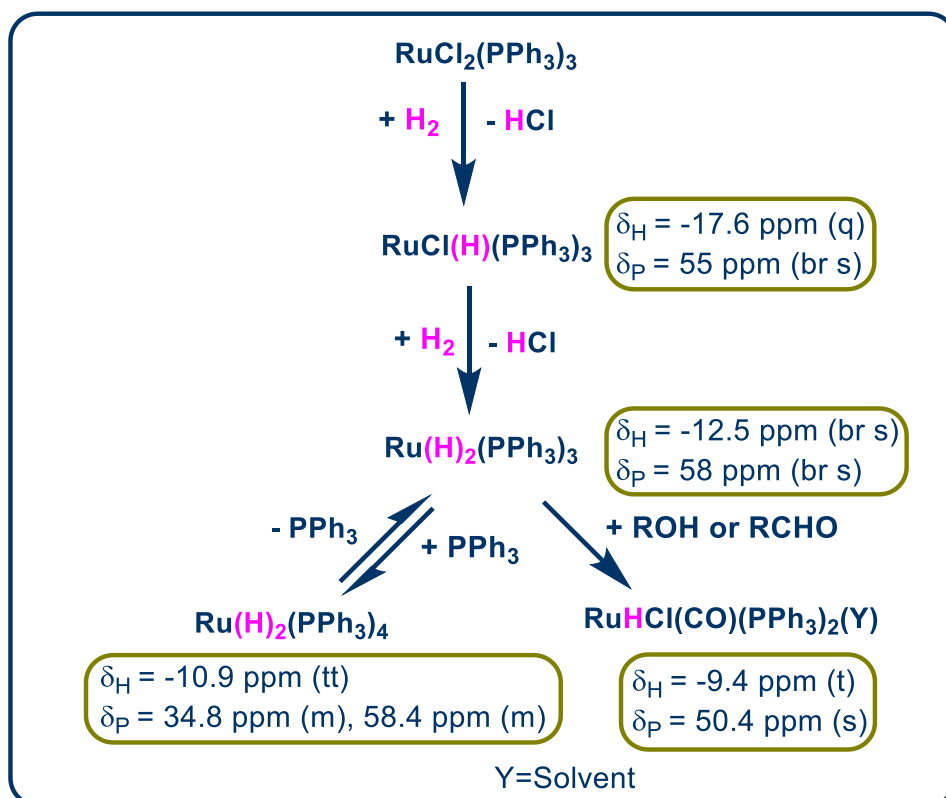
Figure 5. Generation of different species from $RuCl_2(PPh_3)_3$ in the presence of hydrogen.

25
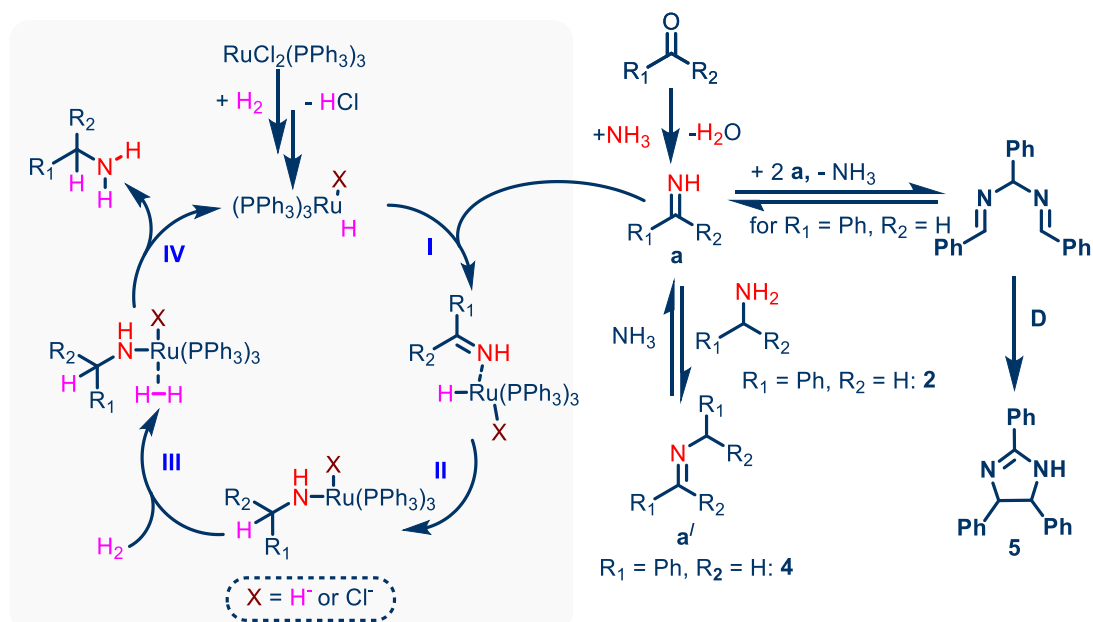
Scheme 21. Proposed reaction mechanism for the RuCl$_2$(PPh$_3$)$_3$-catalyzed reductive amination of carbonyl compounds with ammonia.

3.2 Ultra-small cobalt nanoparticles from molecularly defined Co-salen complexes for catalytic synthesis of amines (*Chemical Science,* 2020,11, 2973-298)

In general, the preparation of nanostructured catalysts involves specific methods and require special instruments. However, the convenient and practical preparation of nanoparticles-based catalysts continues to be important and attracts scientific interest. In this regard, generating nanoparticles *in situ* using suitable precursors in the reaction system is more expedient. Here, the synthesis of in situ generated cobalt nanoparticles from molecularly defined complexes as efficient and selective catalysts for reductive amination reactions is reported.[37] For example, cobalt-N,N-bis(salicylidene)-1,2-phenylenediamine (complex I) in water-THF as solvent in the presence of ammonia and molecular hydrogen at 120 °C formed magnetically separable ultra-small nanoparticles (Co-NPs) (Fig. 6).
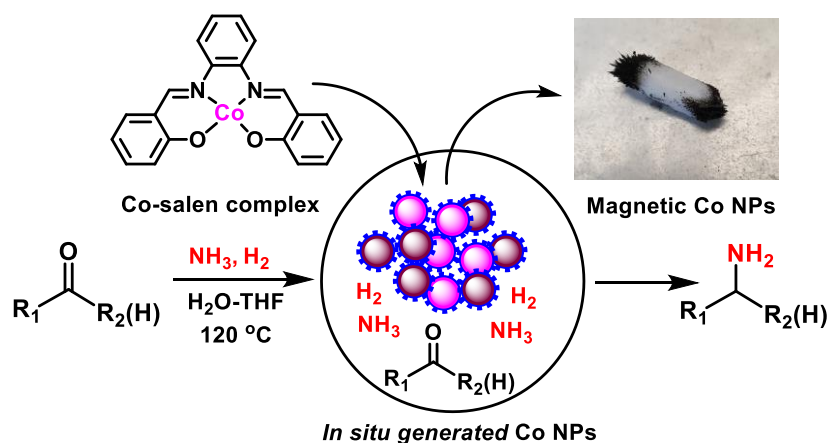
Figure 6. *In situ* generation of Co-NPs from Co-salen complex for reductive aminations.

To explore the reactivity of these Co NPs, preliminary catalytic experiments were carried out for the reductive amination of 4-bromobenzaldehyde **1** to 4-bromobenzylamine **2** in presence ammonia and molecular hydrogen as benchmark reaction (Fig. 5). Testing simple cobalt(II) acetate produced no desired product at all. In contrast, using a mixture of cobalt(II)acetate and N,N-bis(salicylidene)-1,2-phenylenediamine **(L1)** led to the formation of 15% of **2**. Remarkably, the defined complex **Co-L1** (complex I) exhibited excellent activity as well as selectivity in the benchmark reaction (98% of 4-bromobenzylamine). In addition, other molecularly defined Co-salen complexes have also been tested (Fig. 7). Complexes **II-IV** showed good activity (85-90% yield), while complex **V** resulted in lower product yield (50%). In all cases of active complexes, the *in-situ* formation of Co-NPs took place, which catalyzed the reductive amination reaction. Due to their physical properties, the Co NPs could be magnetically separated and were conveniently re-used up to three times (Fig. 7). In addition, the stability of the catalyst system was also confirmed by recycling the NPs after reduced reaction time. For comparison, we also prepared cobalt nanoparticles separately by mixing complex **I**, ammonia and hydrogen under standard reaction condition without the addition of aldehyde. After isolation, they were tested under similar conditions and exhibited comparable activity and selectivity to that of *in situ* generated ones.

Next, the reactivity of these active NPs were compared with related supported NPs. However, addition of carbon or silica support to the reaction led to completely inactive

materials (Fig. 8). On the other hand, materials prepared by immobilization of complex **I** on carbon or silica and subsequent pyrolysis produced catalysts with moderate activity (Fig. 7; 40-50% yield of 2). In addition, specific cobalt nanoparticles have been prepared by using chemical reduction of cobalt salts[88]and tested for their activities. However, none of these cobalt nanoparticles formed the desired product, 4-bromobenzylamine. All these results reveal the superiority of the simply *in situ* generated Co NP´s (Fig 7).
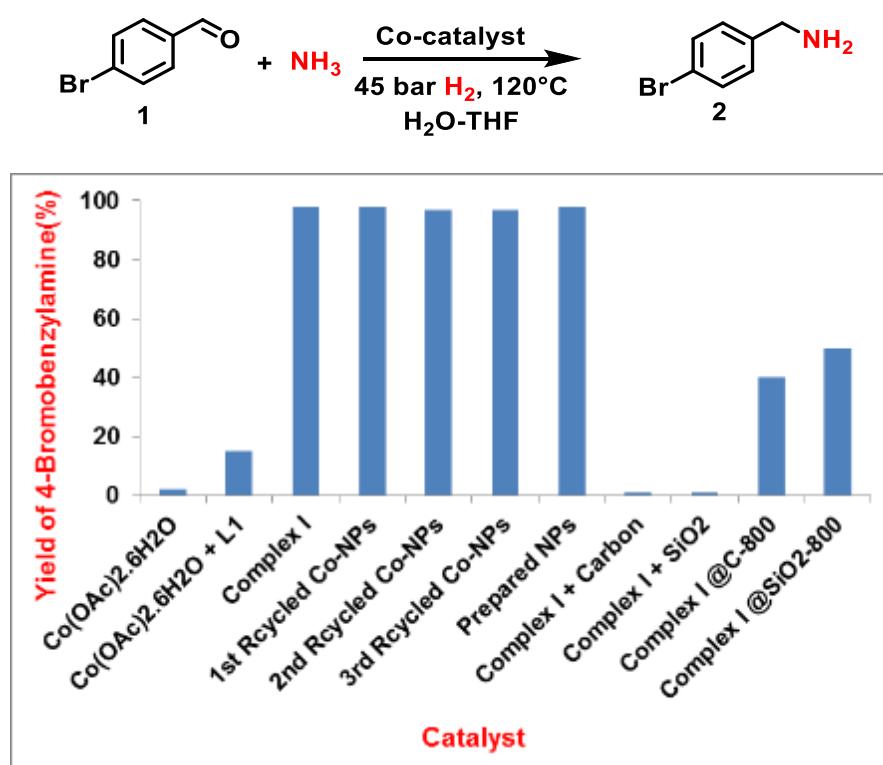
Figure 7. Reductive amination of 4-bromobenzaldehyde: Activity of cobalt catalysts.
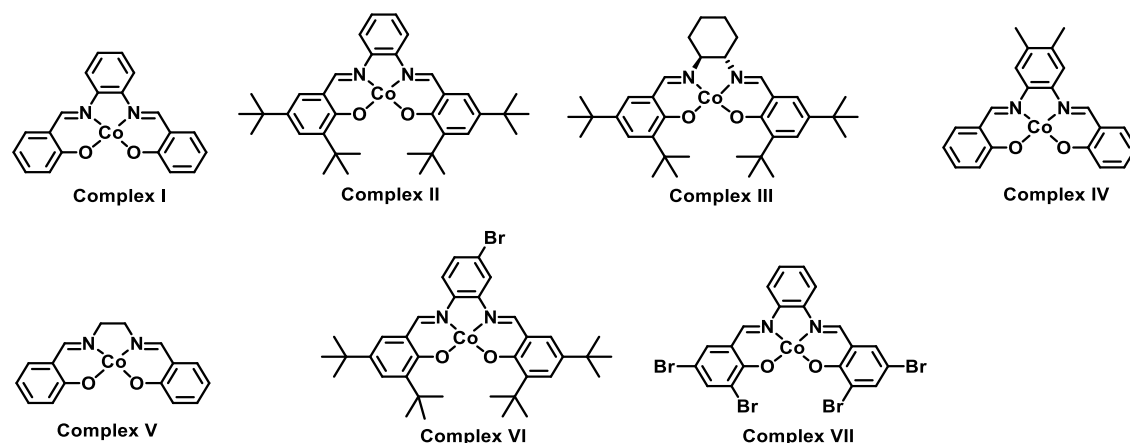
Reaction conditions: 0.5 m mol 4-bromobenzaldehyde, 6 mol% Co-complex, (Co NPs), 5 bar NH₃, 45 bar H₂, 2 mL solvent 2.5 mL (1.5:1 H₂O-THF), 120 °C, 24 h, GC yields using n-hexadecane as standard.
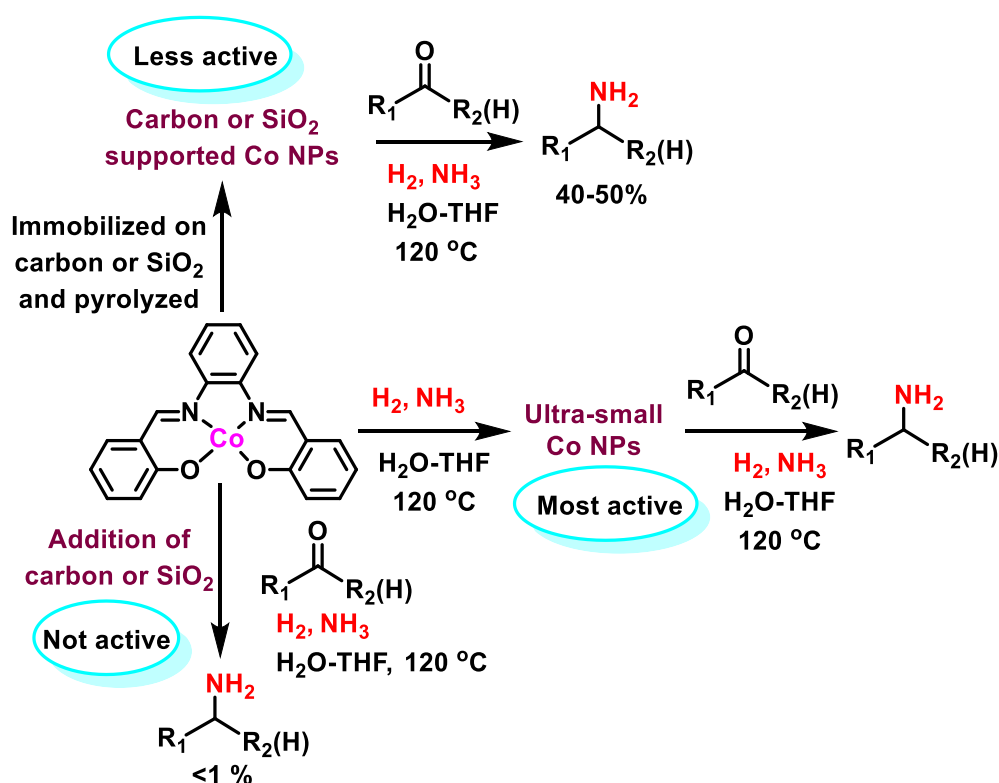
Figure 8. Reductive amination of carbonyl compounds in presence of NH_3 and H_2 using different Co NPs produced from cobalt-salen complex.

Characterizations of *in situ* generated cobalt NPs using transmission electron microscopy (TEM), energy dispersive X-ray spectroscopy (EDX), (X-Ray Diffraction (XRD), and X-ray photoelectron spectroscopy (XPS) revealed the formation of well-defined ultra-small (range 2-4 nm metallic cobalt and cobalt hydroxide nanoparticles embedded in a cobalt-nitrogen framework (Fig. 9).

29
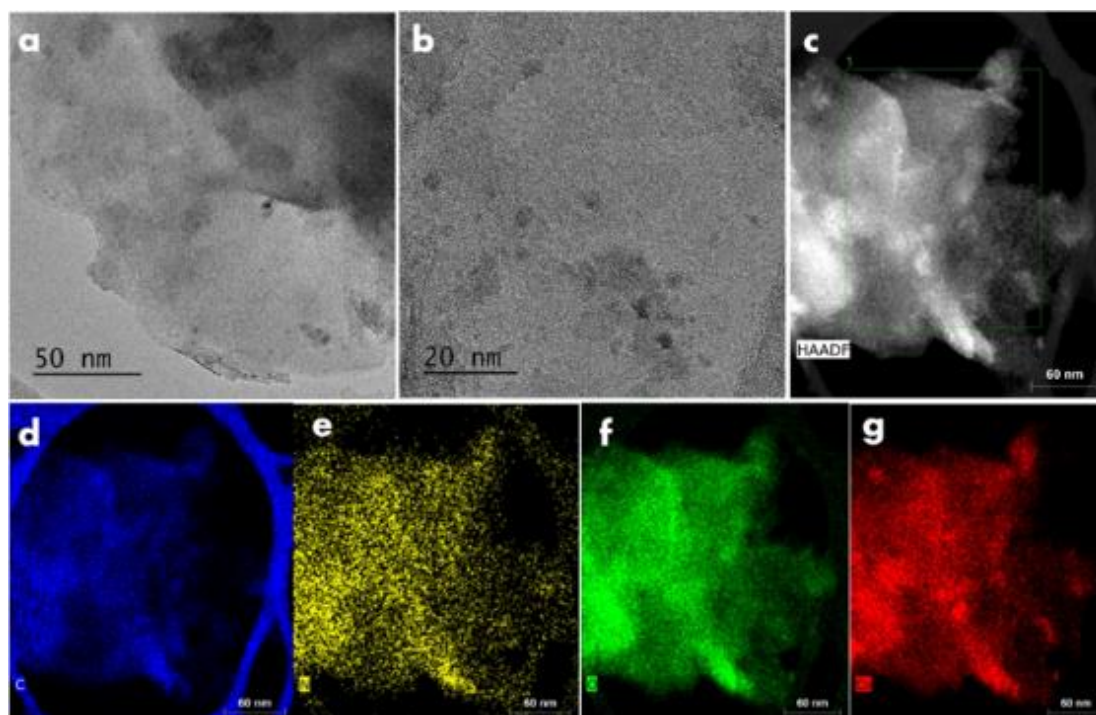
Figure 9. TEM images of *in situ* Co-NPs generated from complex I.

a, b=HRTEM images of cobalt catalyst, C=magnified STEM image, c-g = elemental mapping images where C, N, O and Co are in blue, yellow, green and red colors.

The applicability of these *in situ* generated cobalt NPs was demonstrated for the synthesis of a variety of structurally diverse and functionalized benzylic, heterocyclic and aliphatic linear and branched primary amines from carbonyl compounds and ammonia in presence of molecular hydrogen (schemes 22 and 23).

R–CHO + NH₃ → (In situ Co-nanoparticles / 45 bar H₂, H₂O-THF, 120 °C) → R–CH₂NH₂

3: 89% (89%)ᶜ   **4:** 88%   **5:** 92% (91%)ᶜ   **6:** 91%ᵇ   **7:** 86%

8: 86%   **9:** 91%   **10:** 92% (93%)ᶜ   **2:** 92%   **11:** 91%

12: 88%   **13.** 91%   **14:** 91%   **15:** 92%   **16:** 89% (90%)ᶜ

17: 95% (95%)ᶜ   **18:** 80%   **19.** 90%   **20:** 85%

21: 85%   **22.** 81%   **23:** 89%   **24:** 84%

25. 81%   **26:** 91%   **27:** 87%
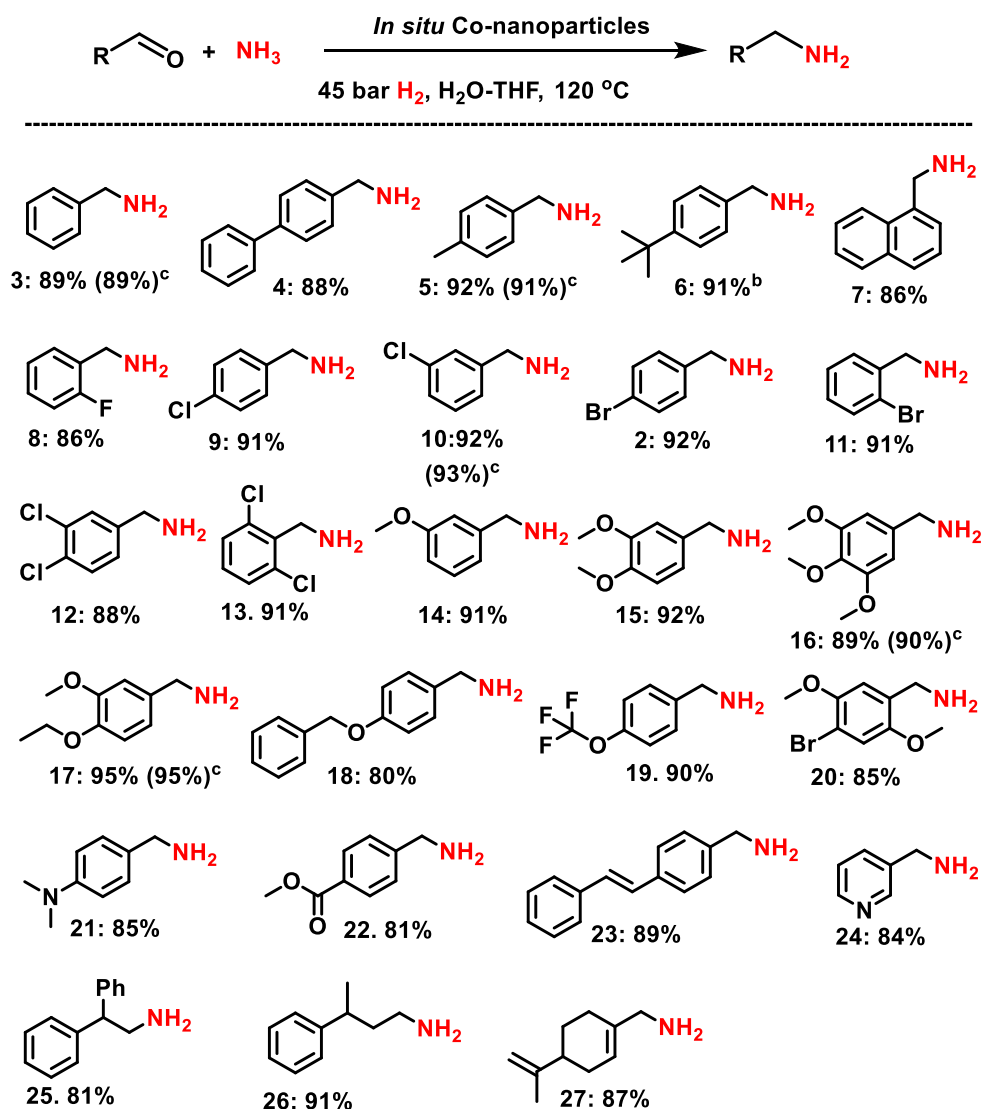
Scheme 22. *In situ* generated Co-nanoparticles catalyzed synthesis of linear primary amines.

[a]Reaction conditions: 0.5 mmol aldehyde, 6 mol% complex **I** (22 mg), 5-7 bar NH₃, 45 bar H₂, 2.5 mL H₂O-THF (1.5 :1 ratio), 120 °C, 24h, isolated yields. [b] Same as [a] at 130°C. [c] same as [a] using prepared and isolated Co-NPs (2 mg; 6.5 mol% Co).
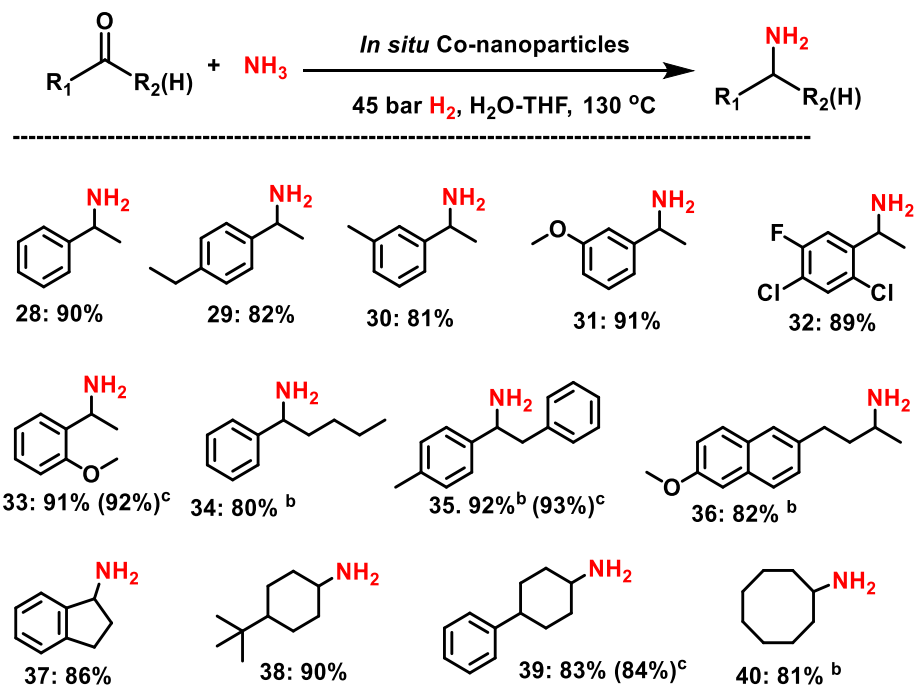
Scheme 23. Synthesis of branched primary amines using *in situ* generated Co-nanoparticles.

[a]Reaction conditions: 0.5 mmol ketone, 6 mol% complex **I** (22 mg) 5-7 bar NH$_3$, 45 bar H$_2$, 2.5 mL H$_2$O, 130 °C, 24 h, isolated yields. [b] Same as [a] in H$_2$O-THF solvent (1.5 :1 ratio). [c] same as [a] using prepared and isolated Co-NPs (2 mg check this correct mol%; 6.5 mol% Co).

Apart from primary amines synthesis, the applicability of these novel Co-nanoparticles was explored for the synthesis of secondary and tertiary amines. Interestingly, testing complex **I**, which generates the active NPs *vide supra* for the reaction of benzaldehyde and aniline at 120 °C in presence of molecular hydrogen (40 bar) led to the formation of imine (N-benzylideneaniline) as the sole product. Under these conditions no nanoparticles could be isolated after the reaction. Apparently, the presence of ammonia and hydrogen are required for the generation of the active NPs. Indeed, using isolated Co NPs, which were prepared from complex **I**, ammonia and hydrogen, led to excellent activity and selectivity for the synthesis of secondary and tertiary amines including N-methyl amines (scheme 23).

Scheme 24. Synthesis of secondary, tertiary and *N*-methyl amines using Co-nanoparticles prepared from complex I.

[a]Reaction conditions: 0.6 mmol aldehyde, 0.5 mmol amine, 2 mg Co-nanoparticles (6.5 mol% Co), 45 bar H_2, 1.5 ml H_2O 130°C, 20 h, isolated yields. [b]Same as [a] using 1 mL Aq. N, N-dimethylamine instead of amine.

3.3 Expedient synthesis of N-methyl- and N-alkylamines by reductive amination using reusable cobalt oxide nanoparticles (*ChemCatChem*, 2018, *10*, 1235-1240)

Reductive amination of aldehydes with nitro compounds or amines for the synthesis of N-alkyl and -methyl amines using carbon-supported, nitrogen-doped graphene activated cobalt oxide (Co_3O_4/NGr@C) was performed in the presence of formic acid-Et_3N mixture. This synthesis using formic acid as hydrogen source under transfer hydrogenation conditions was performed in simple commercially available pressure tubes by avoiding the use of sophisticated pressure equipment. Co_3O_4/NGr@C was

prepared by the immobilization of in situ generated Co-phenanthroline complex on carbon (Vulcan XC 72R) and subsequent pyrolysis at 800 °C under argon for 2h (Fig. 10).[69,70] In addition to phenanthroline, other nitrogen ligands were also used to prepare cobalt-based materials.
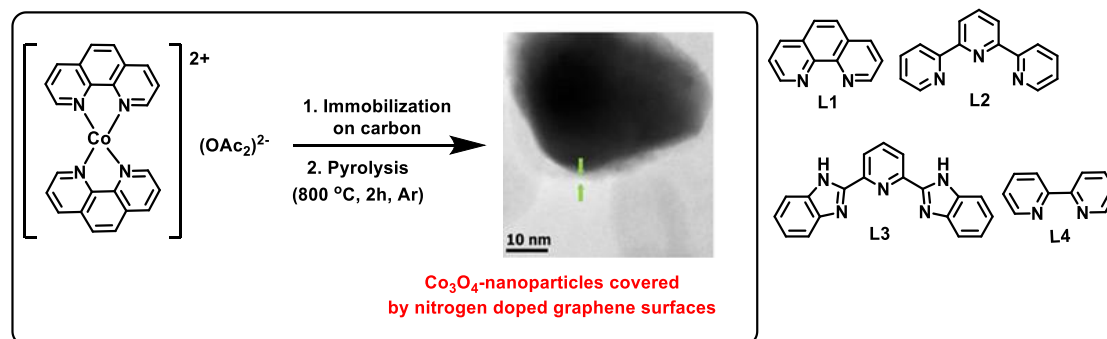
Figure 10. Preparation of Co_3O_4/NGr@C

These cobalt-based materials were tested for the reductive N-methylation of 4-methoxynitrobenzene with aqueous formaldehyde as methylation reagent in presence of formic acid as hydrogen source. The pyrolysis of Co(OAc)$_2$-L1 (L1 = phenanthroline) on carbon led to a highly active catalytic material was produced 4-methoxy-N,N-dimethylaniline in 88% yield (Fig. 11). However, related cobalt materials prepared using ligands L2-L4 showed less activity (25-59%). As expected, homogeneous cobalt complex and pyrolyzed simple cobalt acetate on carbon showed no desired activity.
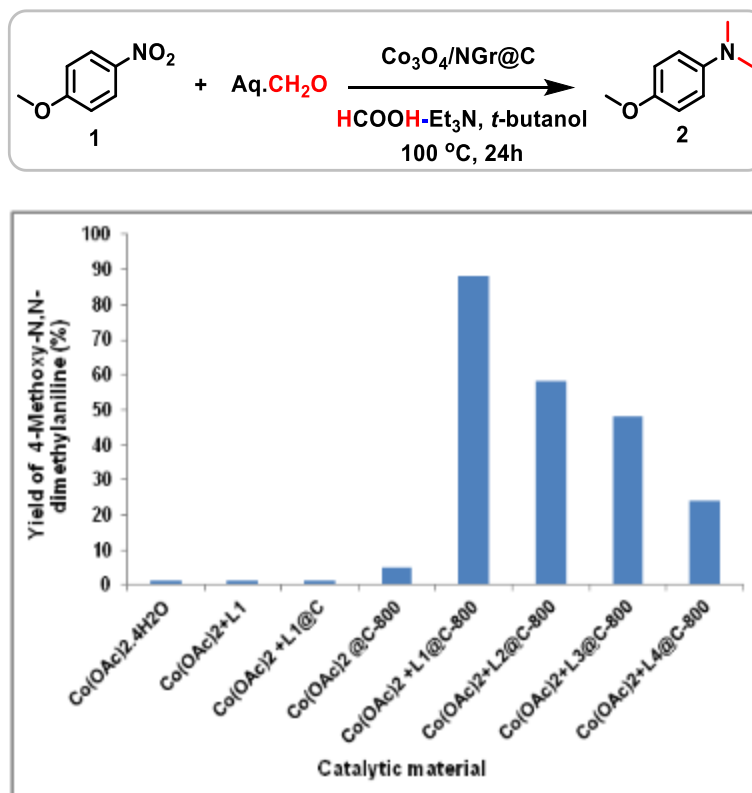
Figure 11. Cobalt-catalyzed reductive N-methylation of 4-methoxynitrobenzene.

The active material (Co₃O₄/NGr@C; Co-L1@C-800) has been characterized by TEM, XPS, EPR and XRD spectral analysis. All these characterization data revealed that the active material contains 2-10 nm Co_3O_4 particles. These cobalt oxide nanoparticles are surrounded by nitrogen-doped graphene surface (Fig. 10). In addition, very small quantity of Co and/or CoO core and a Co_3O_4 shell with a size of 20-80 nm are also present (Fig 10). XPS analysis of the active catalyst showed that Co₃O₄/NGr@C contained pyridine-type nitrogen and pyrrole-type nitrogen atoms as well as quaternary amine species. All these characterization studies confirmed that active material contains mainly nanoscale Co_3O_4 particles, which are surrounded by nitrogen-doped graphene layers. Notably, the formation of nano-sized cobalt oxide particles and the generation of nitrogen-doped graphene layers, which activates Co_3O_4-particles, are important for the activity of catalyst. It is proposed that the interactions of Co-N facilitate the decomposition of formic acid to generate cobalt hydride species in situ, which enhance the reactivity towards reductive amination. Co₃O₄/NGr@C exhibited good to excellent activity and selectivity for the N-methylation of both nitroarenes and amines

using aqueous formaldehyde as methylation source in presence formic acid-Et₃N mixture (scheme 25). As a result, a series of functionalized and structurally diverse N,N/-dimethyl amines have been prepared. N-methylation of nitro-substituted biologically active molecules such as Nimodipin and challenging dinitro compounds was also achieved. In addition to the preparation of aromatic N-methylamines from nitroarenes, this Co-based protocol allowed for the reductive N-methylation of bio-active primary and secondary amines as well as amino acids (scheme 25), which can be exploited for life science applications. As an example, Paroxetine and Duloxetine were N-methylated without affecting other functionalities or the core-structure of the molecules. Notably, phenylalanine and tyrosine amino acid esters have also been dimethylated successfully. In addition, preparation of two drugs such as Amitriptylin and Venlafaxine is showcased.
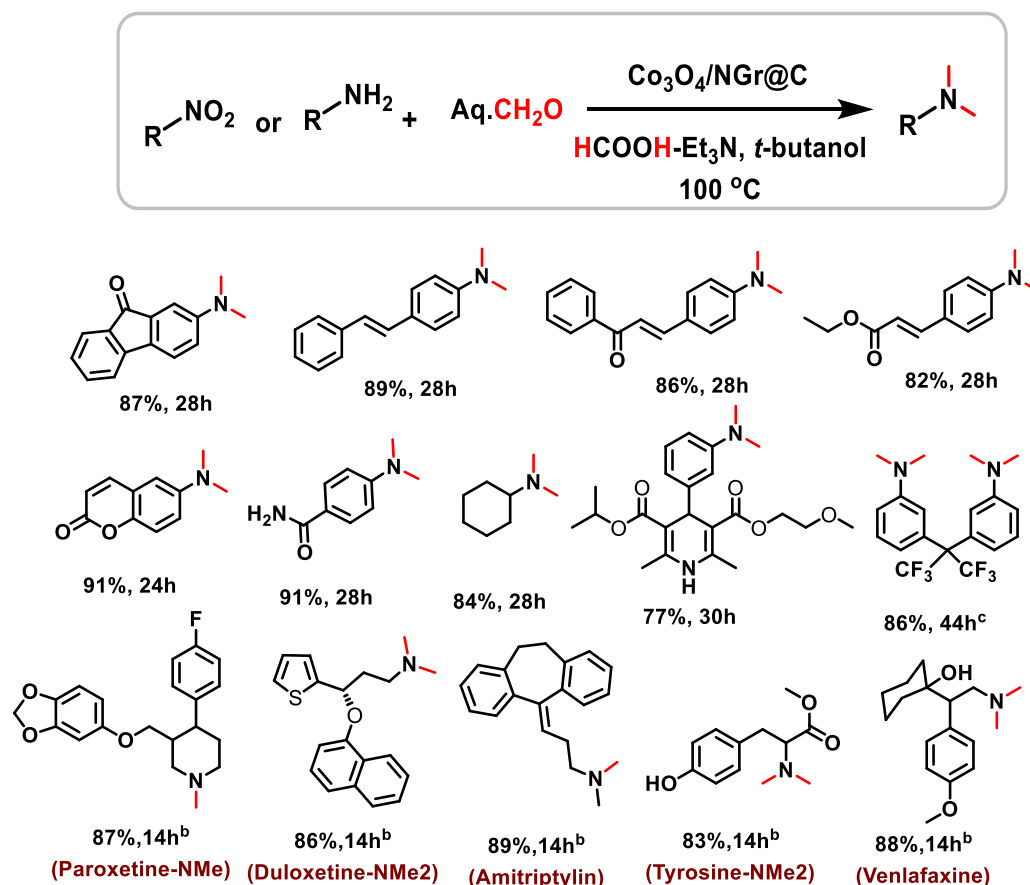
Scheme 25. Co₃O₄/NGr@C catalyzed reductive N-methylation of nitro compounds and amines for the preparation of N-methyl amines.

Reaction conditions: [a] 1 mmol nitroarene, 200 µL aqueous formaldehyde (37 wt% in water) 80 mg Co₃O₄/NGr@C (4 mol% Co), 5.3 mmol formic acid (5.3 equiv. as a HCOOH-Et₃N (5:2) mixture), 3 mL *t*-butanol 100 °C, 24-44 h, isolated yields. [b] 1 mmol amine, 200 µL aqueous formaldehyde (37 wt% in water) 80 mg Co₃O₄/NGr@C (4 mol% Co), 2.2 mmol formic acid (2.2 equiv. as a HCOOH-Et₃N (5:2) mixture), 3 mL *t*-butanol 100 °C, 14 h, isolated yields. [c] same as [a] with 160 mg catalyst, 200 µL aqueous formaldehyde and 10.6 mmol formic acid (10.6 equiv. as a HCOOH-Et₃N (5:2) mixture).

After having demonstrated the preparation of N-methylamines, Co₃O₄/NGr@C was applied for N-alkylation of nitroarenes with aldehydes and selective N-alkylation of amino acid esters and the preparation of existing drug molecules (scheme 26). As a result, phenylalanine and tyrosine amino acid esters are successfully N-alkylated with different aromatic aldehydes. Further on, two existing drug molecules such as Piribedil and Fenpropimorph were prepared. Thus, this benign reductive amination process shows the feasibility for selective late-stage manipulation of amine-based life science molecules.
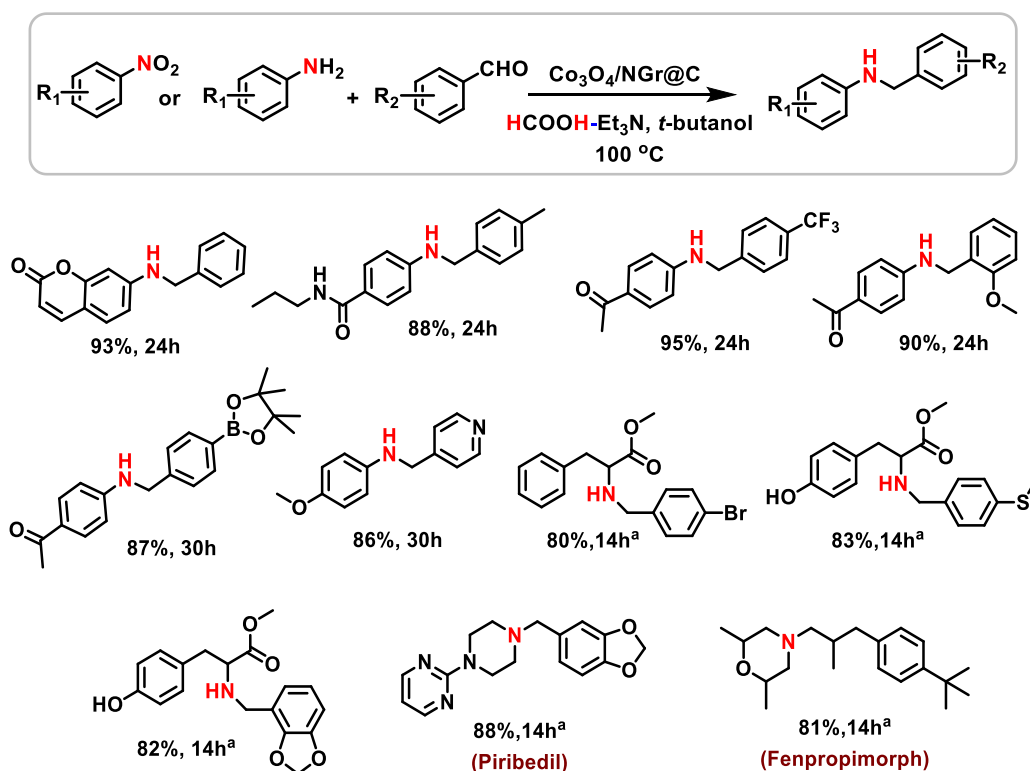
Scheme 26. N-alkylation of amino acids using nanoscale cobalt oxide-catalyst.

Reaction conditions: 1 mmol nitroarene, 1.5 mmol aldehyde, Co$_3$O$_4$/NGr@C (4 mol% Co), 4.3 mmol formic acid (4.3 equiv. as a HCOOH-Et$_3$N (5:2) mixture), 3 mL *t*-butanol 100 °C, 24-44 h, isolated yields. [a] 1 mmol amine, 1.5 mmol aldehyde, Co$_3$O$_4$/NGr@C (4 mol% Co), 1.5 mmol formic acid (1.5 equiv. as a HCOOH-Et$_3$N (5:2) mixture), 3 mL *t*-butanol 100 °C, 14 h, isolated yields.

Finally, practical utility of this protocol has been demonstrated by performing gram scale reactions. Without any improvement of reaction conditions, 1-3 grams of selected nitroarenes have been selectively N-alkylated and -methylated, to produce corresponding secondary and tertiary amines with similar yields to that of 1 mmol scale (scheme 27). These results prove that this protocol can be easily scalable for the preparation of several grams of amines.

18: 85% [a]
(2g Scale)

16: 85% [a]
(1g Scale)

51: 92% [b]
(2g Scale)

42: 88% [b]
(3g Scale)
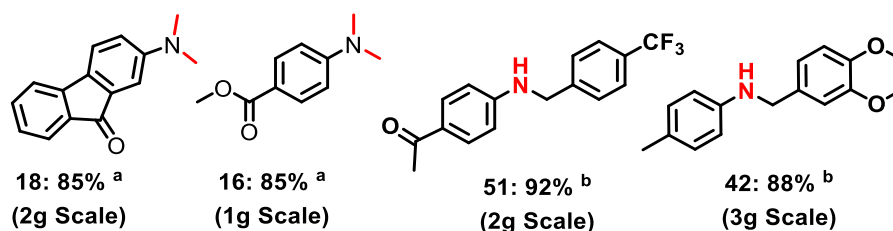
Scheme 27. Demonstrating Co$_3$O$_4$/NGr@C-catalyzed gram scale reactions.

Reaction conditions: [a] 200 μL aqueous formaldehyde (37 wt% in water) 80 mg Co$_2$O$_3$/NGr@C (4 mol% Co), 5.3 mmol formic acid (5.3 equiv. as a HCOOH-Et$_3$N (5:2) mixture) for each 1 mmol nitroarene, 25-30 mL t-butanol 100 °C, 20-30 h, isolated yields. [b] 1.5 mmole aldehyde, 80 mg catalysts and 4.3 mmol formic acid (4.3 equiv. as a HCOOH-Et$_3$N (5:2) mixture) for each 1 mmol nitroarene, 25-30 mL *t*-butanol, 100 °C, 24-30 h, isolated yields.

In general stability, recycling and reusability of a given catalyst are important features for the advancement of sustainable industrial processes. Noticeably, this Co_3O_4/N@C-catalyst is highly stable and conveniently recycled up to 5 times to produced functionalized secondary amine (Fig. 12).
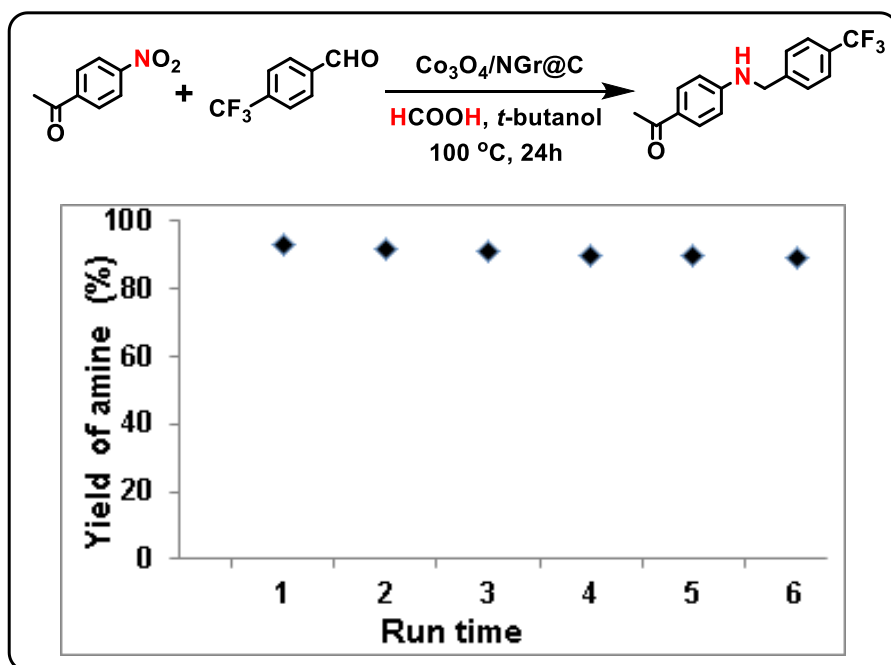
Figure 12. Recycling of Co_3O_4/NGr@C-catalyst for the preparation of functionalized secondary amine.

4. References

1. S. A. Lawrence, S. A. Amines: Synthesis, Properties and Applications (Cambridge University Press, **2004**).

2. A. Ricci, Amino Group Chemistry: From Synthesis to the Life Sciences (Wiley-VCH, **2008**).

3. htts://njardarson. lab. arizona.edu/sites/njardarson. lab. arizona.edu/files/**2018** Top 200 Pharmaceutical Retail sales Poster Low ResFinal V2. Pdf.

4. V. Froidevaux, C. Negrell, S. Caillol, J.-P. Pascault and B. Boutevin, *Chem. Rev.*, **2016**, *116*, 14181-14224.

5. https://www.mordorintelligence.com/industry-reports/amines-market.

6. https://www.grandviewresearch.com/industry-analysis/amines-industry.

7. S. Gomez, J. A. Peters, and T. Maschmeyer, *Adv. Synth. Catal.*, **2002**, *344*, 1037-1057.

8. A. F. Abdel-Magid and S. J. Mehrman, *Org. Process Res. Dev.*, **2006**, *10*, 971-1031.

9. P. T. Rama, S. V. Shyam, P. Jyoti and K. T. Vinod, *Curr. Org. Chem.*, **2008**, *12*, 1093-1115.

10. S. Raoufmoghaddam, *Org. Biomol. Chem.*, **2014**, *12*, 7179-7193.

11. O. I. Afanasyev, E. Kuchuk, D. L. Usanov and D. Chusov, *Chem. Rev.*, **2019**, *119*, 11857-11911.

12. S. D. Roughley and A. M. Jordan, *J. Med. Chem.*, **2011**, *54*, 3451-3479.

13. R. V. Jagadeesh, K. Murugesan, A. S. Alshammari, H. Neumann, M.-M. Pohl, J. Radnik and M. Beller, *Science*, **2017**, *358,* 326-332.

14. G. Hahn, P. Kunnas, N. de Jonge and R. Kempe, *Nat. Catal.*, **2019**, *2*, 71-77.

15. T. Senthamarai, K. Murugesan, J. Schneidewind, N. V. Kalevaru, W. Baumann, H. Neumann, P. C. J. Kamer, M. Beller and R. V. Jagadeesh, *Nat. Commun.,* **2018**, *9*, 4123.

16. K. Murugesan, M. Beller and R. V. Jagadeesh, *Angew. Chem. Int. Ed.*, **2019**, *58*, 5064-5068.

17.   https://erowid.org/archive/rhodium/chemistry/reductive.amination.html

18.   X. Guo, Y. Okamoto, M. R. Schreier, T. R. Ward and O. S. Wenger, *Eur. J. Org. Chem.*, **2020**, 1288–1293.

19.   A. Trowbridge, S. M. Walton and M. J. Gaunt, *Chem. Rev.,* **2020**, *5*, 2613-2692

20.   A. W. Zhipeng, L. Yan-Yu and Z. Ji-Shen, *Curr. Org. Chem.*, **2018**, *15*, 755-761.

21.   F. Shi and X. Cui, *Catalytic Amination for N-Alkylamine Synthesis*; Academic Press: Cambridge, MA, USA, **2018**.

22.   J. G. de Vries, *Science of Synthesis: Catalytic Reduction in Organic Synthesis 2*, Georg Thieme Verlag, Stuttgart, **2018**.

23.   T. C. Nugent, *Chiral Amine Synthesis: Methods, Developments and Applications*, Wiley-VCH, Weinheim, **2010**.

24.   P. G. Andersson and I. J. Munslow, *Modern Reduction Methods*, Wiley-VCH, Weinheim, **2008**.

25.   C. Dume, *Amination of Alcohols by Nucleophlic Substitution or Reductive Amination,* Berichte aus der Chemie, **1999**.

26.   R. J. Ouellette and J. D. Rawn, *Organic Chemistry: Structure, Mechanism, Synthesis, Second Edition*, Academic Press, USA, **2018**.

27.   A. Hassner and I. Namboothiri, *Organic Syntheses Based on Name Reactions (Third Edition)*, **2012**.

28.   B. A. Bunin, *The Combinatorial Index*, Academic Press, San Diego, **1998**.

29.   E. Podyacheva, O. I. Afanasyev, A. A. Tsygankov, M. Makarova and D. Chusov, *Synthesis*, **2019**, *51*, 2667-2677.

30.   W. Li, X. Zhang, *Stereoselective Formation of Amines*, *Topics in Current Chemistry*, Vol. *343*, Springer, Berlin, Heidelberg, **2014**.

31.   K. N. Gusak, Z. V. Ignatovich and E. V. Koroleva, *Russ. Chem. Rev.*, **2015**, *84*, 288-309.

32. E. W. Baxter, A. B. Reitz, *Reductive Aminations of Carbonyl Compounds with Borohydride and Borane Reducing Agents*, Organic Reactions, vol. 59, JohnWiley & Sons, New York, **2002**, pp. 1–714

33. M. Pelckmans, T. Renders, S. Van de Vyver and B. F. Sels, *Green Chem*., **2017**, *19*, 5303–5331.

34. S. Nishimura, *Handbook of Heterogeneous Catalytic Hydrogenation for Organic Synthesis* (John Wiley & Sons Inc., **2001**).

35. P. N. Rylander, *Catalytic Hydrogenation in Organic Synthesis*; Acadamic Press: New York, **1979**.

36. J. H. Schrittwieser, S. Velikogne and W. Kroutil, *Adv. Synth. Catal*., **2015**, *357*, 1655-1685.

37. T. Senthamarai, V. G. Chandrashekhar, M. B. Gawande, N. V. Kalevaru, R. Zboril, P. C. J. Kamer, R. V. Jagadeesh and M. Beller, *Chem Sci.,* **2020**, *11*, 2973-2981.

38. Alcohol amination using homogeneous catalysts: a) Q. Yang, Q. Wanga, and Z. Yu, *Chem. Soc. Rev.,* **2015**, *44*, 2305—2329; b) K.-i. Fujita, K. Yamamoto, R. Yamaguchi, *Org. Lett.,* **2002**, *4*, 2691 –2694; c) C. Gunanathan, D. Milstein, *Angew. Chem., Int. Ed.,* **2008**, *47*, 8661; d) D. Pingen, C. Müller, D. Vogt, *Angew. Chem., Int. Ed.,* **2010**, *49*, 8130; e) M. Utsunomiya, Y. Miyamoto, J. Ipposhi, T. Ohshima, K. Mashima, *Org. Lett.,* **2007**, *9*, 3371–3374; f) C. R. Reddy, E. Jithender, *Tetrahedron.,* **2009**, *50,* 5633 –5635; g) S. Rçsler, M. Ertl, T. Irrgang, R. Kempe, *Angew. Chem. Int. Ed*., **2015**, *54*, 15046 –15050; *Angew. Chem.,* **2015**, *127*, 15260 –15264; h) F. Shi, M. K. Tse, X. Cui, D. Gçrdes, D. Michalik, K. Thurow, Y. Deng, M. Beller, *Angew. Chem. Int. Ed*., **2009**, *48*, 5912 – 5915; *Angew. Chem*., **2009**, *121*, 6026–6029.

39. Alcohol amination heterogeneous catalysts: a) Y. Zhang, X. Qi, X. Cui, F. Shi, Y. Deng, *Tetrahedron Lett.,* **2011**, *52*, 1334; b) F. Shi, M. K. Tse, S. Zhou, M.-M. Pohl, J. Radnik, S. Hebner, K. J-hnisch, A. Breckner, M. Beller, *J. Am. Chem. Soc.,* **2009**, *131*, 1775 –1779; c) S. Nishimoto, B. Ohtani, T. Yoshikawa, T.

Kagiya, *J. Am. Chem. Soc.,* **1983**, *105*, 7180–7182; d) H. Kimura, *Catal. Rev.,* **2011**, *53*, 1; e) C. G. Arellano, K. Yoshida, R. Luque, P. L. Gai, *Green Chem.,* **2010**, *12*, 1281; f) J. Sun, X. Jin, X. F. Zhang, W. Hu, J. Liu, R. Li, *Catal. Commun.*, **2012**, *24*, 30; g) K.-I. Shimizu, N. Imaiida, K. Kon, S. M. A. Hakim Siddiki and A. Satsuma, *ACS Catal.,* **2013**, *3*, 998-1005

40.   a). J. F. Hartwig, *Acc. Chem. Res.*, **2008**, 41, 1534–1544; b). R. J. Lundgren, B. D. Peters, P. G. Alsabeh, M. A. Stradiotto, *Angew. Chem., Int. Ed.,* **2010**, *49*, 4071-4074; c) J. P. Stambuli, R. Kuwano, J. F. Hartwig, *Angew. Chem., Int. Ed.,* **2002**, *41*, 4746-4748; d) A. Köllhofer, T. Pullmann, H. Plenio, *Angew. Chem.Int. Ed.,* **2003**, *42*, 1056-1058; e) A. Ehrentraut, A. Zapf, M. Beller, *Adv. Synth. Catal.,* **2002**, *344*, 209-217; f) D. S. Surry and S. L. Buchwald, *Chem. Sci.*, **2010**, *1*, 13–31.

41.   a) Y. Park, Y. Kim and S. Chang, *Chem. Rev.*, **2017**, 117, 9247−930; b) J. P. Wolfe, S. Wagaw, J.-F. Marcoux, S. L. Buchwald, *Acc. Chem. Res.* **1998**, *31*, 805-818; c) J. Jiao, K. Murakami, K. Itami, *ACS Catal.,* **2016**, *6*, 610-633; d) T. A. Ramirez, B. Zhao, Y. Shi, *Chem. Soc. Rev.,* **2012**, *41*, 931-942.

42.   F. Collet, R. H. Dodda and P. Dauban, *Chem. Commun.*, **2009**, 5061-5074; b) P. Subramanian, G. C. Rudolf, K. P. Kaliappan, *Chem. - Asian J.,* **2016**, *11*, 168-192; c) H. Wang, Y. Wang, C. Peng, J. Zhang, Q. Zhu, *J. Am.Chem. Soc.* **2010**, *132*, 13217-13219; d) K. Takamatsu, K. Hirano, T. Satoh, M. Miura, *J. Org. Chem.,* **2015**, *80*, 3242-3249; f) L.-B. Zhang, S.-K. Zhang, D. Wei, X. Zhu, X.-Q. Hao, J.-H. Su, J.-L. Niu, M.-P Song, *Org. Lett.,* **2016**, *18*, 1318-1321

43.   D. Wang and D. Astruc, *Chem. Rev.* **2015**, *115*, 6621−6686.

44.   Q. Zhang, S.-S. Li, M.-M. Zhu, Y.-M. Liu, H.-Y. He, Y. Cao., Green Chem., **2018**,*18*, 2507–2513.

45.   E. E. Drinkel, R. R. Campedelli, A. M. Manfredi, H. D. Fiedler, F. Nome, *J. Org.Chem*., **2014,** *79*, 2574–2579.

46.   B. C. Ranubri, A. Sakkar, K. G. Sankar and K. Ghosh, *J. Indian chem. soc.,* **1998**, *75*, 690-694

47. P. Zhou, Z. Zhang, L. Jiang, C. Yu, K. Lv, J. Sun, S. Wang, *Applied Catalysis B: Environmental*., **2017**, *210*, 522–532.

48. L. Jiang, P. Zhou, Z. Zhang, S. Jin, and Q. Chi, *Ind. Eng. Chem. Res*., **2017**, *56*, 12556-12565.

49. P. Zhou and Z. Zhang, *ChemSusChem*., **2017**, *10*, 1892 – 1897.

50. T. Senthamarai, K. Murugesan, K. Natte, N. V. Kalevaru, H. Neumann, P. C. J. Kamer, and R. V. Jagadeesh, *ChemCatChem,* **2018***, 10,* 1235-1240,

51. G. Mignonac, *Compt. Rend.*, **1921**, 223.

52. C. F. Winans, *J. Am. Chem. Soc.*, **1939**, *61*, 3566-3567.

53. L. Haskelberg, *J. Am. Chem. Soc.*, **1948**, *70*, 2811-2812.

54. W. Chen, Y. Sun, J. Du, Z. Si, X. Tang, X. Zeng, L. Lin, S. Liu and T. Lei, *J. Chem. Technol. Biotechnol.,* **2018**, *93*, 3028-3034.

55. M. Manzoli, E. C. Gaudino, G. Cravotto, S. Tabasso, R. B. N. Baig, E. Colacino and R. S. Varma, *ACS Sus. Chem. Eng.,* **2019**, 7, 5963-5974.

56. Y. Zhang, H. Yang, Q. Chi and Z. Zhang, *ChemSusChem*, **2019**, *12*, 1246-1255.

57. H. Yuan, J.-P. Li, F. Su, Z. Yan, B. T. Kusema, S. Streiff, Y. Huang, M. Pera-Titus and F. Shi, *ACS Omega.*, **2019**, *4*, 2510-2516.

58. H. Yuan, B. T. Kusema, Z. Yan, S. Streiff and F. Shi, *RSC Adv.,* **2019**, *9*, 38877-38881.

59. C. Bäumler, C. Bauer, R. Kempe, **2020**, 10.1002/cssc.202000856.

60. T. Gross, A. M. Seayad, M. Ahmad and M. Beller, *Org. Lett.,* **2002**, *4*, 2055-2058.

61. A. Behr, A. Wintzer, C. Lübke and M. Müller, *J. Mol. Cat. A: Chem*., **2015**, *405,* 74-82.

62. T. H. Riermeier, U. Dingerdissen, Börner, A. V. Tararov; F. Kadyrov. Weniger, US 6,884,887 B1, **2005**.

63. J. Gallardo-Donaire, M. Ernst, O. Trapp and T. Schaub, *Adv. Synth. Catal.,* **2016**, *358*, 358-363.

64. K. Murugesan, Z. Wei, V. G. Chandrashekhar, H. Neumann, A. Spannenberg, H. Jiao, M. Beller and R. V. Jagadeesh, *Nat. Commun.,* **2019**, *10*, 5443.

65. K. Murugesan, Z. Wei, V. G. Chandrashekhar, H. Neumann, A. Spannenberg, H. Jiao, M. Beller and R. V. Jagadeesh, Chem. Sci., **2020**, *11*, 4332–4339.

66. J. Gallardo-Donaire, M. Hermsen, J. Wysocki, M. Ernst, F. Rominger, O. Trapp, A. S. K. Hashmi, A. Schäfer, P. Comba and T. Schaub, *J. Am. Chem. Soc*., **2018**, *140*, 355-361.

67. X. Tan, S. Gao, W. Zeng, S. Xin, Q. Yin and X. Zhang, *J. Am. Chem. Soc.*, **2018**, *140*, 2024-2027.

68. T. Stemmler, A.-E. Surkus, M.-M. Pohl, K. Junge and M. Beller, *ChemSusChem*., **2014**, *7*, 3012-3016.

69. R. V. Jagadeesh, T. Stemmler, A.-E. Surkus, H. Junge, K. Junge and M. Beller, *Nature Protoc.,* **2015**, *10*, 548.

70. T. Stemmler, F. A. Westerhaus, A.-E. Surkus, M.-M. Pohl, K. Junge and M. Beller, *Green Chem.,* **2014**, *16*, 4535-4540.

71. R. V. Jagadeesh, T. Stemmler, A.-E. Surkus, M. Bauer, M.-M. Pohl, J. Radnik, K. Junge, H. Junge, A. Brückner and M. Beller, Nature Protoc., **2015**, *10*, 916.

72. L. Jiang, P. Zhou, Z. Zhang, Q. Chi and S. Jin, *New J Chem*., **2017**, *41,* 11991-11997.

73. F. Mao, D. Sui, Z. Qi, H. Fan, R. Chen and J. Huang, *RSC Adv*., **2016**, *6*, 94068-94073.

74. Z. Yuan, B. Liu, P. Zhou, Z. Zhang and Q. *Chi, J. Catal*., **2019**, *370*, 347-356.

75. J. E. Cobb et al. *In Encyclopedia of Reagents for Organic Synthesis* (eds. Paquette, L. A. et al.) (John Wiley & Sons, New York, **2004**).

76. S. D. Burke & R. L. Danheiser, *Triphenylphosphine, Handbook of Reagents for Organic synthesis, Oxidizing and Reducing Agents* (Wiley, Hoboken, NJ, **1999**).

77. L. M. Pignolet, *Homogeneous Catalysis with Metal Phosphine Complexes* (Springer US, **2013**).

78. *Wilkinson's catalyst, Comprehensive Organic Name Reactions and Reagents* (**2010**).

79. C. Müller & D. Vogt, Dalton. Trans., **2007**, 5505–5523.

80. J. S. Plummer, M. Shun-Ichi and Z. Changiia, e-EROS Encyclopedia of organic synthesis (John wiley, **2010**).

81. R. H. Crabtree, *Chem. Rev*., **2017**, *117*, 9228–9246.

82. G. Guillena, D. J. Ramon, & M. Yus, *Chem. Rev*., **2010**, *110*, 1611–1641.

83. J. S. M. Sameca, J.-E. Bäckvall, P. G. Andersson, & P. Brandt, *Chem. Soc. Rev.*, **2006**, *35*, 237–248.

84. D. Pingen, M. Lutz, & D. Vogt, *Organometallics*., **2014**, *33*, 1623–1629.

85. D. Evans, J. A. Osborn, F. H. Jardine & G. Wilkinson, *Nature*., **1965**, *208*, 1203–1204.

86. G.-Z. Wang, & J. E. Bäckvall, *Chem. Commun.,* **1992**, 980–982.

87. A. S. Zola, R. U. Ribeiro, J. M. C. Bueno, D. Zanchet, P. A. Arroyo, *J. Exp. Nanoscience.,* **2014**, *9*, 398-405.

5. Contribution to the Publications
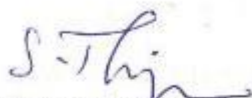
In this chapter, section 5.1 to 5.3, selected publications of this PhD work are presented.

5.1 Simple ruthenium-catalyzed reductive amination enables the synthesis of a broad range of primary amines

Senthamarai, Thirusangumurugan; Murugesan, Kathiravan; Schneidewind, Jocob Kalevaru, Narayana V.; Baumann, Wolfgang; Neumann, Helfried; Kamer, Paul C. J.; Beller, Matthias*; Jagadeesh, Rajenahally V*

Nature Communications, **2018**, *9*, 4123.

In this paper, I planned and executed reaction design and optimization of reaction conditions as well as preparation of catalysts. Performed all catalytic experiments including the isolation and purification of products. In addition, involved in and wrote the manuscript. My contribution as the first author of this paper is approximately 85%.

Signature of the student
(Thirusangumurugan Senthamarai)
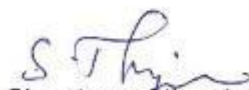
Signature of the supervisor
(Prof. Dr. Matthias Beller)

5.2 Ultra-small cobalt nanoparticles from molecularly-defined Co-salen complexes for catalytic synthesis of amines

Senthamarai, Thirusangumurugan; Chandrashekhar, Vishwas G.; Gawande, Manoj B.; Narayana Kalevaru, V.; Zbořil, Radek; Kamer, Paul C. J.; Rajenahally V. Jagadeesh* and Matthias Beller*

Chemical Science, **2020**, *11*, 2973–2981.

In this work, I designed the plan and prepared catalysts. Performed all catalytic experiments and isolated the reported products. Involved in paper writing. My contribution as the first author of this paper is approximately 85%.

Signature of the student
(Thirusangumurugan Senthamarai)

Signature of the supervisor
(Prof. Dr. Matthias Beller)

5.3 Expedient Synthesis of N-Methyl- and N-alkylamines by reductive amination using reusable cobalt oxide nanoparticles

Senthamarai, Thirusangumurugan; Murugesan, Kathiravan; Natte, kishore; Kalevaru, Narayana V.; Neumann, Helfried; Kamer, Paul C.J.; Jagadeesh, Rajenahally V*.

ChemCatChem, **2018**, *10*, 1235-1240. (with front cover picture)

In this paper, I prepared different catalytic materials and tested for the reaction along with optimization of the reaction, substrate design, complete characterization of the product using analytical technique and wrote the manuscript. My contribution as the first author of this paper is approximately 85%.

Signature of the student
(Thirusangumurugan Senthamarai)

Signature of the supervisor
(Prof. Dr. Matthias Beller)
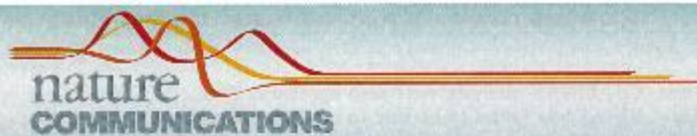
ARTICLE

Simple ruthenium-catalyzed reductive amination enables the synthesis of a broad range of primary amines

Thirusangumurugan Senthamarai[1], Kathiravan Murugesan[1], Jacob Schneidewind [1], Narayana V. Kalevaru[1], Wolfgang Baumann[1], Helfried Neumann[1], Paul C.J. Kamer[1], Matthias Beller [1] & Rajenahally V. Jagadeesh [1]

The production of primary benzylic and aliphatic amines, which represent essential feed-stocks and key intermediates for valuable chemicals, life science molecules and materials, is of central importance. Here, we report the synthesis of this class of amines starting from carbonyl compounds and ammonia by Ru-catalyzed reductive amination using H_2. Key to success for this synthesis is the use of a simple $RuCl_2(PPh_3)_3$ catalyst that empowers the synthesis of >90 various linear and branched benzylic, heterocyclic, and aliphatic amines under industrially viable and scalable conditions. Applying this catalyst, —NH_2 moiety has been introduced in functionalized and structurally diverse compounds, steroid derivatives and pharmaceuticals. Noteworthy, the synthetic utility of this Ru-catalyzed amination protocol has been demonstrated by upscaling the reactions up to 10 gram-scale syntheses. Further-more, in situ NMR studies were performed for the identification of active catalytic species. Based on these studies a mechanism for Ru-catalyzed reductive amination is proposed.

[1] Leibniz-Institut für Katalyse e. V. an der Universität Rostock, Albert-Einstein-Str. 29a, 18059 Rostock, Germany. Correspondence and requests for materials should be addressed to M.B. (email: Matthias.Beller@catalysis.de) or to R.V.J. (email: Jagadeesh.Rajenahally@catalysis.de)

ARTICLE

The development of efficient catalytic reactions for the selective and sustainable synthesis of amines from readily available and inexpensive starting materials by utilizing abundant and green reagents continues to be an important goal of chemical research[1-6]. In particular, the development of simple and easily accessible catalysts for reductive aminations is highly important because these reactions allow for the cost-efficient production of different kinds of amines[7-30]. Among reductive aminations, the reaction of carbonyl compounds with ammonia in presence of molecular hydrogen to produce primary amines is of central importance and continues to be a major challenge[17-30]. In general, amines are essential chemicals used widely in many research areas and industrial productions related to chemistry, medicine, biology, and material science[1-6]. The majority of existing pharmaceuticals, agrochemicals, biomolecules, and natural products contain amine functionalities, which constitute key structural motifs and play vital roles in their functions[1-6]. Among different kinds of amines, primary benzylic and aliphatic amines constitute valuable fine and bulk chemicals, that serve as versatile feedstocks and key intermediates for advanced chemicals, life science molecules and polymers[1-34]. Regarding their synthesis, catalytic reductive amination of carbonyl compounds (aldehydes and ketones) with ammonia in presence of molecular hydrogen represents a waste-free process to access various linear and branched benzylic and aliphatic amines[17-27]. In addition, catalytic amination of alcohols with ammonia also constitutes a sustainable methodology to produce primary amines[35-38]. Apart from transition metal-catalyzed aminations, the Leuckart-Wallach reaction[39-41] and reduction of oxime ethers with borane[42-44] have also been applied. Noteworthy, selective introduction of primary amine moieties in functionalized compounds by utilizing ammonia constitutes a benign and economic methodology[17-27]. Ammonia, which is produced in >175 million tons per year scale, is considered to be an abundant and green chemical used enormously for the large scale production of urea and other fertilizers as well as various basic chemicals[45-50]. Although ammonia is used extensively for the production of simple molecules, its reactions still encounter common problems such as the requirement of high temperatures or pressures and low selectivity towards the formation of a single desired product[45-50]. Hence, the development of more active and selective catalysts for an effective utilization of ammonia, especially for its insertion in advanced and complex molecules, is highly demanded and challenging.

Reductive amination for the preparation of primary amines, especially in industry, is mainly carried out using heterogeneous catalysts[17-23]. Compared to heterogeneous catalysts, homogeneous catalysis for amination of structurally diverse molecules is less studied and remains challenging[24-27]. Transition metal-catalyzed reactions involving ammonia are often difficult to perform or do not even occur. This problem is mainly due to the deactivation of homogeneous catalysts by the formation of stable Werner-type ammine complexes as well as due to the harsh conditions required for the activation of ammonia. In addition, common problems in reductive aminations, such as over alkylation and reduction to the corresponding alcohols, also affect catalyst viability. In order to utilize ammonia successfully and to overcome these problems, there is a need to develop highly efficient homogeneous catalysts, which is the prime task of this investigation. To date, a few catalysts based on Rh-[24,25], Ir-[25] and Ru-[26,27] complexes were reported for the preparation of primary amines from carbonyl compounds and ammonia using hydrogen. Initially, Beller and co-workers[24] have reported a [Rh(COD)Cl]2-TPPTS catalyst system for the synthesis of simple primary amines from aldehydes and aqueous ammonia using NH4OAc as additive. Following this work, Rh[(dppb)(COD)]BF4 and [Rh(COD)

Cl]2-BINAS catalysts were also applied[25]. Next, [Ir(COD)Cl]2-BINAS was found to be able to catalyze the amination of a few simple ketones with ammonia[25]. Regarding Ru-catalysts, RuHCl(CO)(PPh3)3-xantphos/-dppe in presence of Al(OTf)3 is known to catalyze the preparation of simple primary amines from ketones[26]. Recently, RuHCl(CO)(PPh3)3-(S,S)-f-binaphane[27] in presence of NaPF6 or NH4I using NH3, as well as Ru(OAc)2-C3-TunePhos[30] using NH4OAc have been used for enantioselective reductive amination of ketones to obtain chiral primary amines. These homogeneous catalysts, however, have only been applied in (enantioselective) reductive aminations of simple substrates and have not been used for the preparation of functionalized amines. Despite these advances, the design of simpler yet efficient homogeneous catalysts for the preparation of a broad range of structurally diverse primary amines is highly desired and continues to be an important task from both a research and an industry perspective.

In a lot of cases, homogeneous catalysts applied for challenging reactions and advanced organic synthesis operations are based on sophisticated or synthetically demanding metal complexes and ligands. However, a fundamental and economically important principle is that to achieve a convenient and practical chemical synthesis, the catalyst must be simple, effective and commercially available and/or easily accessible. In this regard, triphenylphosphine (PPh3)-based metal complexes are found to be expedient and advantageous for catalysis applications, since PPh3 is a stable and comparatively cheap ligand[51-55]. Among PPh3-based Ru-complexes, RuCl2(PPh3)3 is considered to be the simplest and least expensive one and is also commercially available. Interestingly, RuCl2(PPh3)3 is known to catalyze a number of organic reactions[56-62]. Herein we demonstrate that RuCl2(PPh3)3 is an efficient and highly selective homogeneous precatalyst for reductive amination, allowing the preparation of a variety of primary amines of industrial importance. By applying this Ru-precatalyst and starting from inexpensive and readily available carbonyl compounds (aldehydes, ketones), ammonia and molecular hydrogen, we undertook the synthesis of functionalized and structurally diverse linear and branched benzylic, heterocyclic, and aliphatic amines including drugs and steroid derivatives. Another objective is to demonstrate up-scaling of the homogeneous amination protocol to gram-scale syntheses. Furthermore, efforts were also made to identify catalytically active species and reaction intermediates by performing kinetic and in situ NMR investigations. Based on these studies, a plausible reaction mechanism is proposed.

Results

Selection of catalyst and reaction conditions. Reductive amination of benzaldehyde (1) to benzylamine (2) with ammonia using molecular hydrogen was chosen as a benchmark reaction. At first, in presence of PPh3 different metal precursors were tested. As shown in Table 1, the in situ generated Fe-, Co-, Mn-, Ni- and Cu-PPh3 complexes were not active for the formation of benzylamine (Table 1 entries 1-5). However, in situ generated Ru(II)-PPh3 complexes showed some activity and produced benzylamine in up to 40% yield (Table 1, entries 6 and 7). After observing this reactivity, we next tested in situ generated Ru-complexes with differently substituted PPh3-type ligands as well as simple nitrogen ligands (L1-L10). Among these, Ru-catalysts containing either PPh3 or derivatives with electron donating groups in para position showed the highest activity (Table 2; entries 1,4,5). However, none of the tested nitrogen ligands (L7-L10) produced the desired product (Table 2, entries 7-10). Unfortunately, using in situ generated Ru-complexes the yield of benzylamine did not improve beyond 53% (Table 2).

Table 1 Reductive amination of benzaldehyde: activity of different catalysts

Catalyst (2 mol%)
40 bar H₂, t-amyl alcohol, 130 °C
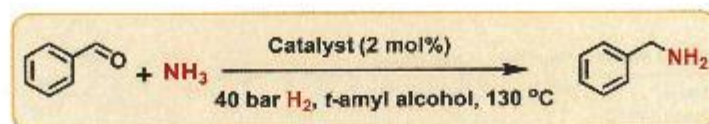
Entry	Metal precursor	L	Yield of benzylamine [%]
1	FeCl₂	PPh₃	nd
2	CoCl₂.6H₂O	PPh₃	nd
3	MnCl₂	PPh₃	nd
4	NiCl₂.6H₂O	PPh₃	nd
5	CuCl₂	PPh₃	nd
6	[RuCl₂(p-cymene)]₂	PPh₃	40
7	[RuCl₂(benzene)]₂	PPh₃	35
8	[RuCl₂(p-cymene)]₂	-	nd
9	-	PPh₃	nd

Reaction conditions: 0.5 mmol benzaldehyde, 2 mol% metal precursor, 6 mol% PPh₃, 5-7 bar NH₃, 40 bar H₂, 1.5 mL t-amyl alcohol, 130 °C, 24 h, GC yields using n-hexadecane as standard L Ligand, nd not detected

Next we turned our interest to molecularly defined Ru-complexes. To our delight, the commercially available complexes RuCl₂(PPh₃)₃ and RuCl₂(PPh₃)₄ showed excellent activity and selectivity for the formation of benzylamine in 92–95% yields (Table 2, entries 11–12). Further, Ru(tris(4-methoxyphenyl)phosphine)₃Cl₂ and Ru(tris(4-chlorophenyl)phosphine)₃Cl₂ were also prepared and tested for their reactivity (Table 2; entries 13 and 14). The former displays similar activity compared to RuCl₂(PPh₃)₃ (Table 2, entry 13), while the latter was less active (Table 2, entry 14), reflecting the same ligand trend observed in case of in situ generated complexes. In presence of highly active catalysts, we observed 4–7 % of benzyl alcohol (3) as the side-product (Table 2, entries 11–13). In case of less-active and or non-active catalysts, undesired side products such as N-benzylidenebenzylamine (4) and 2,4,5-triphenyl-2-imidazoline (5) were formed (Table 2, entries 1–10). Dibenzylamine (6) was not observed under any of these conditions.

Kinetic investigations. After having identified RuCl₂(PPh₃)₃ as one of the most active precatalysts, we performed kinetic investigations on this system and examined the effect of (a) reaction time, (b) catalyst concentration, (c) hydrogen pressure, (d) reaction temperature, (e) ammonia pressure, and (f) substrate (benzaldehyde) concentration on activity and product distribution (Fig. 1). For reaction time, in Fig. 1a it can be seen that after 5 h, secondary imine 4 is predominantly present (ca. 60%), with only 30% of target product 2. Over the course of the reaction, 4, which appears to be an intermediate, is consumed to yield up to 95% 2 after 24 h (for the mechanism of this transformation vide

infra). During the reaction, an increasing amount (up to 4%) of benzyl alcohol is also formed. The cyclic side product 5 can be observed at various reaction times and its amount appears to decrease. This trend, however, is presumably an artifact of the kinetic measurements (see SI). From Fig. 1a it can be concluded that 24 h is an ideal reaction time to obtain maximum yield of 2. Fig. 1b shows how catalyst loading affects the product distribution. At lower (<2 mol%) loadings, increased amounts of intermediate 4 and side product 5 are obtained, while beyond 2 mol% almost no 4 or 5 along with maximum yield of 2 and some benzyl alcohol 3 were observed. A catalyst loading of 2 mol% is therefore necessary to achieve excellent yield of benzylamine. Similar trends in the product distribution are observed for varied H₂ pressure (Fig. 1c) and reaction temperature (Fig. 1d). Thus 40 bar H₂ pressure and 130 °C reaction temperature are found to be optimum to suppress the formation of intermediates/side products (4/5) and to yield maximum amounts of the target product benzylamine. When investigating the effect of ammonia pressure, we found that at less than 5 bar side product 6 (dibenzylamine) is formed in up to 20% (Fig. 1e) yield with a concomitant decrease in the yield of 2. Hence, a minimum NH₃ pressure of 5 bar is required to selectively form the desired product 2 (for mechanistic details vide infra). Further, on increasing the concentration of benzaldehyde (>0.5 mmol) the amount of 5 gradually increases, leading to formation of 5 in up to 80% yield (for 2 mmol benzaldehyde) (Fig. 1e).

Synthesis of linear primary amines from aldehydes. Under optimized reaction conditions, we explored the scope of RuCl₂(PPh₃)₃-catalyzed reductive amination for the synthesis of

Table 2 Reductive amination of benzaldehyde using ruthenium catalysts
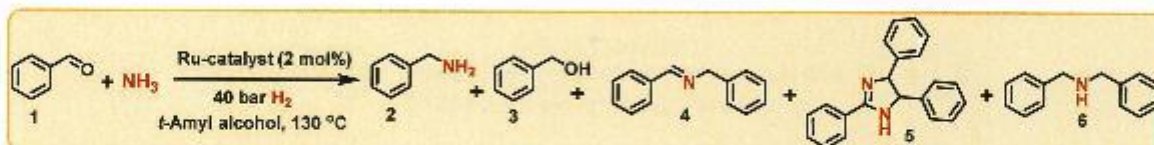
Entry	Ru-precursor/ Defined Ru-catalyst	L	Yield (%)				
			2	3	4	5	6
1[a]	[RuCl₂(p-cymene)]₂	L1	40	2	40	17	-
2[a]	[RuCl₂(p-cymene)]₂	L2	5	-	60	33	-
3[a]	[RuCl₂(p-cymene)]₂	L3	2	-	25	70	-
4[a]	[RuCl₂(p-cymene)]₂	L4	50	5	20	24	-
5[a]	[RuCl₂(p-cymene)]₂	L5	53	4	16	25	-
6[a]	[RuCl₂(p-cymene)]₂	L6	10	2	42	44	-
7[a]	[RuCl₂(p-cymene)]₂	L7	-	-	20	76	-
8[a]	[RuCl₂(p-cymene)]₂	L8	-	-	18	79	-
9[a]	[RuCl₂(p-cymene)]₂	L9	-	-	25	74	-
10[a]	[RuCl₂(p-cymene)]₂	L10	-	-	30	68	-
11[b]	RuCl₂(PPh₃)₃	-	95	4	-	-	-
12[b]	RuCl₂(PPh₃)₄	-	92	7	-	-	-
13[b]	RuCl₂(tris(4-methoxyphenyl)phosphine)₃	-	95	4	-	-	-
14[b]	RuCl₂(tris(4-chlorophenyl)phosphine)₃	-	50	-	49	-	-
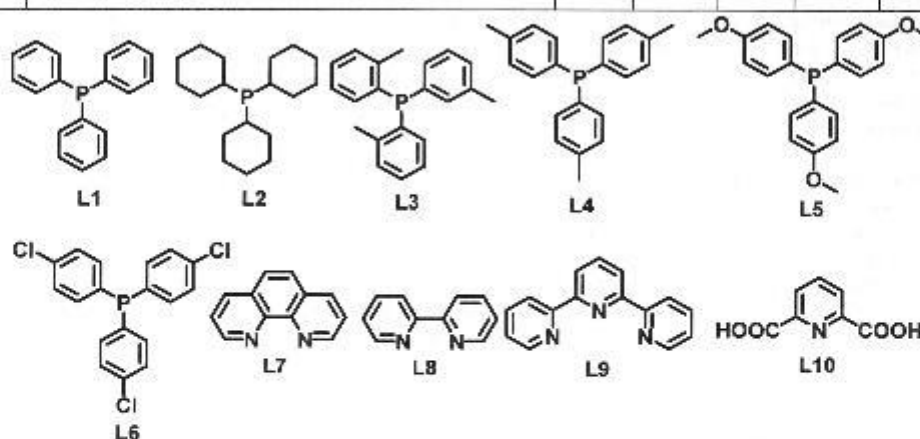
Reaction conditions: [a]0.5 mmol benzaldehyde, 1 mol% [RuCl₂(p-cymene)]₂ (2 mol% with respect to the monomer), 6 mol% ligand, 5-7 bar NH₃, 40 bar H₂ 1.5 mL t-amyl alcohol, 130 °C, 24 h, GC yields using n-hexadecane as standard. [b]Same as 'a' but using 2 mol% defined catalyst.

ARTICLE
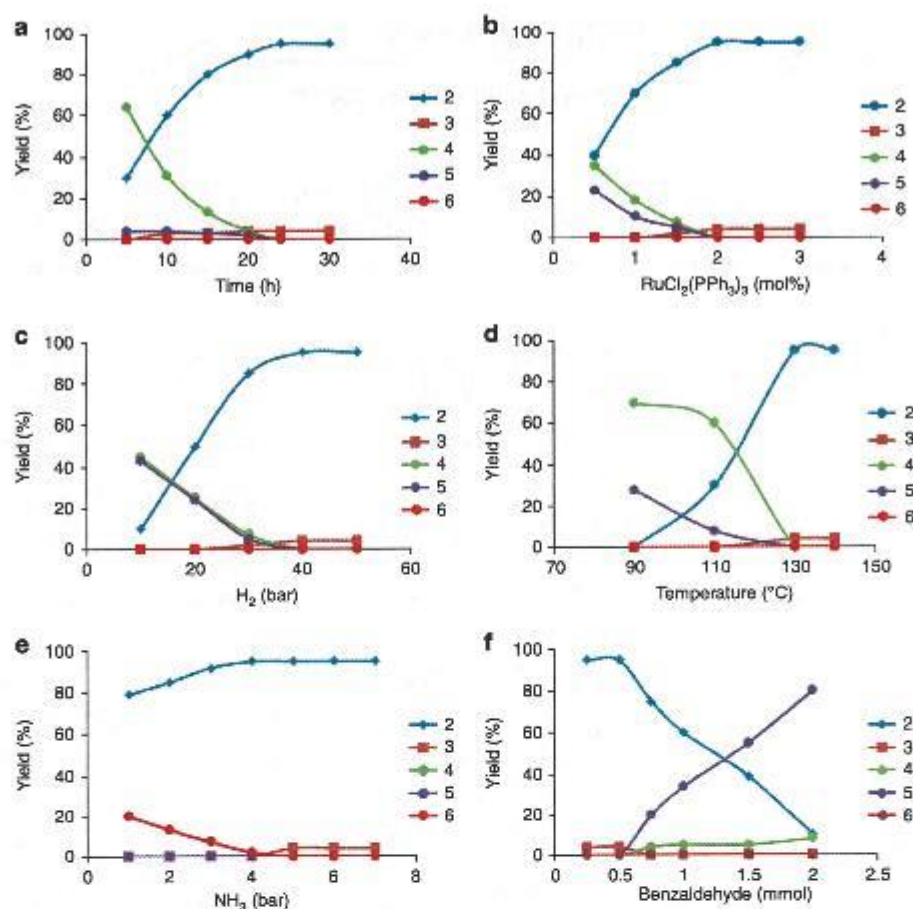
Fig. 1 Kinetic investigations on the Ru-catalyzed reductive amination of benzaldehyde. **a** Yield vs reaction time, **b** yield vs concentration of RuCl₂(PPh₃)₃, **c** yield vs pressure of H₂, **d** yield vs temperature, **e** yield vs pressure of NH₃, **f** yield vs concentration of benzaldehyde. 2 = Yield of benzylamine; 3 = yield of benzyl alcohol; 4 = yield of N-benzylidenebenzylamine; 5 = yield of 2,4,5-triphenyl-4,5-dihydro-1H-imidazole, 6 = yield of dibenzylamine. Reaction conditions: For Fig. 1a: 0.5 mmol benzaldehyde, 2 mol% RuCl₂(PPh₃)₃, 5–7 bar NH₃, 40 bar H₂, 1.5 mL t-amyl alcohol, 130 °C, 5–30 h; for Fig. 1b: 0.5 mmol benzaldehyde, 0.5–3 mol% RuCl₂(PPh₃)₃, 5–7 bar NH₃, 40 bar H₂, 1.5 mL t-amyl alcohol, 130 °C, 24 h; for Fig. 1c: 0.5 mmol benzaldehyde, 2 mol% RuCl₂(PPh₃)₃, 5–7 bar NH₃, 10–50 bar H₂, 1.5 mL t-amyl alcohol, 130 °C, 24 h; for Fig. 1d: 0.5 mmol benzaldehyde, 2 mol% RuCl₂(PPh₃)₃, 5–7 bar NH₃, 40 bar H₂, 1.5 mL t-amyl alcohol, 90–140 °C, 24 h. for Fig. 1e: 0.5 mmol benzaldehyde, 2 mol% RuCl₂(PPh₃)₃, 1–7 bar NH₃, 40 bar H₂, 1.5 mL t-amyl alcohol, 130 °C, 24 h; for Fig. 1f: 0.25–2 mmol benzaldehyde, 2 mol% RuCl₂(PPh₃)₃, 5–7 bar NH₃, 40 bar H₂, 1.5 mL t-amyl alcohol, 130 °C, 24 h. Yields were determined by GC using n-hexadecane as standard

various primary amines. As shown in Fig. 2, industrially relevant and structurally diverse benzylic, heterocyclic, and aliphatic aldehydes underwent reductive amination and offered linear primary amines in good to excellent yields. Simple as well as sterically hindered benzaldehydes were selectively converted to their corresponding benzyl amines in up to 95% yield (Fig. 2; products 2 and 7–13). In order to apply this amination methodology for organic synthesis and drug discovery, achieving a high degree of chemoselectivity is important. In this regard, we conducted the reaction of sensitive halogenated and functionalized benzaldehydes. Delightfully, halogen-substituted benzaldehydes, including more sensitive iodo-substituted compounds, selectively underwent reductive amination without any significant dehalogenation (Fig. 2; products 14–21). Gratifyingly, various functional groups such as ethers, thio-ethers, carboxylic acid-esters and boronic acid-esters, amides and challenging C–C triple bonds were all well-tolerated without being reduced (Fig. 2; products 22–40). In all these cases, the aldehyde group was selectively aminated to produce functionalized amines in up to 88% yield.

Heterocycles are regarded as highly valuable compounds and these motifs serve as integral parts of a large number of life

science molecules and natural products. Thus, the preparation of heterocyclic primary amines is routinely needed en route to the production of pharmaceutically and agriculturally valuable products. Consequently, a series of different heterocyclic amines were synthesized (Fig. 2; products 41–49). The primary amines of pyridine, methylenedioxybenzene and benzodioxane, furan and thiophene were obtained in 87–92% yields.

Success in the amination of aromatic and heterocyclic aldehydes prompted us to validate this catalyst also for aliphatic substrates. Commonly, amination of aliphatic aldehydes is more challenging and most reported catalysts exhibit lower reactivity towards these substrates. In addition, the reaction of aliphatic aldehydes is often troubled by the formation of unwanted aldol reaction products. In spite of these problems, the RuCl₂(PPh₃)₃ precatalyst is found to be highly active and selective for the preparation of aliphatic primary linear amines too (Fig. 2). Accordingly, various primary araliphatic and aliphatic linear amines including allylic ones (products 56 and 57) were obtained in up to 92% yield. Importantly, phenylethylamines (products 50 and 51), which function as monoaminergic neuromodulators and neurotransmitters in the human CNS, have been prepared in up to 90% yield.

ARTICLE
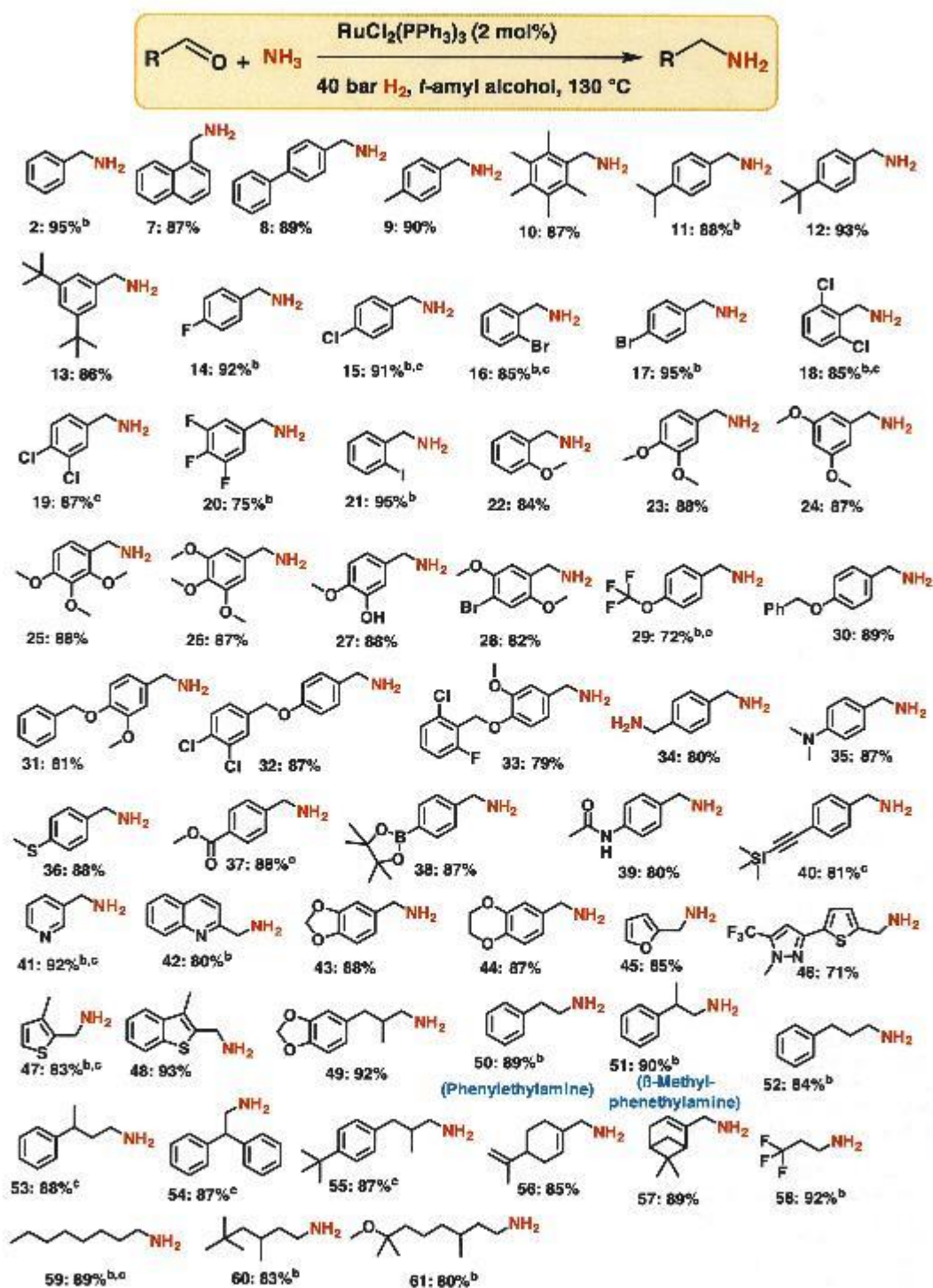
Fig. 2 Ru-catalyzed synthesis of linear primary benzylic, heterocyclic, and aliphatic amines. [a]Reaction conditions: [a]0.5 mmol aldehyde, 2 mol% RuCl₂(PPh₃)₃, 5-7 bar NH₃, 40 bar H₂ 1.5 mL t-amyl alcohol, 130 °C, 24 h, isolated yields. [b]GC yields using n-hexadecane as standard. [c]same as 'a' for 30 h. Isolated as free amines and converted to hydrochloride salts. Corresponding hydrochloride salts were subjected to NMR analysis
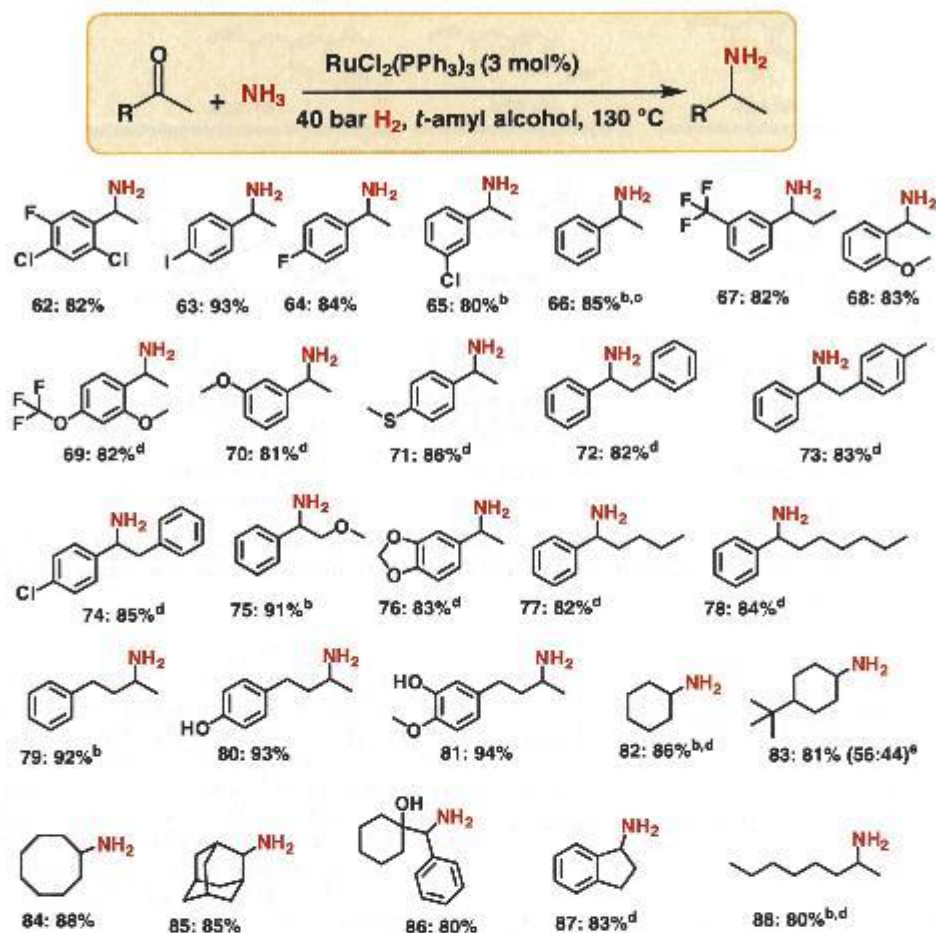
Fig. 3 RuCl$_2$(PPh$_3$)$_3$-catalyzed synthesis of branched primary amines from ketones. [a]Reaction conditions: 0.5 mmol ketone, 3 mol% RuCl$_2$(PPh$_3$)$_3$, 5–7 bar NH$_3$, 40 bar H$_2$ 1.5 mL t-amyl alcohol, 130 °C, 24 h, isolated yields. [b]GC yields using n-hexadecane as standard. [c]Same as 'a' with 1 mol% catalyst. [d]Same as 'a' for 30 h. [e]Diastereomeric ratio. Isolated as free amines and converted to hydrochloride salts. Corresponding hydrochloride salts were subjected to NMR analysis

Synthesis of branched primary amines from ketones. After having successfully performed the reductive amination of aldehydes, we were interested in the general applicability of this ruthenium precatalyst for the synthesis of branched primary amines starting from different ketones (Fig. 3). Compared to aldehydes, the reaction of ketones with ammonia to form primary amines is more difficult. Remarkably, the RuCl$_2$(PPh$_3$)$_3$ precatalyst is also active towards aromatic ketones (Fig. 3). Further, the applicability of this catalyst system was also explored for aliphatic ketones. Here, the aliphatic branched primary amines were obtained in up to 94% yield (Fig. 3).

Applications to life science molecules. To showcase the valuable applications of this amination protocol, we carried out the preparation of existing drugs as well as the introduction of –NH$_2$ moieties into drugs and complex molecules. The amination of important drugs such as Nabumetone, Pentoxifylline, and Azaperone (Fig. 4; products **92–94**) as well as steroid derivatives has been demonstrated (Fig. 4; products **95–97**). Such an insertion of amino groups into life science molecules represents a resourceful technique for further functionalization and modulation of their activities, which is highly useful in drug discovery.

Upscaling for the preparation of amines on gram-scale. In order to show practical utility and to demonstrate potential for

implementation in industrial production, the upscaling of synthetic methodologies is very important. Especially in homogeneous catalysis upscaling is a challenging task. Therefore, to demonstrate the applicability of this homogeneous catalytic amination protocol, we performed gram-scale synthesis of six selected amines. As shown in (see Supplementary Figure 1), 2–10 g of four aldehydes and two ketones were successfully aminated to yield their corresponding primary amines in more or less similar yields to those of 50–100 mg scale reactions.

We were interested to compare our methodology to an established amination protocol. The Leuckart-Wallach reaction is a prime example, finding application also on an industrial scale[39–41]. We therefore subjected 15 aldehydes and ketones, which have been studied in this work, to Leuckart-Wallach reaction conditions[39–41] to prepare the corresponding primary amines. As shown in Supplementary Table 1, the reaction worked well for simple aldehydes/ketones and gave 53–75% of corresponding primary amines (Supplementary Table 1; entries 1–3). For a majority of substituted and structurally diverse as well as heterocyclic aldehydes and ketones it gave poor yields (5–15%) (Supplementary Table 1; entries 4–9). The Leuckart-Wallach reaction failed to yield the desired primary amine for sensitive substrates (e.g., TMS or halogen containing) as well as some (hetero)cyclic and steroid derivatives (Supplementary Table 1; entries 10–15). A majority of the sensitive functional groups were

ARTICLE

89: 85%
(2-Methoxyamphetamine)

90: 92%
(4-Hydroxyamphetamine)

91: 82%
(4-Hydroxy-3-methoxyamphetamine)

92: 90%
(Nabumetone-NH₂)

93: 76%
(Pentoxifylline-NH₂)

94: 80%
(Azaperone-NH₂)

95: 93% (92:8)ᵇ
(Androstanolone-NH₂)

96: 79% (52:48)ᵇ
(Estrone-NH₂)

97: 92% (90:10) ᵇ
(Testosterone propionate-NH₂)
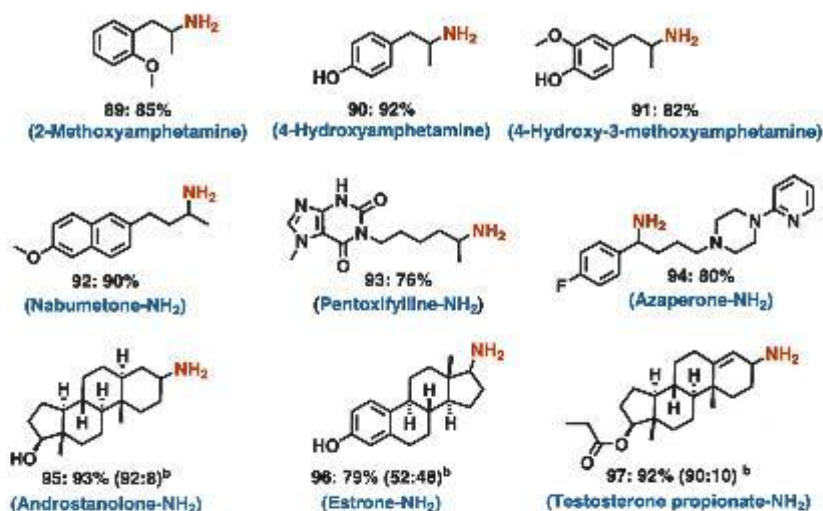
Fig. 4 Synthesis of drugs and amination of complex molecules. ᵃReaction conditions: 0.5 mmol ketone, 3 mol% $RuCl_2(PPh_3)_3$, 5–7 bar NH_3, 40 bar H_2 1.5 mL t-amyl alcohol, 130 °C, 24 h, isolated yields. Isolated as free amines and converted to hydrochloride salts. Corresponding hydrochloride salts were subjected to NMR analysis. ᵇDiastereomeric ratio
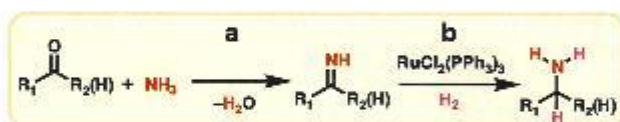
Fig. 5 Ru-catalyzed reductive amination of carbonyl compounds with NH_3 using H_2. a Noncatalytic condensation reaction; b catalytic hydrogenation reaction

not tolerated. Gratifyingly, for all these substrates, the $RuCl_2(PPh_3)_3$ precatalyst using ammonia and hydrogen worked well and produced the corresponding primary amines in 72–93% yields. These results clearly reveal that catalytic reductive amination using $RuCl_2(PPh_3)_3$ is more generally applicable for the preparation of primary amines compared to the traditional Leuckart-Wallach reaction.

Discussion

A general reaction pathway for the catalytic reductive amination of carbonyl compounds is shown in Fig. 5. Initially, the carbonyl compound undergoes condensation with ammonia to form the corresponding primary imine. Subsequently, the intermediate imine is hydrogenated to give the primary amine. The hydrogenation step is catalyzed by a catalytic species derived from the precatalyst, $RuCl_2(PPh_3)_3$.

We were interested to gain mechanistic insight into the hydrogenation step and to determine the nature of the active catalyst species. For this purpose, we studied the interaction of $RuCl_2(PPh_3)_3$ with hydrogen using in situ NMR in a model system consisting solely of the ruthenium precatalyst, methanol and C_6D_6. Figure 6 depicts the hydride region of the obtained ^1H NMR spectra. Initially, even in the absence of H_2, a quartet at $\delta_H = -17.6$ ppm is observed along with a broad singlet at $\delta_P = 55$ ppm in the $^{31}P\{^1H\}$ NMR spectrum (see SI). We assign these signals to $[RuHCl(PPh_3)_3]^{63}$, which is likely formed in small amounts via methanol oxidation. In presence of H_2 (1.5 bar) at room temperature, the quartet corresponding to $[RuHCl(PPh_3)_3]$ broadens[63] and two new hydride signals appear: a broad singlet at $\delta_H = -12.5$ ppm and a triplet of triplets at $\delta_H = -10.9$ ppm. Using ^1H-^{31}P HMBC NMR (see Supplementary Figures 6–13) we

were able to assign the hydride triplet of triplets to two multiplets in the $^{31}P\{^1H\}$ NMR spectrum (at $\delta_P = 34.8$ ppm and $\delta_P = 58.4$ ppm; see SI), which is consistent with the structure of $[Ru(H)_2(PPh_3)_4]^{64}$. We tentatively assign the broad singlet at $\delta_H = -12.5$ ppm to $[Ru(H)_2(PPh_3)_3]$, which is corroborated by the appearance of a broad signal at $\delta_P = 58$ ppm in the $^{31}P\{^1H\}$ NMR spectrum[65]. $[Ru(H)_2(PPh_3)_3]$ would be in equilibrium with $[Ru(H)_2(PPh_3)_4]$ via association/dissociation of a PPh_3 ligand. After 2.5 h at room temperature a new triplet at $\delta_H = -9.4$ ppm appears in the hydride region, which further increases in intensity upon heating to 60 °C. Using ^1H-^{31}P HMBC NMR we could assign this hydride signal to a singlet in the $^{31}P\{^1H\}$ NMR spectrum at $\delta_P = 50.4$ ppm (see Supplementary Figures 6–13). After 1.5 h at 60 °C, it is the dominant species in the hydride region and in the $^{31}P\{^1H\}$ NMR spectrum. The triplet hydride splitting (37 Hz), which collapses to a singlet in the $^1H\{^{31}P\}$ NMR spectrum (see Supplementary Figures 6–13), indicates the presence of just two equivalent PPh_3 ligands. When the $^{31}P\{^1H\}$ NMR experiment is decoupled with reduced power (only aromatic protons are decoupled) the singlet at $\delta_P = 50.4$ ppm splits into a doublet (see Supplementary Figures 6–13), indicating a monohydride structure. Although this species appears to have only two PPh_3 and one hydride ligand, its accumulation indicates high stability under experimental conditions, suggesting the presence of other stabilizing ligands (such as CO). Since $[Ru(H)_2(PPh_3)_3]$ is known to decarbonylate methanol[66] and due to similar spectral characteristics compared to $[RuHCl(CO)(PPh_3)_2(pyrazine)]^{67}$ we tentatively assign this species to the carbonyl-containing complex $[RuHCl(CO)(PPh_3)_2(Y)]$ (with Y possibly being a solvent molecule) formed via methanol decarbonylation.

An overview of the proposed transformation of $RuCl_2(PPh_3)_3$ in our model system is provided in Fig. 7: $RuCl_2(PPh_3)_3$ undergoes a stepwise reaction with H_2 to form $[RuHCl(PPh_3)_3]$ (which is also generated by the reaction with methanol) and $Ru(H)_2(PPh_3)_3$, which is in equilibrium with $Ru(H)_2(PPh_3)_4$. $Ru(H)_2(PPh_3)_3$ can further react via alcohol decarbonylation to form the carbonyl-containing complex $[RuHCl(CO)(PPh_3)_2(Y)]$. While methanol is not present under our reaction conditions for reductive amination, it is known that $RuCl_2(PPh_3)_3$ can also enable the decarbonylation of benzyl alcohols and aldehydes[65], which constitute a majority of our substrates.
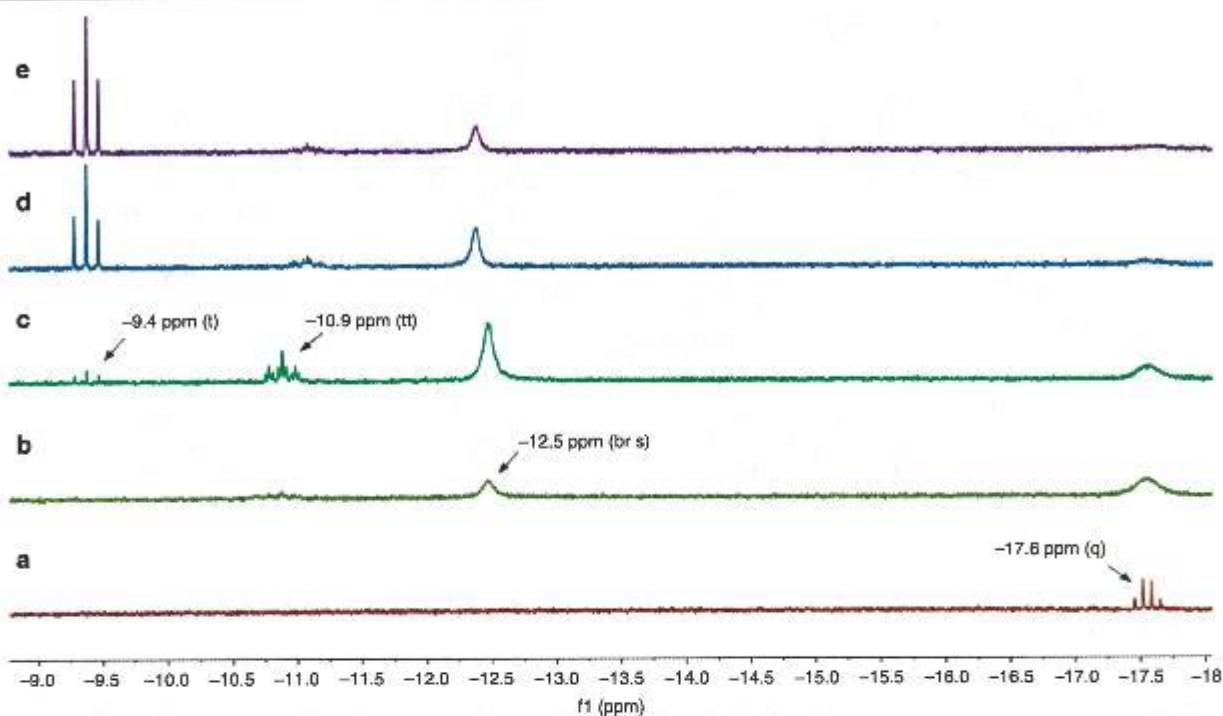
Fig. 6 Hydride region of ^1H NMR spectra of RuCl$_2$(PPh$_3$)$_3$ in C$_6$D$_6$/methanol. **a** RT, argon atmosphere; **b** RT, H$_2$ atmosphere (1.5 bar), 10 min; **c** RT, H$_2$ atmosphere (1.5 bar), 2.5 h; **d** 60 °C, H$_2$ atmosphere (1.5 bar), 30 min; **e** 60 °C, H$_2$ atmosphere (1.5 bar), 1.5 h
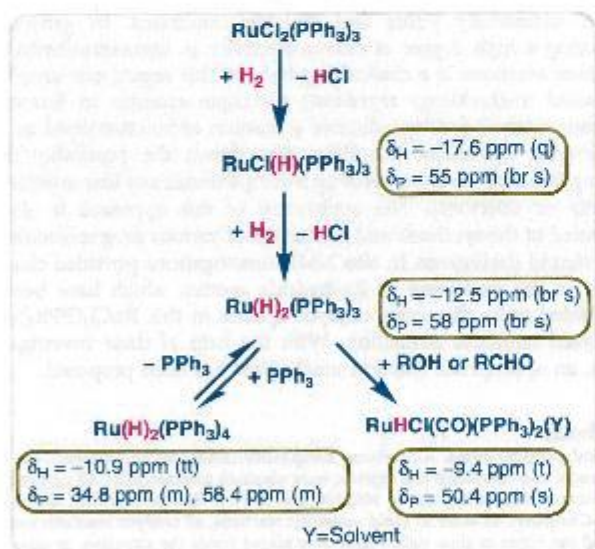
Fig. 7 Generation of different species from RuCl$_2$(PPh$_3$)$_3$ in presence of hydrogen. RuCl$_2$(PPh$_3$)$_2$ = precatalyst; Ru(H)Cl(PPh$_3$)$_3$ and Ru(H)$_2$(PPh$_3$)$_2$ = active catalytic species

Also, a number of previously reported ruthenium systems for reductive amination as well as alcohol amination are based on carbonyl-containing (pre-)catalysts[26,27,35–37]. Therefore, the question arises whether our active catalyst contains a carbonyl ligand or if it conforms to a previously proposed [RuHX(PPh$_3$)$_3$] structure (X = H$^-$ or Cl$^-$)[68,69]. To answer this question, we have compared the catalytic performance of [RuHCl(PPh$_3$)$_3$] and [RuHCl(CO)(PPh$_3$)$_3$] for benzaldehyde amination under standard reaction conditions. Interestingly, [RuHCl(PPh$_3$)$_3$] performs similarly to RuCl$_2$(PPh$_3$)$_3$ (88% benzylamine, 4% benzyl alcohol, 7% dibenzylamine; Supplementary Figure 2). This confirms that [RuHCl(PPh$_3$)$_3$] is part of the transformation cascade (as observed in our model system) which also includes the active catalyst. However, [RuHCl(CO)(PPh$_3$)$_3$] showed poor selectivity under our reaction conditions (3% benzylamine, 5% benzyl alcohol, 90% N-benzylidenebenzylamine; Supplementary Figure 3). In addition, a reported Ru$_3$(CO)$_{12}$/CataCxiumPCy catalytic system, which was used in the amination of alcohols with ammonia[36], was also tested for the reductive amination of cyclohexanone (Supplementary Figure 3). Similarly, this catalyst also showed poor selectivity, yielding only 10% of cyclohexylamine. Therefore, carbonyl-containing complexes are likely not the active species under our reaction conditions. Rather, due to their decreased selectivity, they constitute a possible deactivation pathway for RuCl$_2$(PPh$_3$)$_3$ catalyzed reductive amination. This difference between our observations and previously reported carbonyl-containing ruthenium amination catalysts is attributed to the ligand: carbonyl-containing Ru(II) catalysts typically require bidentate[26] or tridentate[35] ligands. Control experiments have shown significantly decreased yield in the absence of those additional ligands[26]. In contrast, the carbonyl-free catalyst type [RuHX(PPh$_3$)$_3$] appears to be sufficiently active and selective with only PPh$_3$-derived ligands.

After clarifying the pathway for catalyst activation we were interested to investigate the reaction cascade starting from the aldehyde/ketone and ammonia using the benzaldehyde benchmark system. The starting materials can undergo a condensation to form primary imine **A**. Intermediate **A**, however, was never detected in the reaction mixture, presumably due to its high reactivity. Instead (as can be seen in Fig. 1a), secondary imine **4** was determined to be the major intermediate. **4** is formed via condensation of the product **2** with either the starting aldehyde/ketone (releasing water) or via condensation of **2** and **A** (releasing
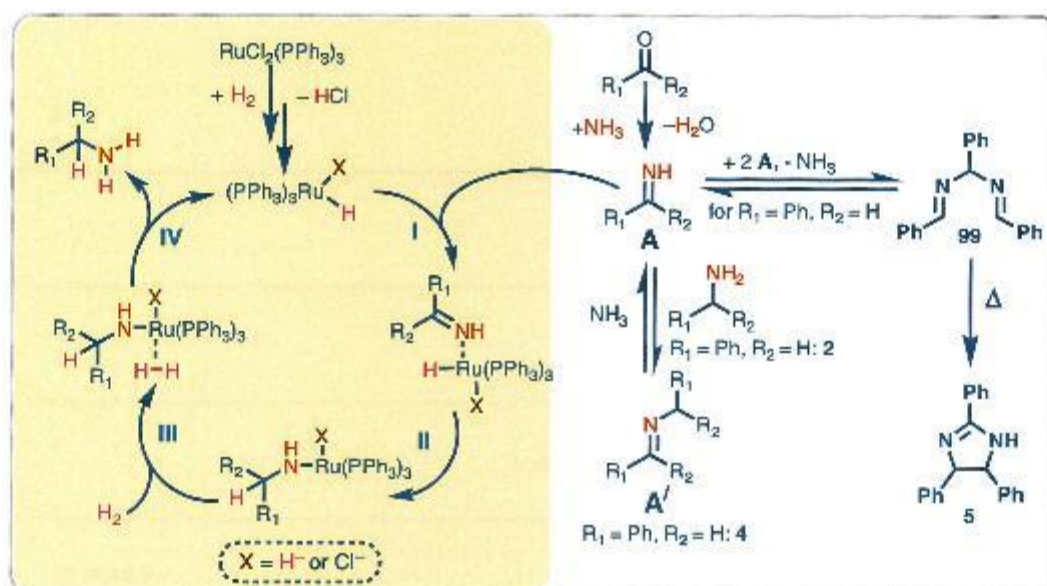
Fig. 8 Proposed reaction mechanism for the RuCl$_2$(PPh$_3$)$_3$-catalyzed reductive amination. **A** Unstable primary imine; **A$'$** stable secondary imine. **5** = 2,4,5-triphenyl-2-imidazoline

NH$_3$). We next reacted isolated **4** under our standard reaction conditions (40 bar H$_2$, 5–7 bar NH$_3$, 24 h, RuCl$_2$(PPh$_3$)$_3$) and found almost quantitative conversion to **2** (Supplementary Figure 4). In contrast, when **4** was reacted in the absence of ammonia, 98% dibenzylamine was obtained after 24 h (Supplementary Figure 4). These results show that **4**, when exposed to NH$_3$, is in an equilibrium with **A** + **2**[70]. While the catalyst is able to hydrogenate both **A** and **4**, **A** is hydrogenated preferentially and is replenished by the equilibrium with **4**. If ammonia is absent or only present in low concentrations (see Fig. 1e), the formation of **A** + **2** from **4** is suppressed, leading to hydrogenation of **4** (yielding dibenzlamine). Furthermore, due to rapid hydrogenation under optimized conditions, the stationary concentration of **A** is low, precluding side reactions of this reactive intermediate. When the hydrogenation does not proceed quickly, however, accumulation and side reactions involving **A** can likely occur. Correspondingly, when a mixture of **4** and benzaldehyde was reacted under standard conditions but without H$_2$, 20% of the cyclic side-product **5** was obtained (the rest being unreacted starting material, see Supplementary Figure 5). Williams et al.[71] and Corey et al.[72] have reported that **A** can trimerize to form **99**, which can subsequently undergo thermal cyclization to form **5** (Fig. 8). This reaction of accumulated **A** likely explains the formation of large amounts of **5** in less active catalyst systems (see Table 1, entries 1–10; Fig. 1).

Based on these observations we propose the following mechanism (Fig. 8): Reaction of a carbonyl compound with NH$_3$ yields primary imine **A**, which can be in an equilibrium with secondary imine **A$'$** via condensation with the product amine. The precatalyst RuCl$_2$(PPh$_3$)$_3$ is activated by H$_2$ to form the the active catalyst species [RuHX(PPh$_3$)$_3$] (X being either H$^-$ or Cl$^-$). This active catalytic species selectively reacts with the primary imine to initially form a substrate complex (**I**). Substrate coordination is followed by hydride insertion (**II**), generating a Ru-amide complex. Coordination of H$_2$ (**III**) followed by hydrogenolysis releases the primary amine as the final product with regeneration of the catalytic species (**IV**).

In conclusion, we demonstrated that using a simple RuCl$_2$(PPh$_3$)$_3$ catalyst, the challenging reductive amination of

carbonyl compounds using ammonia and molecular hydrogen for the selective synthesis of a variety of primary amines is possible. Applying this Ru-based reductive amination, starting from inexpensive aldehydes and ketones, functionalized and structurally diverse linear and branched primary amines have been synthesized under industrially viable and scalable conditions. In general, achieving a high degree of chemoselectivity in amination/hydrogenation reactions is a challenging task. In this regard our simple Ru-based methodology represents a unique example in homogeneous catalysis for the reductive amination of functionalized and challenging molecules. We have also shown the possibility of scaling this amination protocol up to 10 g without any loss in either activity or selectivity. The application of this approach is also extended to the synthesis and amination of various drug molecules and steroid derivatives. In situ NMR investigations provided clear hints on the formation of Ru-hydride species, which have been elucidated to be the active catalytic species in this RuCl$_2$(PPh$_3$)$_3$-catalyzed reductive amination. With the help of these investigations, an appropriate reaction mechanism has been proposed.

Methods

Reductive amination of carbonyl compounds with ammonia. The 8 mL dried glass vial was charged with a magnetic stirring bar and 0.5 mmol of corresponding carbonyl compound (aldehyde or ketone). Then 1.5 mL t-amyl alcohol as solvent and 2–3 mol% RuCl$_2$(PPh$_3$)$_3$ catalysts (2 mol% in case of aldehydes and 3 mol% in case of ketones) were added. The glass vial was fitted with a septum, cap and needle, and placed into a 300 mL autoclave (eight vials with different substrates at a time). The autoclave was flushed with hydrogen twice at 40 bar pressure and then it was pressurized with 5–7 bar ammonia gas and 40 bar hydrogen. The autoclave was

placed into an aluminum block preheated at 140 °C (placed inside 30 min before counting the reaction time in order to attain the reaction temperature) and the reactions were stirred for the required time. During the reaction the inside temperature of the autoclave was measured to be 130 °C and this temperature was used as the reaction temperature. After completion of the reactions, the autoclave was cooled to room temperature. The remaining ammonia and hydrogen were discharged and the vials containing reaction products were removed from the autoclave. The reaction products were analyzed by GC-MS and the corresponding primary amines were purified by column chromatography (silica; n-hexane-ethyl acetate mixture). The resulting amines were converted to their respective hydrochloride salt and characterized by NMR. For conversion into the hydrochloride salt, 1–2 mL methanolic HCl or dioxane HCl (1.5 M HCl in methanol or 4 N HCl in dioxane) was added to the ether solution of the respective amine and stirred at room temperature for 4–5 h. Then, the solvent was removed and the resulting hydrochloride salt of the amine was dried under high vacuum. For determining the yields by GC for selected amines, after completion of the reaction n-hexadecane (100 µL) as standard was added to the reaction vials and the reaction products were diluted with ethyl acetate followed by filtration using a plug of silica and then analyzed by GC.

General procedure for the gram scale reactions. The Teflon or glass fitted 300 (5–10 g) or 500 mL (20 g) (in case 5–20 g) or 100 mL (in case of 2–2.5 g) autoclave was charged with a magnetic stirring bar and the corresponding carbonyl compound (2–20 g). Then 25–150 mL t-amyl alcohol was added. Subsequently, RuCl₂(PPh₃)₃ (amount of catalysts equivalent to 2–3 mol%) was added. The autoclave was flushed with hydrogen twice at 40 bar pressure and then it was pressurized with 5–7 bar ammonia gas and 40 bar hydrogen. The autoclave was placed into an aluminum block preheated to 140 °C (placed 30 min before counting the reaction time in order to attain reaction temperature) and the reaction was stirred for the required time. During the reaction the inside temperature of the autoclave was measured to be 130 °C and this temperature was used as the reaction temperature. After completion of the reaction, the autoclave was cooled to room temperature. The remaining ammonia and hydrogen were discharged and the reaction products were removed from the autoclave. The reaction products were analyzed by GC-MS and the corresponding primary amines were purified by column chromatography (silica; n-hexane-ethyl acetate mixture). The resulting amines were converted to their respective hydrochloride salt and characterized by NMR.

Procedure for the in situ NMR studies. The in situ observation of the Ru-hydrides was performed under hydrogen saturation conditions in a 5 mm glass NMR tube, equipped with a PTFE gas inlet hose and a circulation unit which produces a continuous gas flow through the solution[74,75]. The brown solution of the precursor complex RuCl₂(PPh₃)₃ (50 mg) in 0.5 mL methanol/0.5 mL benzene-d6 was transferred to the NMR tube under Ar. After assembling the device under inert gas and characterizing the solution by its ¹H and ³¹P NMR spectra, the system was filled with neat hydrogen (absolute pressure 1.5 bar). A gas flow of 1 mL min⁻¹ was used to saturate the solution. ¹H and ³¹P NMR spectra were taken at regular intervals to monitor the reaction progress. Changes were immediately observable as shown in Fig. 2. After three hours, the temperature was raised and kept at about 60 °C for another three hours to complete the reaction. No further changes were detected thereafter. The color of the solution was changed to brick-red at the end of the experiment. Note that maintaining a continuous gas flow till the very end was not possible, because black particles of precipitating metallic Ru were clogging the tubing.

Data availability

All data are available from the authors upon reasonable request.

References

1. Lawrence, S. A. Amines: Synthesis, Properties and Applications. (Cambridge University Press, Cambridge, UK, 2004).
2. Ricci, A. Amino Group Chemistry: From Synthesis to the Life Sciences. (Wiley-VCH, Weinheim, 2008).
3. Smith, D. T., Delost, M. D., Qureshi, H. & Njardarson, J. T. Top 200 Pharmaceutical Products by Retail Sales in 2016. https://njardarson.lab.arizona.edu/sites/njardarson.lab.arizona.edu/files/2016Top200PharmaceuticalRetailSalesPosterLowResV3_0.pdf (2017).
4. Roughley, S. D. & Jordan, A. M. The medicinal chemist's toolbox: an analysis of reactions used in the pursuit of drug candidates. J. Med. Chem. 54, 3451–3479 (2011).
5. Froidevaux, V., Negrell, C., Caillol, S., Pascault, J.-P. & Boutevin, B. Biobased amines: from synthesis to polymers; present and future. Chem. Rev. 116, 14181–14224 (2016).
6. Mao, R., Frey, A., Balon, J., Hu, X. & Decarboxylative, C. (sp³)-N cross-coupling via synergetic photoredox and copper catalysis. Nat. Catal. 1, 120–126 (2018).
7. Gomez, S. A., Peters, J. A. & Maschmeyer, T. The reductive amination of aldehydes and ketones and the hydrogenation of nitriles: mechanistic aspects and selectivity control. Adv. Synth. Catal. 344, 1037–1057 (2002).
8. Alinezhad, H., Yavari, H. & Salehian, F. Recent advances in reductive amination catalysis and its applications. Curr. Org. Chem. 19, 1021–1049 (2015).
9. Nugent, T. C. & El-Shazly, M. Chiral amine synthesis-recent developments and trends for enamide reduction, reductive amination, and imine reduction. Adv. Synth. Catal. 352, 753–819 (2010).
10. Wakchaure, V. N., Zhou, J., Hoffmann, S. & List, B. Catalytic asymmetric reductive amination of α-branched ketones. Angew. Chem. Int. Ed. 49, 4612–4614 (2010).
11. Chusov, D. & B. List, B. Reductive amination without an external hydrogen source. Angew. Chem. Int. Ed. 53, 5199–5201 (2014).
12. Natte, K., H. Neumann, H., Jagadeesh, R. V. & Beller, M. Convenient iron-catalyzed reductive aminations without hydrogen for selective synthesis of N-methylamines. Nat. Commun. 8, 1344 (2017).
13. Jagadeesh, R. V. et al. Hydrogenation using iron oxide-based nanocatalysts for the synthesis of amines. Nat. Protoc. 10, 548–557 (2015).
14. Reductive amination. https://www.reagentguides.com/reagent-guides/reductive-amination (2015).
15. Gusak, K. N., Ignatovich, Z. V. & Koroleva, E. V. New potential of the reductive alkylation of amines. Russ. Chem. Rev. 84, 288–309 (2015).
16. Senthamarai, T. et al. Expedient synthesis of N-methyl- and N-alkylamines by reductive amination using reusable cobalt oxide nanoparticles. ChemCatChem 10, 1235–1240 (2018).
17. Jagadeesh, R. V. et al. MOF-derived cobalt nanoparticles catalyze a general synthesis of amines. Science 358, 326–332 (2017).
18. Komanoya, T., Kinemura, T., Kita, Y., Kamata, Y. K. & Hara, M. Electronic effect of ruthenium nanoparticles on efficient reductive amination of carbonyl compounds. J. Am. Chem. Soc. 139, 11493–11499 (2017).
19. Nakamura, Y., Kon, K., Touchy, A. S., Shimizu, K.-i. & Ueda, W. Selective synthesis of primary amines by reductive amination of ketones with ammonia over supported Pt catalysts. ChemCatChem 7, 921–924 (2015).
20. Liang, G. et al. Production of primary amines by reductive amination of biomass-derived aldehydes/ketones. Angew. Chem. Int. Ed. 56, 3050–3054 (2017).
21. Wang, Z. Mignonac reaction. In Comprehensive organic name reactions and reagents. (John Wiley & Sons, New Jersey, 2010).
22. Chatterjee, M., Takayuki Ishizaka, T. & Kawanami, H. Reductive amination of furfural to furfurylamine using aqueous ammonia solution and molecular hydrogen: an environmentally friendly approach. Green. Chem. 18, 487–496 (2016).
23. Reductive amination review. https://erowid.org/archive/rhodium/chemistry/reductive.amination.html (2004).
24. Gross, T., Seayad, A. M., Ahmad, M. & Beller, M. Synthesis of primary amines: first homogeneously catalyzed reductive amination with ammonia. Org. Lett. 4, 2055–2058 (2002).
25. Riermeier, T. et al. Method for producing amines by homogeneously catalyzed reductive amination of carbonyl compounds. US 6, 884–887 B1 (2005).
26. Gallardo-Donaire, J., Ernst, M., Trapp, O. & Schaub, T. Direct synthesis of primary amines via ruthenium-catalysed amination of ketones with ammonia and hydrogen. Adv. Synth. Catal. 358, 358–363 (2016).
27. Gallardo-Donaire, J. et al. Direct asymmetric ruthenium-catalyzed reductive amination of alkyl-aryl ketones with ammonia and hydrogen. J. Am. Chem. Soc. 140, 355–361 (2018).
28. Ogo, S., Uehara, K., Abura, T. & Fukuzumi, S. pH-Dependent chemoselective synthesis of α-amino acids. Reductive amination of α-keto acids with ammonia catalyzed by acid-stable iridium hydride complexes in water. J. Am. Chem. Soc. 126, 3020–3021 (2004).
29. Kadyrov, R. & Riermeier, T. H. Highly enantioselective hydrogen-transfer reductive amination: catalytic asymmetric synthesis of primary amines. Angew. Chem. Int. Ed. 42, 5472–5474 (2003).
30. Tan, X. et al. Asymmetric synthesis of chiral primary amines by ruthenium-catalyzed direct reductive amination of alkyl aryl ketones with ammonium salts and molecular H₂. J. Am. Chem. Soc. 140, 2024–2027 (2018).
31. Yan, T., Feringa, B. L. & Barta, K. Iron catalysed direct alkylation of amines with alcohols. Nat. Commun. 5, 5602 (2014).
32. Meindl, W. R., Angerer, E. V., Schoenenberger, H. & Ruckdeschel, G. Benzylamines: synthesis and evaluation of antimycobacterial properties. J. Med. Chem. 27, 1111–1118 (1984).
33. Yan, T., Feringa, B. L. & Barta, K. Direct N-alkylation of unprotected amino acids with alcohols. Sci. Adv. 3, eaao6494 (2017).
34. Goldacre, R. J. Mode of action of benzylamine sulphonamide ('Marfanil'). Nature 154, 796–797 (1944).

ARTICLE

35. Gunanathan, C. & Milstein, D. Selective synthesis of primary amines directly from alcohols and ammonia. *Angew. Chem. Int. Ed.* 47, 8661–8664 (2008).

36. Imm, S., Bähn, S., Neubert, L., Neumann, H. & Beller, M. An efficient and general synthesis of primary amines by ruthenium-catalyzed amination of secondary alcohols with ammonia. *Angew. Chem. Int. Ed.* 49, 8126–8129 (2010).

37. Pingen, D., Müller, C. & Vogt, D. Direct amination of secondary alcohols using ammonia. *Angew. Chem. Int. Ed.* 49, 8130–8133 (2010).

38. Bähn, S. et al. The catalytic amination of alcohols. *ChemCatChem* 3, 1853–1864 (2011).

39. Leuckart, R. Ueber eine neue bildungsweise von tribenzylamin. *Ber* 18, 2341–2344 (1885).

40. Moore, M. L. *Organic Reactions* (Wiley, Hoboken, NJ, 2011).

41. Crosley, F. S. & Moore, M. L. Studies on Leuckart reaction. *J. Org. Chem.* 9, 529–536 (1944).

42. Feuer, H. & Braunstein, D. M. Reduction of oximes, oxime ethers, and oxime esters with diborane. *Nov. Synth. Amines J. Org. Chem.* 34, 1817–1821 (1969).

43. Huang, X. et al. Asymmetric synthesis of primary amines via the spiroborate-catalyzed borane reduction of oxime ethers. *Org. Lett.* 9, 1793–1796 (2007).

44. Mirjafary, Z., Abdoli, M., Saeidian, H., Boroon, S. & Kakanejadifard, A. Oxime ethers as versatile precursors in organic synthesis: a review. *RSC Adv.* 5, 79361–79384 (2015).

45. Ammonia. https://pubchem.ncbi.nlm.nih.gov/compound/ammonia (2016).

46. Appl, M. in *Ullmann's Encyclopedia of Industrial Chemistry*, 7th edn. (ed. Wiley-VCH) (Wiley, New York, 2011).

47. van Gysel, A. B. & Musin, W. in *Ullmann's Encyclopedia of Industrial Chemistry*, 7th edn. (ed. Wiley-VCH) (Wiley, New York, 2011).

48. Schirmann, P. & Bourdauducq, J.-P. in *Ullmann's Encyclopedia of Industrial Chemistry*, 7th edn. (ed. Wiley-VCH) (Wiley, New York, 2011).

49. Klinkenberg, J. L. & Hartwig, J. F. Catalytic organometallic reactions of ammonia. *Angew. Chem. Int. Ed.* 50, 86–95 (2011).

50. Schranck, J. & Tlili, A. Transition-metal-catalyzed monoarylation of ammonia. *ACS Catal.* 8, 405–418 (2018).

51. Cobb, J. E. et al. In *Encyclopedia of Reagents for Organic Synthesis* (eds. Paquette, L. A. et al.) (John Wiley & Sons, New York, 2004).

52. Burke, S. D. & Danheiser, R. L. *Triphenylphosphine, Handbook of Reagents for Organic synthesis, Oxidizing and Reducing Agents* (Wiley, Hoboken, NJ, 1999).

53. Pignolet, L. M. *Homogeneous Catalysis with Metal Phosphine Complexes* (Springer US, 2013).

54. Wilkinson's catalyst, *Comprehensive Organic Name Reactions and Reagents* (2010).

55. Müller, C. & Vogt, D. Phosphinines as ligands in homogeneous catalysis: Recent developments, concepts and perspectives. *Dalton. Trans.* 5505–5523 (2007).

56. Plummer, J. S., Shun-Ichi, M. & Changjia, Z. Dichlorotris (triphenylphosphine)ruthenium(II), *e-EROS Encyclopedia of Reagents for Organic Synthesis* (John Wiley, 2010).

57. Crabtree, R. H. Homogeneous transition metal catalysis of acceptorless dehydrogenative alcohol oxidation: applications in hydrogen storage and to heterocycle synthesis. *Chem. Rev.* 117, 9228–9246 (2017).

58. Guillena, G., Ramon, D. J. & Yus, M. Hydrogen autotransfer in the N-alkylation of amines and related compounds using alcohols and amines as electrophiles. *Chem. Rev.* 110, 1611–1641 (2010).

59. Samec, J. S. M., Bäckvall, J.-E., Andersson, P. G. & Brandt, P. Mechanistic aspects of transition metal-catalyzed hydrogen transfer reactions. *Chem. Soc. Rev.* 35, 237–248 (2006).

60. Pingen, D., Lutz, M. & Vogt, D. Mechanistic study on the ruthenium-catalyzed direct amination of alcohols. *Organometallics* 33, 1623–1629 (2014).

61. Evans, D., Osborn, J. A., Jardine, F. H. & Wilkinson, G. Homogeneous hydrogenation and hydroformylation using ruthenium complexes. *Nature* 208, 1203–1204 (1965).

62. Wang, G.-Z. & Bäckvall, J. E. Ruthenium-catalysed transfer hydrogenation of imines by propan-2-ol. *Chem. Commun.* 980–982 (1992).

63. Kirss, R. U., Eisenschmid, T. C. & Eisenberg, R. Para hydrogen induced polarization in hydrogenation reactions catalyzed by ruthenium phosphine complexes. *J. Am. Chem. Soc.* 110, 8564–8566 (1988).

64. Samouel, H., Miloserdov, F. M., Escudero-Adán, E. C. & Grushin, V. V. Solid-state structure and solution reactivity of [(Ph₃P)₄Ru(H)₂] and related Ru(II) complexes used in catalysis: a reinvestigation. *Organometallics* 33, 7279–7283 (2014).

65. Mazziotta, A. & Madsen, R. Ruthenium-catalyzed dehydrogenative decarbonylation of primary alcohols. *Eur. J. Org. Chem.* 36, 5417–5420 (2017).

66. Van der Sluys, L. S., Kubas, G. J. & Caulton, K. G. Reactivity of (dihydrogen) dihydridotris(triphenylphosphine)ruthenium. Dimerization to form

67. Małecki, J. G. & Kruszynski, R. Synthesis, crystal and spectroscopic characterization of [RuIICl(CO)(PPh₃)₂(pyrazine)]. *J. Coord. Chem.* 60, 2085–2095 (2007).

68. Aranyos, A., Csjernyik, G., Szabo, K. S. & Bäckvall, J. E. Evidence for a ruthenium dihydride species as the active catalyst in the RuCl₂(PPh₃)-catalyzed hydrogen transfer reaction in the presence of base. *Chem. Commun.* 351–352 (1999).

69. Masters, C. *Homogeneous Transition-Metal Catalysis: A Gentle Art.* 51–55 (Chapman & Hall, 1981).

70. Krupka, J., Dluhoš, L. & Mrózek, L. Evaluation of benzylamine production via reductive amination of benzaldehyde in a slurry reactor. *Chem. Eng. Technol.* 40, 870–877 (2017).

71. Williams, O. F. & Bailar, J. C. The stereochemistry of complex inorganic compounds. XXIV. Cobalt stilbenediamine complexes. *J. Am. Chem. Soc.* 81, 4464–1469 (1959).

72. Corey, E. J. & Kühnle, P. N. M. A simplified synthesis of (±)–1,2-diphenyl-1,2-diaminoethane (1) from benzaldehyde and ammonia. Revision of the structures of the long-known intermediates "hydrobenzamide" and "amarine". *Tetrahedron Lett.* 38, 8631–8634 (1997).

73. Samouel, H., Vladimir, V. & Grushin, V. V. New, highly efficient, simple, safe, and scalable synthesis of [(Ph₃P)₃Ru(CO)(H)₂]. *Organometallics* 32, 4440–4443 (2013).

74. Baumann, W., Manasi, S., Heller, D. & Borns, S. Gas bubbles in the NMR tube: an easy way to investigate reactions with gases in the liquid phase. *Magn. Reson. Chem.* 35, 701–706 (1997).

75. Baumann, W., Börner, A., Selent, D. Gas injection and circulation device for tracking of reactions in the liquid phase involving gaseous reactants under normal and high pressure by means of nuclear magnetic resonance spectroscopy (NMR spectroscopy pressure) under steady state conditions. DE103331493B4, 2008.

Author contributions

R.V.J., T.S., K.M., M.B., and N.V.K. planned and developed the project. T.S., K.M., R.V.J., J.S., N.V.K., H.N., and P.C.J.K. designed the experiments. T.S. and K.M. performed catalytic experiments. W.B. and J.S. performed in situ NMR experiments. R.V.J., J.S., N.V.K., T.S., K.M., P.C.J.K., and M.B. wrote the paper. R.V.J. and M.B. supervised the project.

Additional information

Supplementary Information accompanies this paper at https://doi.org/10.1038/s41467-018-06416-6.

Contribution to the Publications

Chemical Science

EDGE ARTICLE

Check for updates

Ultra-small cobalt nanoparticles from molecularly-defined Co–salen complexes for catalytic synthesis of amines†

Thirusangumurugan Senthamarai,[a] Vishwas G. Chandrashekhar,[a] Manoj B. Gawande, [b] Narayana V. Kalevaru, [a] Radek Zbořil, [b] Paul C. J. Kamer, [a] Rajenahally V. Jagadeesh [*a] and Matthias Beller [*a]

We report the synthesis of *in situ* generated cobalt nanoparticles from molecularly defined complexes as efficient and selective catalysts for reductive amination reactions. In the presence of ammonia and hydrogen, cobalt–salen complexes such as cobalt(II)–N,N'-bis(salicylidene)-1,2-phenylenediamine produce ultra-small (2–4 nm) cobalt-nanoparticles embedded in a carbon–nitrogen framework. The resulting materials constitute stable, reusable and magnetically separable catalysts, which enable the synthesis of linear and branched benzylic, heterocyclic and aliphatic primary amines from carbonyl compounds and ammonia. The isolated nanoparticles also represent excellent catalysts for the synthesis of primary, secondary as well as tertiary amines including biologically relevant N-methyl amines.

Introduction

In recent years, 3d metal-based nanoparticles (NPs) emerged as promising catalysts for the synthesis of functionalized and complex organic molecules for advanced applications in life and material sciences.[1] Traditionally, such syntheses are performed using homogeneous organometallic complexes,[2] which are often sensitive and more difficult to recycle compared to heterogeneous materials.[1,2] For the preparation of stable but at the same time active and selective NPs, the use of suitable precursors and optimal methods is crucial.[1] Commonly, nanoparticles are prepared by chemical reduction processes, calcination or pyrolysis in the presence of suitable supports and metal precursors. The resulting materials are applied particularly in industrially-relevant bench mark reactions of less functionalized molecules.[2] However, in recent years there is an increasing interest to use such catalysts for advanced organic synthesis, specifically for the preparation of life science products.[1] In this respect, the preparation of specific NPs by immobilization and pyrolysis of organometallic complexes or metal organic frameworks (MOFs) on heterogeneous supports attracted also attention.[1,4] These supported NPs show high

activity and selectivity for the preparation of functionalized amines,[1d-f] nitriles,[1k,4c] carboxylic acid derivatives,[1f,h] and cyclo-aliphatic compounds.[1j] Although this preparation represents a highly useful tool to produce novel nano-structured catalysts on lab-scale, the upscaling can be difficult and requires specialized equipment.[1,4] Thus, the use of alternative, more convenient methods is highly desired. One possibility is the practical *in situ* generation of active heterogeneous NPs.[5] Based on this idea, herein we report a straightforward approach for the generation of cobalt-based NPs *in situ* from molecularly-defined metal complexes and their application in reductive amination reactions using ammonia and molecular hydrogen (Fig. 1).

The resulting amines represent privileged molecules widely used in chemistry, medicine, biology, and material science.[6] For their synthesis, catalytic reductive amination of carbonyl compounds using molecular hydrogen is widely applied as cost-
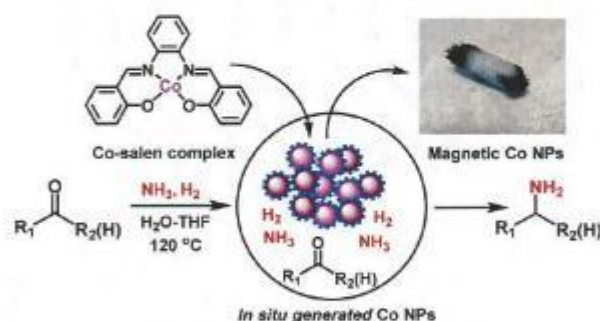
Fig. 1 *In situ* generation of Co-NPs for reductive aminations.

*a*Leibniz-Institut für Katalyse e. V. an der Universität Rostock, Albert-Einstein-Str. 29a, 18059 Rostock, Germany. E-mail: jagadeesh.rajenahally@catalysis.de; matthias.beller@catalysis.de

*b*Regional Centre of Advanced Technologies and Materials, Department of Physical Chemistry, Faculty of Science, Palacký University, Olomouc, Šlechtitelů 27, Olomouc, 78371, Czech Republic

† Electronic supplementary information (ESI) available. See DOI: 10.1039/c9sc04963k

effective methodology in both academic research and industry.[1c,A,7–10] Among reductive aminations, the synthesis of primary amines, which can be easily functionalized to high value products, continues to be especially important.[1c,A,/A–10] Regarding catalysts for this reaction, precious metals-based ones are known to a large extent.[8,9] However, in recent years Co-[1c] and Ni[1A,/]-based nanocatalysts have successfully been developed in addition to RANEY® nickel.[10]

Results and discussion

In situ generation of Co-NPs and their activities

Following our concept, we initially investigated the reaction of cobalt salen complexes to obtain NPs. For example, using the cobalt–N,N'-bis(salicylidene)-1,2-phenylenediamine (complex I) in water–THF as solvent in the presence of ammonia and molecular hydrogen at 120 °C a black precipitate of Co NPs is formed, which can be magnetically separated (Fig. 1 and S3†). To explore their reactivity, preliminary catalytic experiments were carried out for the reductive amination of 4-bromobenzaldehyde 1 to 4-bromobenzylamine 2 in presence of ammonia and molecular hydrogen (Fig. 2). Indeed, using a mixture of cobalt(II) acetate and N,N'-bis(salicylidene)-1,2-phenylenediamine (L1) led to the formation of 15% of 2. In contrast, testing simple cobalt(II) acetate under the same conditions produced no desired product. Remarkably, the defined complex Co-L1 (complex I) exhibited excellent activity as well as selectivity in the bench mark reaction (98% of 4-bromobenzylamine). In addition, other molecularly-defined Co–salen complexes have also been tested (Fig. S1†) and complexes II–IV showed good activity (85–90% yield), while complex V resulted in lower product yield (50%). In all cases of active complexes, the reaction mixtures turned black after some hours. Hence, we assumed the *in situ* formed cobalt-NPs are the "real" active species for the reductive amination reaction. To confirm this, we performed a standard mercury test in the presence of complex I and after addition of 15 mg Hg the reductive amination reaction did not occur. Hot filtration of NPs and testing the filtrate for the reaction showed that Co-NPs did not go into solution as soluble particles. Studying the course of the benchmark reaction at different intervals of time showed a prolonged catalyst preformation time and only after 10 h 4-bromobenzylamine started to form (Fig. S3†). Apparently, complex I generated nanoparticles slowly, which then catalyze the desired amination process. For comparison, we also prepared cobalt nanoparticles separately by mixing complex I, ammonia and hydrogen (see S7a†). After isolation, they were tested under similar conditions and exhibited comparable activity and selectivity to that of *in situ* generated ones. Due to their physical properties, the Co NPs could be magnetically separated and were conveniently re-used up to three times (Fig. 2). However, after the third cycle we observed a significant decrease in activity and selectivity. In addition, the stability of the catalyst system was also confirmed by recycling the NPs after reduced reaction time (Fig. S4†). Next, we compared the reactivity of these active NPs with related supported NPs. However, addition of carbon or silica support to the reaction led to completely inactive materials (Fig. 2). On the other hand, materials prepared by immobilization of complex I on carbon or silica and subsequent pyrolysis produced catalysts with moderate activity (Fig. 2; 40–50% yield of 2). In addition, specific cobalt nanoparticles have been prepared by using chemical reduction of cobalt salts[11] and tested for their activities. However, none of these cobalt nanoparticles formed the desired product, 4-bromobenzylamine (Table S1,† entries 5–6). All these results reveal the superiority of the simply *in situ* generated Co NPs (Fig. 3).

Characterization of *in situ* Co-NPs

To understand the reactivity and to know the structural features of the most active cobalt nanoparticles, we performed detailed
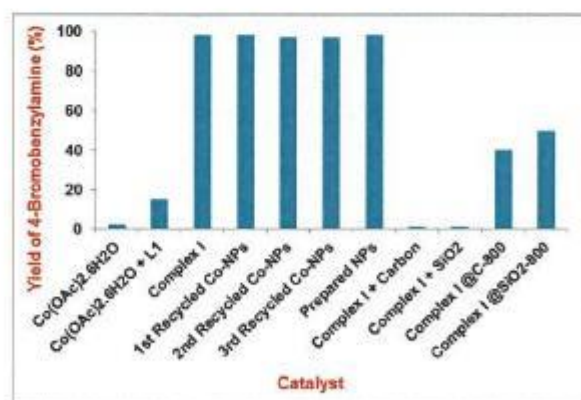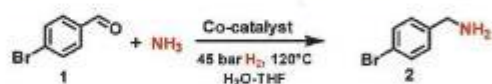
Fig. 2 Reductive amination of 4-bromobenzaldehyde: Activity of cobalt catalysts[a]. [a]Reaction conditions: 0.5 mmol 4-bromobenzaldehyde, 6 mol% Co-complex, (Co NPs), 5 bar NH_3, 45 bar H_2, 2.5 mL H_2O–THF (1.5 : 1), 120 °C, 24 h, GC yields using n-hexadecane as standard.
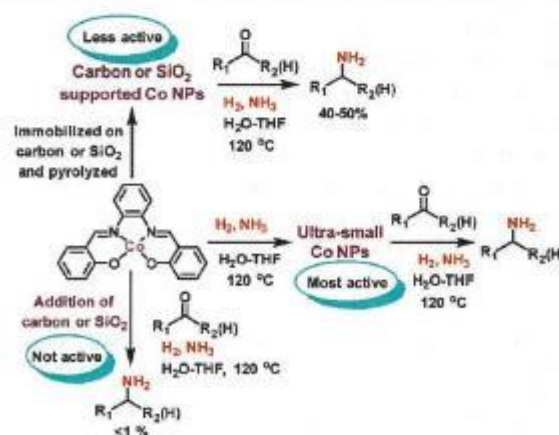
Fig. 3 Reductive amination of carbonyl compounds in presence of NH_3 and H_2 using different Co NPs produced from cobalt–salen complex.

Edge Article

characterizations using transmission electron microscopy (TEM), energy dispersive X-ray spectroscopy (EDX), X-ray diffraction (XRD), and X-ray photoelectron spectroscopy (XPS).

TEM analysis of cobalt-particles at different magnification showed sheets and at some places thread bundles like morphology where cobalt nanoparticles are embedded in carbon and nitrogen framework (Fig. 4). Further detailed morphological investigations were performed by HRTEM-STEM analysis. A close inspection of HRTEM images at 20 nm, revealed the presence of ultra-small (range 2–4 nm) cobalt nanoparticles (Fig. 4 and S6†) supported on graphitic carbon. The HAADF-elemental mapping displayed a homogeneous distribution of the cobalt nanoparticles (Fig. 4). In case of the recycled catalyst, we observed that these particles were still intact and there are no noticeable changes in the morphology (Fig. S8†).

XRD patterns of *in situ* generated and reused Co-nanoparticles do not show variations on the phase composition (Fig. S9†). Two allotropes of metallic cobalt have been identified, one with face centered cubic arrangement (Co-fcc, space group $Fm\bar{3}m$, PDF card 01-089-7093), and the other one with hexagonal closed packing (Co-hcp, space group $P6_3/mmc$, PDF card 01-089-7373). Elemental analysis of the bulk material showed 96.8 wt% of Co, 0.15 wt% of C and only 0.5 wt% of N. Complementary, XPS analysis displayed the presence of larger amounts of C, N, and O (C = 34.4, N = 1.2, O = 47.24 and Co = 16.8 at%) on the surface (Fig. S10†). The high resolution XP spectra of NPs in C1s region can be deconvoluted into five peak components with binding energies of 284.6, 285.6, 286.5, 288.5 and 289.4 eV corresponding to C–C sp^2, C–C sp^3, C–O/C–N, and

C=O, and O=C–O type bonds with individual atomic% of 64.09, 19.30, 8.59, 3.20 and 4.82 respectively, showing the graphitic nature of the carbon material (Fig. 5a). The presence of a specific N1s peak at 399.7 confirms pyrrolic nitrogen (Fig. 5b). The three peak components at 529.5, 531.4, and 532.9 eV in O1s spectra originate from the presence of Co(OH)$_2$ (6.99%), C=O (73.09%), and O–C on the surface of cobalt (19.92%). This reveals partial oxidation at the surface of the optimal material (Fig. 5c). In agreement, the two main component peaks having binding energy at 780.7 eV (50.81%) and 782.5 eV (22.54%) confirm the presence of Co^{2+} (Co(OH)$_2$) (Fig. 5d).[12a] Three small peaks having binding energies at 778.09 (2.45%), 781.09 (0.59%) and 783.09 (0.35%) eV indicate presence of metallic cobalt.[12b]

The HR-XPS of reused catalysts revealed that there is no shifting of binding energy in Co 2p$_{3/2}$ peak but the ratio of metallic cobalt *vs.* cobalt hydroxide was slightly changed (Fig. S11d†). On the other hand, no perceptible change in the binding energies of C1s and N1s was discerned except for the slight shifting of the pyrrolic nitrogen peak from 399.7 eV to 400.2 eV, thus reiterating no apparent alteration in the chemical nature of the carbon shell of the catalyst (Fig. S11a and b†).

It is interesting to note that these cobalt-particles exhibit ferromagnetic behaviour with distinct values of coercivity field and remanent magnetization (Fig. S12†). Ferromagnetic behaviour at room temperature is due to the stronger effect of the magnetic dipole interaction compared with thermal fluctuations. We do not observe any blocking temperature suggesting the size of nanoparticles above 10–15 nm (*e.g.* the system is not superparamagnetic at room temperature).
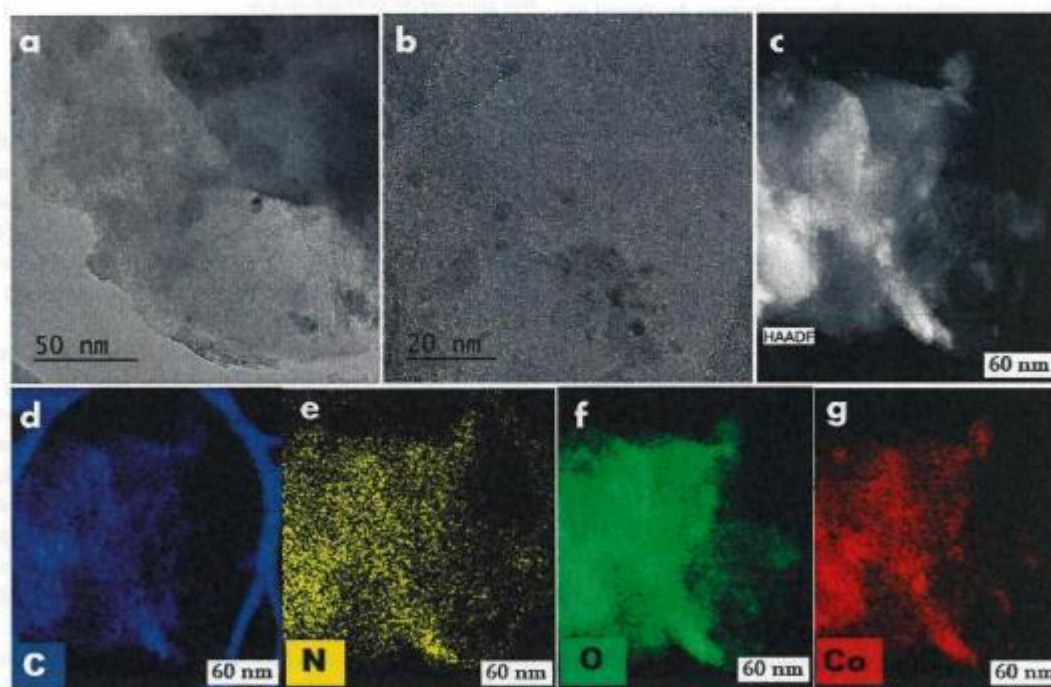
Fig. 4 TEM images of *in situ* generated Co-NPs from complex I. (a and b) HRTEM images of cobalt catalyst, (C) magnified STEM image, (d–g) elemental mapping images where C, N, O and Co are in blue, yellow, green and red colours.
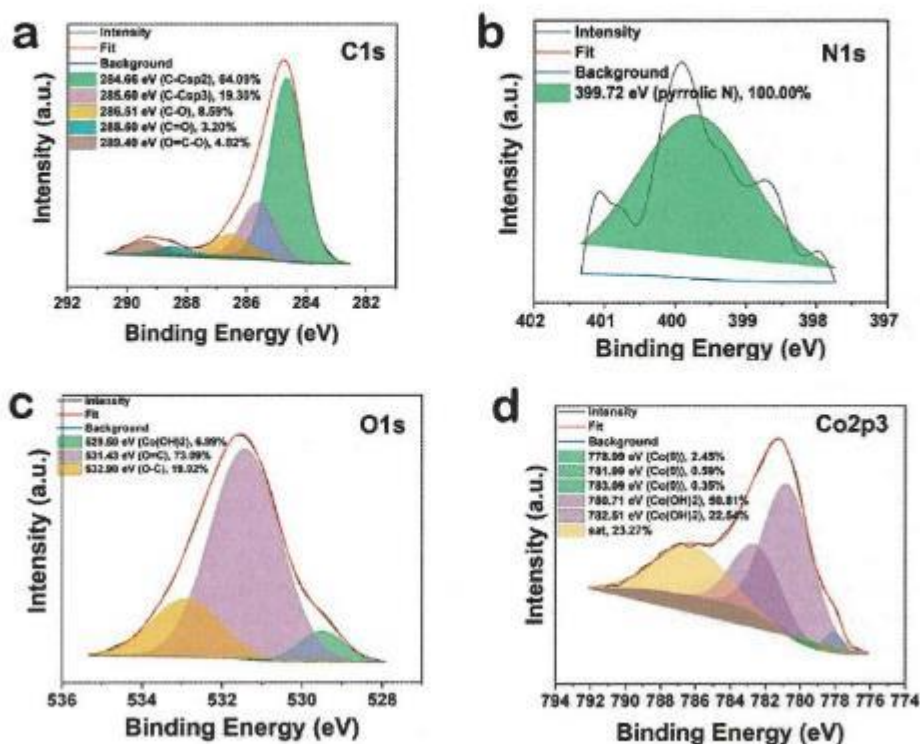
Fig. 5 HR-XPS spectra of *in situ* generated Co NPs.

Synthesis of linear primary amines

Then, we tested the general applicability of our *in situ* generated nanoparticles for the synthesis of primary amines. As shown in Schemes 1 and 2, a variety of structurally diverse and functionalized benzylic, heterocyclic and aliphatic linear and branched primary amines can be prepared in good to excellent yields. Simple and substituted aldehydes underwent smooth reaction to give primary benzylic amines in up to 92% yield (Scheme 1, products 3–7). For example, fluoro-, chloro-, and bromo-substituted benzaldehydes produced corresponding amines without significant dehalogenations in 86–92% yields (Scheme 1, entries 8–12). Different functionalized benzylic amines containing methoxy, trifluoromethoxy, dimethylamino, and ester groups as well as C–C double bonds were synthesized in up to 95% yield (Scheme 1, products 14–23). In addition to benzylic amines, primary aliphatic ones were also prepared under similar conditions (Scheme 1, products 25–27). Interestingly, the natural product perillaldehyde was successfully aminated to produce the corresponding amine in 87% yield (product 27).

Synthesis of branched primary amines

Next, we tested the reductive amination of ketones (Scheme 2), which is more challenging compared to aldehydes.

Nevertheless, at higher temperature (130 °C) nine aromatic and six aliphatic branched primary amines were prepared in up to 92% yield. In addition, separately prepared Co NPs from complex I, gave similar yields of amines to those obtained by *in situ* generated nanoparticles.

Synthesis of secondary and tertiary amines

Apart from primary amines synthesis, we explored the applicability of Co-NPs for the synthesis of secondary and tertiary amines. Interestingly, testing complex I which generates the active NPs *vide supra* for the reaction of benzaldehyde and aniline at 120 °C in presence of molecular hydrogen (40 bar) led to the formation of imine (N-benzylideneaniline) as the sole product. Under these conditions no nanoparticles could be isolated after the reaction.

Apparently, the presence of both ammonia and hydrogen are required for the generation of the active NPs! Indeed, using isolated Co NPs, which were prepared from complex I, ammonia and hydrogen, led to excellent activity and selectivity for the synthesis of secondary and tertiary amines including N-methyl amines (Scheme 3). As representative examples different benzaldehydes were reacted with substituted anilines and the corresponding N-benzylanilines were obtained in 87–98% yields (Scheme 1; products 41–45). Similarly, reactions of different benzaldehydes with benzylic and aliphatic amines produced selectively the corresponding secondary and tertiary amines (Scheme 3; products 46–55). In addition, aliphatic aldehydes and 4-fluoroaniline underwent reductive amination and gave the corresponding secondary amines (Scheme 3, products 56–57). Finally, N,N'-dimethylamines

Edge Article

Chemical Science
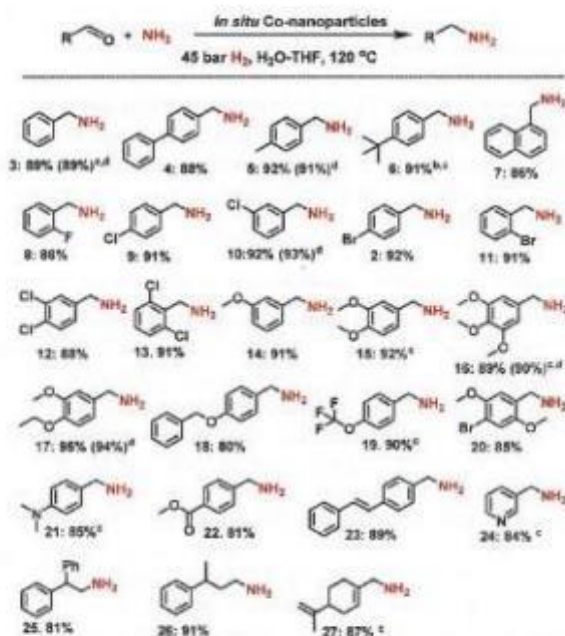
Scheme 1 *In situ* generated Co-nanoparticles catalyzed synthesis of linear primary amines from aldehydes[a]. [a]Reaction conditions: 0.5 mmol aldehyde, 6 mol% complex I (22 mg), 5–7 bar NH_3, 45 bar H_2, 2.5 mL H_2O–THF (1.5 : 1), 120 °C, 24h, isolated yields. [b] Same as 'a' at 130 °C. [c] Same as 'a' in 2.5 mL H_2O. [d] same as 'a' using prepared and isolated Co-NPs from complex I (2 mg; 6.5 mol% Co).
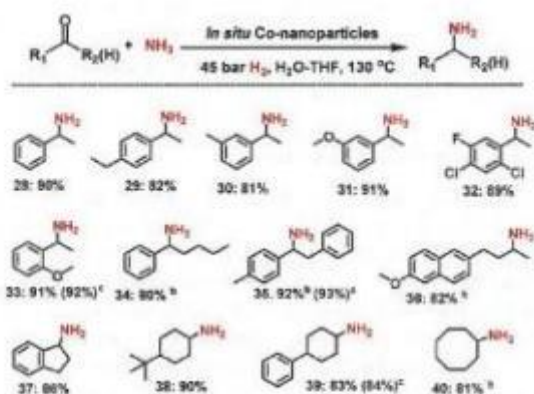
Scheme 2 Synthesis of branched primary amines from ketones using *in situ* generated Co-nanoparticles[a]. [a]Reaction conditions: 0.5 mmol ketone, 6 mol% complex I (22 mg) 5–7 bar NH_3, 45 bar H_2, 2.5 mL H_2O, 130 °C, 24 h, isolated yields. [b] Same as 'a' in H_2O–THF (1.5 : 1 ratio). [c]Using prepared and isolated Co-NPs from complex I (2 mg; 6.5 mol% Co).

were also prepared from three different aldehydes and aqueous *N,N*-dimethyl amine (Scheme 3, products 58–60).

Reaction upscaling

In order to demonstrate the synthetic utility of this novel reductive amination protocol, we performed the amination of 5
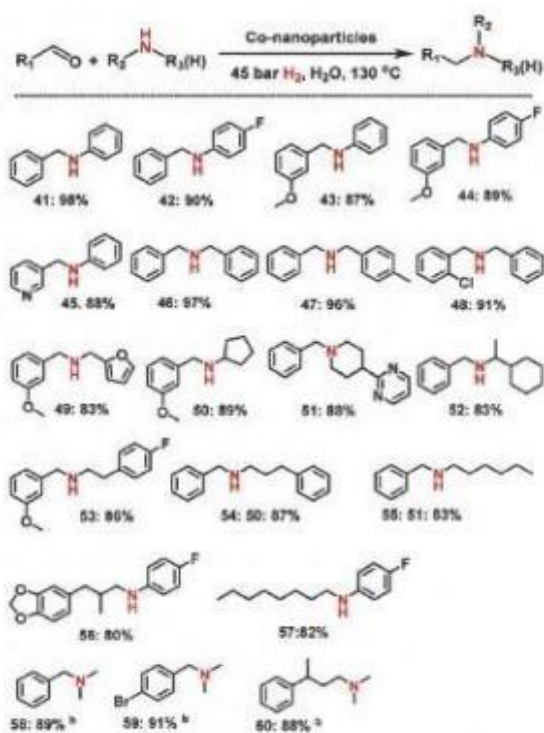
Scheme 3 Synthesis of secondary, tertiary and *N*-methyl amines using Co-nanoparticles prepared from complex I[a]. [a]Reaction conditions: 0.6 mmol aldehyde, 0.5 mmol amine, 2 mg Co-NPS (6.5 mol% Co), 45 bar H_2, 2.5 mL H_2O, 130 °C, 20 h, isolated yields. [b]Same as 'a' using 1 mL aq. *N,N*-dimethylamine instead of amine.

carbonyl compounds in 5–10 g scale (Scheme 4). As expected, all the tested reactions could be successfully upscaled and the yields (92–96%) of the corresponding primary amines were comparable to that of small scale (0.5 mmol) reactions.

Experimental

General considerations

All substrates were obtained commercially from various chemical companies and their purity has been checked before use. Cobalt(II) acetate tetrahydrate (cat no. 208396–50G), salicylaldehyde, phenylenediamine and other ligand precursors were purchased from Sigma-Aldrich. Silica (silicon(IV) oxide,
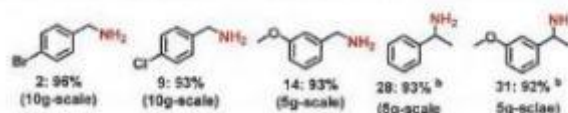
Scheme 4 Gram-scale synthesis of selected primary amines using *in situ* generated Co-NPs[a]. [a]Reaction conditions: 5–10 g of carbonyl compound, weight of complex I corresponds to 6 mol%, 5–7 bar NH_3, 45 bar H_2, 75–150 mL H_2O–THF (1 : 1), 120 °C, 24h, isolated yields. [b] Same as 'a' at 130 °C in 75 mL H_2O.

amorphous fumed, S.A. 300–350 m^2 g^{-1}) was obtained from Alfa Aesar. Carbon powder, VULCAN® XC72R with Code XVC72R and CAS No. 1333-86-4 was obtained from Cabot Corporation Prod. The pyrolysis experiments were carried out in a Nytech-Qex oven.

X-ray diffraction patterns were recorded with an Empyrean (PANalytical, The Netherlands) diffractometer in the Bragg–Brentano geometry, Co-Kα radiation (40 kV, 30 mA, λ = 0.1789 nm) equipped with a PIXcel3D detector (1D mode) and programmable divergence and diffracted beam anti-scatter slits. The measurement range was 2θ: 5–105°, with a step size of 0.026°. The identification of crystalline phases was performed using the High Score Plus software (PANalytical) that includes the PDF-4$^+$ database.

TEM images were obtained using a HRTEM TITAN 60-300 with X-FEG type emission gun, operating at 80 kV. This microscope is equipped with a Cs image corrector and a STEM high-angle annular dark-field detector (HAADF). The point resolution is 0.06 nm in TEM mode. The elemental mappings were obtained by STEM-Energy Dispersive X-ray Spectroscopy (EDS) with an acquisition time of 20 min. For HRTEM analysis, the powder samples were dispersed in ethanol and ultrasonicated for 5 min. One drop of this solution was placed on a copper grid with holey carbon film.

XPS surface investigation has been performed on the PHI 5000 VersaProbe II XPS system (Physical Electronics) with monochromatic Al-Kα source (15 kV, 50 W) and photon energy of 1486.7 eV. Dual beam charge compensation was used for all measurements. All the spectra were measured in the vacuum of 1.3 × 10^{-7} Pa and at room temperature of 21 °C. The analyzed area on each sample was a spot of 200 μm in diameter. The survey spectra were measured with pass energy of 187.850 eV and electronvolt step of 0.8 eV while for the high resolution spectra was used pass energy of 23.500 eV and electronvolt step of 0.2 eV. The spectra were evaluated with the MultiPak (Ulvac – PHI, Inc.) software. All binding energy (BE) values were referenced to the carbon peak C 1s at 284.80 eV.

Magnetic properties of cobalt-nanoparticles were analyzed using a Quantum Design Physical Properties Measurement System (PPMS Dynacool system) with the vibrating sample magnetometer (VSM) option. The experimental data were corrected for the diamagnetism and signal of the sample holder. The temperature dependence of the magnetization was recorded in a sweep mode of 1 K min^{-1} in the zero-field-cooled (ZFC) and field-cooled (FC) measuring regimes. To get the ZFC magnetization curve, the sample was firstly cooled down from 300 to 5 K in a presence of zero magnetic field and the measurement was carried out on warming from 5 to 300 K under the external magnetic field (1000 Oe). In the case of the FC magnetization measurements, the sample was cooled from 300 to 5 K in an external magnetic field (1000 Oe) and the measurement was carried out on warming from 5 to 300 K at the same value of the external magnetic field (1000 Oe). Hysteresis loops were measured at room temperature (300 K) and at low temperature (5 K).

GC conversion and yields were determined by GC-FID, HP6890 with FID detector, column HP530 m × 250 mm ×

0.25 μm. ^{1}H, ^{13}C, NMR data were recorded on a Bruker ARX 300 and Bruker ARX 400 spectrometers using DMSO-d$_6$ and CDCl$_3$ solvents.

All catalytic reactions were carried out in 300 mL and 100 mL autoclaves (PARR Instrument Company). In order to avoid unspecific reactions, catalytic reactions were carried out either in glass vials, which were placed inside the autoclave, or glass/Teflon vessel fitted autoclaves.

Preparation of Co–salen complexes (see scheme S1†)

(a) Preparation of salen ligand (L1). Salicylaldehyde (4 mmol; in 15 mL ethanol), 1,2-phenylenediamine (2 mmol; in 10 mL ethanol) were separately dissolved in ethanol. Then, the ethanolic solution of 1,2-phenylenediamine was slowly added to salicylaldehyde solution. The resulting reaction mixture was refluxed at 80 °C for 8 h to obtain a solid compound. The reaction mixture was cooled to room temperature and the product was isolated by filtration. Then, the solid product was washed with 30 mL of cold ethanol twice and dried *in vacuo* to get corresponding salen ligand (L1) in 98% yield. Other salen ligands were prepared by using similar method.

(b) Preparation of Co–salen complex (complex I).[13] 1 g of Co(OAc)$_2$·4H$_2$O, (4 mmol; in 15 mL ethanol) and 1.28 g of *N,N'*-bis(salicylidene)-1,2-phenylenediamine (ligand L1) (4 mmol; in 20 mL ethanol) were separately dissolved in ethanol. The cobalt acetate solution was slowly added to the solution of ligand. The resulting red suspension was refluxed for 18 h at 80 °C to give a reddish-brown solid compound. The obtained solid compound was filtered. Then the obtained solid compound was washed with 10 mL of cold ethanol and dried *in vacuo* to get corresponding cobalt salen complex I in 94% yield. The same procedure was applied to prepare other cobalt salen complexes using different salen ligands.

Procedure for reductive amination

(a) Procedure for the synthesis of primary amines. The magnetic stirring bar, 0.5 mmol of the carbonyl compound (aldehyde or ketone) and 22 mg complex I (in case of *in situ* generated Co NPs) or 2 mg of prepared and isolated Co NPs were transferred to an 8 mL glass vial. Then, 2 mL of solvent (water or THF/H$_2$O (1.5 : 1)) was added and the vial was fitted with septum, cap and needle. The reaction vials (8 vials with different substrates at a time) were placed into a 300 mL autoclave. The autoclave was flushed with hydrogen twice at 40 bar pressure and then it was pressurized with 5–7 bar ammonia and 45 bar hydrogen. The autoclave was placed into an aluminium block preheated at 135 °C in case of aldehydes and 145 °C in case of ketones and the reactions were stirred for the required time. During the reaction, the inside temperature of the autoclave was measured to be 120 °C in case of aldehydes and 130 °C in case of ketones and this temperature was used as the reaction temperature. After completion of the reactions, the autoclave was cooled to room temperature. The remaining ammonia and hydrogen were discharged and the vials containing reaction products were removed from the autoclave. The reaction mixtures containing the products were filtered off and washed

thoroughly with ethanol. The reaction products were analyzed by GC-MS. The crude product was purified by column chromatography using ethyl acetate and *n*-heptane as the eluent. The corresponding primary amines were converted to their respective hydrochloride salt and characterized by NMR and GC-MS analysis. For converting into hydrochloride salt of amine, 0.3–0.5 mL 7 M HCl in dioxane or 1.5 M HCl in methanol was added to the dioxane solution of respective amine and stirred at room temperature for 4–5 h. Then, the solvent was removed and the resulted hydrochloride salt of amine was dried under high vacuum. The yields were determined by GC for the selected amines: after completing the reaction, *n*-hexadecane (100 µL) as standard was added to the reaction vials and the reaction products were diluted with ethyl acetate followed by filtration using plug of silica and then analyzed by GC.

(b) **Procedure for the synthesis of secondary and tertiary amines.** The magnetic stir bar, 0.5 mmol of amine and 0.6 mmol aldehyde were transferred to an 8 mL glass vial. Then 2 mg of Co NPs and 2 mL of water as solvent were added. The vial was fitted with septum, cap and needle. The reaction vials (8 vials with different substrates at a time) were placed into a 300 mL autoclave. The autoclave was flushed with hydrogen twice at 40 bar pressure and then it was pressurized 45 bar hydrogen. The autoclave was placed into an aluminium block preheated at 145 °C and the reactions were stirred for the required time. During the reaction, the inside temperature of the autoclave was measured to be 130 °C and this temperature was used as the reaction temperature. After completion of the reactions, the autoclave was cooled to room temperature. The remaining hydrogen was discharged and the vials containing the reaction products were removed from the autoclave. The reaction mixtures containing the products were filtered off and washed thoroughly with ethanol. The reaction products were analyzed by GC-MS. The crude product was purified by column chromatography using ethyl acetate and *n*-heptane as the eluent. The corresponding amines were characterized by NMR and GC-MS analysis.

Isolation of *in situ* generated cobalt nanoparticles

After the completion of the reductive amination reaction of carbonyl compound in presence of ammonia and hydrogen as described in Section S3a,† the *in situ* generated cobalt nanoparticles from the solution containing products were separated using the magnetic stir bar. Then, they were separated from the magnetic stir bar and washed with water and ethanol. Finally the recycled Co NPs were dried under vacuum and stored in a glass vial.

Elemental analysis (wt%): Co = 96.8% C = 0.15% and N = 0.5%.

Recycling of *in situ* generated cobalt-nanoparticles

A magnetic stirring bar and 5 mmol 4-bromobenzaldehyde were transferred to a glass fitted 100 mL autoclave and then 20 mL THF–water (1.5 : 1) was added. Subsequently, 20 mg isolated *in situ* generated Co NPs were added. The autoclave was flushed with 40 bar hydrogen and then it was pressurized with 5–7 bar

ammonia gas and 45 bar hydrogen. The autoclave was placed into the heating system and the reaction was allowed to progress at 120 °C (temperature inside the autoclave) by stirring for 24 h. After completion of the reaction, the autoclave was cooled and the remaining ammonia and hydrogen pressure was discharged. To the reaction products, 200 µL *n*-hexadecane as standard was added. The catalyst was then separated by centrifugation and the supernatant containing the reaction products was subjected to GC analysis for determining conversion and yield. The separated catalyst was then washed with ethanol, dried under vacuum and used without further purification or reactivation for the next run.

Gram-scale reactions

The Teflon or glass fitted 300 mL autoclave was charged with a magnetic stirring bar and 5–10 g of carbonyl compound (aldehyde or ketone) and complex I (weight of complex I corresponds 6 mol%). Then, 75–150 mL of solvent (THF/H$_2$O (1.5 : 1) in case of aldehyde and H$_2$O in case of ketones) was added and the autoclave was flushed with hydrogen twice at 40 bar pressure. Afterwards, it was pressurized with 5–7 bar ammonia and 45 bar hydrogen. The autoclave was placed into an aluminium block preheated at 135 °C in case of aldehydes and 145 °C in case of ketones and the reactions were stirred for the required time. During the reaction, the inside temperature of the autoclave was measured to be 120 °C in case of aldehydes and 130 °C in case of ketones and this temperature was used as the reaction temperature. After completion of the reaction, the autoclave was cooled to room temperature and the remaining ammonia and hydrogen were discharged. The reaction mixtures containing the products were filtered off and washed thoroughly with ethanol. The reaction products were analysed by GC-MS and the crude primary amine product was purified by column chromatography using ethyl acetate and *n*-heptane as the eluent.

Preparation of cobalt-nanoparticles

(a) **Preparation of Co NPs from complex I.** A magnetic stir bar and 1.0 g of cobalt–salen complex (complex I) were transferred to a glass fitted 100 mL autoclave. Then, 20 mL THF–water (1 : 1) was added. The autoclave was flushed with 40 bar hydrogen and then it was pressurized with 5–7 bar ammonia and 45 bar hydrogen. The autoclave was placed into the heating system and the reaction was allowed to progress at 120 °C (temperature inside the autoclave) by stirring for 24 h. After 24 h of reaction time, the autoclave was removed from the heating system and cooled to room temperature. The remaining ammonia and hydrogen pressure was discharged. The cobalt nanoparticles formed were separated from solution by using the magnetic stir bar. Then, the nanoparticles were separated from the magnetic stir bar and washed with water and ethanol. Finally obtained nanoparticles were dried under vacuum and stored in a glass vial.

(b) **Preparation of carbon and silica supported Co-nanoparticles.** In a 50 mL round bottomed flask, cobalt salen complex (316.8 mg) and 25 mL of ethanol were refluxed at 80 °C

for 15 minutes. To this, 700 mg of Vulcan XC 72R carbon powder or SiO_2 was added and then the whole reaction mixture was refluxed at 80 °C for 4–5 h. The reaction mixture was cooled to room temperature and the ethanol was removed in vacuum. The solid sample obtained was dried in high vacuum, after which it was grinded to a fine powder. Then, the grinded powder was pyrolyzed at 800 °C for 2 hours under an argon atmosphere and cooled to room temperature.

(c) **Preparation of other cobalt nanoparticles reported in literature.**[11] *Method-I*: 1.0 g of cobalt acetate and 1.5 mL of oleic acid were mixed in 40 mL of diphenyl ether (DPE) and the reaction mixture was heated to 200 °C under N_2 atmosphere. Then, 1.0 mL of TOP (trioctylphosphine) was added and the mixture was again heated to 250 °C. Subsequently, the reducing solvent such as 4.0 g of 1,2-dodecanediol dissolved in 10 mL DPE at 80 °C, was injected into the reaction mixture. Then whole reaction mixture was held at 250 °C for 30 min until the completion of the reduction. The reaction products were cooled to room temperature and ethanol was added to precipitate nanoparticles. The formed cobalt nanoparticles were separated by centrifugation and were finally dried and stored in glass vial.

Method-II: 2 mmol of cobalt acetate and 0.4 mmol of oleic acid were mixed in 1 mL ethanol. Then, 3 mmol of $NaBH_4$ dissolved in 1 mL of ethanol, was slowly added to the above mixture at room temperature under stirred condition. The whole mixture was stirred at room temperature for 4 h. The formed cobalt nanoparticles were separated by centrifugation and finally dried and stored in glass vial.

Conclusions

In conclusion, we demonstrated that the *in situ* formation of cobalt nanoparticles from molecularly defined precursors is straightforward and convenient. Such approach can be used as a versatile tool to prepare selective and active heterogeneous catalysts. In our specific case, Co NPs are formed from cobalt–salen complexes (*e.g.* cobalt(II)–*N,N'*-bis(salicylidene)-1,2-phenylenediamine) in the presence of ammonia and hydrogen. Thereby, well-defined ultra-small metallic cobalt and cobalt hydroxide nanoparticles embedded in a cobalt–nitrogen framework are formed. The resulting NPs are stable in the presence of air and water and allow for the preparation of various functionalized and structurally diverse linear and branched benzylic, heterocyclic and aliphatic primary amines as well as secondary and tertiary amines. Moreover, they can be easily magnetically separated enabling easy catalyst recycling and product purification.

Conflicts of interest

There are no conflicts to declare.

Acknowledgements

Notes and references

1 (a) D. Wang and D. Astruc, *Chem. Soc. Rev.*, 2017, **46**, 816–854; (b) L. Liu and A. Corma, *Chem. Rev.*, 2018, **8**, 4981–5079; (c) X. Cui, X. Dai, Y. Deng and F. Shi, *Chem.–Eur. J.*, 2013, **19**, 3665–3675; (d) R. V. Jagadeesh, A.-E. Surkus, H. Junge, M.-M. Pohl, J. Radnik, J. Rabeah, H. Huan, V. Schünemann, A. Brückner and M. Beller, *Science*, 2013, **342**, 1073–1076; (e) R. V. Jagadeesh, K. Murugesan, A. S. Alshammari, H. Neumann, M.-M. Pohl, J. Radnik and M. Beller, *Science*, 2017, **358**, 326–332; (f) L. He, F. Weniger, H. Neumann and M. Beller, *Angew. Chem., Int. Ed.*, 2016, **55**, 12582–12594; (g) T. Schwob and R. Kempe, *Angew. Chem., Int. Ed.*, 2016, **55**, 15175–15179; (h) G. Hahn, P. Kunnas, N. de Jonge and R. Kempe, *Nat. Catal.*, 2018, **2**, 71–77; (i) K. Murugesan, M. Beller and R. V. Jagadeesh, *Angew. Chem., Int. Ed.*, 2019, **58**, 5064–5068; (j) K. Murugesan, T. Senthamarai, A. S. Alshammari, R. M. Altamimi, C. Kreyenschulte, M.-M. Pohl, H. Lund, R. V. Jagadeesh and M. Beller, *ACS Catal.*, 2019, **9**, 8581–8591; (k) R. V. Jagadeesh, T. Stemmler, A.-E. Surkus, M. Bauer, M.-M. Pohl, J. Radnik, K. Junge, H. Junge, A. Brückner and M. Beller, *Nat. Protoc.*, 2015, **10**, 916–926; (l) T. Schwob, P. Kunnas, N. de Jonge, C. Papp, H. P. Steinrück and R. Kempe, *Sci. Adv.*, 2019, **5**, eaav3680; (m) T. Schwob, M. Ade and R. Kempe, *ChemSusChem*, 2019, **12**, 3013–3017.
2 (a) G. W. Parshall and S. D. Ittel, *Homogeneous Catalysis: The Applications and Chemistry of Catalysis by Soluble Transition Metal Complexes*, Weily, 1992; (b) P. W. N. M. van Leeuwen and J. C. Chadwick, *Homogeneous Catalysts: Activity – Stability – Deactivation*, Wiley-VCH, 2011; (c) B. Cornils, W. A. Herrmann, M. Beller and R. Paciello, *Applied Homogeneous Catalysis with Organometallic Compounds*, Wiley-VCH, 2017; (d) B. A. Averill, J. A. Moulijn, R. A. van Santen and P. W. N. M. van Leeuwen, *Catalysis: An integrated approach*, Elsevier, 1997.
3 (a) L. Filipponi and D. Sutherland, *Nanotechnologies: Principles, Applications, Implications and Hands-on Activities*, European Commission, European Union, 2012; (b) M. B. Gawande, S. P. Branco and R. S. Varma, *Chem. Soc. Rev.*, 2013, **42**, 3371–3393; (c) M. B. Gawande, A. Goswami, T. Asefa, H. Guo, A. V. Biradar, D. L. Peng, R. Zboril and R. S. Varma, *Chem. Soc. Rev.*, 2015, **44**, 7540–7590; (d) P. Munnik, P. E. De Jongh and K. P. De Jong, *Chem. Rev.*, 2015, **115**, 6687–6718; (e) M. Sankar, N. Dimitratos, P. J. Miedziak, P. P. Wells, C. J. Kielye and G. J. Hutchings,

Chem. Soc. Rev., 2012, **41**, 8099–8139; (*f*) F. Tao, *Metal Nanoparticles for Catalysis: Advances and Applications*, Royal Society of Chemistry, 2014; (*g*) E. M. van Schrojenstein Lantman, T. Deckert-Gaudig, A. J. G. Mank, V. Deckert and B. M. Weckhuysen, *Nat. Nanotechnol.*, 2012, **7**, 583–586; (*h*) J. J. H. B. Sattler, J. Ruiz-Martinez, E. Santillan-Jimenez and B. M. Weckhuysen, *Chem. Rev.*, 2014, **114**, 10613–10653; (*i*) A. Balanta, C. Godard and C. Claver, *Chem. Soc. Rev.*, 2011, **40**, 4973–4985.

4 (*a*) S. Dang, Q.-L. Zhu and Q. Xu, *Nat. Rev. Mater.*, 2017, **3**, 17075; (*b*) J. Tang and Y. Yamauchi, *Nat. Chem.*, 2016, **8**, 638–639; (*c*) K. Shen, X. Chen, J. Chen and Y. Li, *ACS Catal.*, 2016, **6**, 5887–5903.

5 (*a*) N. Yan, Y. Yuan and P. J. Dyson, *Dalton Trans.*, 2013, **42**, 13294–13304; (*b*) Da. Cantillo, M. Baghbanzadeh and C. O. Kappe, *Angew. Chem., Int. Ed.*, 2012, **51**, 10190–10193; (*c*) J. Holz, C. Pfeffer, H. Zuo, D. Beierlein, G. Richter, E. Klemm and R. Peters, *Angew. Chem., Int. Ed.*, 2019, **58**, 10330–10334; (*d*) L. Zadoina, K. Soulantica, S. Ferrere, B. Lonetti, M. Respaud, A. F. Mingotaud, A. Falqui, A. Genovese, B. Chaudret and M. Mauzac, *J. Mater. Chem.*, 2011, **21**, 6988–6994.

6 (*a*) A. Ricci, *Amino group chemistry: From synthesis to the life sciences*, Wiley-VCH, 2008; (*b*) Top 200 drugs production, National Science Foundation, *J Chem. Educ.*, 2010, **87**, 1348; (*c*) S. A. Lawrence, *Amines: synthesis, properties and applications*, Cambridge University Press, 2004; (*d*) F. Shi and X. Cui, *Catalytic amination for N-alkyl amine synthesis*, Academic Press, 2018; (*e*) W. R. Meindl, E. V. Angerer, H. Schoenenberger and G. Ruckdeschel, *Med. Chem.*, 1984, **27**, 1111–1118; (*f*) V. Froidevaux, C. Negrell, S. Caillol, J.-P. Pascault and B. Boutevin, *Chem. Rev.*, 2016, **116**, 14181–14224; (*g*) T. Yan, B. L. Feringa and K. Barta, *Nat. Commun.*, 2014, **5**, 5602.

7 (*a*) S. Gomez, J. A. Peters and T. Maschmeyer, *Adv. Synth. Catal.*, 2002, **344**, 1037–1057; (*b*) H. Alinezhad, H. Yavari and F. Salehian, *Curr. Org. Chem.*, 2015, **19**, 1021–1049; (*c*) T. C. Nugenta and M. El-Shazlya, *Adv. Synth. Catal.*, 2010, **352**, 753–819; (*d*) K. Natte, H. Neumann, R. V. Jagadeesh and M. Beller, *Nat. Commun.*, 2017, **8**, 1344; (*e*) https://reagentguides.com/reagent-guides/reductive-amination/list-of-reagents/hydrogen-metal-catalysts-precious-and-base-

metal; (*f*) K. N. Gusak, Z. V. Ignatovich and E. V. Koroleva, *Russ. Chem. Rev.*, 2015, **84**, 288–309.

8 (*a*) Y. Nakamura, K. Kon, A. S. Touchy, K.-I. Shimizu and W. Ueda, *ChemCatChem*, 2015, **7**, 921–924; (*b*) G. Liang, A. Wang, L. Li, G. Xu, N. Yan and T. Zhang, *Angew. Chem., Int. Ed.*, 2017, **56**, 3050–3054; (*c*) T. Komanoya, T. Kinemura, Y. Kita, Y. K. Kamata and M. Hara, *J. Am. Chem. Soc.*, 2017, **139**, 11493–11499; (*d*) M. Chatterjee, T. Ishizakaa and H. Kawanami, *Green Chem.*, 2016, **18**, 487–496.

9 (*a*) T. Gross, A. M. Seayad, M. Ahmad and M. Beller, *Org. Lett.*, 2002, **4**, 2055–2058; (*b*) T. Riermeier, K.-J. Haack, U. Dingerdissen, A. Börner, V. Tararov and R. Kadyrov, *US Pat.*, 6884887B1, 2005; (*c*) J. Gallardo-Donaire, M. Ernst, O. Trapp and T. Schaub, *Adv. Synth. Catal.*, 2016, **358**, 358–363; (*d*) J. Gallardo-Donaire, M. H. Wysocki, M. Ernst, F. Rominger, O. Trapp, A. Stephen, L. Hashmi, A. Schaefer, P. Comba and T. Schaub, *J. Am. Chem. Soc.*, 2018, **140**, 355–361; (*e*) S. Ogo, K. Uehara, T. Abura and S. Fukuzumi, *J. Am. Chem. Soc.*, 2014, **126**, 3020–3021; (*f*) R. Kadyrov and T. H. Riermeier, *Angew. Chem., Int. Ed.*, 2003, **42**, 5472–5474; (*g*) T. Senthamarai, K. Murugesan, J. Schneidewind, N. V. Kalevaru, W. Baumann, H. Neumann, P. C. J. Kamer, M. Beller and R. V. Jagadeesh, *Nat. Commun.*, 2018, **9**, 4123; (*h*) X. Tan, S. Gao, W. Zeng, S. Xin, Q. Yin and X. Zhang, *J. Am. Chem. Soc.*, 2018, **140**, 2024–2027.

10 (*a*) Z. Wang, *"Mignonac reaction" in comprehensive organic name reactions and reagents*, Wiley, 2010; (*b*) https://erowid.org/archive/rhodium/chemistry/reductive.amination.html, 2004.

11 A. S. Zola, R. U. Ribeiro, J. M. C. Bueno, D. Zanchet and P. A. Arroyo, *J. Exp. Nanosci.*, 2014, **9**, 398–405.

12 (*a*) J. Yang, H. Liu, W. N. Martens and R. L. Frost, *J. Phys. Chem.*, 2010, **114**, 111–119; (*b*) C. D. Wagner, L. E. Davis, J. F. Moulder and G. E. Mullenberg, *Handbook of X-ray Photoelectron Spectroscopy*, Minnesota: Perkin-Elmer Corporation, 1978.

13 (*a*) A. A. Khandar, B. Shaabani, F. Belaj and A. Bakhtiari, *Inorg. Chim. Acta*, 2007, **360**, 3255–3264; (*b*) A. van Den Bergen, K. S. Murray and B. O. West, *J. Organomet. Chem.*, 1971, **33**, 89–96.

Expedient Synthesis of N-Methyl- and N-Alkylamines by Reductive Amination using Reusable Cobalt Oxide Nanoparticles

Thirusangumurugan Senthamarai,[a] Kathiravan Murugesan,[a] Kishore Natte,[a, b]
Narayana V. Kalevaru,[a] Helfried Neumann,[a] Paul C. J. Kamer,[a] and
Rajenahally V. Jagadeesh*[a]

N-Methyl- and N-alkylamines represent important fine and bulk chemicals that are extensively used in both academic research and industrial production. Notably, these structural motifs are found in a large number of life-science molecules and play vital roles in regulating their activities. Therefore, the development of convenient and cost-effective methods for the synthesis and functionalization of amines by using earth-abundant metal-based catalysts is of scientific interest. In this regard, herein we report an expedient reductive amination process for the selective synthesis of N-methylated and N-alkylated amines by using nitrogen-doped, graphene-activated nanoscale Co_3O_4-based catalysts. Starting from inexpensive and easily accessible nitroarenes or amines and aqueous formaldehyde or aldehydes in the presence of formic acid, this cost-efficient reductive amination protocol allows the synthesis of various N-methyl- and N-alkylamines, amino acid derivatives, and existing drug molecules.

Amines, which are produced on a multimillion ton scale per annum, represent highly privileged chemicals that are used extensively in research laboratories, industrial production, and drug discovery.[1] The majority of the existing life-science molecules and natural products contain amino groups, which constitute key scaffolds and play vital roles in their functions.[1c] Owing to the enormous utilization and "noble" applications of amines, the development of more cost-effective and convenient methods for their synthesis and functionalization starting from easily available feedstocks and abundant reagents continues to be an actual and important task for organic synthesis and the chemical industry. Regarding their synthesis and functionalization, catalytic reductive amination is a method that is used widely in research laboratories and industries.[2–4] In general, most known reductive aminations have been performed by using high-pressure molecular hydrogen in the presence of precious-metal-based catalysts.[2,3] In recent years, a few non-noble-metal-based catalysts have also been developed for these reactions.[4] However, for the laboratory preparation of amines, to avoid the use of high-pressure hydrogen and specialized equipment, alternative methods are highly desired. In this regard, complementary to molecular hydrogen is formic acid, which is a nontoxic and easily handled chemical. Noteworthy, this abundant and cost-effective liquid serves as a suitable hydrogen-storage material[5] and has been used in transfer hydrogenation reactions for the preparation of various chemicals.[6,7] Hence, reductive aminations performed with the use of formic acid represent useful and operationally simple procedures.[6] To achieve more sustainable and cost-efficient reductive amination processes to access highly functionalized and structurally diverse amines, the use of appropriate catalysts is crucial.

With respect to modern, state-of-the-art catalysts, there exists increasing interest in earth-abundant metal-based systems owing to their high abundance, low cost, and low toxicity.[8,9] In recent years, molecularly defined non-noble metal complexes have been successfully developed for selected organic synthesis for reactions for which noble metals were previously required.[8] However, most homogeneous complexes are sensitive and need synthetically demanding ligand systems. In contrast to these homogeneous complexes, nanomaterial-based heterogeneous catalysts are highly preferable for the advancement of more sustainable processes, because these materials are extremely stable, easily separable, and reusable.[10,11] Despite the existence of thousands of such materials, most of them work under drastic conditions and are difficult to apply for the refinement of complex molecules. Hence, the search for new materials and suitable precursors to produce active and selective nanocatalysts, especially those based on base metals, continues to attract the attention of academic and industrial researchers. In this regard, we previously introduced nitrogen-ligated cobalt complexes as precursors to produce nitrogen-doped graphene (NGr)-activated nanoscale Co_3O_4 particles supported on carbon under pyrolysis (Co_3O_4/NGr@C catalysts).[12a] Remarkably, these cobalt-oxide nanoparticles were shown to be excellent catalysts for highly selective redox reactions involving functionalized molecules.[4f–g,7d,12] Motivated by these cobalt materials (Co_3O_4/NGr@C) and on the basis of our continuous work to develop sustainable processes for amines synthesis, herein we demonstrate the synthesis of N-methyl- and N-al-

[a] T. Senthamarai, K. Murugesan, Dr. K. Natte, Dr. N. V. Kalevaru,
Dr. H. Neumann, Prof. Dr. P. C. J. Kamer, Dr. R. V. Jagadeesh
Leibniz-Institut für Katalyse e. V. an der Universität Rostock
Albert-Einstein-Str. 29a, 18059 Rostock (Germany)
E-mail: Jagadeesh.Rajenahally@catalysis.de

[b] Dr. K. Natte
CSIR-Indian Institute of Petroleum
Haridwar Road Dehradun 248005 (India)

kylamines starting from nitro compounds or amines and aqueous formaldehyde or aldehydes.

Typically, the immobilization and subsequent pyrolysis of in situ generated nitrogen-ligated Co complexes on commercial carbon (Vulcan XC72R) at 800 °C under an argon atmosphere produces nanoscale Co_3O_4 particles and generates specific nitrogen-doped graphene surfaces that surround cobalt-oxide particles.[12a] (Figure 1)

1. Immobilization on carbon

2. Pyrolysis (800 °C, 2h, Ar)

Co_3O_4-nanoparticles covered by nitrogen doped graphene surfaces
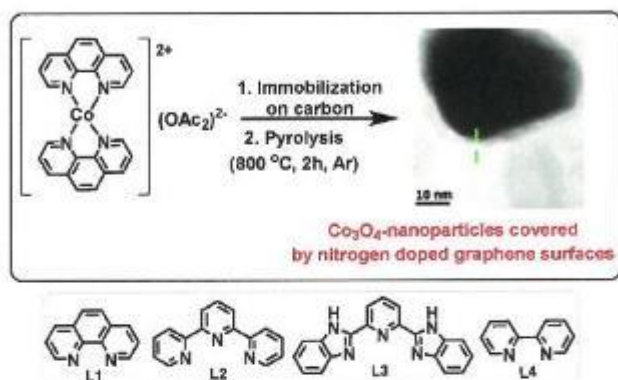
Figure 1. Conversion of a homogeneous cobalt–nitrogen complex into nitrogen-doped, graphene-activated nanoscale Co_3O_4 particles supported on carbon.

To demonstrate the applicability of our cobalt-based materials for reductive N-methylation, 4-methoxynitrobenzene was treated with aqueous formaldehyde as a methylation reagent in the presence of formic acid as the hydrogen source. As seen from Figure 2, pyrolysis of in situ generated cobalt–nitrogen complexes with different ligands on carbon exhibited varying
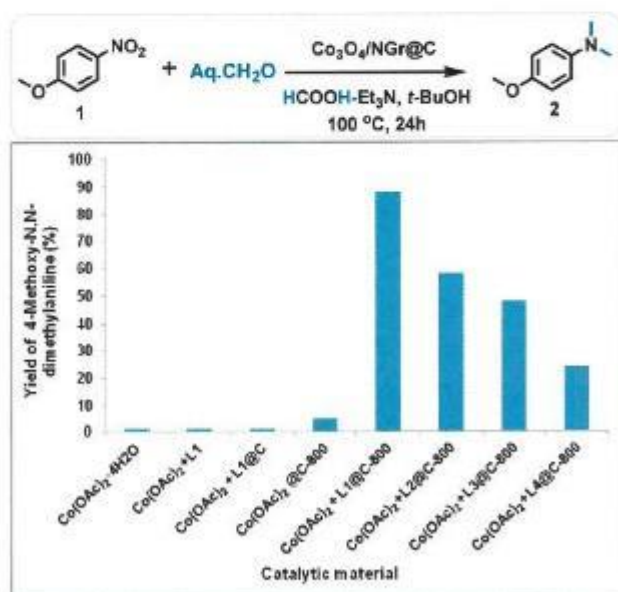
Figure 2. Cobalt-catalyzed reductive N-methylation of 4-methoxynitrobenzene: activity of cobalt catalysts.

catalytic activities. The pyrolysis of Co(OAc)$_2$–L1 (L1 = phenanthroline) on carbon led to a highly active catalytic material and produced 4-methoxy-N,N-dimethylaniline in 88% yield (Figure 2). However, related cobalt materials prepared by using ligands L2–L4 showed lower activity (25–59%). As expected, the homogeneous cobalt complex and pyrolyzed simple cobalt acetate on carbon showed no activity.

The active material Co–L1@C-800 was characterized by transmission electron microscopy (TEM), X-ray photoelectron spectroscopy (XPS), electron paramagnetic resonance (EPR) spectroscopy, and X-ray diffraction (XRD) analysis[12a,c] (for detailed characterization, see the Supporting Information). The characterization data reveal that the active material mainly contains Co_3O_4 particles of 2–10 nm size. These cobalt-oxide nanoparticles are surrounded by a nitrogen-doped graphene layers (Figure 3; also see Figures S2 and S3 in the Supporting Information). In addition, a very small Co and/or CoO core and
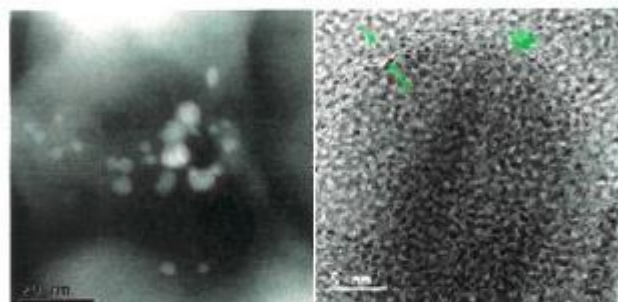
Figure 3. TEM images of the Co_3O_4/NGr@C catalyst: Images of nanoparticle distribution (right) and visualization of the formed nitrogen-doped graphene layers (left).

a Co_3O_4 shell with a size of 20–80 nm are also present (Figures 3, S2, and S3). The nature of the nitrogen species was determined by XPS analysis, which showed three distinct peaks in the N 1s spectra with electron binding energies of 399.0, 400.8, and 402.3 eV (Figure S7). The lowest binding energy peak is recognized as pyridine-type nitrogen, which is bound to a metal ion. The next electron binding energy of 400.8 eV is characteristic for pyrrole-type nitrogen. Finally, the peak at an electron binding energy of 402.3 eV is assigned to quaternary amine species. These characterization studies confirm that the active material contains mainly nanoscale Co_3O_4 particles, which are surrounded by nitrogen-doped graphene layers. Notably, the formation of nanosized cobalt-oxide particles and the generation of nitrogen-doped graphene layers, which activate the Co_3O_4 particles, are important for the activity of the catalyst. The Co–N interactions can facilitate decomposition of formic acid to generate hydrogen in situ and also enhance the reactivity of the reductive amination reaction.

With the active material (Co_3O_4/NGr@C) and the set of optimized conditions in hand, we performed the reductive N-methylation of nitroarenes by using aqueous formaldehyde in the presence of formic acid. Among the different kinds of amines, N-methylated derivatives are of special interest, as this small motif plays a vital role in regulating the biological and

pharmaceutical properties of all kinds of life-science molecules.[13] In addition, the N-methyl moiety present in bioactive molecules such as peptides and DNA controls biological functions and also plays a significant role in the actions of enzymes and antibodies and in pharmacokinetics and drug delivery.[13] On the laboratory scale, especially in drug discovery, N-methylamines have been prepared by using activated, but toxic methyl compounds such as methyl iodide and dimethyl sulfate, which generate significant amounts of waste.[14] However, in industry these products are frequently synthesized by Eschweiler–Clarke methodology[15] and catalytic reductive aminations, in which the corresponding amine and formaldehyde are converted into N-methylamines in the presence of hydrogen or a stoichiometric amount of reducing agents.[16] Despite these methods, the development of selective protocols involving the use of earth-abundant metal-based catalysts is highly desired.[13f]

In general, N-methylated (hetero)aromatic amines are prepared starting from the corresponding anilines.[15–18] However, anilines are produced by the hydrogenation of nitroarenes.[19] Therefore, a straightforward and direct synthesis of N-methylamines from nitroarenes is advantageous in terms of step economy and the price of substrates.[4i,13f,20] Indeed, 26 various nitroarenes underwent reductive amination to produce N-methylamines in good to excellent yields by using our cobalt catalyst (Scheme 1).

For both drug discovery and organic synthesis, the introduction of an N-methyl moiety in structurally diverse molecules is of central importance. In this regard, selective transformation of the nitro group into the N-methylamine functionality in the presence of sensitive halides, OH groups, SH groups, ketones, esters, amides, and C=C bonds was achieved with product yields of 83–91% (Scheme 1). Next, N,N-dimethylcyclohexane was prepared from the corresponding nitro compound, which showed that this catalyst was also active for aliphatic nitro compounds. Further, N-methylation of a nitro-substituted biologically active molecule (i.e., nimodipin) and challenging dinitro compounds was also performed (Scheme 1, products 25–27).

In addition to the preparation of aromatic N-methylamines from nitroarenes, our protocol allows for the reductive N-methylation of bioactive primary and secondary amines as well as amino acids (Scheme 2), which can be exploited for life-science applications. As an example, paroxetine and duloxetine were N-methylated without affecting other functionalities or the core structures of the molecules (Scheme 2, products 31 and 32). Notably, phenylalanine and tyrosine amino acid esters were also dimethylated successfully (Scheme 2, products 33 and 34). In addition, the two drugs amitriptylin and venlafaxine were prepared (Scheme 2, products 35 and 36).

After having demonstrated the preparation of N-methylamines, we applied our catalyst to the N-alkylation of nitroarenes with aldehydes (Scheme 3). Although a few non-noble-metal-based catalysts have been used for reductive N-alkylations, they exhibited poor reactivity and selectivity for challenging substrates.[4] Expediently, upon using our cobalt nanocatalyst, structurally diverse alkylamines were prepared
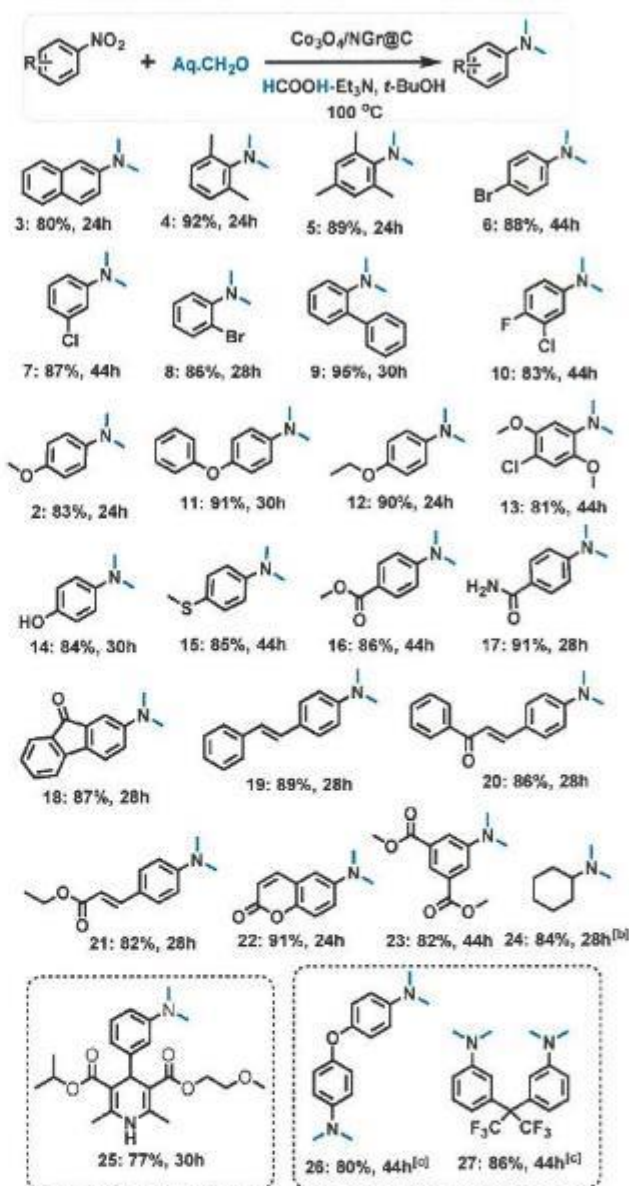
Scheme 1. Nanoscale Co₃O₄-catalyzed synthesis of N-methylamines from nitroarenes.[a] [a] Reaction conditions: nitroarene (1 mmol), formaldehyde (37 wt% in water, 200 µL) Co₃O₄/NGr@C (80 mg, 4 mol% Co), formic acid [5.3 mmol, 5.3 equiv. as a HCOOH/Et₃N (5:2) mixture], tBuOH (3 mL), 100 °C, 24–44 h; yields of isolated products are given. [b] GC yield using n-hexadecane (100 µL) as a standard. [c] Reaction conditions: nitroarene (1 mmol), formaldehyde (37 wt% in water, 200 µL) Co₃O₄/NGr@C (160 mg, 4 mol% Co), formic acid [10.6 mmol, 10.6 equiv. as a HCOOH/Et₃N (5:2) mixture], tBuOH (3 mL), 100 °C, 24–44 h.

(Scheme 3). Clearly, we demonstrated the viability of this method for the synthesis of complex and more challenging amines. As seen from Scheme 3, both functionalized nitroarenes and aldehydes reacted smoothly and produced secondary amines in good to excellent yields. Thus, the unique feature of this catalyst in that it can be used for both reductive N-methylation and N-alkylation reactions was demonstrated.

Next, an interesting application was presented for the selective N-alkylation of amino acid esters and the preparation of
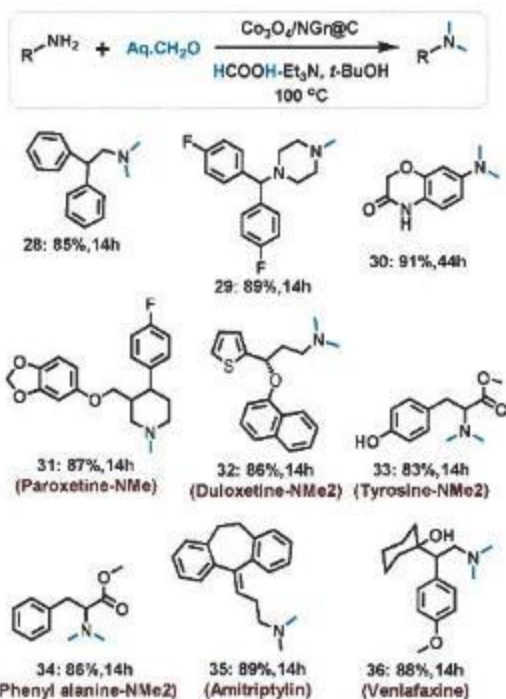
Scheme 2. Cobalt-oxide-catalyzed N-methylation of interesting amines and life-science molecules. Reaction conditions: amine (1 mmol), formaldehyde (37 wt% in water, 200 µL) Co_3O_4/NGr@C (80 mg, 4 mol% Co), formic acid [2.2 mmol, 2.2 equiv. as a HCOOH/Et$_3$N (5:2) mixture], tBuOH (3 mL), 100°C, 14 h; yields of isolated products are given.

existing drug molecules (Scheme 4). As a result, phenylalanine and tyrosine amino acid esters were successfully N-alkylated with different aromatic aldehydes (Scheme 4, products **55–61**). Notably, N-alkylated and N-methylated amino acid derivatives are widely distributed in nature, and such molecules are used in pharmaceutical, chemical, and biological processes. Further, two existing drug molecules, piribedil and fenpropimorph (Scheme 4, products **62** and **63**), were prepared. Thus, this benign reductive amination process shows feasibility for selective late-stage manipulation of amine-based life-science molecules.

Finally, the practical utility was demonstrated by performing gram-scale reactions. Without changing the reaction conditions, selected nitroarenes (1–3 g) were N-alkylated and N-methylated to produce the corresponding amines with yields similar to those obtained on a 1 mmol scale (Scheme 5). These results prove that this protocol can be easily scaled for the preparation of several grams of amines.

In general, the stability, recycling, and reusability of a given catalyst are important features for the advancement of sustainable industrial processes. Noticeably, this Co_3O_4/N@C catalyst is highly stable and can be conveniently recycled up to five times to produce functionalized secondary amine (Figure 4).

In summary, we developed a selective and convenient reductive amination process for the preparation of N-methyl- and N-alkylamines by using an earth-abundant cobalt-based
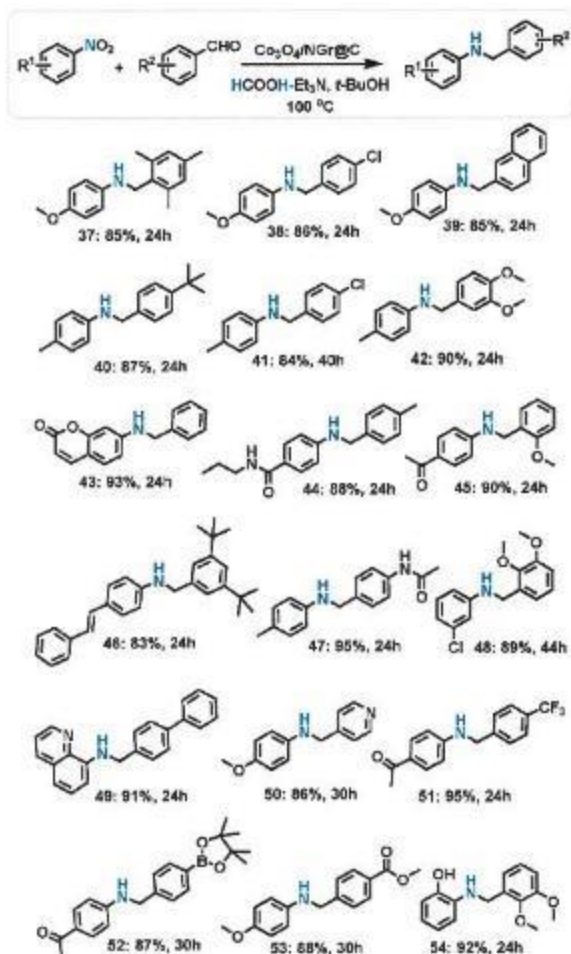
Scheme 3. Co_3O_4/NGr@C-catalyzed reductive amination of nitroarenes with aldehydes for the synthesis of N-alkylated amines. Reaction conditions: nitroarene (1 mmol), aldehyde (1.5 mmol), Co_3O_4/NGr@C (4 mol% Co), formic acid [4.3 mmol, 4.3 equiv. as a HCOOH/Et$_3$N (5:2) mixture], tBuOH (3 mL), 100°C, 24–44 h; yields of isolated products are given.
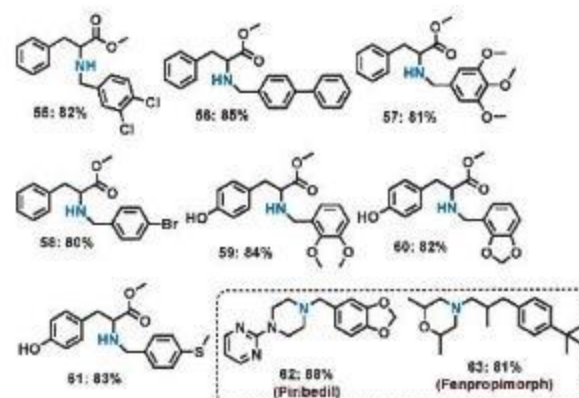
Scheme 4. N-Alkylation of amino acids by using a nanoscale cobalt-oxide catalyst. Reaction conditions: amine (1 mmol), aldehyde (1.5 mmol), Co_3O_4/NGr@C (4 mol% Co), formic acid [1.5 mmol, 1.5 equiv. as a HCOOH/Et$_3$N (5:2) mixture], tBuOH (3 mL), 100°C, 14 h; yields of isolated products are given.

18: 85%[a] (2g Scale)
16: 85%[a] (1g Scale)
51: 92%[b] (2g Scale)
42: 88%[b] (3g Scale)
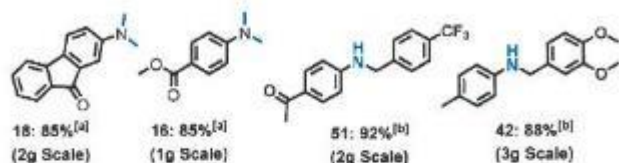
Scheme 5. Demonstrating the Co₃O₄/NGr@C-catalyzed reductive amination protocol for gram-scale reactions.[a,b] [a] Reaction conditions: formaldehyde (37 wt% in water, 200 µL), Co₃O₄/NGr@C (80 mg, 4 mol% Co), formic acid [5.3 mmol, 5.3 equiv. as a HCOOH/Et₃N (5:2) mixture] for each 1 mmol nitroarene, tBuOH (25–30 mL), 100°C, 20–30 h; yields of isolated products are given. [b] Reaction conditions: aldehyde (1.5 mmol), catalyst (80 mg), and formic acid [4.3 mmol, 4.3 equiv. as a HCOOH/Et₃N (5:2) mixture] for each 1 mmol nitroarene, tBuOH (25–30 mL), 100°C, 24–30 h; yields of isolated products are given.
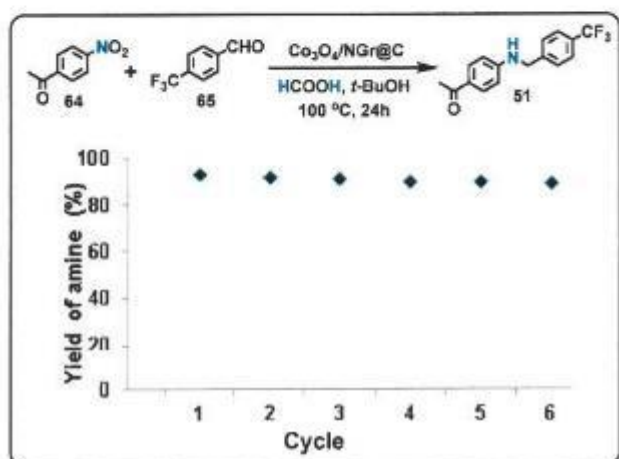
Figure 4. Recycling of the Co₃O₄/NGr@C catalyst for the preparation of functionalized secondary amines. Reaction conditions: 4-nitroacetophenone (5 mmol), 4-(trifluoromethyl)benzaldehyde (7.5 mmol), catalyst (400 mg, 4 mol% Co), formic acid [21.5 mmol, 4.3 equiv. as a HCOOH/Et₃N (5:2) mixture], tBuOH (10 mL), 100°C, 24–30 h; yields were determined by GC by using n-hexadecane (250 µL) as a standard.

nanocatalyst. Starting from nitroarenes or amines and aqueous formaldehyde or aldehydes, this operationally simple and cost-effective protocol allowed the synthesis of structurally diverse and functionalized N-methylated and N-alkylated amines. The synthetic utility of this method was established by the functionalization and preparation of life-science molecules and amino acid derivatives. Using a single cobalt-based catalyst, reductive N-methylation and N-alkylation reactions were both successfully performed.

Acknowledgements

Conflict of interest

The authors declare no conflict of interest.

[1] a) S. A. Lawrence, *Amines: Synthesis properties and applications*, Cambridge University Press, Cambridge, **2004**; b) A. Ricci, *Amino group chemistry: From synthesis to the life sciences*, Wiley-VCH, Weinheim, **2008**; c) http://njardarson.lab.arizona.edu/sites/njardarson.lab.arizona.edu/files/Top200PharmaceuticalProductsRetailSales2015LowRes.pdf; d) S. D. Roughley, A. M. Jordan, *J. Med. Chem.* **2011**, *54*, 3451–3479; e) V. Froidevaux, C. Negrell, S. Caillol, J.-P. Pascault, B. Boutevin, *Chem. Rev.* **2016**, *116*, 14181–14224; f) T. Yan, B. L. Feringa, K. Barta, *Nat. Commun.* **2014**, *5*, 5602.

[2] For revisions on reductive aminations, see: a) S. Gomez, J. A. Peters, T. Maschmeyer, *Adv. Synth. Catal.* **2002**, *344*, 1037–1057; b) H. Alinezhad, H. Yavari, F. Salehian, *Curr. Org. Chem.* **2015**, *19*, 1021–1049.

[3] a) B. Sreedhar, P. Surendra Reddy, D. Keerthi, *J. Org. Chem.* **2009**, *74*, 8806–8809; b) L. Li, Z. Niu, S. Cai, Y. Zhi, H. Li, H. Rong, L. Liu, L. Liu, W. He, Y. Li, *Chem. Commun.* **2013**, *49*, 6843–6845; c) L. Hu, X. Cao, D. Ge, H. Hong, Z. Guo, L. Chen, X. Sun, J. Tang, J. Zheng, J. Lu, H. Gu, *Chem. Eur. J.* **2011**, *17*, 14283–14287; d) M. Pintado-Sierra, A. M. Rasero-Almansa, A. Corma, M. Iglesias, F. Sánchez, *J. Catal.* **2013**, *299*, 137–145; e) C. del Pozo, A. Corma, M. Iglesias, F. Sánchez, *J. of Catal.* **2012**, *291*, 110–116; f) D. B. Bagal, R. A. Watile, M. V. Khedkar, K. P. Dhake, B. M. Bhanage, *Catal. Sci. Technol.* **2012**, *2*, 354–358; g) S. Ogo, K. Uehara, T. Abura, S. Fukuzumi, *J. Am. Chem. Soc.* **2004**, *126*, 3020–3021; h) G. Liang, A. Wang, L. Li, G. Xu, N. Yan, T. Zhang, *Angew. Chem. Int. Ed.* **2017**, *56*, 3050–3054; *Angew. Chem.* **2017**, *129*, 3096–3100.

[4] a) A. Pagnoux-Ozherelyeva, N. Pannetier, M. D. Mbaye, S. Gaillard, J.-L. Renaud, *Angew. Chem. Int. Ed.* **2012**, *51*, 4976–4980; *Angew. Chem.* **2012**, *124*, 5060–5064; b) F. Mao, D. Sui, Z. Qi, H. Fan, R. Chen, J. Huang, *RSC Adv.* **2016**, *6*, 94068–94073; c) F. Santoro, R. Psaro, N. Ravasio, F. Zaccheria, *ChemCatChem* **2012**, *4*, 1249–1254; d) T. Stemmler, A.-E. Surkus, M.-M. Pohl, K. Junge, M. Beller, *ChemSusChem* **2014**, *7*, 3012–3016; e) R. V. Jagadeesh, T. Stemmler, A.-E. Surkus, H. Junge, K. Junge, M. Beller, *Nat. Protoc.* **2015**, *10*, 548–557; f) S. Pisiewicz, T. Stemmler, A.-E. Surkus, K. Junge, M. Beller, *ChemCatChem* **2015**, *7*, 62–64; g) T. Stemmler, F. A. Westerhaus, A.-E. Surkus, M.-M. Pohl, K. Junge, M. Beller, *Green Chem.* **2014**, *16*, 4535–4540; h) R. V. Jagadeesh, K. Murugesan, A. S. Alshammari, H. Neumann, M.-M. Pohl, J. Radnik, M. Beller, *Science* **2017**, *358*, 326–332.

[5] D. Mellmann, P. Sponholz, H. Junge, M. Beller, *Chem. Soc. Rev.* **2016**, *45*, 3954–3988.

[6] a) C. Wang, A. Pettman, J. Basca, J. Xiao, *Angew. Chem. Int. Ed.* **2010**, *49*, 7548–7552; *Angew. Chem.* **2010**, *122*, 7710–7714; b) Q. Zhang, S.-S. Li, M.-M. Zhu, Y. M. Liu, H.-Y. He, Y. Cao, *Green Chem.* **2016**, *18*, 2507–2513; c) P. Zhou, Z. Zhang, *ChemSusChem* **2017**, *10*, 1892–1897; d) P. Zhou, Z. Zhang, L. Jiang, C. Yu, K. Lv, J. Sun, S. Wang, *Applied Catal. B: Environ.* **2017**, *210*, 522–532.

[7] a) T. Touge, T. Nara, M. Fujiwhara, Y. Kayaki, T. Ikariya, *J. Am. Chem. Soc.* **2016**, *138*, 10084–10087; b) O. Soltani, M. A. Ariger, H. Vázquez-Villa, E. M. Carreira, *Org. Lett.* **2010**, *12*, 2893–2895; c) G. Wienhöfer, I. Sorribes, A. Boddien, F. Westerhaus, K. Junge, H. Junge, R. Llusar, M. Beller, *J. Am. Chem. Soc.* **2011**, *133*, 12875–12879; d) R. V. Jagadeesh, D. Banerjee, P. B. Arockiam, H. Junge, K. Junge, M.-M. Pohl, J. Radnik, A. Brückner, M. Beller, *Green Chem.* **2015**, *17*, 898–902; e) R. V. Jagadeesh, K. Natte, He. Junge, M. Beller, *ACS Catal.* **2015**, *5*, 1526–1529; f) R. Shen, T. Chen, Y. Zhao, R. Qiu, Y. Zhou, S. Yin, X. Wang, M. Goto, L.-B. Han, *J. Am. Chem. Soc.* **2011**, *133*, 17037–17044; g) M. Zeng, L. Li, S. B. Herzon, *J. Am. Chem. Soc.* **2014**, *136*, 7058–7067; h) J. M. R. Narayanam, J. W. Tucker, C. R. J. Stephenson, *J. Am. Chem. Soc.* **2009**, *131*, 8756–8757.

[8] For catalysis with earth abundant metals, see: a) R. M. Bullock, *Catalysis without precious metals*, Wiley, Hoboken, **2010**; b) M. Albrecht, R. Bedford, B. Plietker, *Organometallics* **2014**, *33*, 5619–5621; c) D. Wang, D. Astruc, *Chem. Soc. Rev.* **2017**, *46*, 816–854; d) R. Morris Bullock, *Chem*

2017, 2, 444–446; e) I. Roger, M. A. Shipman, M. D. Symes, *Nat. Chem. Rev.* **2017**, *1*, DOI:10.1038/s41570-016-0003; f) J. L. Que, W. B. Tolman, *Nature* **2008**, *455*, 333–340; g) I. Bauer, H.-J. Knölker, *Chem. Rev.* **2015**, *115*, 3170–3387; h) G. Cahiez, A. Moyeux, *Chem. Rev.* **2010**, *110*, 1435–1462; i) W. Zhang, F. Wang, S. D. McCann, D. Wang, P. Chen, S. S. Stahl, G. Liu, *Science* **2016**, *353*, 1014–1018; j) Y.-F. Wang, K. K. Toh, E. P. J. Ng, S. Chiba, *J. Am. Chem. Soc.* **2011**, *133*, 6411–6421; k) T. M. Gøgsig, J. Kleimark, S. O. N. Lill, S. Korsager, A. T. Lindhardt, P.-O. Norrby, T. Skrydstrup, *J. Am. Chem. Soc.* **2012**, *134*, 443–452.

[9] For Price of metals, see: http://www.metalprices.com/.

[10] a) *Nanotechnologies: Principles, applications, implications and hands-on activities*, European Commission, European Union, **2012**; b) V. Polshettiwar, T. Asefa, *Nanocatalysis: Synthesis and applications*, Wiely, Hoboken, **2013**.

[11] a) M. Sankar, N. Dimitratos, P. J. Miedziak, P. P. Wells, C. J. Kiely, G. J. Hutchings, *Chem. Soc. Rev.* **2012**, *41*, 8099–8139; b) H. M. Torres Galvis, J. H. Bitter, C. B. Khare, M. Ruitenbeek, A. I. Dugulan, K. P. de Jong, *Science* **2012**, *335*, 835–838; c) J. Zečević, G. Vanbutsele, K. P. de Jong, J. A. Martens, *Nature* **2015**, *528*, 245–248.

[12] a) F. A. Westerhaus, R. V. Jagadeesh, G. Wienhöfer, M.-M. Pohl, J. Radnik, A.-E. Surkus, J. Rabeah, K. Junge, H. Junge, M. Nielsen, A. Brückner, M. Beller, *Nat. Chem.* **2013**, *5*, 537–543; b) R. V. Jagadeesh, H. Junge, M.-M. Pohl, J. Radnik, A. Brückner, M. Beller, *J. Am. Chem. Soc.* **2013**, *135*, 10776–10782; c) R. V. Jagadeesh, T. Stemmler, A.-E. Surkus, M. Bauer, M.-M. Pohl, J. Radnik, K. Junge, H. Junge, A. Brückner, M. Beller, *Nat. Protoc.* **2015**, *10*, 916–926; d) R. V. Jagadeesh, H. Junge, M. Beller, *Nat. Commun.* **2014**, *5*, 4123.

[13] a) J. Chatterjee, F. Rechenmacher, H. Kessler, *Angew. Chem. Int. Ed.* **2013**, *52*, 254–269; *Angew. Chem.* **2013**, *125*, 268–283; b) J. Chatterjee, C. Gilon, A. Hoffman, H. Kessler, *Acc. Chem. Res.* **2008**, *41*, 1331–1342; c) A. D. Goldberg, C. D. Allis, E. Bernstein, *Cell* **2007**, *128*, 635–638; d) G. Egger, G. N. Liang, A. Aparicio, P. A. Jones, *Nature* **2004**, *429*, 457–463; e) E. L. Barreiro, A. E. Kümmerle, C. A. M. Fraga, *Chem. Rev.* **2011**, *111*, 5215–5246; f) K. Natte, H. Neumann, R. V. Jagadeesh, M. Beller, *Nat. Commun.* **2017**, *8*, 1344.

[14] a) M. B. Smith, J. March, *J. March's advanced organic chemistry: Reactions, mechanisms, and structure*, 6th Ed., Wiley, Hoboken, **2007**;

b) H. K. R. Santhapuram, A. Dutta, O. E. Hutt, G. I. Georg, *J. Org. Chem.* **2008**, *73*, 4705–4708.

[15] a) W. Eschweiler, *Ber. Dtsch. Chem. Ges.* **1905**, *38*, 880–882; b) H. T. Clarke, H. B. Gillespie, S. Z. Weisshaus, *J. Am. Chem. Soc.* **1933**, *55*, 4571–4687.

[16] a) M. Tanis, G. Rauniyar, **1992**, US5105013 A; b) I. Sorribes, K. Junge, M. Beller, *Chem. Eur. J.* **2014**, *20*, 7878–7883; c) L. Zhu, L.-S. Wang, B. Li, W. Li, B. Fu, D. van der Waals, L. E. Heim, C. Gedig, F. Herbrik, S. Vallazza, M. H. Prechtl, *ChemSusChem* **2016**, *9*, 2343–2347; e) R. A. da Silva, I. H. S. Estevam, L. W. Bieber, *Tetrahedron Lett.* **2007**, *48*, 7680–7682; f) S. H. Pine, B. L. Sanchez, *J. Org. Chem.* **1971**, *36*, 829–832; g) N. B. Godfrey, US3210349A, **1965**; h) C. Wu, R. Li, D. Dearborn, Y. Wang, *Int. J. Org. Chem.* **2012**, *2*, 202–223; i) N. Y. Man, W. Li, S. G. Stewart, X. F. Wu, *Chimia* **2015**, *69*, 345–347; j) K. Okabe, Y. Yokota, K. Matsutani, T. Imanaka, US4757144 A, **1988**; k) K. C. Waterman, W. B. Arikpo, M. B. Fergione, T. W. Graul, B. A. Johnson, B. C. Macdonald, M. C. Roy, R. J. Timpano, *J. Pharm. Sci.* **2008**, *97*, 1499–1507.

[17] a) K. Natte, H. Neumann, M. Beller, R. V. Jagadeesh, *Angew. Chem. Int. Ed.* **2017**, *56*, 6384–6394; *Angew. Chem.* **2017**, *129*, 6482–6492.

[18] a) Y. Li, I. Sorribes, T. Yan, K. Junge, M. Beller, *Angew. Chem. Int. Ed.* **2013**, *52*, 12156–12160; *Angew. Chem.* **2013**, *125*, 12378–12382; b) Y. Li, X. Fang, K. Junge, M. Beller, *Angew. Chem. Int. Ed.* **2013**, *52*, 9568–9571; *Angew. Chem.* **2013**, *125*, 9747–9750; c) S. Das, F. D. Bobbink, G. Laurenczy, P. J. Dyson, *Angew. Chem. Int. Ed.* **2014**, *53*, 12876–12879; *Angew. Chem.* **2014**, *126*, 13090–13093; d) Y. Li, X. Cui, K. Dong, K. Junge, M. Beller, *ACS Catal.* **2017**, *7*, 1077–1086.

[19] a) A. Corma, P. Serna, *Science* **2006**, *313*, 332–334; b) R. V. Jagadeesh, A.-E. Surkus, H. Junge, M.-M. Pohl, J. Radnik, J. Rabeah, H. Huan, V. Schünemann, A. Brückner, M. Beller, *Science* **2013**, *342*, 1073–1076.

[20] a) X. Cui, Y. Zhang, Y. Deng, F. Shi, *Chem. Commun.* **2014**, *50*, 13521–13524; b) Y. Yu, Q. Zhang, S.-S. Li, J. Huang, Y.-M. Liu, H.-Y. He, Y. Cao, *ChemSusChem* **2015**, *8*, 3029–3035.

6. Appendix

6.1 Stable and Reusable Nanoscale Fe_2O_3-catalyzed Aerobic Oxidation Process for the Selective Synthesis of Nitriles and Primary Amides.
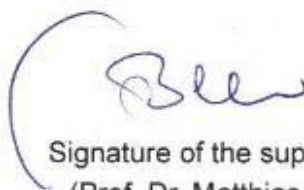
Murugesan, Kathiravan; Senthamarai, Thirusangumurugan; Sohail, Manzar; Sharif, Muhammad; Kalevaru, Narayana V.; Jagadeesh, Rajenahally V*.

Green Chemistry, **2018**, *20*, 266-273.

In this manuscript, I performed analyzing the data and co-wrote the paper. My contribution as the second author of this paper is approximately 20-30%.

Signature of the student
(Thirusangumurugan Senthamarai)
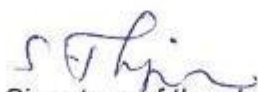
Signature of the supervisor
(Prof. Dr. Matthias Beller)

6.2 Cobalt-based Nanoparticles Prepared from MOF-carbon Templates as Efficient Hydrogenation Catalysts

Murugesan, Kathiravan; Senthamarai, Thirusangumurugan; Sohail, Manzar Alshammari, Ahmad S.; Pohl, Marga-Martina; Beller, Matthias*; Jagadeesh, Rajenahally V*.

Chemical Science, **2018**, *9*, 8553-8560.

In this manuscript, I performed analyzing the data and co-wrote the paper. My contribution as the second author of this paper is approximately 20%.

Signature of the student
(Thirusangumurugan Senthamarai)
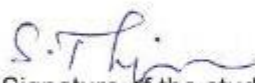
Signature of the supervisor
(Prof. Dr. Matthias Beller)

6.3 Cobalt-nanoparticles Catalyzed Efficient and Selective Hydrogenation of Aromatic Hydrocarbons

Murugesan, Kathiravan; Senthamarai, Thirusangumurugan; Alshammari, Ahmad S.; Altamimi, Rashid M.; Kreyenschulte, Carsten; Pohl, Marga-Martina; Lund, Henrik; Rajenahally V. Jagadeesh* and Matthias Beller*

ACS Catalysis, **2019**, *9*, 8581–8591

In this manuscript, I performed analyzing the data and co-wrote the paper. My contribution as the second author of this paper is approximately 15-20%.

Signature of the student
(Thirusangumurugan Senthamarai)

Signature of the supervisor
(Prof. Dr. Matthias Beller)

6.4 Reductive amination using cobalt-based nanoparticles for synthesis of amines
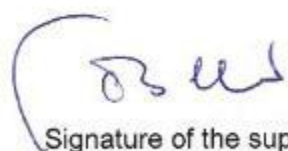
Kathiravan Murugesan, Vishwas G. Chandrashekhar, Thirusangumurugan Senthamarai, Rajenahally V. Jagadeesh* and Matthias Beller*

Journal: *Nature Protocols,* **2020,** https://doi.org/10.1038/s41596-019-0258-z.

Author contributions:

In this manuscript, I performed checking the correction of manuscript. My contribution as the second author of this paper is approximately 10-15%.

Signature of the student
(Thirusangumurugan Senthamarai)

Signature of the supervisor
(Prof. Dr. Matthias Beller)

6.5 Catalytic Reductive Aminations Using Molecular Hydrogen for the Synthesis of Different Kinds of Amines
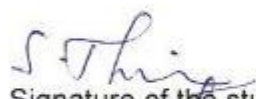
Murugesan, Kathiravan[$]; Senthamarai, Thirusangumurugan[$]; Chandrashekhar, Vishwas G[$].; Natte, Kishore; Beller, Matthias*; Jagadeesh, Rajenahally V*.

([$]1st, 2nd and 3rd authors equally contributed and co-first authors)
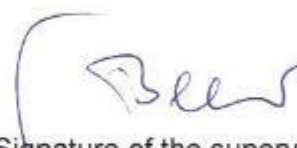
Chemical Society Review, **2020** (revised)

Author contributions:

In this work, I searched the related publications and Co-wrote the manuscript. My contribution as the first author of this paper is approximately 30%.

Signature of the student
(Thirusangumurugan Senthamarai)

Signature of the supervisor
(Prof. Dr. Matthias Beller)

Green Chemistry

PAPER

Check for updates
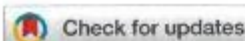
Stable and reusable nanoscale Fe₂O₃-catalyzed aerobic oxidation process for the selective synthesis of nitriles and primary amides†

Kathiravan Murugesan,[a] Thirusangumurugan Senthamarai,[a] Manzar Sohail,[b] Muhammad Sharif,[b] Narayana V. Kalevaru[a] and Rajenahally V. Jagadeesh [ID] *[a]

The sustainable introduction of nitrogen moieties in the form of nitrile or amide groups in functionalized molecules is of fundamental interest because nitrogen-containing motifs are found in a large number of life science molecules, natural products and materials. Hence, the synthesis and functionalization of nitriles and amides from easily available starting materials using cost-effective catalysts and green reagents is highly desired. In this regard, herein we report the nanoscale iron oxide-catalyzed environmentally benign synthesis of nitriles and primary amides from aldehydes and aqueous ammonia in the presence of 1 bar O₂ or air. Under mild reaction conditions, this iron-catalyzed aerobic oxidation process proceeds to synthesise functionalized and structurally diverse aromatic, aliphatic and heterocyclic nitriles. Additionally, applying this iron-based protocol, primary amides have also been prepared in a water medium.

1. Introduction

The development of iron-catalyzed reactions for modern state-of-the-art organic synthesis is an important goal of chemical research.[1,2] Remarkably, the high abundance, lower price and lower toxicity of iron make it an ideal metal for catalysis applications,[1,2] and it can be a suitable candidate for replacing existing precious metal-based catalysts. Compared to homogeneous iron complexes, heterogeneous catalysts based on nanostructured iron materials are more practical and cost-efficient catalytic systems due to their ease of separation, reusability and stability.[1d,2a,3] In order to realize more environmentally benign syntheses, iron catalyzed reactions should exploit the use of green and renewable reagents under mild reaction conditions.[1c,d,4–7] Clearly, iron-catalyzed syntheses utilizing atmospheric O₂ or air[1c,d,4–7] and ammonia[8] that demonstrate exquisite selectivity represent a more sustainable process that is crucial for the advancement of academic research and industrial production. Therefore, the development of iron catalyzed aerobic oxidation reactions is highly desired for the pro-

duction of valuable chemicals, especially nitriles and amides. It is worth noting that nitriles and amides represent major building blocks and central intermediates for the synthesis of advanced chemicals, life science molecules and materials.[9–13] Furthermore, these structural motifs have been found to be integral parts of bio-active molecules and natural products.[13–17]

While simple nitriles have been prepared by industrial ammoxidation processes under harsh conditions (>300 °C in the gas phase),[18] functionalized and structurally diverse nitriles still rely on toxic cyanation reactions.[19] The limitations of ammoxidation and drawbacks of cyanation inspired the search for alternative sustainable routes for the synthesis of nitriles from suitable starting materials. In this regard, the catalytic oxidative conversion of alcohols[20] or aldehydes[20a,21] using ammonia represents a green method to produce various nitriles.

Complementary to alcohols are aldehydes, which are readily available fine and bulk chemicals, and they serve as suitable starting materials for the preparation of various chemicals such as amines,[22] carboxylic acids,[23] alcohols,[24] esters[25] and heterocycles,[26] as well as for C–C bond forming reactions that enable the preparation of an array of interesting molecules[24a–c,27]. In particular, the recently reported Fe-[23a] and Cu-[23b] catalyzed oxidative conversions of aldehydes to carboxylic acids are quite interesting. Regarding the synthesis of nitriles from aldehydes, few methods have been reported using different nitrogen sources, such as hexamethyldisilazane (HMDS),[28] hydroxyl-

[a]Leibniz-Institut für Katalyse e. V. an der Universität Rostock, Albert-Einstein-Str. 29a, 18059 Rostock, Germany. E-mail: Jagadeesh.Rajenahally@catalysis.de
[b]The Center of Research Excellence in Nanotechnology (CENT) and Department of Chemistry, King Fahd University of Petroleum and Minerals, Dhahran 31261, Saudi Arabia
†Electronic supplementary information (ESI) available. See DOI: 10.1039/c7gc02627g

Green Chemistry

amine,[29] NaN₃,[30] K₃[Fe(CN)₆][31] and ammonia,[20a,21,32] using different catalysts. Unfortunately, except ammonia all of these reagents are either toxic or produce stoichiometric amounts of waste. Remarkable ammonia is considered to be a green and abundant nitrogen source for the preparation of nitrogen containing compounds. With regards to the utilization of ammonia for the synthesis of nitriles from aldehydes, various oxidants and catalysts have already been reported.[20a,b,21,32–34] Among these, iodine and iodine-containing compounds were commonly employed.[32] However these reagents are not only sensitive and hazardous, but also produce significant amounts of waste. Hence these reagents are not suitable from a green chemistry perspective. Next, Ru-based catalysts were used under harsh conditions (130 °C and 6 bar air).[20a,b] In addition to ruthenium, Cu,[21] Ni,[33a] and Mg–Mn[33b] based systems are also used to catalyze the reaction of aldehydes and ammonia to obtain nitriles. Among these, the Cu/TEMPO/bipyridin catalyst system works under mild reaction conditions (25 °C and 1 bar O₂).[21a] Even though this catalyst works under mild reaction conditions, it is a homogeneous catalyst and cannot be recycled.[21a] In addition, the use of NaOH additive and narrower substrate scope have hindered its practical utility for the sustainable synthesis of nitriles.[21a] Furthermore, other oxidants/catalysts such as trichloroisocyanuric acid (TCCA),[34a] tetrabutylammonium tribromide (TBATB),[34b] chloramine-T (CAT)[34c] and ceric ammonium nitrate (CAN)[34d] have also been used for the preparation of nitriles from aldehydes and ammonia. Again these compounds led to the formation of a significant amount of waste and hence they are not considered as green oxidants. Overall, most of these methodologies have disadvantages regarding the use of toxic and waste generating reagents, poor selectivity or narrower substrate scope for the synthesis of functionalized and structurally diverse nitriles. Hence, greener and more efficient methodologies are required for the synthesis of advanced nitriles from aldehydes using heterogeneous iron-based catalysts under mild reaction conditions. In this regard, herein we report the application of a reusable iron oxide catalyst for the synthesis of a variety of nitriles from aldehydes and aqueous ammonia under mild reaction conditions. Compared to previously reported catalysts (Fig. 1), our iron-based catalyst is more
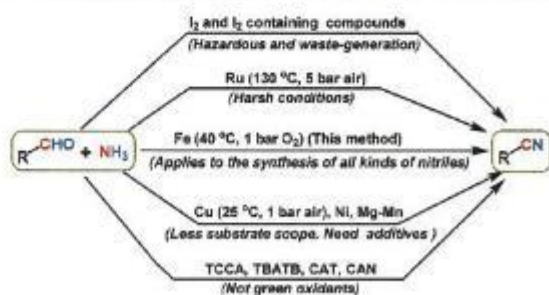
advantageous and allows the synthesis of functionalized and structurally diverse nitriles. Notably, the synthetic utility and practical applicability of this catalyst have been demonstrated by performing gram-scale syntheses and recycling the catalyst. In addition to the synthesis of nitriles, a greener protocol for the preparation of amides is also demonstrated using iron-based catalysts, starting from aldehydes and ammonia in a water medium.

2. Results and discussion

2.1. Preparation of nanoscale Fe₂O₃-based (Fe₂O₃-N/C) catalysts

In 2013, we developed nanoscale Fe₂O₃-based particles activated by nitrogen doped graphene layers for catalysis applications (Fe₂O₃-N/C).[2a] Inspired by these materials and based on our objective to develop iron-based sustainable chemical processes, herein we demonstrate the synthesis of all kinds of aromatic, heterocyclic and aliphatic nitrile as well as primary amides starting from aldehydes and aqueous ammonia using 1 bar of molecular oxygen or air. Typically, this Fe₂O₃-based catalyst has been prepared (Fig. 2) by impregnation of an *in situ* generated Fe(II)(1,10-phenanthroline)₃(OAc)₂ complex on commercial carbon (Vulcan XC 72R) and subsequent pyrolysis at 800 °C for 2 h in an argon atmosphere (Fe-phen/C-800; phen = 1,10-phenanthroline).[2a] The detailed preparation and characterization of this material by transmission electron microscopy (TEM), X-ray photoelectron spectroscopy (XPS), electron paramagnetic resonance (EPR) spectroscopy, and Mössbauer spectroscopy has been reported in our previously published paper[2a] (see also ESI†). The Fe-phen/C-800 catalyst was characterized by the formation of nanoscale Fe₂O₃ particles (2–5 and 20–80 nm), which are surrounded by 3–5 nitrogen doped graphene layers (Fig. S1A†). In contrast to the active material, the inactive material, Fe(OAc)₂/C-800, prepared without phenanthroline contained much larger and well facetted Fe₂O₃ particles with a size of 100–800 nm. In this case there was no formation of graphene layers and hence these particles are not surrounded by graphene layers.

The X-ray photoelectron spectra for the N 1s electrons (Fig. S3A†) of the Fe₂O₃-N/C (Fe-phen/C-800) catalyst reveal

Fig. 1 The synthesis of nitriles from aldehydes and ammonia using different catalysts/oxidants: a comparison of our method with previously reported methods.
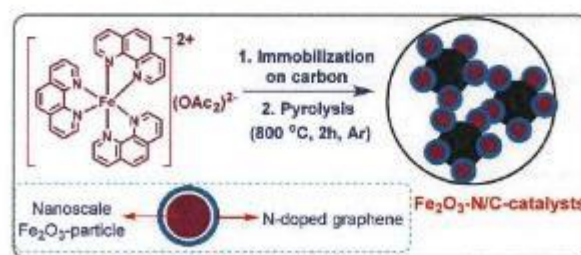
Fig. 2 The preparation of nitrogen doped graphene activated nanoscale Fe₂O₃-particles supported on carbon.

that there are three N 1s peaks that occur at 398.3 eV, 399.3 eV and 401.0 eV. The first two peaks are assigned to the pyridinic nitrogens and Fe–N centers respectively. The peak observed at 401.0 eV is assigned to nitrogen in a grapheme-like structure. In the XPS for the Fe 2p electrons, two peaks corresponding to Fe species in the near-surface region were observed (Fig. S3B†). The first (major) appeared at 712.4 eV and the second (minor) at 709.9 eV. The first peak is due to the presence of Fe^{3+} species (more likely Fe_2O_3) while the second peak is assigned to Fe^{2+} species. Fe^{2+} species are in a minor proportion compared to Fe^{3+} species. By XPS analysis, in the Fe-phen/C-800 catalyst both the Fe^{3+} (major) and Fe^{2+} (minor) species are present on the surface of the material. However, the bulk composition is somewhat different to the surface composition. In the bulk, we can see the presence of mainly the Fe^{3+} species (in the form of Fe_2O_3). The presence of Fe_2O_3 in the bulk composition was confirmed by EPR spectroscopy and Mössbauer spectral analysis (Fig. S4 and S5; see ESI† for more details). Based on the reactivity and detailed spectroscopic characterization of the active (Fe-phen/C-800) and inactive (Fe(OAc)/ C-800) catalysts, the active sites of the catalyst consist mainly of nanoscale Fe_2O_3 particles, which are surrounded by the nitrogen species of the graphene layers. Both the nano-sized particles and the Fe–N interactions are responsible for the remarkable activity of this catalyst. Thus, the active sites appear to be Fe–N_x centers that govern the catalytic activities.

2.2. Reaction design for the synthesis of nitriles

Using our Fe-phen/C-800 catalyst (Fe_2O_3-N/C), we started to investigate the preparation of nitriles from suitable starting materials using aqueous ammonia in the presence of 1 bar molecular oxygen at a mild temperature (<50 °C) in conventional apparatus (in a glass vial using a balloon), without the use of any special equipment or an autoclave. Under these conditions, first we tested benzyl alcohol at 40 °C with 1 bar O_2 in the presence of the Fe_2O_3-N/C catalyst and found that no reaction occurred to produce the desired benzonitrile. However, to our surprise the reaction of benzaldehyde selectively gave benzonitrile in a 96% yield (Table 1, entry 6). Obviously, the homogeneous catalyst systems based on iron acetate or iron acetate/phenanthroline were found to be inactive (Table 1, entries 1 and 2). Similarly, the unpyrolyzed Fe-phen@C material, pyrolyzed simple iron acetate on carbon (Fe (OAc)$_2$@C-800) and bulk Fe_2O_3 were also not active (Table 1, entries 3–5). After getting excellent results using the Fe_2O_3-N/C catalyst, and establishing a set of mild reaction conditions, we explored the applicability of this methodology for the preparation of nitriles from aldehydes and aqueous ammonia. As seen from Schemes 1–3, structurally diverse and functionalized aromatic, heterocyclic and challenging aliphatic nitriles have been synthesized from various aldehydes.

2.3. Synthesis of structurally diverse aryl nitriles

Aryl nitriles, which are an important motif found in a majority of nitrile containing life science molecules, especially in the central nervous system (CNS), cardiovascular and anti-HIV

Table 1 The preparation of benzonitrile from benzaldehyde and aqueous ammonia using iron catalysts: a comparison of the catalytic activity

Entry	Catalyst	Yield of benzonitrile (%)
1[a]	Fe(OAc)$_2$	<1
2[a]	Fe(OAc)$_2$ + phen	<1
3[b]	Fe-phen@C	<1
4[b]	Fe(OAc)$_2$@C-800	<3
5[b]	Bulk Fe$_2$O$_3$	<1
6[b]	Fe-phen@C-800	96

Carbon = Vulcan XC72R, phen = phenanthroline. Materials were pyrolyzed at 800 °C for 2h under argon and bulk Fe_2O_3 was obtained commercially (>96% Fe basis).[a] Homogeneous catalysis reaction conditions: 0.5 mmol benzaldehyde, 300 µL aq. NH$_3$ (28–30% NH$_3$ basis), 0.015 mmol Fe(OAc)$_2$, 0.045 mmol phenanthroline, 1 bar O_2 (balloon), 2 mL t-amyl alcohol, 40 °C, 24 h. GC yields determined using 100 µL n-hexadecane as standard. [b] Heterogeneous catalysis reaction conditions: 0.5 mmol benzaldehyde, 300 µL aq. NH$_3$ (28–30% NH$_3$ basis), weight of catalyst corresponds to 3 mol% Fe, 1 bar O_2 (balloon), 2 mL t-amyl alcohol, 40 °C, 24 h. GC yields determined using 100 µL n-hexadecane as standard.
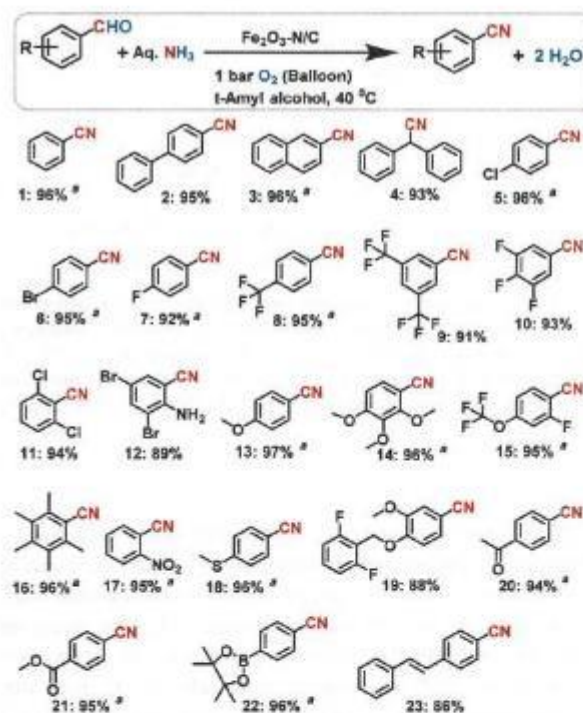
Scheme 1 The Fe_2O_3-N/C-catalyzed synthesis of structurally diverse and functionalized benzonitriles. Reaction conditions: 0.5 mmol aldehyde, 200–300 µL aq. NH$_3$ (28–30% NH$_3$ basis), 30 mg catalyst (3 mol% Fe), 1 bar O_2 (balloon), 2 mL t-amyl alcohol, 40 °C, 24 h. Isolated yields are shown. [a] Yields were determined by GC using 100 µL n-hexadecane as standard.

Green Chemistry

Paper
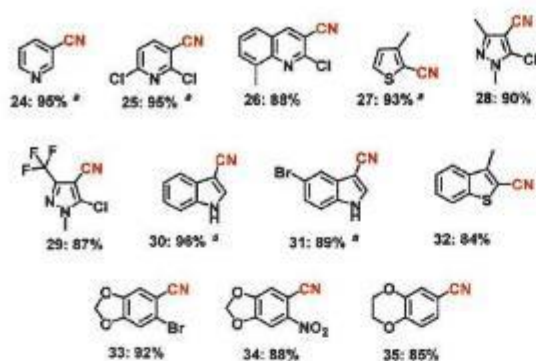
Scheme 2 The preparation of cyano-heterocycles using the Fe$_2$O$_3$-N/C catalyst. Reaction conditions: 0.5 mmol aldehyde, 200–300 µL aq. NH$_3$ (28–30% NH$_3$ basis), 30 mg catalyst (3 mol% Fe), 1 bar O$_2$ (balloon), 2 mL t-amyl alcohol, 40 °C, 24 h. Isolated yields are shown. ^{a} Yields were determined by GC using 100 µL n-hexadecane as standard.
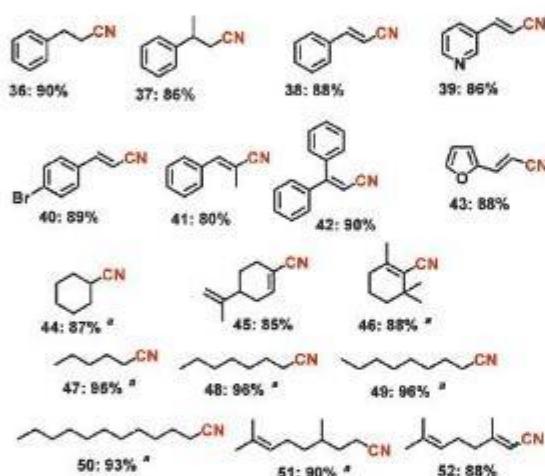
Scheme 3 The synthesis of challenging aliphatic nitriles using the Fe$_2$O$_3$-N/C catalyst. Reaction conditions: 0.5 mmol aldehyde, 200–300 µL aq. NH$_3$ (28–30% NH$_3$ basis), 30 mg catalyst (3 mol% Fe), 1 bar O$_2$ (balloon), 2 mL t-amyl alcohol, 40 °C, 24 h. Isolated yields are shown. ^{a} Yields were determined by GC by using 100 µL n-hexadecane as standard.

drugs,[14] were obtained in good to excellent yields (Scheme 1). Interestingly, halogenated benzonitriles, which encounter selectivity problems when made by typical cyanation reactions, were prepared in 89–97% yields (Scheme 1). The resulting halogenated benzonitriles serve as precursors for agrochemicals, pesticides and engineering materials. As an example, 2,6-dichlorobenzonitrile (DCBN), which is a herbicide and a key intermediate in the preparation of various potential pesticides and the engineering of highly thermally resistant plastics, was obtained in a 94% yield (Scheme 1; product 11). This particular reaction is of high commercial significance and is also a very challenging topic in the field of heterogeneous

catalysis under gas phase conditions due to steric hindrance (i.e. due to the substitution of two deactivating chlorine atoms in the *ortho* positions). The yield of DCBN achieved in the present study is much higher than that of state of the art catalysts (Y_{DCBN} = ca. 80% only). Also, functionalized benzaldehydes underwent selective reactions to produce challenging benzonitriles in yields of up to 97% (Scheme 1).

2.4. Synthesis of heterocyclic nitriles

Next, cyano-substituted heterocycles and aryl nitriles bearing heterocyclic backbones were synthesized in 84–96% yields (Scheme 2). In general, heterocyclic nitriles have been found to be key starting materials for the preparation of various active subunits of medicinal and biological molecules.

2.5. Synthesis of challenging aliphatic nitriles

In subsequent efforts, various aliphatic aldehydes, that are difficult to react, were chosen as potential substrates to produce their corresponding nitriles in good to excellent yields (up to 96%, Scheme 3). More interestingly, the allylic nitriles, which are important starting compounds for allylic amines, were obtained without further oxidation of their olefinic group (Scheme 3).

2.6. Green synthesis of primary amides

The creation of amide functionalities[35–37] is highly important in chemistry, medicine and biology because they play a major role in the amplification and configuration of life science molecules, peptides, proteins and materials.[13,16,17] In general, primary amides have been prepared by the reaction of carboxylic acids or their activated derivatives, such as acid chlorides and anhydrides, with ammonia. Nevertheless for the synthesis of this important class of amides, more environmentally benign procedures are required. In addition to alcohols,[37a,b] the synthesis of primary amides from aldehydes and ammonia has also been carried out using manganese oxide,[37a] Rh,[38a] KMnO$_4$[38b] and iodine.[38c] However, the use of iron-based heterogeneous catalysts for the synthesis of primary amides is obviously more advantageous.

After having successfully demonstrated the preparation of important nitriles, we have further extended the potential scope of the Fe$_2$O$_3$-N/C catalyst for the direct and one-pot synthesis of primary amides from benzaldehyde and aqueous ammonia. Interestingly, this catalyst was also observed to be active and selective for the preparation of even primary amides (Scheme 4). However, to achieve sufficient activity and selectivity, the reaction temperature and pressure had to be raised to a certain extent and the reaction conditions needed to be adjusted accordingly. In a water medium, we were able to convert aldehydes into primary amides using aqueous ammonia and air in a yield of up to 91% (Scheme 4).

The reaction pathway for the formation of nitriles and amides is presented in Scheme 5. In the first step, the formation of the intermediate, a primary imine was formed from an aldehyde and ammonia. In the presence of the Fe$_2$O$_3$-N/C
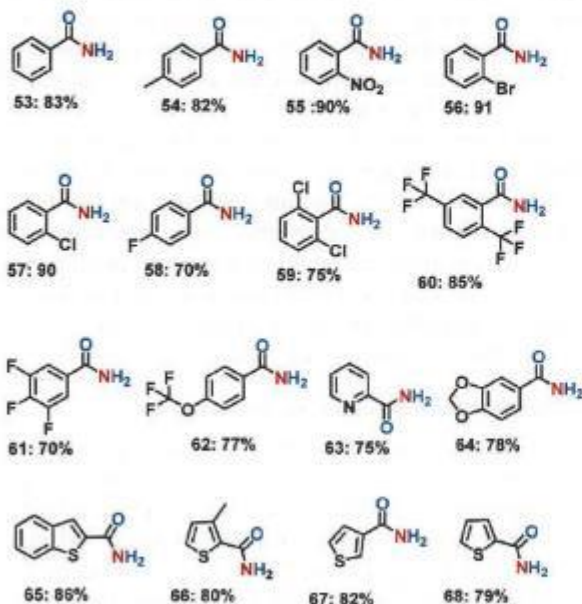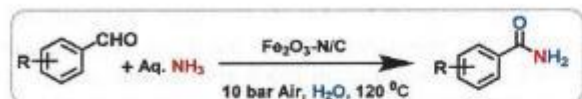
Scheme 4 The nanoscale Fe$_2$O$_3$-catalysed synthesis of amides from aldehydes and aqueous ammonia. Reaction conditions: 0.5 mmol aldehyde, 100 µL aq. NH$_3$ (28–30% NH$_3$ basis), 50 mg catalyst (5.0 mol% Fe), 10 bar air, 3 mL H$_2$O, 120 °C, 24 h. Isolated yields are shown.
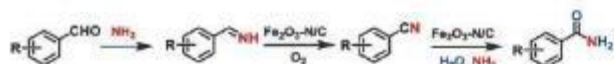
Scheme 5 The reaction pathway for the Fe$_2$O$_3$-N/C-catalyzed synthesis of nitriles and amides from aldehydes and ammonia.

catalyst, this unstable imine underwent oxidation to produce a nitrile. In the final step, in presence of water and ammonia, the formed nitrile was hydrolyzed to produce a primary amide. The production of the amide from the nitrile requires a higher temperature to proceed under forcing conditions. In order to confirm the formation mechanism of the amide, we performed the reaction of benzonitrile in water at 120 °C in the presence of aq. ammonia and a catalyst. In this case, the formation of benzamide in an 80% yield was observed. This result clearly evidenced that water is required for the formation of amides from aldehydes and ammonia. Due to the involvement of a two step reaction, the obtained yields of the amides are somewhat lower than those of the nitriles. In this case the unreactive nitrile was observed as the other product.

2.7. Scale up studies for gram scale synthesis

In order to demonstrate the synthetic and practical utility of this approach using our iron-catalyzed synthetic protocol, we also performed the gram scale (*i.e.* 1 to 5 g) reactions. In the

Scheme 6 Demonstrating the gram scale reactions for the synthesis of some selected nitriles over the Fe$_2$O$_3$-N/C catalyst. Reaction conditions: 2–5 g substrate, the weight of the catalyst corresponds to 3 mol% Fe, 200 µL aq. NH$_3$ for every 0.5 mmol substrate, 40 °C, 10–50 mL *t*-amyl alcohol, 1 bar O$_2$ (balloon), 24–30 h. Isolated yields are shown.

interest of scale up, a few grams of some selected aldehydes were converted to their corresponding nitriles under identical reaction conditions. The yields of the desired nitriles obtained from these tests are very much comparable and quite consistent with those obtained from the small (0.5 mmol) scale tests (Scheme 6).

2.8. Stability and recyclability of the Fe$_2$O$_3$-N/C catalyst

In general, the stability, recyclability and reusability features of any catalyst are very important for the advancement of sustainable industrial processes. Noticeably, our Fe$_2$O$_3$-N@C catalyst is highly stable and can be conveniently recycled up to 5 times without any significant loss of catalytic activity and selectivity (Fig. 3). The recycled catalyst was subjected to ICP analysis and it was found that there was no leaching of iron in the recycled catalyst.

The stability of the catalyst was also tested by performing kinetic studies (Fig. S6†). The effect of ammonia concentration, reaction time, amount of catalyst, concentration of substrate (benzaldehyde) and pressure of O$_2$ on the yield of benzonitrile was studied (Fig. S6†). Noticeably, the catalyst is stable and exhibited similar catalytic activity in the presence of an excess of ammonia (1 mL), with a prolonged reaction time and at a high pressure of O$_2$ (5 bar). As seen from the kinetic plots (Fig. S6†), on increasing the reaction time, catalyst amount and ammonia concentration, the yield of benzonitrile
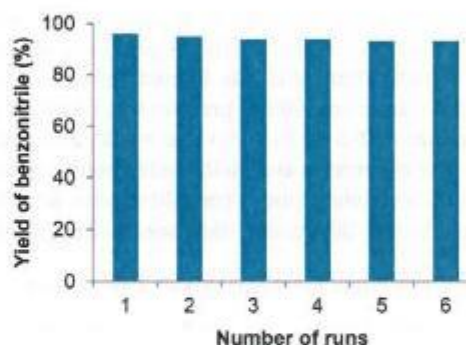
Fig. 3 Recyclability of the Fe$_2$O$_3$-N/C catalyst for the synthesis of benzonitrile. Reaction conditions: 1 mmol benzalydehyde, 60 mg catalyst (3.2 mol% Fe), 400 µL aq. NH$_3$ (28–30% NH$_3$ basis), 1 bar O$_2$ (balloon), 4 mL *t*-amyl alcohol, 40 °C, 24 h. Yields were determined by GC using *n*-hexadecane as standard.

increased and the highest yield was observed for the reaction that took 24 h with 30 mg of catalyst, in the presence of 200 µL aq. ammonia and one bar O_2.

3. Experimental section

3.1. Procedure for the preparation of the Fe₂O₃-N/C (Fe-phen/C-800) catalyst (1 g)[2a]

Appropriate amounts of $Fe(OAc)_2$ and 1,10-phenanthroline corresponding to 3 wt% of Fe in a 1 : 3 molar ratio of Fe to phenathroline were stirred in ethanol for 30 minutes at room temperature. Then, carbon powder (VULCAN® XC72R, Cabot Corporation Prod. Code XVC72R, CAS no. 1333-86-4) was added and the whole reaction mixture was stirred at 60 °C for 12–15 hours. The reaction mixture was cooled to room temperature and the ethanol was removed *in vacuo*. The solid material obtained was dried at 60 °C for 12 hours, after which it was ground to a fine powder. Then, the powdered material was pyrolyzed at 800 °C for 2 hours under an argon atmosphere and then cooled to room temperature.

Elemental analysis of Fe₂O₃-N/C (pyrolyzed Fe-phen/C at 800 °C) (wt%): C = 91.1, H = 0.19, N = 2.69, Fe = 2.95.

3.2. General procedure for the preparation of nitriles

An 8 mL oven dried glass vial was charged with a magnetic stirrer bar and 0.5 mmol of the appropriate aldehyde and then 2 mL *t*-amyl alcohol was added. Next, 30 mg Fe₂O₃-N/C (*i.e.* Fe-phen/C-800) catalyst (3 mol% Fe) was added followed by the addition of 200–300 µL aq. NH_3 (28–30% NH_3 basis). The glass vial was fitted with a septum and screw cap. Then a balloon containing 1 bar O_2 was connected to the reaction vial *via* a needle and the reaction was allowed to proceed for 24 h at 40 °C under continuous stirring. After completion of the reaction, the reaction vial was cooled down to room temperature and the excess O_2 was gradually discharged. Then, the catalyst was filtered-off, and washed with ethyl acetate. The solvent from the filtrate containing the reaction products and unreacted substrates (if any) was removed *in vacuo* and the target nitrile was purified by column chromatography. In the case of determining the yields by GC, 100 µL *n*-hexadecane was added to the reaction vial containing the products, and diluted with ethyl acetate. Then, this was filtered through a plug of silica and the filtrate containing product was analysed by GC (HP-6890, column HP-5 30 m × 250 mm × 0.25 µm) equipped with a FID. The conversion and yields were determined on the basis of the GC area counts using pre-calibrations. All products were analyzed by GC, GC-MS and NMR spectroscopy analysis.

3.3. General procedure for the preparation of amides

A magnetic stirrer bar and the appropriate aldehydes were transferred to an 8 mL glass vial and then 3 mL H_2O was added. Later on, 50 mg Fe₂O₃-N/C (*i.e.* Fe-phen/C-800) catalyst (5 mol% Fe) was added followed by the addition of 100 µL aq. NH_3. Then, the vial was fitted with a septum, cap and needle. The reaction vials (*i.e.* 8 vials in each test) were placed into a

300 mL autoclave (PARR Instrument Company, USA) and then the autoclave was pressurized with 10 bar of air. The autoclave was placed into an aluminium block and the temperature of the aluminium block was set to be 120 °C inside the autoclave. The reactions were allowed to progress under continuous stirring for the required time at 120 °C. In this set-up the temperature of the aluminium block was set to more than 120 °C (130–140 °C) in order to attain exactly 120 °C inside the autoclave. After completion of the reaction, the excess air that remained in the autoclave was slowly depressurized and then the samples were removed from the autoclave. Afterwards, the catalyst was filtered-off and washed with methanol. The solvent from the filtrate containing the reaction products was removed *in vacuo* and the corresponding amide was purified by column chromatography. All products were analyzed by GC-MS and NMR spectroscopy analysis.

3.4. Procedure for the gram scale reactions

The reactions were performed similarly to the procedure mentioned in section 3.2, in a 100 or 300 mL glass fitted autoclave with the following conditions; 2–5 g aldehyde, a corresponding 3 mol% Fe, 200 µL aq. NH_3 for every 0.5 mmol substrate, 40 °C, 10–50 mL *t*-amyl alcohol, 24–30 h. After completion of the reaction, the autoclave was cooled to room temperature and the remaining air was discharged. The catalyst from the reaction mixture was filtered off and washed with ethyl acetate. The solvent from the filtrate containing the reaction products was removed *in vacuo*. The corresponding nitrile was purified by column chromatography (silica and an *n*-hexane–ethyl acetate mixture). All products were analyzed by GC-MS and NMR spectroscopy analysis.

3.5. Procedure for recycling the catalyst

The recycling of the catalyst was carried out for the synthesis of benzonitrile using the same procedure given in section 3.2 under the following reaction conditions: 1 mmol benzaldehyde, 60 mg Fe₂O₃-N/C (Fe-phen/C-800) (3% Fe), 400 µL aq. NH_3, 1 bar O_2, 4 mL *t*-amyl alcohol, 40 °C, 24 h; yields were determined by GC using 100 µL *n*-hexadecane as standard. In each run, after the reaction, the catalyst was separated by centrifugation, washed thoroughly with ethyl acetate and dried under vacuum. Then, the dried catalyst was used further, without any purification or re-activation. The recycled catalyst and centrifugate containing the reaction products were subjected to ICP analysis. This analysis showed that the content of Fe in the recycled catalysts had not decreased (2.94) and also Fe was not detected in the centrifugate.

4. Conclusions

In conclusion, we have demonstrated a green method for the preparation of nitriles and primary amides starting from various easily accessible aldehydes by making use of a combination of an earth abundant Fe-based nano-catalyst and green reagents such as atmospheric O_2 or air and inexpensive

Paper

aqueous ammonia. Under operationally simple and mild reaction conditions, this iron-based catalyst is highly reactive and selective for the synthesis of a series of functionalized and structurally diverse aromatic, heterocyclic and aliphatic nitriles. Additionally, this aerobic green oxidative method has been applied in the preparation of primary amides. Moreover, the synthetic utility and practical applicability of this method were demonstrated by up scaling the reactions to gram scales (1–5 g scale) and recycling of the catalyst.

Conflicts of interest

There are no conflicts to declare.

Acknowledgements

References

1 For selected reviews and books on iron catalysis: (a) S. Enthaler, K. Junge and M. Beller, *Angew. Chem., Int. Ed.*, 2008, **47**, 3317–3321; (b) C. Bolm, *Nat. Chem.*, 2009, **1**, 420; (c) C. Bolm, J. Legros, J. Le Paih and L. Zani, *Chem. Rev.*, 2004, **104**, 6217–6254; (d) I. Bauer and H.-J. Knölker, *Chem. Rev.*, 2015, **115**, 3170–3387; (e) K. Gopalaiah, *Chem. Rev.*, 2013, **113**, 3248–3296; (f) B. Plietker, in *Iron Catalysis in Organic Chemistry*, Wiley-VCH, Weinheim, Germany, 2008.

2 For selected examples of iron catalysis: (a) R. V. Jagadeesh, A.-E. Surkus, H. Junge, M.-M. Pohl, J. Radnik, J. Rabeah, H. Huan, V. Schünemann, A. Brückner and M. Beller, *Science*, 2013, **342**, 1073–1076; (b) J. R. Ludwig, P. M. Zimmerman, J. B. Gianino and C. S. Schindler, *Nature*, 2016, **533**, 374–379; (c) K. Adams, A. K. Ball, J. Birkett, L. Brown, B. Chappell, D. M. Gill, P. K. T. Lo, N. J. Patmore, C. R. Rice, J. Ryan, P. Raubo and J. B. Sweeney, *Nat. Chem.*, 2017, **9**, 396–401; (d) R. K. Sharma, S. Dutta, S. Sharma, R. Zboril, R. S. Varma and M. B. Gawande, *Green Chem.*, 2016, **18**, 3184–3209.

3 For selected examples and reviews on iron nanocatalysis: (a) R. V. Jagadeesh, T. Stemmler, A.-E. Surkus, H. Junge, K. Junge and M. Beller, *Nat. Protoc.*, 2015, **10**, 548–557; (b) H. M. T. Galvis, J. H. Bitter, C. B. Khare, M. Ruitenbeek, A. l. Dugulan and K. P. de Jong, *Science*, 2012, **335**, 835–838; (c) V. Polshettiwar, R. Luque, A. Fihri, H. Zhu, M. Bouhrara and J.-M. Basset, *Chem. Rev.*, 2011, **111**, 3036–3075.

4 (a) L. Que Jr. and W. B. Tolman, *Nature*, 2008, **455**, 333–340; (b) W. N. Oloo and L. Que Jr., *Acc. Chem. Res.*, 2015, **48**, 2612–2621.

5 S. S. Stahl and S. J. Lippard, Dioxygen and Alkane Activation by Iron-Containing Enzymes in *Iron Metabolism: Inorganic Biochemistry and Regulatory Mechanisms*, Wiley, 2008.

6 X. Jiang, J. Zhang and S. Ma, *J. Am. Chem. Soc.*, 2016, **138**, 8344–8347.

7 M. O. Ratnikov, X. Xu and M. P. Doyle, *J. Am. Chem. Soc.*, 2013, **135**, 9475–9479.

8 J. L. Klinkenberg and J. F. Hartwig, *Angew. Chem., Int. Ed.*, 2011, **50**, 86–95.

9 (a) R. C. Larock, *Comprehensive Organic Transformations: A Guide to Functional Group Preparations*, Wiley-VCH, New York, 2nd edn, 1999; (b) A. J. Aatiadi in *Preparation and Synthetic Applications of Cyano Compounds*, ed. S. Patai and R. Rappaport, Wiley, 2010.

10 M. Movassaghi and M. D. Hill, *Nat. Protoc.*, 2007, **2**, 2018–2023.

11 J. Yang, M. R. Karver, W. Li, S. Sahu and N. K. Devaraj, *Angew. Chem., Int. Ed.*, 2012, **51**, 5222–5225.

12 T. Wang and N. Jiao, *Acc. Chem. Res.*, 2014, **47**, 1137–1145.

13 G. Arthur, *The Amide Linkage: Selected Structural Aspects in Chemistry, Biochemistry, and Materials Science*, Wiley-Interscience, 2000.

14 F. F. Fraser, Y. Lihua, P. C. Ravikumar, L. Funk and B. C. Shook, *J. Med. Chem.*, 2010, **53**, 7902–7917.

15 S. T. Murphy, H. L. Case, E. Ellsworth, S. Hagen, M. Huband, T. Joannides, C. Limberakis, K. R. Marotti, A. M. Ottolini, M. Rauckhorst, J. Starr, M. Stier, C. Taylor, T. Zhu, A. Blaser, W. A. Denny, G. L. Lu, J. B. Smaill and F. Rivault, *Bioorg. Med. Chem. Lett.*, 2007, **17**, 2150–2155.

16 A. Graul and J. Castaner, *Drugs Future*, 1997, **22**, 956–968.

17 S. D. Roughley and A. M. Jordan, *J. Med. Chem.*, 2011, **54**, 3451–3479.

18 (a) A. Martin and V. N. Kalevaru, *ChemCatChem.*, 2010, **2**, 1504–1522; (b) F. Cavani, G. Centi and P. Marion, *Metal Oxide Catalysis*, ed. S. D. Jackson and J. S. J. Hargreaves, Wiley-VCH Verlag GmbH, 2009; (c) R. K. Grasselli and M. A. Tenhover, *Handbook of Heterogeneous Catalysis*, ed. G. Ertl, H. Knözinger, F. Schüth and J. Weitkamp, Wiley-VCH, Weinheim, 2008, pp. 3489–3517; (d) A. Martin and B. Lücke, *Catal. Today*, 2000, **57**, 61–70.

19 (a) P. Anbarasan, T. Schareina and M. Beller, *Chem. Soc. Rev.*, 2011, **40**, 5049–5067; (b) M. Sundermeier, A. Zapf, S. Mutyala, W. Baumann, J. Sans, S. Weiss and M. Beller, *Chem. – Eur. J.*, 2003, **9**, 1828–1836.

20 (a) T. Oishi, K. Yamaguchi and N. Mizuno, *Angew. Chem., Int. Ed.*, 2009, **48**, 6286–6288; (b) T. Oishi, K. Yamaguchi and N. Mizuno, *Top. Catal.*, 2010, **53**, 479–486; (c) W. Yin, C. Wang and H. Huang, *Org. Lett.*, 2013, **15**, 1850–1853; (d) R. V. Jagadeesh, T. Stemmler, A.-E. Surkus, M. Bauer, M.-M. Pohl, J. Radnik, K. Junge, H. Junge, A. Brückner and M. Beller, *Nat. Protoc.*, 2015, **10**, 916–926; (e) R. V. Jagadeesh, H. Junge and M. Beller, *Nat. Commun.*,

Green Chemistry

Paper

2014, **5**, 4123; (f) S. Shang, W. Dai, L. Wang, Y. Lv and S. Gao, *Chem. Commun.*, 2017, **53**, 1048–1051.

21 (a) L. M. Dornan, Q. Cao, J. C. A. Flanagan, J. J. Crawford, M. J. Cook and M. J. Muldoon, *Chem. Commun.*, 2013, **49**, 6030–6032; (b) M. Bhardwaj, M. Kour and S. Paul, *RSC Adv.*, 2016, **6**, 99604–99614.

22 (a) S. Gomez, J. A. Peters and T. Maschmeyer, *Adv. Synth. Catal.*, 2002, **344**, 1037–1057; (b) H. Alinezhad, H. Yavari and F. Salehian, *Curr. Org. Chem.*, 2015, **19**, 1021–1049; (c) O.-Y. Lee, K.-L. Law and D. Yang, *Org. Lett.*, 2009, **11**, 3302–3305.

23 (a) H. Yu, S. Ru, G. Dai, Y. Zhai, H. Lin, S. Han and Y. Wei, *Angew. Chem., Int. Ed.*, 2017, **56**, 3867–3871; (b) M. Liu and C.-J. Li, *Angew. Chem., Int. Ed.*, 2016, **55**, 10806–10810.

24 (a) H. Wang, X.-J. Dai and C.-J. Li, *Nat. Chem.*, 2017, **9**, 374–378; (b) L. Pu, *Acc. Chem. Res.*, 2014, **47**, 1523–1535; (c) F. Meng, F. Haeffner and A. H. Hoveyda, *J. Am. Chem. Soc.*, 2014, **136**, 11304–11307; (d) S. Fleischer, S. Zhou, K. Junge and M. Beller, *Angew. Chem., Int. Ed.*, 2013, **52**, 5120–5124; (e) X. Tan, G. Wang, Z. Zhu, C. Ren, J. Zhou, H. Lv, X. Zhang, L. Wa Chung, L. Zhang and X. Zhang, *Org. Lett.*, 2016, **18**, 1518–1521.

25 (a) E. E. Finney, K. A. Ogawa and A. J. Boydston, *J. Am. Chem. Soc.*, 2012, **134**, 12374–12377; (b) B. E. Marki and K. A. Scheidt, *Org. Lett.*, 2008, **10**, 4331–4334; (c) R. A. Green, D. Pletcher, S. G. Leach and R. C. D. Brown, *Org. Lett.*, 2015, **17**, 3290–3293; (d) B. R. Travis, M. Sivakumar, G. O. Hollist and B. Borhan, *Org. Lett.*, 2003, **5**, 1031–1034; (e) S. D. Sarkar, S. Grimme and A. Studer, *J. Am. Chem. Soc.*, 2010, **132**, 1190–1191; (f) R. Lerebours and C. Wolf, *J. Am. Chem. Soc.*, 2006, **128**, 13052–13053.

26 (a) D. W. Piotrowski, A. S. Kamlet, A.-M. R. Dechert-Schmitt, J. Yan, T. A. Brandt, J. Xiao, L. Wei and M. T. Barrila, *J. Am. Chem. Soc.*, 2016, **138**, 4818–4823; (b) D. Mahesh, P. Sadhu and T. Punniyamurthy, *J. Org. Chem.*, 2015, **80**, 1644–1650; (c) V. Zuliani, G. Cocconcelli, M. Fantini, C. Ghiron and M. Rivara, *J. Org. Chem.*, 2007, **72**, 4551–4553; (d) S. Hati, P. K. Dutta, S. Dutta, P. Munshi and S. Sen, *Org. Lett.*, 2016, **18**, 3090–3093.

27 (a) Y. Bernhard, B. Thomson, V. Ferey and M. Sauthier, *Angew. Chem., Int. Ed.*, 2017, **56**, 7460–7464; (b) M. Silvi, E. Arceo, I. D. Jurberg, C. Cassani and P. Melchiorre, *J. Am. Chem. Soc.*, 2015, **137**, 6120–6123; (c) V. Andrushko and N. Andrushko, *Stereoselective Synthesis by Bond Formation, Stereoselective Synthesis of Drugs and Natural Products*, Wiley VCH, Germany, 2013.

28 (a) C. B. Kelly, K. M. Lambert, M. A. Mercadante, J. M. Ovian, W. F. Bailey and N. E. Leadbeater, *Angew. Chem., Int. Ed.*, 2015, **54**, 4241–4245; (b) C. Fang, M. Li, X. Hu, W. Mo, B. Hu, N. Sun, L. Jin and Z. Shen, *Adv. Synth. Catal.*, 2016, **358**, 1157–1163.

29 (a) J. K. Augustine, R. N. Atta, B. K. Ramappa and C. Boodappa, *Synlett*, 2009, 3378–3382; (b) J.-L. Zhu, F.-Y. Lee, J.-D. Wu, C.-W. Kuo and K.-S. Shia, *Synlett*, 2007, 1317–1319; (c) E. Wang and G. Lin, *Tetrahedron Lett.*, 1998, **39**, 4047–4050; (d) M. A. Alia and T. Punniyamurthya, *Adv. Synth. Catal.*, 2010, **352**, 288–292.

30 B. V. Rokade and K. R. Prabhu, *J. Org. Chem.*, 2012, **77**, 5364–5370.

31 Q. Wu, Y. Luo, A. Lei and J. You, *J. Am. Chem. Soc.*, 2016, **138**, 2885–2888.

32 (a) S. Talukdar, J.-L. Hsu, T.-C. Chou and J.-M. Fang, *Tetrahedron Lett.*, 2001, **42**, 1103–1105; (b) A. C. Lele, N. H. P. Desai and M. S. Degani, *J. Pharm. Res.*, 2014, **7**, 934–936; (c) A. G. Choghamarani, M. A. Zolfigol, M. Hajjami and S. Sardari, *Synth. Commun.*, 2013, **43**, 52–58; (d) V. N. Telvekar, K. N. Patel, H. S. Kundaikar and H. K. Chaudhari, *Tetrahedron Lett.*, 2008, **49**, 2213–2215; (e) V. N. Telvekar, R. A. Rane and T. V. Namjoshi, *Synth. Commun*, 2010, **40**, 494–497; (f) N. D. Arote, D. S. Bhalerao and K. G. Akamanchi, *Tetrahedron Lett.*, 2007, **48**, 3651–3653; (g) S. Bag, N. R. Tawari and M. S. Degani, *ARKIVOC*, 2009, **xiv**, 118–123.

33 (a) S. Yamazaki and Y. Yamazaki, *Chem. Lett.*, 1990, 571–574; (b) G. Lai, N. K. Bhamare and W. K. Anderson, *Synlett*, 2001, 230–231.

34 (a) H. Veisi, *Synthesis*, 2010, 2631–2635; (b) Y.-Z. Zhu and C. Cai, *Monatsh. Chem.*, 2010, **141**, 637–639; (c) Y.-Z. Zhu, X.-Q. Zhang, F. Liu, H.-M. Gu and H.-L. Zhu, *Synth. Commun.*, 2013, **43**, 2943–2948; (d) L. Wang, C. Shen, H.-P. Wang, W.-Y. Zhou, F.-A. Sun, M.-Y. He and Q. Chen, *J. Chem. Res.*, 2012, **36**, 460–462.

35 (a) V. R. Pattabiraman and J. W. Bode, *Nature*, 2011, **480**, 471–479; (b) C. L. Allen and J. M. J. Williams, *Chem. Soc. Rev.*, 2011, **40**, 3405–3415.

36 (a) M. B. Smith, *Compendium of Organic Synthetic Methods*, Wiley, New York, 2001, p. 9; (b) E. Valeur and M. Bradley, *Chem. Soc. Rev.*, 2009, **38**, 606.

37 (a) K. Yamaguchi, H. Kobayashi, T. Oishi and N. Mizuno, *Angew. Chem., Int. Ed.*, 2012, **51**, 544–547; (b) J. F. Soule, H. Miyamura and S. Kobayashi, *J. Am. Chem. Soc.*, 2011, **133**, 18550–18553; (c) C. Tang and N. Jiao, *Angew. Chem., Int. Ed.*, 2014, **53**, 6528–6532; (d) F.-L. Zhang, Y.-F. Wang, G. H. Lonca, X. Zhu and S. Chiba, *Angew. Chem., Int. Ed.*, 2014, **53**, 4390–4394; (e) J. Zhang, Y. Liu, S. Chiba and T.-P. Loh, *Chem. Commun.*, 2013, **49**, 11439–11441; (f) S. L. Zultanski, J. Zhao and S. S. Stahl, *J. Am. Chem. Soc.*, 2016, **138**, 6416–6419; (g) C. Gunanathan, Y. Ben-David and D. Milstein, *Science*, 2007, **317**, 790–792.

38 (a) H. Peng, H. Xu, H. Wu, K. Zhang and P. Wu, *Chem. Commun.*, 2013, **49**, 2709; (b) D. Antoniak, A. Sakowicz, R. Loska and M. Mąkosza, *Synlett*, 2015, **26**, 84–86; (c) J.-J. Shie and J.-M. Fang, *J. Org. Chem.*, 2003, **68**, 1158–1160.
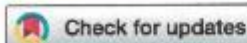
Chemical Science

EDGE ARTICLE

Check for updates

Cobalt-based nanoparticles prepared from MOF–carbon templates as efficient hydrogenation catalysts†

Kathiravan Murugesan, [ID] [a] Thirusangumurugan Senthamarai,[a] Manzar Sohail, [ID] [ab] Ahmad S. Alshammari,[c] Marga-Martina Pohl,[a] Matthias Beller [ID] *[a] and Rajenahally V. Jagadeesh [ID] *[a]

The development of efficient and selective nanostructured catalysts for industrially relevant hydrogenation reactions continues to be an actual goal of chemical research. In particular, the hydrogenation of nitriles and nitroarenes is of importance for the production of primary amines, which constitute essential feedstocks and key intermediates for advanced chemicals, life science molecules and materials. Herein, we report the preparation of graphene shell encapsulated Co_3O_4- and Co-nanoparticles supported on carbon by the template synthesis of cobalt-terephthalic acid MOF on carbon and subsequent pyrolysis. The resulting nanoparticles create stable and reusable catalysts for selective hydrogenation of functionalized and structurally diverse aromatic, heterocyclic and aliphatic nitriles, and as well as nitro compounds to primary amines (>65 examples). The synthetic and practical utility of this novel non-noble metal-based hydrogenation protocol is demonstrated by upscaling several reactions to multigram-scale and recycling of the catalyst.

Introduction

The development of base metal catalysts for sustainable and cost-effective processes is an actual and long standing goal of chemical research in academia and industry.[1-3] Among the different synthetic technologies, catalytic hydrogenations represent a versatile tool box for the preparation of numerous fine and bulk chemicals, fuels, and life science molecules.[4-10] Until today, on a practical scale these reactions mainly rely on precious metal-based catalysts,[4-9] as well as RANEY® nickel.[4-10] However, the availability and high price of precious metals, and selectivity problems and sensitivity of RANEY® Ni spurred interest towards alternative catalysts.[1-3,11-18] In this respect, reusable supported nanoparticles are attractive due to easy separation, accessibility of active sites, control of size, and prospect of mild reaction conditions.[15-25] Traditionally, supported metal nanoparticles are prepared by thermal (pyrolysis or calcination) or chemical reduction of the respective metal salts on heterogeneous supports.[19-25] Despite the synthesis of

literally thousands of such catalytic materials, the majority of them does not permit for the refinement of functionalized and complex molecules.[19-25] However in recent years, more potent materials were prepared by using specific precursors such as metal–nitrogen complexes[15-17,26] or structure-controlling templates.[27-35] In this respect, metal organic frameworks (MOFs) built from metal ions and different organic linkers can be assembled in a highly flexible manner.[20-27] So far, MOFs proved to be suitable for gas separation and storage, but also interesting catalytic applications have been realized,[27-30] especially *via* subsequent pyrolysis processes.[31-34] Complementary to these materials, most recently we described the use of cobalt-diamine-dicarboxylic acid-based MOFs as precursors for the preparation of supported nanoparticles and single Co atoms, which exhibit excellent catalytic activity for reductive aminations.[35] In this case, both the nitrogen and carboxylic acid linker was necessary to produce an active material. In continuation of our efforts to develop cost-efficient materials[36] for sustainable catalysis, herein we describe the expedient preparation of a cobalt-terephthalic acid MOF–carbon template, which forms after pyrolysis graphene shell encapsulated Co_3O_4/Co particles. The resulting nanoparticles are supported on carbon, which creates stable and reusable catalysts for selective hydrogenations of aliphatic and aromatic nitriles and nitro compounds (Fig. 1).

The resulting amines are of interest to chemistry, medicine, biology, biochemistry and material science.[37-43] For example, amine motifs constitute an integral part of the majority of life

[a]Leibniz-Institut für Katalyse e. V. an der Universität Rostock, Albert-Einstein-Str. 29a, 18059 Rostock, Germany. E-mail: Matthias.Beller@catalysis.de; Jagadeesh. Rajenahally@catalysis.de

[b]The Center of Research Excellence in Nanotechnology (CENT), King Fahd University of Petroleum and Minerals, Dhahran 31261, Saudi Arabia

[c]King Abdulaziz City for Science and Technology, Riyadh 11442, Saudi Arabia

† Electronic supplementary information (ESI) available. See DOI: 10.1039/c8sc02807a
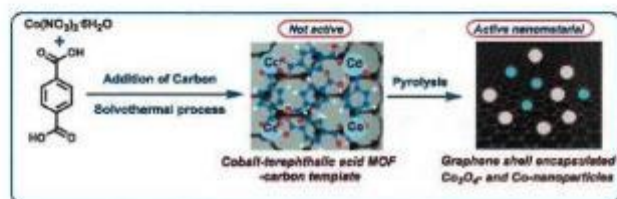
Fig. 1 Preparation of graphene encapsulated cobalt oxide- and cobalt-nanoparticles supported on carbon by the pyrolysis of cobalt-terephthalic acid MOF–carbon template.

science molecules and natural products.[37-43] In fact, among 200 existing drugs, more than 170 contain at least one nitrogen atom regulating their activities.[37] Among the different kinds of amines, primary amines attract special interest because they can be easily further transformed; thus constitute central intermediates for the production of specialty chemicals, pharmaceuticals, agrochemicals, dyes and polymers. In industry primary benzylic, aliphatic and aromatic amines are often prepared by the hydrogenation of the corresponding nitriles[44-46] and nitroarenes,[15,16,47-53] respectively. Apart from traditional noble metal-catalysts,[44-46] Raney®-nickel[54-57] or -cobalt,[57] Fe,[58,59] Co,[60-64] and Mn[65]-based catalysts have recently been disclosed. Despite these achievements, still the development of active and selective nanocatalysts based on earth abundant metals is desired.

Results and discussion

Catalyst preparation and activity studies

At the start of our investigations, we prepared a cobalt-terephthalic acid MOF template on carbon by reacting cobalt nitrate and terephthalic acid (1 : 3) in DMF with carbon powder at 150 °C. After slow evaporation of solvent, the corresponding material was pyrolyzed at different temperatures (400, 600, 800, and 1000 °C) under inert atmosphere. The activity of the prepared potential catalysts was tested for the hydrogenation of benzonitrile to benzylamine as a bench mark reaction. Among these, cobalt-terephthalic acid MOF@C-800 was the most active material. However, a mixture of the desired benzylamine (<15%) and several side products such as N-benzylidenebenzylamine and dibenzylamine were observed (Table 1, entry 1). To suppress their formation, the reaction was performed in presence of hydrogen and ammonia. The latter is known to control the selective formation of primary amines from nitriles (Fig. S1†). Advantageously, under these conditions benzylamine was obtained in 97% yield (Table 1, entry 2). Other materials such as pyrolyzed cobalt nitrate on carbon (cobalt nitrate@C-800), unpyrolyzed MOF–carbon template (cobalt-terephthalic acid MOF@C) and isolated MOF (cobalt-terephthalic acid MOF) were also tested and none of these materials were active (Table 1, entries 3–5). As expected, cobalt nitrate and cobalt-terephthalic acid under homogeneous reaction conditions were also not active (Table 1, entries 6–7). Further, the cobalt-terephthalic acid MOF was pyrolyzed directly without carbon

Table 1 Hydrogenation of benzonitrile to benzylamine: activity of cobalt catalysts[a]

Entry	Catalyst	Conv. (%)	Yield (%)
1[b]	Cobalt-terephthalic acid MOF@C-800	>99	<15
2[c]	Cobalt-terephthalic acid MOF@C-800	>99	97
3[c]	Cobalt nitrate@C-800	<5	<2
4[c]	Cobalt-terephthalic acid MOF@C	<2	<1
5[c]	Cobalt-terephthalic acid MOF	<2	<1
6[d]	Cobalt nitrate + terephthalic acid	<2	<1
7[d]	Co(NO$_3$)$_2$·6H$_2$O	<2	<1
8[e]	Cobalt-terephthalic acid MOF-800	>99	96

[a] Materials are pyrolyzed at 800 °C for 2 h under argon. Cobalt content in the pyrolyzed sample supported on carbon = 4.5 wt%. [b] Reaction conditions: Heterogeneous catalysis conditions = 0.5 mmol benzonitrile, 25 mg catalyst (3.8 mol% Co), 3 mL toluene, 25 bar H$_2$, 120 °C, 15 h. [c] Same as 'a' with 5 bar NH$_3$. [d] Homogeneous catalysis conditions = 0.5 mmol benzonitrile, 0.02 mmol Co(NO$_3$)$_2$·H$_2$O, 0.06 mmol linker, 3 mL toluene, 25 bar H$_2$, 5 bar NH$_3$, 120 °C, 15 h. [e] Material was prepared by the direct pyrolysis (800 °C, 2 h Ar) of MOF without carbon support.

support and tested for its catalytic activity. Interestingly, this material was also found to be active and produced 96% of benzylamine (Table 1, entry 8). However, due to the high cobalt content (40% wt%), this catalyst (cobalt-terephthalic acid MOF-800) exhibits less stability compared to the cobalt-terephthalic acid MOF@C-800.

To further optimize the benchmark reaction and to study the course of the formation of products, we varied different parameters such as ammonia concentration, reaction time, amount of catalyst, and hydrogen pressure in the presence of the optimal catalyst (cobalt-terephthalic acid MOF@C-800). As shown in Fig. S2,† complete conversion of benzonitrile (0.5 mmol-scale) and formation of benzylamine as the sole desired product was observed in presence of 20 mg of catalyst at 20 bar of H$_2$.

Characterization of the active nano-catalyst

In order to understand the structural features of the most active material, cobalt-terephthalic acid MOF@C-800 was characterized using Cs-corrected STEM (scanning transmission electron microscopy), XRD (X-ray diffraction), EPR (electron paramagnetic resonance), and XPS (X-ray photoelectron spectroscopy) spectral analysis. TEM analysis of the active material
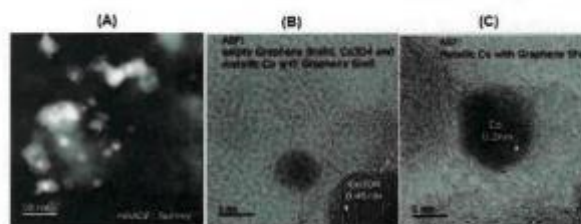
Fig. 2 TEM images of cobalt-terephthalic acid MOF@C-800 catalyst showing Co$_3$O$_4$ and Co-nanoparticles (A) and metallic cobalt particles encapsulated in graphene shells (B and C).

Edge Article

revealed the formation of cobalt oxide (Co_3O_4) particles with 5–30 nm size (Fig. 2). In addition, the material also contained metallic cobalt nanoparticles. Interestingly, both types of nanoparticles are encapsulated within graphene shells (Fig. 2). In contrast, the inactive material cobalt nitrate@C-800 contained hollow Co_3O_4 particles above 50 nm size (Fig. S4†). Notably, this material contained no graphene shells. Further, the formation of Co_3O_4-particles was confirmed by XRD data (Fig. S7†). Also, XRD analysis revealed the formation of cobalt-terephthalic acid MOF (Fig. S8†).

To understand the nature of the active metal species in more detail, EPR measurements were performed, too. Cobalt-terephthalic acid MOF@C-800 displayed a broad signal with a resonance peak observed at 3391 G with full width at half maximum (FWHM) 1640 G (Fig. S9†). The g value 2.572 observed was about 23% higher than the g value of free electron (2.00) in space. This indicates Co in higher oxidation states (Co^{2+}/Co^{3+}). The observation of only one peak indicates the presence of one paramagnetic species predominantly.[66] Further, to confirm the presence of Co_3O_4, we performed XPS analysis of Co2p and O1s electrons for cobalt-terephthalic acid MOF@C-800 (Fig. S10†). The binding energy values of its most intense Co2p signals match very closely to the presence of Co_3O_4 at the surface of the catalyst. The $Co2p^{3/2}$ and $Co2p^{1/2}$ peaks appeared at 779.75 eV and 794.91 eV, respectively. The $Co2p^{3/2}$–$Co2p^{1/2}$ splitting energy of 15.16 eV is also in close agreement with the presence of Co_3O_4. Weak peaks, which are the characteristics of Co^{2+} in Co_3O_4, support the absence of other CoO species. It is generally known that in Co_3O_4, the $Co2p^{3/2}$ spectrum of cobalt oxide is representative for high spin Co^{2+} and low spin Co^{3+} ions.[67,68] The O1s surface spectra showed a significant broadening towards higher binding energy and was deconvoluted in three components. The first peak at 529.05 eV is representative of a cobalt oxide network, while the second peak present at 531.60 eV could be related to the presence of hydroxyl groups in the inner surface. The third broad peak at 535.23 eV is related to water adsorbed at the surface.[69] The BET surface area of cobalt-terephthalic acid MOF@C-800 is 158.4 m^2 g^{-1} and the corresponding average pore size is 7.96 nm (Fig. S9 and S10†). Notably, TEM analysis revealed the formation of both Co_3O_4 and metallic Co nanoparticles in the most active sample (cobalt-terephthalic acid MOF@C-800). However, XPS and XRD analyses detected only Co_3O_4-particles. This might be due to the small quantity or size of metallic cobalt particles, which are difficult to detect by XRD or XPS.

Hydrogenation of functionalized (hetero)aromatic nitriles

With the optimal material (cobalt-terephthalic acid MOF@C-800) in hand, we investigated the scope and general applicability for the hydrogenation of nitriles. As shown in Fig. 3 and 4, various functionalized and structurally diverse benzonitriles, heterocyclic nitriles and challenging aliphatic ones smoothly underwent hydrogenation to produce the corresponding primary amines in good to excellent yields. For example, 8 different halogenated benzylic amines, which constitute common building blocks in the chemical industry, were
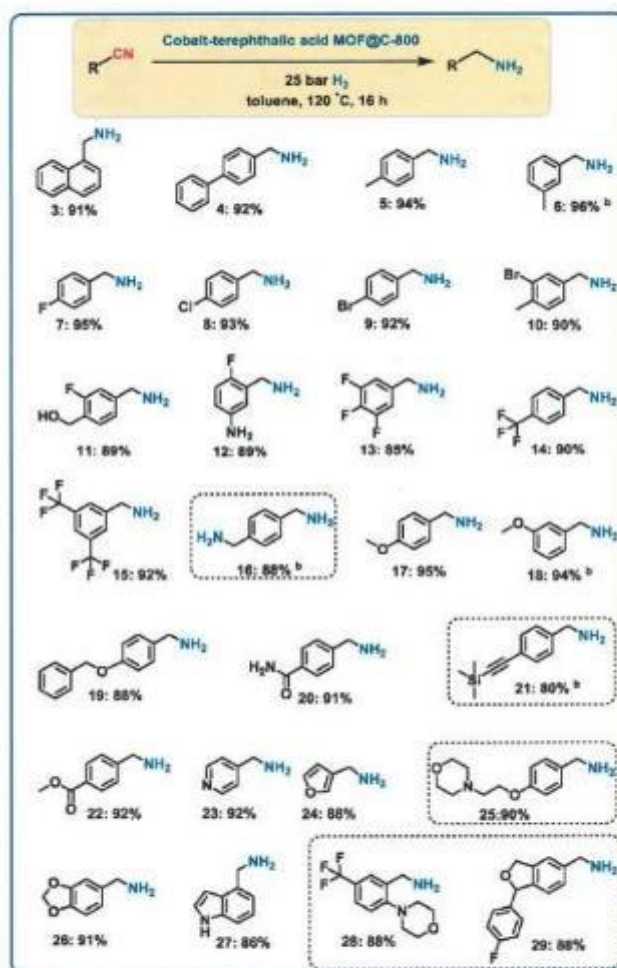
Fig. 3 Cobalt-terephthalic acid MOF@C-800-catalyzed hydrogenation of benzonitriles and cyano-heterocycles to primary amines[a]. [a]Reaction conditions: 0.5 mmol benzonitrile, 25 mg catalyst (3.8 mol% Co), 3 mL toluene, 25 bar H_2, 5 bar NH_3, 120 °C, 16 h, isolated yields. [b]GC yields using 100 μL n-hexadecane. Isolated as respective hydrochloride salts.

obtained in 85–95% yield without significant dehalogenations (Fig. 3; products 7–14). In order to apply this protocol for advanced organic synthesis and drug discovery, achieving high chemo-selectivity is of crucial importance. In this regard, we were pleased to find excellent hydrogenation selectivity in the presence of amide, ester, and even C–C double and triple bonds (Fig. 3; products 17–21). Furthermore, diverse heterocyclic amines have been prepared from the corresponding nitriles (Fig. 3; products 23–29).

Hydrogenation of aliphatic nitriles

Next, we performed the hydrogenation of aliphatic nitriles to the corresponding primary amines (Fig. 4). Compared to aromatic nitriles, such hydrogenations are in general more difficult and need harsher conditions. Fortunately, this catalyst
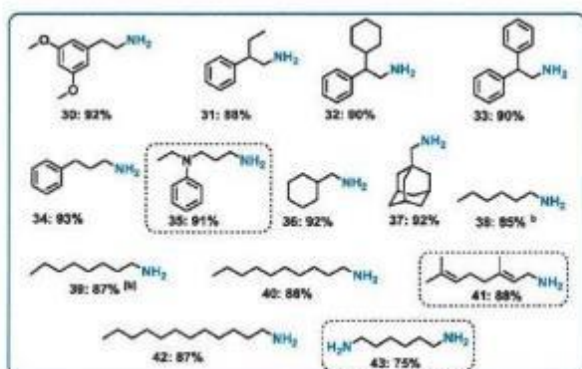
Fig. 4 Hydrogenation of aliphatic nitriles catalyzed Co₃O₄/Co-nanoparticles. [a]Reaction conditions: 0.5 mmol benzonitrile, 25 mg catalyst (3.8 mol% Co), 3 mL toluene, 25 bar H₂, 5 bar NH₃, 120 °C, 16 h, isolated yields. [b]GC yields using 100 μL n-hexadecane. Isolated as respective hydrochloride salts.

is similar active and selective for the hydrogenation of aliphatic substrates, too. As a result, aliphatic amines including long chain, (bi)cyclic and as well as allylic ones were obtained in up to 93% yield (Fig. 4). The preparation of hexamethylenediamine in 75%—a central precursor for nylon 66 polymer (Fig. 4; product 43)—highlights the industrial relevance of this methodology.

Chemoselective hydrogenation of nitroarenes to anilines

After having demonstrated the reduction of nitriles, we speculated on the utility of our cobalt-catalyst for other hydrogenations to give amines.

In this context, several nitroarenes were hydrogenated to produce the corresponding anilines with excellent yields (Fig. 5–6). Similar to nitriles, aromatic, heterocyclic and aliphatic nitro compounds were selectively reduced. For example, halogenated anilines were obtained in up to 95% yield without dehalogenation (Fig. 5; products 48–54). Most interestingly, 4-iodonitrobenzene, which is a highly sensitive compound, led in 95% to the corresponding aniline (Fig. 5; product 53). In other structurally diverse and functionalized molecules the nitro group was also selectively reduced. As a result, hydroxyl groups, aldehyde, ketone, ester, amide, and C–C double bonds were untouched.

Hydrogenation of nitro heterocycles and nitroalkanes

Next, 5 representative nitro-substituted heteroarenes were hydrogenated to produce amino-substituted N-heterocycles (Fig. 6; products 70–75). For example, the resulting 8-amino-quinoline (product 71) represents a key intermediate for preparation of primaquine, tafenoquine and pamaquine drugs, which are used in the treatment of malaria. Finally, nitro-cyclohexane and 1-nitrohexane were tested. It should be noted that most of the known nitro reduction catalysts either show poor reactivity or do not work at all for aliphatic nitro compounds. Favorably, using this novel cobalt catalyst both
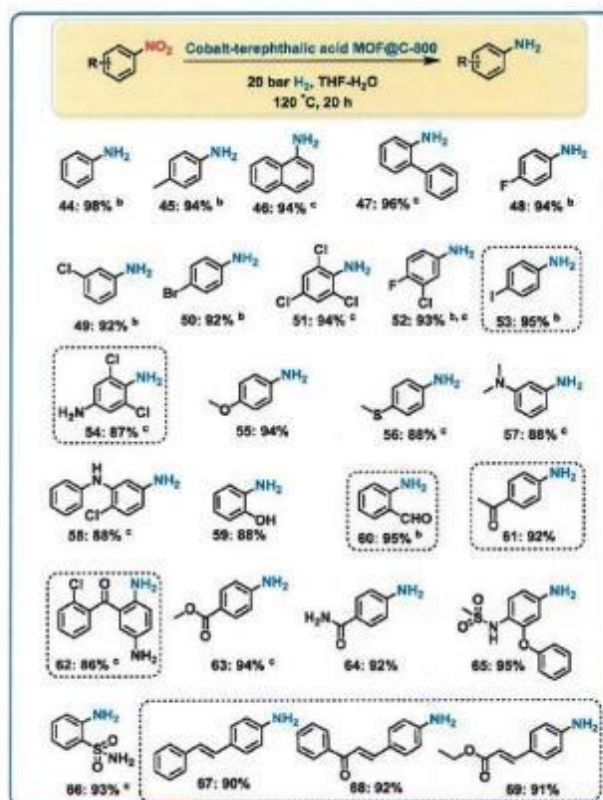
Fig. 5 Cobalt-terephthalic acid MOF@C-800-catalyzed hydrogenation of functionalized nitroarenes to anilines[a]. [a]Reaction conditions: 0.5 mmol nitroarene, 25 mg catalyst (3.8 mol% Co), 3 mL THF–H₂O (1 : 1), 20 bar H₂, 120 °C, 20 h, isolated yields. [b]GC yields using 100 μL n-hexadecane. [c]With 40 bar H₂.

compounds were successfully hydrogenated and produced primary amines in 78 and 91% yield, respectively (Fig. 6; products 76 and 77).

Demonstrating scale-up and catalyst recycling

To complement the synthetic viability of the catalyst system and the developed protocols, upscaling of selected reactions and
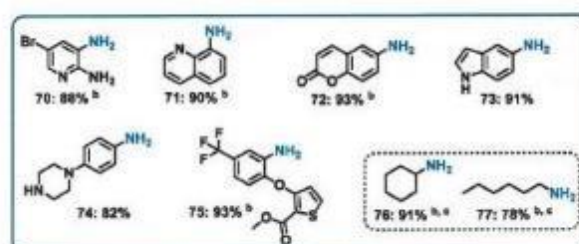
Fig. 6 Hydrogenation of nitro-heterocycles and aliphatic nitro compounds catalyzed cobalt-terephthalic acid MOF@C-800-catalyst. [a]Reaction conditions: 0.5 mmol nitro compound, 25 mg catalyst (3.8 mol% Co), 3 mL THF–H₂O (1 : 1), 20 bar H₂, 120 °C, 20 h, isolated yields. [b]With 40 bar H₂ in 3 mL t-butanol solvent. [c]GC yields using 100 μL n-hexadecane.

recycling of catalyst are presented. The hydrogenation of three nitriles two nitroarenes on gram-scale (2–5 g) proceeded easily and in all cases similar yields to mg-scale reactions were obtained (Fig. 7).

In addition, these cobalt oxide nanoparticles proved to be highly stable in the benchmark hydrogenation and were recycled and reused for 5 times without significant loss of catalytic activity (Fig. 8). TEM analysis of the reused catalyst showed that there is no change in the structure of metallic Co particles (Fig. S5 and S6†). However, a change in the structure of the cobalt oxide particles was observed. Some of these particles migrate out from graphene shells and form new structures on carbon support (Fig. S5 and S6†).

Experimental

General considerations

All nitriles and nitroarenes were obtained commercially from various chemical companies. Cobalt(ii) nitrate hexahydrate, terephthalic acid were obtained from Sigma-Aldrich. Dry toluene, 99.8% was obtained from across chemicals. Carbon powder, VULCAN® XC72R with Code XVC72R and CAS no. 1333-86-4 was obtained from Cabot Corporation Prod. The pyrolysis experiments were carried out in Nytech-Qex oven. Before using, the purity of nitriles and nitroarenes has been checked.

The TEM measurements were performed at 200 kV with an aberration-corrected JEM-ARM200F (JEOL, Corrector: CEOS). The microscope is equipped with a JED-2300 (JEOL) energy-dispersive X-ray-spectrometer (EDXS). The aberration corrected STEM imaging (High-Angle Annular Dark Field (HAADF) and Annular Bright Field (ABF) were performed under the following conditions. HAADF and ABF both were done with a spot size of approximately 0.1 nm, a convergence angle of 30–36° and collection semi-angles for HAADF and ABF of 90–170 mrad and 11–22 mrad respectively. The solid samples were deposited without any pretreatment on a holey carbon supported Cu-grid (mesh 300) and transferred to the microscope.
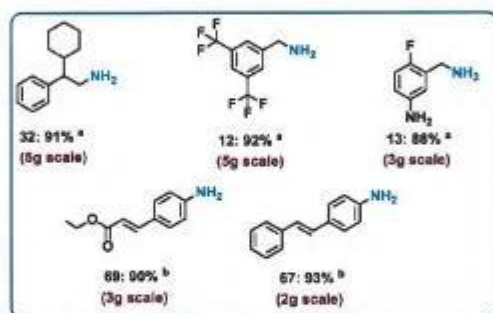
Fig. 7 Representing the practical utility of the cobalt-catalyzed hydrogenation protocol for gram scale reactions. Reaction conditions: [a]3–5 g nitrile, 25 mg catalyst (3.8 mol% Co) for each for each 0.5 mmol substrate, 25 bar H_2, 5 bar NH_3, 120 °C, 20–60 mL toluene 16 h, Isolated respective hydrochloride salts. [b]2–3 g nitroarene 25 mg catalyst (3.8 mol% Co) for each 0.5 mmol substrate, 40 bar H_2, 120 °C, 20–40 mL THF–H_2O (1 : 1), 20 h, isolated yields.
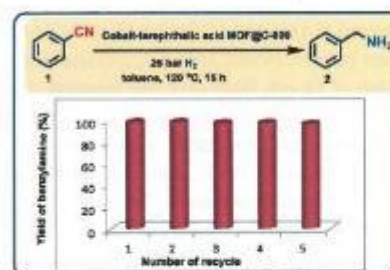
Fig. 8 Demonstrating the recycling of cobalt-terephthalic acid MOF@C-800-catalyst for the hydrogenation of benzonitrile to benzylamine. Reaction condition: 5 mmol benzonitrile, 250 mg catalyst, (3.8 mol% Co), 20 mL toluene, 25 bar H_2, 5 bar NH_3, 120 °C, 16 h, GC yields using n-hexadecane standard.

XRD powder pattern were recorded either on a Panalytical X'Pert diffractometer equipped with a Xcelerator detector or on a Panalytical Empyrean diffractometer equipped with a PIXcel 3D detector system. Both were used with automatic divergence slits and Cu kα1/α2 radiation (40 kV, 40 mA; λ = 0.015406 nm, 0.0154443 nm). Cu β-radiation was excluded by using nickel filter foil. Peak positions and profile were fitted with pseudo-Voigt function using the HighScore Plus software package (Panalytical). Phase identification was done by using the PDF-2 database of the International Center of Diffraction Data (ICDD).

EPR spectra were recorded in X-band at 273 K on a Adani Spinscan X-band electron paramagnetic resonance (EPR) spectrometer equipped with cavity Q factor and MW power measurement with a magnetic field modulation capability of 10–250 kHz. The data were measured at microwave frequency = 9.48 GHz; modulation amplitude = 8 G; modulation frequency = 100 kHz as reported in the reference.

XPS data was obtained with a VG ESCALAB220iXL (Thermo-Scientific) with monochromatic Al Kα (1486.6 eV) radiation. The electron binding energies EB were obtained without charge compensation. For quantitative analysis the peaks were deconvoluted with Gaussian–Lorentzian curves, the peak area was divided by a sensitivity factor obtained from the element specific Scofield factor and the transmission function of the spectrometer.

All catalytic experiments were carried out in 300 mL and 100 mL autoclaves (PARR Instrument Company). In order to avoid unspecific reactions, all catalytic reactions were carried out either in glass vials, which were placed inside the autoclave, or glass/Teflon vessel fitted autoclaves.

GC and GC-MS were recorded on Agilent 6890N instrument. GC conversion and yields were determined by GC-FID, HP6890 with FID detector, column HP530 m × 250 mm × 0.25 μm.

^{1}H, ^{13}C NMR data were recorded on a Bruker ARX 300 and Bruker ARX 400 spectrometers using DMSO-d6, CD_3OD and $CDCl_3$ solvents.

Procedure for the preparation of cobalt-terephthalic acid MOFs–carbon template and graphene shell encapsulated cobalt-based nanoparticles

A 50 mL dried round bottomed flask was charged with magnetic stirring bar and 1.52 mmol of cobalt(ii) nitrate hexahydrate and

4.58 mmol of terephthalic acid. Then 25–30 mL of DMF was added and stirred at 140–150 °C for 20–30 min. To this mixture, 1.5 g of carbon powder (VULCAN® XC72R) was added followed by the addition of 15 mL DMF and the reaction mixture again was stirred at 150 °C for 4–5 h by fixing reflux condenser. Then, the reflux condenser and magnetic stirring bar were removed and the round bottomed flask containing reaction products were. Then, the round bottomed flask containing reaction mixture was placed into an aluminium block preheated at 150 °C and allowed to stand without stirring and closing for 20–22 h at 150 °C in order to slow evaporation of DMF and to form Co–MOF–carbon template *via* solvothermal process. After complete drying, the material was cooled to room temperature and grinded to fine powder. The powdered material was pyrolyzed at 800 °C for 2 hours under an argon atmosphere and then cooled to room temperature after pyrolysis. (Elemental analysis (wt%): cobalt-terephthalic acid MOF@C-800: Co = 4.5, C = 90.70%, H = 0.25%.

Procedure for the preparation and isolation of cobalt-terephthalic acid MOFs

A 50 mL dried round bottomed flask was charged with magnetic stirring bar, 0.52 mmol of cobalt(II) nitrate hexahydrate and 4.58 mmol of terephthalic acid. Then 25–30 mL of DMF was added and stirred at 140–150 °C for 20–30 min. Then, the round bottomed flask containing reaction mixture was placed into an aluminium block preheated at 150 °C and stirred for 20–30 minutes by fixing reflux condenser. Then, the reflux condenser and magnetic stirring bar were removed and the round bottomed flask containing reaction products were allowed to stand without stirring and closing for 20–24 h at 150 °C in order to slow evaporation of DMF and to form Co–MOFs *via* solvothermal process. Afterward the product obtained was cooled down to room temperature and washed with hot DMF and then dried at 150 °C and at high vacuum.

General procedure for the hydrogenation of nitriles

The magnetic stirring bar and 0.5 mmol corresponding nitrile compound was transferred to 8 mL glass vial and then 3 mL solvent (toluene) was added. Then, 25 mg of catalyst was added and the vial was fitted with septum, cap and needle. The reaction vials (8 vials with different substrates at a time) were placed into a 300 mL autoclave. The autoclave was flushed with hydrogen twice at 25 bar pressure and then it was pressurized with 5 bar ammonia gas and 25 bar hydrogen. The autoclave was placed into an aluminium block preheated at 130 °C (placed 30 minutes before counting the reaction time in ordered to attain reaction temperature) and the reactions were stirred for required time. During the reaction the inside temperature of the autoclave was measured to be 120 °C and this temperature was used as the reaction temperature. After the completion of the reactions, the autoclave was cooled to room temperature. The remaining ammonia and hydrogen were discharged and the vials containing reaction products were removed from the autoclave. The catalyst was filtered off and washed with ethyl acetate. The filtrate containing product was subjected to

evaporation to remove solvent and ammonia. The crude product was diluted with ether and 1–2 mL methanol HCl or dioxane HCl (1.5 M HCl in methanol or 4 N HCl in dioxane) was added and stirred at room temperature for 4–5 h to obtain hydrochloride salt of amine. Then, the solvent was removed and the resulted hydrochloride salt of amine is dried under high vacuum. For determining the yields using GC analysis, after completing the reaction *n*-hexadecane (100 μL) as standard was added to the reaction vials and the reaction products were diluted with ethyl acetate followed by filtration using plug of silica and then analyzed by GC.

General procedure for the hydrogenation of nitro compounds

The magnetic stirring bar and corresponding nitro compound (0.5 mmol) were transferred to the glass vial and then 3 mL solvent (water–THF or tertiary butanol) was added. Then, 25 mg of catalyst was added and the vial was fitted with septum, cap and needle. The reaction vials (8 reaction vials at a time in case of 0.5 mmol scale) were placed into a 300 mL autoclave. The autoclave was flushed with hydrogen twice at 30 bar pressure and then it was pressurized to 20 bar or 40 bar hydrogen pressure. The autoclave was placed into an aluminium block (placed 30 minutes before counting the reaction time in ordered to attain reaction temperature) preheated at 130 °C and the reactions were stirred for required time. During the reaction the inside temperature of the autoclave was measured to be 120 °C and this temperature was used as the reaction temperature. After the completion of the reaction, the autoclave was cooled to room temperature. The remaining hydrogen was discharged and the samples were removed from the autoclave. Catalyst from the reaction mixture was filtered off and washed with THF and then ethyl acetate. The solvent form filtrate containing reaction product was removed *in vacuo*. The corresponding aniline was purified by column chromatography (silica; *n*-hexane-ethyl acetate mixture). Then, dried over anhydrous Na₂SO₄ and the solvent was removed *in vacuo*. For determining the yields using GC analysis, after completing the reaction *n*-hexadecane (100 μL) as standard was added to the reaction vials and the reaction products were diluted with THF followed by filtration using plug of silica and then analyzed by GC.

Procedure for up-scaling the reactions

For the hydrogenation of nitriles. To a Teflon or glass fitted 300 mL or 1.0 L autoclave, the magnetic stirring bar and corresponding nitriles were transferred and then 120–150 mL of dry toluene was added. Then after, required amount of catalyst (25 mg for each 0.5 mmol substrate) was added. The autoclave was flushed with hydrogen twice at 30 bar pressure and then it was pressurized with 5 bar ammonia gas and 25 bar hydrogen. The autoclave was placed into an aluminium block preheated at 130 °C (placed 30 minutes before counting the reaction time in ordered to attain reaction temperature) and the reaction was stirred for required time. During the reaction the inside temperature of the autoclave was measured to be 120 °C and this temperature was used as the reaction temperature. After the completion of the reaction, the autoclave was cooled to room

temperature. The remaining ammonia and hydrogen were discharged and the reaction products were removed from the autoclave. The solid catalyst was filtered off and washed thoroughly with ethyl acetate. The reaction products were analyzed by GC-MS and the corresponding primary amines were converted to their respective hydrochloride salt and characterized.

For the hydrogenation of nitroarenes. To a Teflon or glass fitted 300 mL or 1.0 L autoclave, the magnetic stirring bar and corresponding nitrocompounds were transferred and then 120–150 mL of THF–H$_2$O was added. Then after, required amount of catalyst (25 mg for each 0.5 mmol substrate) was added. The autoclave was flushed with hydrogen twice at 30 bar pressure and 40 bar hydrogen. The autoclave was placed into an aluminium block preheated at 130 °C (placed 30 minutes before counting the reaction time in ordered to attain reaction temperature) and the reaction was stirred for required time. During the reaction the inside temperature of the autoclave was measured to be 120 °C and this temperature was used as the reaction temperature. After the completion of the reaction, the autoclave was cooled to room temperature. The remaining hydrogen was discharged and the reaction products were removed from the autoclave. The solid catalyst was filtered off and washed thoroughly with ethyl acetate. The reaction products were analyzed by GC-MS and the corresponding anilines were isolated.

Procedure for catalyst recycling

The magnetic stirring bar and 5 mmol benzonitrile were transferred to glass fitted 100 mL autoclave and then 20 mL dry toluene was added. Then after, 250 mg of catalyst was added. The autoclave was flushed with 30 bar hydrogen and then it was pressurized with 5 bar ammonia gas and 25 bar hydrogen. The autoclave was placed into heating system and reactions were allowed to progress at 120 °C (temperature inside the autoclave) by stirring for required time. After the completion of the reaction, the autoclave was cooled and the remaining ammonia and hydrogen were discharged. To the reaction products, 250 μL n-hexadecane as standard was added. The catalyst was then separated by centrifugation and the centrifugate containing reaction products was subjected to GC analysis for determining the yield of benzyl amine. The separated catalyst by centrifugation was then washed with ethyl acetate, dried under vacuum and used without further purification or reactivation for the next run.

Conclusions

In conclusion, we prepared cobalt nanoparticles encapsulated in graphene shells supported on carbon by pyrolysis of simple cobalt salts and terephthalic acid (TPA). Compared to other recently developed nano-catalysts, this Co–TPA–carbon catalyst does not require nitrogen-doping for activity, which opens new avenues for catalyst design. The presented material constitutes a general base-metal hydrogenation catalyst, which allows for selective reduction of a series of functionalized and structurally diverse aromatic, heterocyclic and aliphatic nitriles, as well as

nitro compounds. The synthetic utility and practicability of this cobalt-based hydrogenation protocol was further established by performing gram-scale synthesis and recycling of the catalyst.

Conflicts of interest

There are no conflicts to declare.

Acknowledgements

Notes and references

1 J. Maes, E. A. Mitchell and B. U. W. Maes, *Base metals in catalysis: From zero to hero in green and sustainable medicinal chemistry: Methods, tools and strategies for the 21st century pharmaceutical industry*, L. Summerton, H. F. Sneddon, L. C. Jones and J. H. Clark, Royal Society of Chemistry, 2016.

2 Chem 21, *Base metal catalysis*, http://learning.chem21.eu/media/pdf/27/base-metal-catalysis-a4.pdf.

3 P. J. Chirik and R. Morris, *Acc. Chem. Res.*, 2015, **48**, 2495.

4 P. N. Rylander, *Hydrogenation methods (best synthetic methods)*, Academic Press, 1990; P. N. Rylander, *Catalytic hydrogenation in organic syntheses*, Academic Press, 1979; P. N. Rylander, *Catalytic hydrogenation over platinum metals*, Academic Press, 2012.

5 S. Nishimura, *Handbook of heterogeneous catalytic hydrogenation for organic synthesis*, Wiley, New York, 2001.

6 K. R. Westerterp and K. B. van Gelder, *Stud. Surf. Sci. Catal.*, 1997, **108**, 47–67.

7 J. Pritchard, G. A. Filonenko, R. van Putten, E. J. M. Hensen and E. A. Pidko, *Chem. Soc. Rev.*, 2015, **44**, 3808–3833.

8 I. Karamé, *Hydrogenation*, InTech, 2012.

9 H.-U. Blaser, C. Malan, B. Pugin, F. Spindler, H. Steiner and M. Studer, *Adv. Synth.*, 2003, **345**, 103–151.

10 S. H. Tucker, *J. Chem. Educ.*, 1950, **27**, 489.

11 For price of metals, see: http://www.metalprices.com/.

12 A. Extance, *Base metal catalysts strike hydrogenation gold, chemistry world*, http://kuchem.kyoto-u.ac.jp/chembio/theme1.pdf.

13 R. M. Bullock, *Science*, 2013, **342**, 1054–1055.

14 S. Borman, Catalysts that are less precious, *Chem. Eng. News*, 2013, **91**, 27.

15 R. V. Jagadeesh, A.-E. Surkus, H. Junge, M.-M. Pohl, J. Radnik, J. Rabeah, H. Huan, V. Schünemann, A. Brückner and M. Beller, *Science*, 2013, **342**, 1073–1076.

16 F. A. Westerhaus, R. V. Jagadeesh, G. Wienhöfer, M.-M. Pohl, J. Radnik, A.-E. Surkus, J. Rabeah, K. Junge, H. Junge, M. Nielsen, A. Brückner and M. Beller, *Nat. Chem.*, 2013, **5**, 537–543.

17 R. V. Jagadeesh, T. Stemler, A. E. Surkus, H. Junge, K. Junge and M. Beller, *Nat. Protoc.*, 2015, **10**, 548–557.

100

18 E. de Smit and B. M. Weckhuysen, *Chem. Soc. Rev.*, 2008, **37**, 2758–2781.

19 L. Filipponi and D. Sutherland, *Nanotechnologies: Principles, applications, implications and hands-on activities*, European Commission, European Union, 2012.

20 V. Polshettiwar and T. Asefa, *Nanocatalysis: Synthesis and Applications*, Wiley, 2013.

21 P. Serp and K. Philippot, *Nanomaterials in Catalysis*, Wiley, 2012.

22 M. Sankar, N. Dimitratos, P. J. Miedziak, P. P. Wells, C. J. Kiely and G. J. Hutchings, *Chem. Soc. Rev.*, 2012, **41**, 8099–8139.

23 J. Zečević, G. Vanbutsele, K. P. de Jong and J. A. Martens, *Nature*, 2015, **528**, 245–248.

24 P. Munnik, P. E. de Jongh and K. P. de Jong, *Chem. Rev.*, 2015, **115**, 6687–6718.

25 E. M. van Schrojenstein Lantman, T. Deckert-Gaudig, A. J. G. Mank, V. Deckert and B. M. Weckhuysen, *Nat. Nanotechnol.*, 2012, **7**, 583–586.

26 L. He, F. Weniger, H. Neumann and M. Beller, *Angew. Chem. Int. Ed.*, 2016, **55**, 12582–12594.

27 H. Furukawa, K. E. Cordova, M. O'Keeffe and O. M. Yaghi, *Science*, 2013, **341**, 1230444.

28 A. Corma, H. García and F. X. Llabrés i Xamena, *Chem. Rev.*, 2010, **110**, 4606–4655.

29 H. Wang, Q.-L. Zhu, R. Zou and Q. Xu, *Chem*, 2017, **2**, 52–80.

30 L. Zhu, X.-Q. Liu, H.-J. Jiang and L.-B. Sun, *Chem. Rev.*, 2017, **117**, 8129–8176.

31 P. Pachfule, D. Shinde, M. Majumder and Q. Xu, *Nat. Chem.*, 2016, **8**, 718–724.

32 J. Tang and Y. Yamauchi, *Nat. Chem.*, 2016, **8**, 638–639.

33 W. Xia, A. Mahmood, R. Zou and Q. Xu, *Energy Environ. Sci.*, 2015, **8**, 1837–1866.

34 (a) K. Shen, X. Chen, J. Chen and Y. Li, *ACS Catal.*, 2016, **6**, 5887–5903; (b) X. Wang and Y. Li, *J. Mol. Catal. A: Chem.*, 2016, **420**, 56–65; (c) J. Long, K. Shen and Y. Li, *ACS Catal.*, 2017, **7**, 275–284.

35 R. V. Jagadeesh, K. Murugesan, A. S. Alshammari, H. Neumann, M.-M. Pohl, J. Radnik and M. Beller, *Science*, 2017, **358**, 326–332.

36 The applied linker, terephthalic acid (TPA) belongs to the most available carboxylic acids; see for example: R. J. Sheehan, *Terephthalic Acid, Dimethyl Terephthalate, and Isophthalic Acid, Ullmann's Encyclopedia of Industrial Chemistry*, Wiley-VCH, Weinheim, 2011.

37 S. A. Lawrence, *Amines: synthesis, properties and applications*, Cambridge University Press, 2004.

38 A. Ricci, *Amino group chemistry: from synthesis to the life sciences*, Wiley-VCH, 2008.

39 http://njardarson.lab.arizona.edu/sites/njardarson.lab.arizona.edu/files/Top200PharmaceuticalProductsRetailSales2015LowRes.pdf.

40 S. D. Roughley and A. M. Jordan, *J. Med. Chem.*, 2011, **54**, 3451–3479.

41 J. Li, J. S. Cisar, C. Zhou, B. Vera, H. Williams, A. D. Rodríguez, B. F. Cravatt and D. Romo, *Nat. Chem.*, 2013, **5**, 510–517.

42 T. Yan, B. L. Feringa and K. Barta, *Nat. Commun.*, 2014, **5**, 5602.

43 J. Maes, T. R. M. Rauws and B. U. W. Maes, *Chem.–Eur. J.*, 2013, **19**, 9137–9141.

44 D. B. Bagal and B. M. Bhanage, *Adv. Synth. Catal.*, 2015, **357**, 883–900.

45 S. Werkmeister, K. Junge and M. Beller, *Org. Process Res. Dev.*, 2014, **18**, 289–302.

46 C. de Bellefon and P. Fouilloux, *Catal. Rev.*, 1994, **36**, 459–506.

47 H.-U. Blaser, H. Steiner and M. Studer, *Chem. Cat. Chem.*, 2009, **1**, 210–221.

48 M. Orlandi, D. Brenna, R. Harms, S. Jost and M. Benaglia, *Org. Process Res. Dev.*, 2018, **22**, 430–445.

49 A. Corma and P. Serna, *Science*, 2006, **313**, 332–334.

50 T. Schwob and R. Kempe, *Angew.Chem. Int .Ed.*, 2016, **55**, 15175–15179.

51 D. Formenti, F. Ferretti, C. Topf, A.-E. Surkus, M.-M. Pohl, J. Radnik, M. Schneider, K. Junge and M. Beller, *J. Catal.*, 2017, **351**, 79–89.

52 B. Sahoo, D. Formenti, C. Topf, S. Bachmann, M. Scalone, K. Junge and M. Beller, *ChemSusChem*, 2017, **10**, 3035–3039.

53 P. Zhou, L. Jiang, F. Wang, K. Deng, K. Lv and Z. Zhang, *Sci. Adv.*, 2017, **3**, e1601945.

54 W. Huber, *J. Am. Chem. Soc.*, 1944, **66**, 876–879.

55 R. Novi, *Hydrogenation of aliphatic nitriles over nickel catalysts modified by formaldehyde*, PhD thesis, ETH Zürich, Switzerland, 2004, DOI: 10.3929/ethz-a-004877494.

56 P. Kukula, M. Studer and H.-U. Blaser, *Adv. Synth. Catal.*, 2004, **346**, 1487–1493.

57 R. J. Allain and G. D. Smith, *US Pat.*, 4375003A, 1983.

58 C. Bornschein, S. Werkmeister, B. Wendt, H. Jiao, E. Alberico, W. Baumann, H. Junge, K. Junge and M. Beller, *Nat. Commun.*, 2014, **5**, 4111.

59 S. Chakraborty, G. Leitus and D. Milstein, *Chem. Comm.*, 2016, **52**, 1812–1815.

60 S. Mukherjee, D. Srimani, S. Chakraborty, Y. Ben-David and D. Milstein, *J. Am. Chem. Soc.*, 2015, **137**, 8888–8891.

61 P. Ji, K. Manna, Z. Lin, X. Feng, A. Urban, Y. Song and W. Lin, *J. Am. Chem. Soc.*, 2017, **139**, 7004–7011.

62 F. Chen, C. Topf, J. Radnik, C. Kreyenschulte, H. Lund, H. Schneider, A.-E. Surkus, L. He, K. Junge and M. Beller, *J. Am. Chem. Soc.*, 2016, **138**, 8781–8788.

63 W. A. Butte and W. J. Murtaugh, *US Pat.*, 4186146A, 1980.

64 K. Tokmic, B. J. Jackson, A. Salazar, T. J. Woods and A. R. Fout, *J. Am. Chem. Soc.*, 2017, **139**, 13554–13561.

65 S. Elangovan, C. Topf, S. Fischer, H. Jiao, A. Spannenberg, W. Baumann, R. Ludwig, K. Junge and M. Beller, *J. Am. Chem. Soc.*, 2016, **138**, 8809–8814.

66 J. G. McAlpin, Y. Surendranath, M. Dincă, T. A. Stich, S. A. Stoian, W. H. Casey, D. G. Nocera and R. D. Britt, *J. Am. Chem. Soc.*, 2010, **132**, 6882–6883.

67 N. S. McIntyre, D. D. Johnston, L. L. Coatsworth, R. D. Davidson and J. R. Brown, *Surf. Interface Anal.*, 1990, **15**, 265–27268.

68 S. C. Petitto and M. A. Langell, *J. Vac. Sci. Technol., A*, 2004, **22**, 1690.

69 L. Armelao, *Surf. Sci. Spect.*, 2001, **8**, 14.

Cobalt-Nanoparticles Catalyzed Efficient and Selective Hydrogenation of Aromatic Hydrocarbons

Kathiravan Murugesan,[†] Thirusangumurugan Senthamarai,[†] Ahmad S. Alshammari,[‡] Rashid M. Altamimi,[‡] Carsten Kreyenschulte,[†] Marga-Martina Pohl,[†] Henrik Lund,[†] Rajenahally V. Jagadeesh,*,[†] and Matthias Beller*,[†]

[†]Leibniz-Institut für Katalyse e.V. an der Universität Rostock, Albert-Einstein Str. 29a, Rostock D-18059, Germany
[‡]King Abdulaziz City for Science and Technology, P.O. Box 6086, Riyadh 11442, Saudi Arabia

S *Supporting Information*

ABSTRACT: The development of inexpensive and practical catalysts for arene hydrogenations is key for future valorizations of this general feedstock. Here, we report the development of cobalt nanoparticles supported on silica as selective and general catalysts for such reactions. The specific nanoparticles were prepared by assembling cobalt-pyromellitic acid-piperazine coordination polymer on commercial silica and subsequent pyrolysis. Applying the optimal nanocatalyst, industrial bulk, substituted, and functionalized arenes as well as polycyclic aromatic hydrocarbons are selectively hydrogenated to obtain cyclohexane-based compounds under industrially viable and scalable conditions. The applicability of this hydrogenation methodology is presented for the storage of H_2 in liquid organic hydrogen carriers.

SiO₂ supported Co-nanoparticles

KEYWORDS: *arenes, cyclohexanes, co-nanoparticles, hydrogenations, catalysis*

■ INTRODUCTION

Aromatic hydrocarbons represent an essential feedstock for the chemical industry and their applications range from life sciences to bulk and fine chemicals as well as polymers and fuels.[1,2] In fact, the basic substrates such as benzene, toluene, and xylene are produced on >100 million tons per annum.[3,4] Moreover, condensed arenes are available from oil refining on large scale.[4] Because of their importance and abundance, synthetic organic chemistry in the past century and even today focused to a large extent on their functionalization.[1,2,5,6] In general, hydrogenations of arenes constitute green and 100% atom-efficient processes for the synthesis of cyclohexane-based products,[1,2,7−35] which are also used in industries, drug development, material sciences, and energy sector.[7−14] Because of the high stability of the benzene ring, the majority of catalysts for this transformation are based on precious metals.[15−37] In fact, the state-of-the-art systems constitute Ru[15−25] and Rh.[15−19,26−35] For the advancement of sustainable arene hydrogenation, the development of more earth abundant metal catalysts is of central importance. In this respect, so far, nickel[38−43] including Raney nickel,[44] as well as few other Co[38,42−48]-based catalysts are known for the hydrogenation of benzene and other simple substrates. However, in general, these catalysts exhibit poor selectivity and low stability for recycling and have not been applied for diverse compounds.[38−48] Thus, cost-efficient and chemo-, regio-, and stereo-selective hydrogenation of structurally challenging aromatic hydrocarbons in the presence of heterogeneous base metal catalysts are highly important and continue to attract significant interest.

In recent years, supported nanostructured materials had tremendous impact on the chemical industry and the innovation of chemical processes.[49−62] Key for the implementation of these materials is the preparation of active nanoparticles on appropriate supports using inexpensive precursors and applying convenient, easy to follow up, and reproducible methods.[49−62] In this regard, pyrolysis of (in situ generated) organometallic complexes,[51,58−62] metal organic frameworks (MOFs),[52,63−67] and coordination polymers (CPs)[67−74] allows for the synthesis of unique catalytic materials. Notably, metal containing CPs can be easily engineered by variation of metal ions and organic linkers.[67−74] Following this concept, the selection of suitable linkers for the preparation of active nanoparticles with the precise size and shape is most important. Advantageously, a plethora of carboxylic acid- and nitrogen-based linkers are available to prepare different CPs. Here, we describe the preparation of cobalt-based CPs using inexpensive pyromellitic acid (PMA) and piperazine (PZ) linkers and their use as convenient precursor and structure directing template. Supporting these CPs on commercial silica (AEROSIL) and subsequent pyrolysis creates reusable cobalt nanoparticles for the hydro-
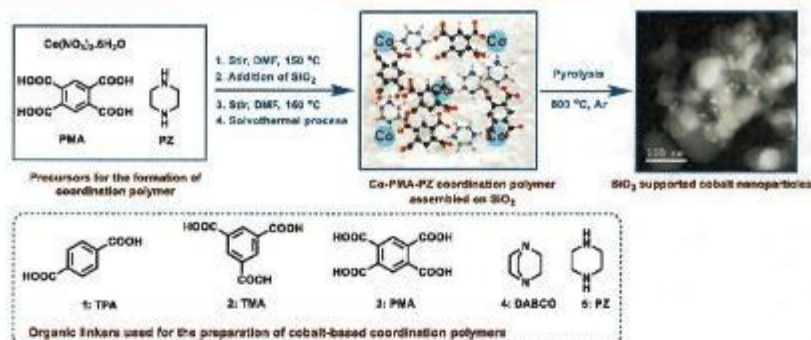
Figure 1. Synthesis of supported cobalt nanoparticles using CPs as precursors and structure-controlling templates.
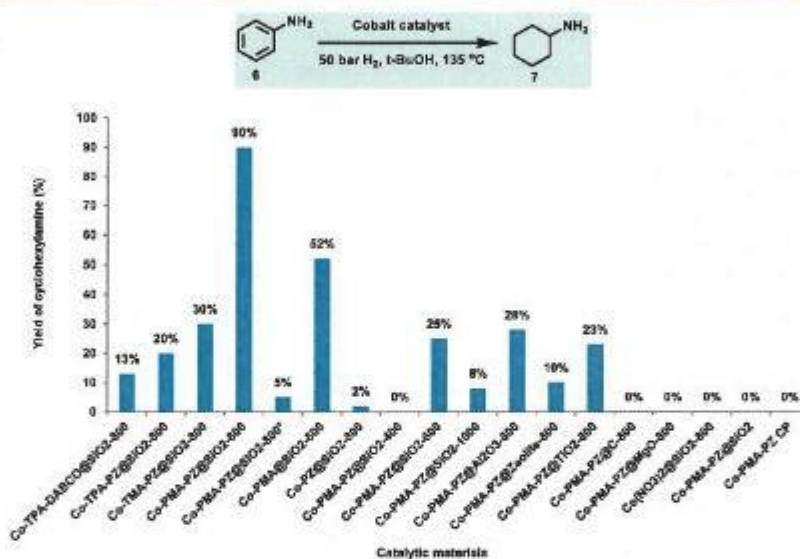
Figure 2. Hydrogenation of aniline to cyclohexylamine: activity of cobalt catalysts. Reaction conditions: 1 mmol aniline, 120 mg catalyst (9 mol % Co), 50 bar H_2, 4 mL t-BuOH, 135 °C, 24 h, yields were determined by GC using n-hexadecane standard. *Catalyst was prepared using polymeric material reported in ref 74.

genation of industrially important and structurally diverse arenes.

RESULTS AND DISCUSSION

Preparation of Cobalt-Based Nanocatalysts. First, we generated different cobalt-based CPs in situ in N,N-dimethylformamide (DMF) combining $Co(NO_3)_2 \cdot 6H_2O$ with different carboxylic acids such as terephthalic acid (TPA; 1,4-benzenedicarboxylic acid; 1), trimesic acid (1,3,5-benzenetricarboxylic acid; TMA; 2), PMA (1,2,4,5-benzenetetracarboxylic acid; PMA; 3), and nitrogen linker, for example, 1,4-diazabicyclo[2.2.2]octane (triethylendiamine; DABCO; 4) and PZ (diethylenediamine; PZ; 5) (Figure 1).

The resulting materials were assembled on different supports (SiO_2, Al_2O_3, ZSM-5 TiO_2, carbon, and MgO) and then pyrolyzed under argon to obtain the respective nanomaterials (see the Experimental Section for detailed preparation). Hereafter, these materials are labeled as Co-acid linker-amine linker@support-x, where x denotes the pyrolysis temperature.

Initially, all of the prepared materials were tested for the hydrogenation of industrially important aniline to cyclohexylamine as a benchmark reaction (Figure 2). Cyclohexylamine is used as a valuable intermediate for pharmaceuticals (e.g., mucolytics, analgesics, bronchodilators) and herbicides. Furthermore, it is the precursor for accelerators for vulcanization and an effective corrosion inhibitor. First, we tested Co-TPA-DBCO@SiO$_2$-800 material prepared using TPA and DABCO linkers, which were used previously for the preparation of cobalt-based MOFs and nanocatalysts.[52,66] Interestingly, this catalyst showed some activity (13%). Variation of the nitrogen linker from DABCO to PZ gave Co-TPA-PZ@SiO$_2$-800 with increased product yield (20%). Further preparation of CPs using different benzene carboxylic acid linkers and PZ resulted in more active materials. Among these, Co-CPs based on PMA and piparazine (PZ) linkers produced the best catalyst (Co-PMA-PZ@SiO$_2$-800), which led to 90% cyclohexylamine. The reported cobalt-CP[74] using $CoCl_2 \cdot 6H_2O$, PMA and PZ linkers with a molar ratio of 1:1:3 was also prepared and immobilized on SiO_2. Pyrolysis of this

material at 800 °C under argon produced a much less active catalyst for the formation of cyclohexylamine (5%). To produce an active catalyst, 3 equivalents of each of PMA and PZ linkers with respect to cobalt are required. The X-ray powder diffraction (XRD) pattern of cobalt-PMA-PZ CP is given in Figure S1. Comparison with materials made from single linkers, Co-PMA@SiO$_2$-800 and Co-PZ@SiO$_2$-800, showed activity (52%) for the former one, whereas the latter is almost inactive. Similarly, cobalt nitrate@SiO$_2$-800, the nonpyrolyzed Co-PMA-PZ@SiO$_2$ and corresponding Co-PMA-PZ CP were not active too. In addition to the different linkers, the effect of the pyrolysis temperature was also studied. The material pyrolyzed at 400 °C (Co-PMA-PZ@SiO$_2$-400) again is completely inactive, whereas pyrolysis at 600 °C and 1000 °C (Co-PMA-PZ@SiO$_2$-600; Co-PMA-PZ@SiO$_2$-1000) showed little activity (25 and 8%, respectively). Further, to know the effect of supports, different supported materials prepared using Co-PMA-PZ CP were also tested. Among these Al$_2$O$_3$, TiO$_2$, and zeolite-supported catalysts showed some activity (10–28%). However, carbon- and MgO-supported ones are completely inactive.

Catalysis and Synthetic Applications. *Hydrogenation of Bulk and Functionalized Arenes.* With the successful catalyst Co-PMA-PZ@SiO$_2$-800 for the benchmark process of aniline to cyclohexylamine in hand, we carried out its general applicability for the hydrogenation of various aromatic hydrocarbons. As shown in Schemes 1–4, this catalyst allows

Scheme 1. Co-PMA-PZ@SiO$_2$-800 Catalyzed Hydrogenation of Bulk and Functionalized Arenes to Obtain Value-Added Cyclohexanes[a]
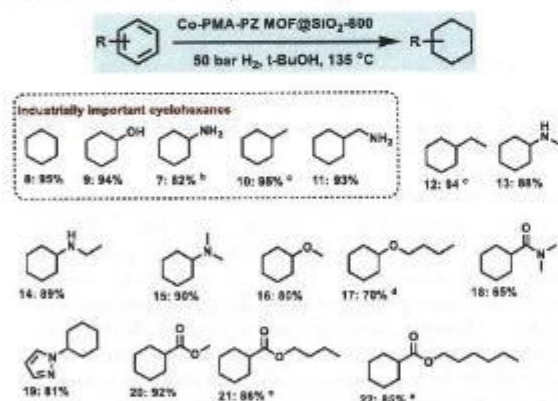
[a]Reaction conditions: 1 mmol substrate, 120 mg catalyst (9 mol % Co), 50 bar H$_2$, 4 mL t-BuOH, 135 °C, 24 h, yields were determined by gas chromatography (GC) using n-hexadecane standard. [b]Nitrobenzene was used as substrate to obtain cyclohexylamine. [c]At 150 °C for 48 h. [d]At 150 °C for 34 h. [e]For 40 h and isolated yields.

for the selective hydrogenation of diverse functionalized and substituted arenes, including annulated compounds to cyclic aliphatic hydrocarbons. Several bulk chemicals including benzene, toluene, and phenol were hydrogenated to produce industrially important products in excellent yields (Scheme 1 products 8–11). As an example, cyclohexane is used for the production of KA oil (mixture of cyclohexanone and cyclohexanol), adipic acid, and caprolactam. This product, which is currently produced (>5 million tons/annum) using

either Ni or Pt catalysts at >160 °C,[75,76] is conveniently formed in 95% yield at 135 °C and 50 bar H$_2$ (Scheme 1; product 8). Similarly, methylcyclohexane used as energy fuel is obtained in 95% (product 10). Apart starting from aniline, cyclohexylamine can be prepared directly from nitrobenzene in 82% yield (Scheme 1; product 7). It is worthwhile to mention here that cyclohexylamine is industrially produced by the hydrogenation of aniline (see benchmark reaction), which is obtained from nitrobenzene. In this respect, the production of cyclohexylamine directly from nitrobenzene has obvious advantages with respect to step- and cost-economy. The preference of this catalyst for chemoselective arene hydrogenation is showcased using functionalized substrates containing amine, ether, amide, ester, and pyrazole groups (Scheme 1; products 13–22). In all these cases, the benzene ring was selectively reduced by tolerating these functional groups.

Hydrogenation of Multiring Aromatic Hydrocarbons. In case of aromatic hydrocarbons with multiple rings, the reduction of one in the presence of others is generally more challenging and most of the known catalysts are less selective for such substrates.[15–48] However, using Co-PMA-PZ@SiO2-800 catalyst regioselective hydrogenation of one ring in case of naphthalenes, biphenyl, diphenyl methane, fluorine and xanthene molecules took place at 135 °C (Scheme 2; products

Scheme 2. Hydrogenation of Aromatic Hydrocarbons with Multiple Rings Using Co-PMA-PZ@SiO$_2$-800[a]
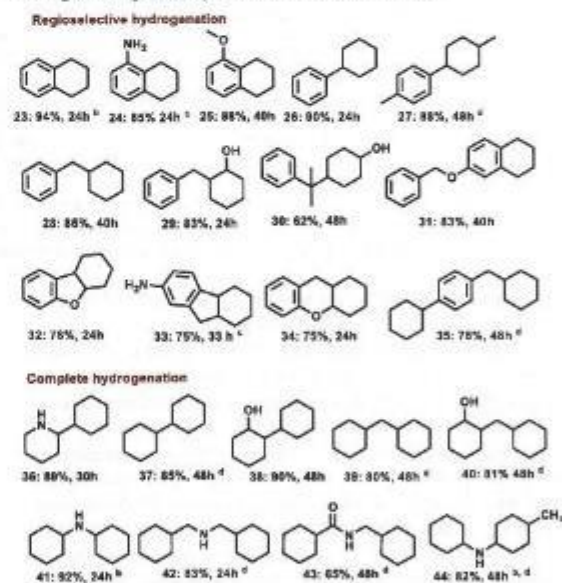
[a]Reaction conditions: 1 mmol substrate, 120 mg catalyst (9 mol % Co), 50 bar H$_2$, 4 mL t-BuOH, 135 °C, isolated yields. [b]In 4 mL i-PrOH and GC yield using n-hexadecane. [c]In 4 mL t-BuOH and 100 µL H$_2$O. [d]150 °C.

23–35). Notably, some of these partially hydrogenated derivatives are of increasing interest as intermediates for energy technologies. As an example, cyclohexylbenzene (CHB; product 26) is used as electrolyte additive in lithium ion batteries. Interestingly, at slightly elevated temperature (150 °C) we achieved full hydrogenation in selected molecules. As a

Scheme 3. Diastereoselective Hydrogenation of Substituted Phenols and Arenes[a]

45: 94%, 24h, (16:84)[b]   38: 88%, 48h (27:73)[b]   29: 75%, 24h (5: 95)[b]

40: 88%, 48h (30:70)[b,a]   46: 94%, 24h (93: 7)[b]   47: 92%, 24h (72:28)[b]

48: 91%, 30h (82:18)   49: 95%, 24h (29: 71%)[b]   50: 82%, 24h (30:70%)[b,d]

51: 93%, 24h (23:77)[b]   52: 92%, 30h (27:73)[b]   30: 62%, 48h (28:72)[b]

53: 92%, 24h (28:72)[b]   54: 82%, 48h (48:52)[b]

44: 82%, 48h (48:52)[b,c,d]   27: 88%, 48h (75:25)[b,a]

Hydrogenation of thymol

55: (Thymol) → Co-PMA-PZ MOF@SiO2-800, 50 bar H2, 150°C → 56 : 92%[d] (Isomeric mixture with 71% of (±)-Isomenthol)

57: 88%[d] (Isomeric mixture)
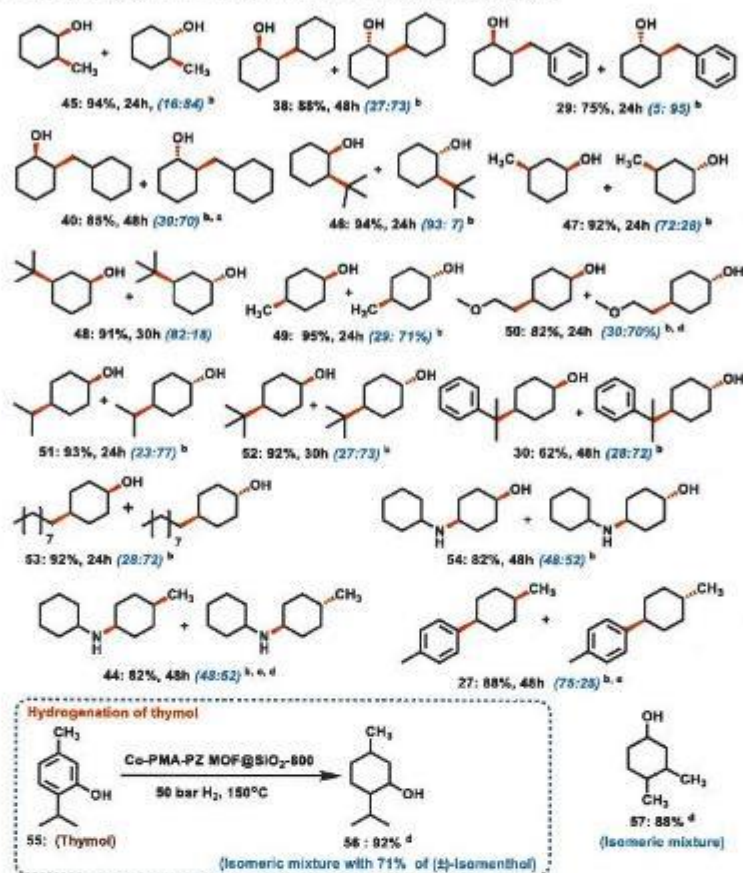
[a]Reaction conditions: 1 mmol substrate, 120 mg catalyst (9 mol % Co), 50 bar H2, 4 mL t-BuOH, 135 °C, 24 h, isolated yields. Cis–trans isomers selectivity was determined by NMR spectral analysis. [b]At 150 °C. [c]In 4 mL i-PrOH. [d]1 g substrate, 9 mol % catalyst, 15 mL t-BuOH, 150 °C, 48 h, isolated yields. Isomeric ratio in case of 2-isopropyl-5-methylcyclohexanol was determined by GC.

result, 9 bicyclic aliphatic hydrocarbons were obtained in up to 92% yields (Scheme 2; products 36–44).

Diastereoselective Hydrogenation Process. A major challenge for any new arene hydrogenation catalyst to be implemented in synthetic chemistry is the diastereoselective hydrogenation of multiple substituted derivatives.[20,23,26,35,77] In general, such reactions offer a unique possibility to synthesize platform molecules for new pharmaceuticals, agrochemicals, and fine chemical applications. Unfortunately, relatively, a few catalysts have been applied for such transformations.[20,23,26,37,77] Among these, notable works are based on Rh[26] and Ru[20] for the preparation fluorinated cycloalkanes and substituted cyclohexanols, respectively.

To evaluate the potential of our Co-PMA-PZ@SiO2-800 system in this context, the hydrogenation of a series of substituted phenols for the preparation of cyclohexanols was performed. Apart from being interesting intermediates, the present hydroxyl group can be easily further functionalized. As shown in Scheme 3, various di- and trisubstituted phenols underwent hydrogenation to give the corresponding diastereoisomers in good to excellent yields (Scheme 3). 1,2-Disubstituted phenols with methyl, cyclohexyl, and benzyl groups lead preferentially to the thermodynamically more stable trans products in up to 95% selectivity (Scheme 3;

products 29, 38,40). On the other hand, 2-tert-butylphenol gave the corresponding cis product with 93% selectivity (Scheme 3; product 46). To understand this observation, isomerization experiments of both cis- and trans-2-methylcyclohexanol were performed under the typical hydrogenation conditions. However, no isomerization occurred. Similar to the 1,2-disubstituted phenols, the related 1,4-derivatives yield preferentially the thermodynamically more stable trans isomers (Scheme 3; products 30, 44, 49–54). An exception is the formation of 27, which is explained by the stronger coordination of the second arene ring to the catalyst surface, which leads to the cis-product. In case of 1,3-disubstituted phenols, the cis products were preferentially formed, which is also explained by their increased thermodynamic stability (Scheme 3; products 47–48). To showcase the selective hydrogenation of disubstituted anilines and biaryls, N-phenyltoluidine and 4,4'-dimethylbiphenyl, respectively, were also reduced in high yields (Scheme 3; products 44 and 27). As an example for the reduction of trisubstituted arenes, the hydrogenation of thymol (2-isopropyl-5-methylphenol; 55) was investigated, which is industrially important for the synthesis of menthol isomers.[78] At 150 °C, full conversion of thymol was observed using our novel base metal catalyst yielding 71% of (±)-isomenthol.[78]

ACS Catalysis

Scheme 4. Application of Cobalt-Catalyzed Hydrogenation Process for the Storage of H₂ in LOHCs[a]

Hydrogenation of Marlotherm SH: A potential LOHC

58: >99 Conv. (Marlotherm SH (MSH)) → 59: 2% (MSH-H6) + 60: 86% (MSH-H12) + 61: 10% (MSH-H18)

Total H₂ storage = 66%

H₂ Carrier	% H₂ storage	H₂ Carrier	% H₂ storage
4-Benzylbiphenyl 62: >99% Conv.	73%	Methylbenzene 66: >99% Conv.	99%
Diphenylmethane 63: >99% Conv.	92%	Ethylbenzene 67: 97% Conv.	96%
4-Propylbiphenyl 64: >99% Conv.	78%	Benzene 68: >99% Conv.	99% [b]
Biphenyl 65: >99% Conv.	92%		
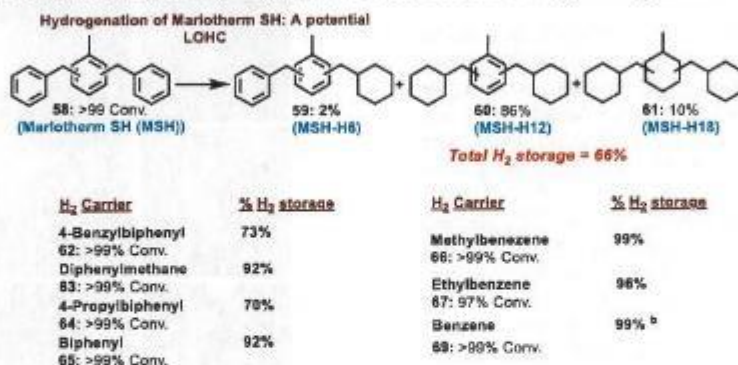
[a]Reaction conditions: 2 mmol substrate, 240 mg catalyst (9 mol % Co), 50 bar H₂, 8 mL t-BuOH, 150 °C, 48 h. [b]At 135 °C, 24 h.

Scheme 5. Representing the Synthetic Utility of Cobalt-Catalyzed Hydrogenation Process for Gram-Scale Reactions[a]

20: 87%, 24h (1g scale) 26: 91%, 24h (1g scale) 25: 85%, 40h (2g scale) 21: 89%, 40h (2g scale) 45: 92%, 24h (3g scale)

41: 92%, 24h [†] (3g scale) 7: 92%, 24h (10g scale) 8: 93%, 24h (25g scale) 9: 93% (25g scale) 55: 93%, 48h [‡] (25g scale)
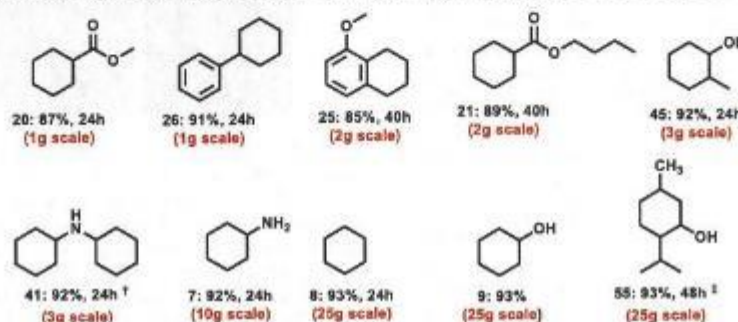
[a]Reaction conditions: 1−25 g substrate, 4.5 mol % catalyst, t-BuOH solvent (10 v for each 1 g substrate), 135 °C. [*]With 9 mol % catalyst. [†]In i-PrOH solvent.

Applicability of Cobalt Nanoparticles for the Storage of H₂ in LOHC. Catalytic hydrogenation reactions constitute a key element for the transformation of renewable energy (wind, PV, etc.) into chemical energy carriers. In this context, the storage of hydrogen in liquid organic hydrogen carriers (LOHCs) has attracted significant interest in recent years.[79−81] In general, different arenes such as benzene, methylbenzene, diphenylmethane, bipyridine, and dibenzyltoluene are considered as LOHCs. For example, the latter compound is readily available and technically applied as heat transfer oil (MARLOTHERM SH, MSH).[79−81] Regarding the known catalysts for this transformation, commercially available Ru/Al₂O₃ was used for the hydrogenation of MSH (45% storage of hydrogen at 150 °C).[81] Using our cobalt catalyst at 150 °C, hydrogenation of MSH yielded three different isomers with overall hydrogen storage of 65% (Scheme 4). In addition, other selected molecules reacted smoothly and resulted in up to 99% hydrogen storage (Scheme 4).

Synthetic Utility Co-Catalyzed Arenes Hydrogenation Protocol. After having demonstrated several applications of this novel Co-PMA-PZ@SiO₂-800 material, reaction upscaling and catalyst recycling were showcased. Consequently, several arenes were hydrogenated to obtain corresponding cyclohexanes in up to 25 g (Scheme 5). Notably, all of these reactions were carried out using lower catalyst loading (4.5 mol % Co).

Recycling and reusability of the catalyst was performed using phenol hydrogenation. It was recycled up to 4 times without

significant loss of activity and in all cases, the yield of cyclohexanol was >90% (Figure 3). In addition to recycling, we also tested the stability of the Co-PMA-PZ@SiO₂-800 catalyst by performing recycling of the catalyst at reduced reaction time (Figure S22). At 10 h of reaction time, the yield of cyclohexanol in each run was rapidly decreased (Figure S22). These studies showed that the catalyst is not stable and deactivation occurred. Hence, 24 h of the reaction time is
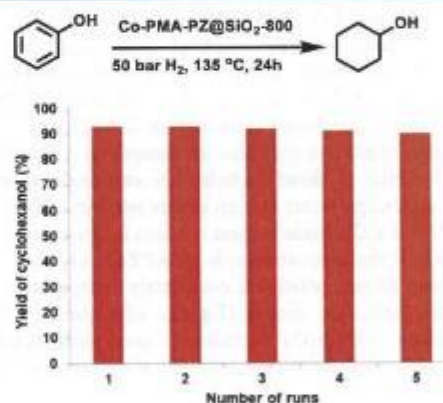
Figure 3. Catalyst recycling for the hydrogenation of phenol to cyclohexanol. Reaction conditions: 10 g phenol (106 mmol), 6.35 g catalyst (4.5 mol %), 100 mL t-BuOH, 135 °C, 24 h.

required to obtain >90% cyclohexanol in up to 5th run (Figure 3)

Characterization of Co-Based Nanocatalysts. In order to identify the structural features and to understand the varying catalytic activities of these novel cobalt-based materials, we characterized the active catalyst (Co-PMA-PZ@SiO₂-800), less active (Co-TPA-PZ@SiO₂-800, Co-PMA@SiO₂-800), and completely inactive materials (Co-PZ@SiO₂-800) using X-ray powder diffraction (XRD), Brunauer–Emmett–Teller (BET), scanning transmission electron microscopy (STEM), electron energy loss spectroscopy (EELS), and energy-dispersive X-ray spectroscopy (EDXS) and X-ray photoelectron spectroscopy (XPS). XRD analysis revealed that the most active catalyst contains metallic cobalt particles along with some Co_3O_4 (Figure S2). In case of less active materials, a mixture of metallic Co and oxidic cobalt (Co_3O_4 and CoO) particles were present (Figures S3 and S4). However, in case of the inactive material, the presence of mainly Co_3O_4 particles was observed (Figure S5). Another nonactive material, cobalt nitrate@SiO₂-800 also contained mainly metal oxide particles (Figure S6). BET measurements revealed the importance of the surface area for the catalyst activity which increased in the order of 42 (Co-PZ@SiO₂-800), 77 (Co-PMA@SiO₂-800) to 155 m²/g (Co-PMA-PZ@SiO₂-800) (Figures S8–S10).

The STEM analysis of the most active material revealed the formation of cobalt nanoparticles with sizes between 5 and 20 nm of different compositions. Contrast in high-angle annular dark field (HAADF) micrographs shows the presence of probably metallic Co particles tightly covered in graphitic carbon and particles of Co oxide (Figure 4A) more loosely attached to carbon and the support. Unfortunately, during EDXS and EELS measurements, the morphology of the Co-containing particles changed somewhat under the extended influence of the electron beam and formation of particles similar to such Co oxide crystallites was observed. Therefore, EELS data cannot be used to determine the exact nature of the Co species, for example, by fingerprinting the fine structure of the Co-L edge in the EELS data (Figures S12 and S13A).[82] Additionally, there is a carbon phase containing N attached to the SiO₂ support as seen in the EELS elemental maps. High-resolution HAADF images of a free hanging carbon structure indicate the presence of even heavier atoms in this phase; however, the density was too low for EDXS or EELS analysis (Figure S14). In case of the less active material prepared using TPA and PZ linkers (Co-TPA-PZ@SiO₂-800), metallic cobalt particles are surrounded by graphitic shells and Co oxide particles show little contact to carbon structures when attached to the silica support (Figures 4B and S13B). The Co-PMA@SiO₂-800 material contained generally small (<15 nm) with a few large polycrystalline particles as exceptions (Figures 4C and S13C). Some of these particles are encapsulated within large well-ordered graphitic carbon others without carbon shell and probably of a Co oxide variant are also located directly on silica. In case of the inactive sample (Co-PZ@SiO₂-800), large particles up to 85 nm, which are completely encapsulated within graphitic shells, are found (Figures 4D and S13D). In addition, some Co/Co_3O_4 particles in core shell structures were also observed, however, with no clear connection to carbon structures.

Further XPS analysis for Co-PMA-PZ@SiO₂-800, Co-PMA@SiO₂-800, and Co-PZ@SiO₂-800 samples has been conducted to understand in more detail the states of cobalt and nitrogen at the surface of the catalysts (Figure S15). In the
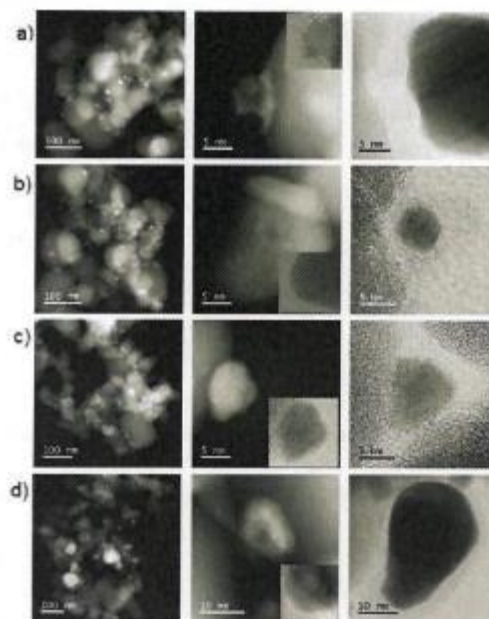
Figure 4. STEM-HAADF and -ABF images of silica supported cobalt catalysts. Left column shows HAADF images of the general structure, the middle column shows details of Co oxide particles with ABF images as an inset to highlight possible carbon structures, and the right column shows ABF images with details of Co particles, with tightly packed graphitic covering of metallic Co particles where these metallic particles are present, (a) Co-PMA-PZ@SiO₂-800, (b) Co-TPA-PZ@SiO₂-800, (c) Co-PMA@SiO₂-800, and (d) Co-PZ@SiO₂-800.

most active catalyst, (Co-PMA-PZ@SiO₂-800) the deconvolution of Co 2p peaks shows the presence of two types of Co-species (Figure S15a; left image). The peak at 778.55 eV represents metallic cobalt (Co $2p_{3/2}$), while the peak at 780.51 eV denotes Co^{2+} ($2p_{3/2}$) species (Figure S15a; left image). The corresponding Co $2p_{1/2}$ peaks are observed at 794.43 and 796.45 eV. Co $2p_{3/2}$ and Co $2p_{1/2}$ peak energy splitting was found to be 15.88 eV for Co(0) and 15.90 eV for Co^{2+}.[83] The catalyst Co-PMA@SiO₂-800 also contains mixed oxidation states for Co-species (Figure S15b; left image). A peak at 778.49 eV represents the presence of Co $2p_{3/2}$ in the metallic state, whereas a peak at 779.92 eV can be assigned to Co^{2+} species. Although, a peak for Co^{3+} could not be deconvoluted, however, the presence of strong satellite peaks at 786.43 and 802.20 eV are indicative for multiple oxidized Co species, as satellite peaks arise due to spin–spin interactions of different Co species.[83,84] The Co-PZ@SiO₂-800 material also shows the presence of two cobalt species (Figure S15c; left image); however, the absence of a peak around 778.5 eV indicates that metallic Co is not present.[85] The peaks present at 779.91 and 781.52 eV can be assigned to $2p_{3/2}$ Co^{2+} and Co^{3+} species. The corresponding $2p_{1/2}$ peaks are present at 793.52 and 795.45 eV for both these species (Figure S15c; left image). In these three catalysts, surface concentration and states of N vary due to the use of different ligands in the pyrolysis process. Clearly, the presence of different linkers affects the graphitization process and the occurrence of N at the surface.[86] Nevertheless, in all these samples, N 1s spectra are complicated due to the low concentrations of N on the surface and also its interaction with cobalt, carbon, and SiO₂.[86–88] For Co-PMA-PZ@SiO₂-800,

ACS Catalysis

which was prepared using $Co(NO_3)_2$, PMA, and PZ, N 1s spectra could be deconvoluted to three N 1s peaks within the catalyst structure (Figure S15a; right image). The binding energies centered at 399.35, 401.36, and 403.88 eV can be assigned to pyridinic N, pyrrolic N, and graphitic N, respectively.[86,87] In contrast, the sample Co-PMA@SiO$_2$-800, which was prepared form $Co(NO_3)_2$, PMA, contains only two types of N (Figure S15b; right image). Deconvolution results fitting of two N-peaks centered at binding energies of 399.4 and 400.1 eV. Compared to Co-PMA-PZ@SiO$_2$-800, in this case, graphitic N is absent at the surface. The presence of N in this sample obviously comes from cobalt nitrate. The material Co-PZ@SiO$_2$-800 prepared by $Co(NO_3)_2$ and PZ also contains two types of N 1s peaks centered at 401.21 and 404.05 eV (Figure S15c; right image). In this case, pyridinic N is absent. Further to know the phases of cobalt, in situ XRD analysis has been performed (Figures S16–S21). If the catalyst is decomposed, the formation of CoO has to be observed at 800 °C under a helium (He) flow of 10 mL/min. However, the catalyst cooled down, and the product of the thermal treatment was investigated ex situ and observed only Co$_3$O$_4$. According to this result, the experiments were performed by flushing with He (10 mL/min) for approximately 25 min. Then, the gas flow was stopped, and the temperature program was started. After heating to 800 °C (25 °C/min heating rate), the diffraction data were collected over a period of 2 h (each 10 min) and the cooling of the sample were monitored by the collection of diffraction data each 100 °C step. In this experiment, the formation of metallic Co can be stated. Then, the metallic Co is oxidized to Co$_3$O$_4$ during the cooling process. An additional experiment was also carried out to check the amount of O$_2$ during heating, isothermal, and cooling procedure by the analysis of the gas passed through an empty capillary. The value of the O$_2$ concentration was constant over the whole experiment (heating to 800 °C, 30 min isothermal, cooling to 25 °C, heating rate: 25 °C/min).

All of these characterization studies revealed that in the most active material (Co-PMA-PZ@SiO$_2$-800) different types cobalt nanoparticles are present. Metallic Co particles tend to be covered in graphitic shells possibly isolating them, whereas a large fraction of Co oxide particles connects to the carbon matrix containing nitrogen and possibly highly disperse Co. The nitrogen content indicates that PMA with PZ as the linker forms these structures which in accordance with the BET results seems to enhance the active surface area of the catalyst strongly when compared to the pure support.

■ CONCLUSIONS

In conclusion, we have developed efficient cobalt-based nanocatalysts for general and selective hydrogenation of aromatic hydrocarbons to produce the corresponding aliphatic products, which serve as essential compounds in chemical and life science industries as well as for energy and material sciences. Key to success for this hydrogenating process is the graphitic shell-encapsulated cobalt nanoparticles prepared by the template synthesis of cobalt–PMA–PZ CP on commercial silica and subsequent pyrolysis under an inert atmosphere. This cobalt-based protocol proceeds for the hydrogenation of industrial bulk, substituted, and functionalized arenes as well as polycyclic aromatic hydrocarbons under industrially viable and scalable conditions. In addition, this catalyst system has been applied for the diastereoselective hydrogenation of multiple substituted phenols and arenes. The utility and applicability of

this hydrogenation methodology is demonstrated by catalyst recycling and gram-scale synthesis as well as for the storage of H$_2$ in LOHC.

■ EXPERIMENTAL SECTION

General Consideration. All substrates were obtained commercially from various chemical companies. Cobalt(II) nitrate hexahydrate (cat no. 139267-100G), PZ (ReagentPlus, ≥99%; cat. no. P45907) 1,4-diazabicyclo[2.2.2]octane (DABCO; ReagentPlus, ≥99%; cat. no. D27802-25G), TPA (cat no. 185361; 98%), and titanium(IV) oxide (TiO$_2$; cat no. 718467; ≥99.5%) were obtained from Sigma-Aldrich. PMA (cat no. B23099; 96%), 1,3,5-benzenetricarboxylic acid (TMA; cat no. A15947; 98%), zeolite ZSM-5 ammonium (ZSM-5; cat no. 45879), and magnesium oxide (MgO; cat no. 43196; 99.95%) were obtained from Alfa Aesar. t-Butanol (t-buOH, code-390690025; 99.8%) was obtained from Across chemicals. Silica (AEROSIL OX 50) was obtained from Evonik. Carbon powder, VULCAN XC72R with code XVC72R and CAS no. 1333-86-4 was obtained from Cabot Corporation Prod. The pyrolysis experiments were carried out in a Nytech Qex oven. Before using, the purity of the substrate has been checked.

STEM measurements were performed at 200 kV with aberration-corrected JEM-ARM200F (JEOL, Corrector: CEOS). The microscope was equipped with a JED-2300 (JEOL) energy-dispersive X-ray-spectrometer and Enfinium ER (GATAN) electron energy-loss spectrometer with dual EELS for chemical analysis. HAADF and annular bright field (ABF) detectors were used for general imaging; the annular dark field detector was used for position control for EELS acquisition. Dual EELS was done at a camera length of 4 cm, an illumination semi angle of 27.8 mrad, and a filter entrance aperture semi angle of 41.3 mrad using the low loss region for compensation of energy shifts during acquisition. The solid samples were deposed without any pretreatment on a holey carbon supported Cu-grid (mesh 300) and transferred to the microscope.

XRD powder pattern were recorded on a PANalytical X'Pert diffractometer equipped with a XCelerator detector using automatic divergence slits and Cu Kα1/α2 radiation (40 kV, 40 mA; λ = 0.15406, 0.154443 nm). Cu β-radiation was excluded using a nickel filter foil. The measurements were performed in 0.0167° steps and 100 s of data collecting time per step. The samples were mounted on silicon zero background holders. The obtained intensities were converted from automatic to fixed divergence slits (0.25°) for further analysis. Peak positions and the profile were fitted with Pseudo-Voigt function using the HighScore Plus software package (PANalytical). Phase identification was done by using the PDF-2 database of the International Center of Diffraction Data (ICDD).

BET surface areas of the catalysts were determined on a NOVA 4200e instrument by N$_2$-physisorption at −196 °C. Prior to the measurements, the known amount of the catalyst was evacuated for 2 h at 220 °C to remove physically adsorbed water.

In situ XRD studies were preformed on a Stoe Stadi P equipped with a Stoe ht2-in situ oven and a Mythen 1K detector in Debye–Scherrer geometry using a Mo-X-ray tube [50 kV, 40 mA, Kα1: 0.70930 Å, Ge(111)]. Temperature correction was applied by measurement of well-known phase transitions of standard materials (AgNO$_3$, KClO$_4$, Ag$_2$SO$_4$, SiO$_2$, K$_2$SO$_4$, K$_2$CrO$_4$, WO$_3$, BaCO$_3$). Gas dosage was done via

a Bronkhorst mass flow controller. The sample to investigate was grinded, pressed to pellets by a pressure of 10 tons, crushed, and sieved to fraction of 100–150 μm. The fraction was filled to a quartz glass capillary (approx. 2 mm outer diameter, 1 mm inner diameter, opened on both sides) to a height of approx. 8 mm and fixed by quartz glass wool at both sides. The loading of the catalyst precursor was increased to 20 wt % to obtain data of reliable quality after the decomposition of the precursor. The capillary was mounted into the in situ chamber, and the capillary was flushed with He (10 mL min^{-1}) for 20 min. The gas flow was switched off before starting the heating. The sample was heated to 800 °C (25 °C min^{-1}), and the temperature was kept constant for 2 h while recording diffraction data every 10 min (stationary measurement, 300 s of acquisition time). The cooling process (25 °C min^{-1}) was monitored each 100 °C step.

All catalytic experiments were carried out in 300 and 100 mL autoclaves (PARR Instrument Company). In order to avoid unspecific reactions, all catalytic reactions were carried out either in glass vials, which were placed inside the autoclave or glass/Teflon vessel-fitted autoclaves.

GC and GC–mass spectrometry (MS) were recorded on Agilent 6890N instrument. GC conversion and yields were determined by GC-FID, HP6890 with a FID detector, column HP5 30 m × 250 mm × 0.25 μm.

^{1}H and ^{13}C NMR data were recorded on Bruker ARX 300 and Bruker ARX 400 spectrometers using DMSO-d_6, CD$_3$OD and CDCl$_3$ solvents.

HRMS data were recorded on a mass spectrometer MAT 95 XP (Thermo Electron), 70 eV.

Procedure for the Catalyst Preparation. *Preparation of Co-PMA-PZ@SiO$_2$ Template (3 g Preparation) and Pyrolysis To Obtain Nanomaterial.* In a 50 mL round-bottom flask, cobalt(II) nitrate hexahydrate (444.5 mg; 1.5 mmol) and PZ (395.2 mg; 4.5 mmol) were stirred for 5 min in 15 mL of DMF at 150 °C. To this mixture, the already dissolved (by heating) PMA (1.16 g; 4.5 mmol) in 10 mL of DMF was added. Then, the round-bottom flask containing the reaction mixture was placed into an aluminum block preheated at 150 °C and stirred for 20–30 min after fixing a reflux condenser to the round-bottom flask. Then, 1.2 g of silica (AEROSIL OX 50) was added followed by the addition of 15 mL of DMF, and the reaction mixture was stirred again at 150 °C for 4–5 h. Then, the reflux condenser was removed, and the round-bottom flask containing the reaction product was allowed to stand without stirring and closing for 20 h at 150 °C in order to slowly evaporate DMF and to grow the cobalt-CP template on carbon. After the evaporation of the solvent and ensuring the complete drying, the material was cooled to room temperature and grinded to give a fine powder. The powdered material was pyrolyzed at the defined temperature (400, 600, 800, or 1000 °C) for 2 h under an argon atmosphere and then cooled to room temperature after pyrolysis.

Elemental analysis (wt %): Co-PMA-PZ@SiO$_2$-800: Co = 4.6%, C = 16.98%, H = 0.10%, Si = 32.59% N = 0.81%.

The same procedure has been applied for the preparation of other supported materials.

Preparation of Co-PMA-PZ CP. In a 50 mL round-bottom flask, cobalt(II) nitrate hexahydrate (444.5 mg) and PZ (395.2 mg) were stirred for 5 min in 15 mL DMF at 150 °C, and to this mixture the already dissolved PMA (by heating) (1.16 g) in 10 mL DMF was added. Then, the round-bottom flask containing a reaction mixture was placed into an aluminum

block preheated at 150 °C and stirred for 1 h after fixing a reflux condenser to the round-bottom flask. Then, the reflux condenser was removed, and the reaction mixture was allowed to stand without stirring for 1–2 h at 150 °C. A pink colored cobalt-CP was formed and filtered through filter paper and washed 3–4 times with hot DMF (15–20 mL each time). The washed material was dried at 140–150 °C in an oven for 15 h and then finally dried under high vacuum at room temperature for 4–5 h.

General Procedure for the Hydrogenation of Arenes. A magnetic stirring bar and 1.0 mmol of the corresponding arene were transferred to a glass vial (8 mL), and 3 mL of the solvent (t-BuOH) was added. Then, 120 mg of the catalyst (Co-PMA-PZ@SiO$_2$-800; 9 mol % Co) was added, and the vial was fitted with a septum, cap, and needle. The reaction vials (eight vials with different substrates at a time) were placed into a 300 mL autoclave. The autoclave was flushed with 30 bar hydrogen twice, and then, it was pressurized with 50 bar of hydrogen. The autoclave was placed into an aluminum block preheated at 145 °C (placed 30 min before counting the reaction time in order to attain reaction temperature), and the reactions were stirred for the required time. During the reaction, the inside temperature of the autoclave was measured to be 135 °C, and this temperature was used as the reaction temperature. After completion of the reactions, the autoclave was cooled to room temperature. The remaining hydrogen was discharged, and the vials containing the reaction products were removed from the autoclave. The solid catalyst was filtered off and washed thoroughly with ethyl acetate. The reaction products were analyzed by GC–MS. The corresponding products were purified by column chromatography (silica; n-hexane–ethyl acetate mixture) and characterized by NMR and GC–MS analysis.

Procedure for the Yields Determined by GC for Selected Compounds. After completion of the reactions, n-hexadecane (100 μL) was added as the standard to the reaction vials, and the reaction products were diluted with ethyl acetate followed by filtration using plug of silica and then analyzed by GC.

Procedure for Gram Scale Reactions. To a Teflon or glass fitted 300 mL or 1.0 L autoclave, a magnetic stirring bar and the corresponding arene were transferred and 20–250 mL of t-BuOH was added. After adding the required amount of catalyst (Co-PMA-PZ@SiO$_2$-800; 4.5 mol % Co; 60 mg for each 1.0 mmol substrate), the autoclave was flushed with 40 bar hydrogen twice, and then, it was pressurized with 40 bar hydrogen. The autoclave was placed into an aluminum block preheated at 145 °C (placed 30 min before counting the reaction time in ordered to attain reaction temperature), and the reaction was stirred for the required time. During the reaction, the inside temperature of the autoclave was measured to be 135 °C, and this temperature was used as the reaction temperature. After completion of the reaction, the autoclave was cooled to room temperature. The remaining hydrogen was discharged, and the reaction products were removed from the autoclave. The solid catalyst was filtered off and washed thoroughly with ethyl acetate. The reaction products were analyzed by GC–MS, and the corresponding products were purified by column chromatography (silica; n-hexane–ethyl acetate mixture) and characterized by NMR and GC–MS spectral analysis.

Procedure for Catalyst Recycling. A magnetic stirring bar and 106 mmol of phenol were transferred to a 300 mL autoclave, and then, 70 mL t-BuOH was added. After adding

6.3 g of catalyst (Co-PMA-PZ@SiO$_2$-800; 4.5 mol % Co), the autoclave was flushed with 40 bar hydrogen, and then, it was pressurized with 50 bar hydrogen. The autoclave was placed into the heating system, and reactions were allowed to progress at 135 °C (temperature inside the autoclave) by stirring for the required time. After the completion of the reaction, the autoclave was cooled and the remaining hydrogen was discharged. To the reaction mixture, 250 μL n-hexadecane as standard was added. The catalyst was separated by centrifugation and the filtrate was subjected to GC analysis for determining the yield of cyclohexanol. The separated catalyst was washed with ethyl acetate, dried under vacuum, and used without further purification or reactivation for the next run.

■ ASSOCIATED CONTENT

Ⓢ Supporting Information

The Supporting Information is available free of charge on the ACS Publications website at DOI: 10.1021/acscatal.9b02193.

> Additional materials characterization data and NMR data and spectra (PDF)

■ AUTHOR INFORMATION

Corresponding Authors

*E-mail: jagadeesh.rajenahally@catalysis.de (R.V.J.).
*E-mail: matthias.beller@catalysis.de (M.B.).

ORCID ⊙

Kathiravan Murugesan: 0000-0003-1678-7728
Carsten Kreyenschulte: 0000-0002-2371-4909
Rajenahally V. Jagadeesh: 0000-0001-6079-0962
Matthias Beller: 0000-0001-5709-0965

Notes

The authors declare no competing financial interest.

■ ACKNOWLEDGMENTS

■ REFERENCES

(1) Mortier, J. Arene Chemistry: Reaction Mechanisms and Methods for Aromatic Compounds: John Wiley & Sons, 2016.
(2) Astruc, D. Modern Arene Chemistry; Wiley-VCH, 2002.
(3) Niziolek, A. M.; Onel, O.; Floudas, C. A. Production of benzene, toluene, and xylenes from natural gas via methanol: Process synthesis and global optimization. AIChE J. 2016, 62, 1531–1556.
(4) Speight, J. G. Handbook of Petroleum Refining; CRC Press, 2016.
(5) March, J. Advanced Organic Chemistry: Reactions, Mechanisms, and Structure, 4th ed.; John Wiley & Sons, 1992.
(6) Caron, S. Practical Synthetic Organic Chemistry: Reactions, Principles, and Techniques; John Wiley & Sons, 2011.
(7) Olah, G. A.; Molnar, A.; Prakash, G. K. S. Hydrocarbon Chemistry, 3rd ed.; John Wiley & Sons, 2017.
(8) Olah, G. A.; Prakash, G. K. S. Electrophilic Reactions on Alkanes in Alkanes and Cycloalkanes; Patai, S., Rappoport, Z., Eds.; Wiley 1992.
(9) Bond, G. C. Metal-Catalysed Reactions of Hydrocarbons; Springer, 2005.
(10) https://commons.wikimedia.org/wiki/Category:Cyclohexane_derivatives, (accesssed March 11, 2019).

(11) Debenham, J. S.; Graham, T. H.; Verras, A.; Zhang, Y.; Clements, M. J.; Kuethe, J. T.; Madsen-Duggan, C.; Liu, W.; Bhatt, U. R.; Chen, D.; Chen, Q.; Garcia-Calvo, M.; Geissler, W. M.; He, H.; Li, X.; Lisnock, J.; Shen, Z.; Tong, X.; Tung, E. C.; Wiltsie, J.; Xu, S.; Hale, J. J.; Pinto, S.; Shen, D.-M. Discovery and optimization of orally active cyclohexane-based prolylcarboxypeptidase (PrCP) inhibitors. Bioorg. Med. Chem. Lett. 2013, 23, 6228–6233.
(12) Hughes, M. D.; Xu, Y.-J.; Jenkins, P.; McMorn, P.; Landon, P.; Enache, D. I.; Carley, A. F.; Attard, G. A.; Hutchings, G. J.; King, F.; Stitt, E. H.; Johnston, P.; Griffin, K.; Kiely, C. J. Tunable gold catalysts for selective hydrocarbon oxidation under mild conditions. Nature 2005, 437, 1132–1135.
(13) Hegetschweiler, K. A rigid, cyclohexane-based polyamino-polyalcohol as a versatile building block for tailored chelating agents. Chem. Soc. Rev. 1999, 28, 239–249.
(14) Chida, N.; Sato, T. Synthesis of Natural Products Containing Cyclohexane Units Utilizing the Ferrier Carbocyclization Reaction. Chem. Rec. 2014, 14, 592–605.
(15) Dyson, P. J. Arene hydrogenation by homogeneous catalysts: fact or fiction? Dalton Trans. 2003, 2964–2974.
(16) Qi, S.-C.; Wei, X.-Y.; Zong, Z.-M.; Wang, Y.-K. Application of supported metallic catalysts in catalytic hydrogenation of arenes. RSC Adv. 2013, 3, 14219–14232.
(17) Lu, S.-M.; Zhou, Y.-G. Hydrogenation of arenes and hetarenes in Science of Synthesis. Stereosel. Synth. 2011, 1, 257–294.
(18) Gual, A.; Godard, C.; Castillón, S.; Claver, C. Soluble transition-metal nanoparticles-catalysed hydrogenation of arenes. Dalton Trans. 2010, 39, 11499–11512.
(19) Bianchini, C.; Meli, A.; Vizza, F. Hydrogenation of Arenes and Heteroaromatics, From Handbook of Homogeneous Hydrogenation; de Vries, J. G., Elsevier, C. J., Eds.; Wiley-VCH 2007.
(20) Maegawa, T.; Akashi, A.; Yaguchi, K.; Iwasaki, Y.; Shigetsura, M.; Monguchi, Y.; Sajiki, H. Efficient and Practical Arene Hydrogenation by Heterogeneous Catalysts under Mild Conditions. Chem.—Eur. J. 2009, 15, 6953–6963.
(21) Cui, X.; Surkus, A.-E.; Junge, K.; Topf, C.; Radnik, J.; Kreyenschulte, C.; Beller, M. Highly selective hydrogenation of arenes using nanostructured ruthenium catalysts modified with a carbon–nitrogen matrix. Nat. Commun. 2016, 7, 11326.
(22) Dwivedi, A. D.; Rai, R. K.; Gupta, K.; Singh, S. K. Catalytic Hydrogenation of Arenes in Water Over In Situ Generated Ruthenium Nanoparticles Immobilized on Carbon. ChemCatChem 2017, 9, 1930–1938.
(23) Li, H.; Wang, Y.; Lai, Z.; Huang, K.-W. Selective Catalytic Hydrogenation of Arenols by a Well-Defined Complex of Ruthenium and Phosphorus-Nitrogen PN3-Pincer Ligand Containing a Phenanthroline Backbone. ACS Catal. 2017, 7, 4446–4450.
(24) Morioka, Y.; Matsuoka, A.; Binder, K.; Knappett, B. R.; Wheatley, A. E. H.; Naka, H. Selective hydrogenation of arenes to cyclohexanes in water catalyzed by chitin-supported ruthenium nanoparticles. Catal. Sci. Technol. 2016, 6, 5801–5805.
(25) Miao, S.; Liu, Z.; Han, B.; Huang, J.; Sun, Z.; Zhang, J.; Jiang, T. Ru Nanoparticles Immobilized on Montmorillonite by Ionic Liquids: A Highly Efficient Heterogeneous Catalyst for the Hydrogenation of Benzene. Angew. Chem., Int. Ed. 2006, 45, 266–269.
(26) Wiesenfeldt, M. P.; Nairoukh, Z.; Li, W.; Glorius, F. Hydrogenation of fluoroarenes: Direct access to all-cis-(multi)-fluorinated cycloalkanes. Science 2017, 357, 908–912.
(27) Schulz, J.; Roucoux, A.; Patin, H. Stabilized Rhodium(0) Nanoparticles: A Reusable Hydrogenation Catalyst for Arene Derivatives in a Biphasic Water-Liquid System. Chem.—Eur. J. 2000, 6, 618–624.
(28) Bianchini, C.; Dal Santo, V.; Meli, A.; Moneti, S.; Moreno, M.; Oberhauser, W.; Psaro, R.; Sordelli, L.; Vizza, F. Hydrogenation of Arenes over Catalysts that Combine a Metal Phase and a Grafted Metal Complex: Role of the Single-Site Catalyst. Angew. Chem., Int. Ed. 2003, 42, 2636–2639.
(29) Barbaro, P.; Bianchini, C.; Dal Santo, V.; Meli, A.; Moneti, S.; Psaro, R.; Scaffidi, A.; Sordelli, L.; Vizza, F. Hydrogenation of Arenes

over Silica-Supported Catalysts That Combine a Grafted Rhodium Complex and Palladium Nanoparticles: Evidence for Substrate Activation on Rhsingle-site–PdmetalMoieties. *J. Am. Chem. Soc.* 2006, 128, 7065–7076.

(30) Yan, N.; Yuan, Y.; Dyson, P. J.; Yan, N.; Yuan, Y.; Dyson, P. J. Rhodium nanoparticle catalysts stabilized with a polymer that enhances stability without compromising activity. *Chem. Commun.* 2011, 47, 2529–2531.

(31) Motoyama, Y.; Takasaki, M.; Yoon, S.-H.; Mochida, I.; Nagashima, H. Rhodium Nanoparticles Supported on Carbon Nanofibers as an Arene Hydrogenation Catalyst Highly Tolerant to a Coexisting Epoxide Group. *Org. Lett.* 2009, 11, 5042–5045.

(32) Park, K. H.; Jang, K.; Kim, H. J.; Son, S. U. Near-Monodisperse Tetrahedral Rhodium Nanoparticles on Charcoal: The Shape-Dependent Catalytic Hydrogenation of Arenes. *Angew. Chem., Int. Ed.* 2007, 46, 1152–1155.

(33) Dykeman, R. R.; Yuan, Y.; Yan, N.; Asakura, H.; Teramura, K.; Tanaka, T.; Dyson, P. J. Rational Design of a Molecular Nanocatalyst-Stabilizer that Enhances both Catalytic Activity and Nanoparticle Stability. *ChemCatChem* 2012, 4, 1907–1910.

(34) Tran, B. L.; Fulton, J. L.; Linehan, J. C.; Lercher, J. A.; Bullock, R. M. Rh(CAAC)-Catalyzed Arene Hydrogenation: Evidence for Nanocatalysis and Sterically Controlled Site-Selective Hydrogenation. *ACS Catal.* 2018, 8, 8441–8449.

(35) Miyamura, H.; Suzuki, A.; Yasukawa, T.; Kobayashi, S. Polysilane-Immobilized Rh-Pt Bimetallic Nanoparticles as Powerful Arene Hydrogenation Catalysts: Synthesis, Reactions under Batch and Flow Conditions and Reaction Mechanism. *J. Am. Chem. Soc.* 2018, 140, 11325–11334.

(36) Bartlesville, F.-N. Hydrogenation of benzene in the presence of water. U.S. Patent 6,013,847 A, 2000.

(37) Mévellec, V.; Roucoux, A.; Ramirez, E.; Philippot, K.; Chaudret, B. Surfactant-Stabilized Aqueous Iridium(0) Colloidal Suspension: An Efficient Reusable Catalyst for Hydrogenation of Arenes in Biphasic Media. *Adv. Synth. Catal.* 2004, 346, 72–76.

(38) Kang, X.; Liu, H.; Hou, M.; Sun, X.; Han, H.; Jiang, T.; Zhang, Z.; Han, B. Synthesis of Supported Ultrafine Non-noble Subnanometer-Scale Metal Particles Derived from Metal-Organic Frameworks as Highly Efficient Heterogeneous Catalysts. *Angew. Chem., Int. Ed.* 2016, 55, 1080–1084.

(39) Lu, L.; Rong, Z.; Du, W.; Ma, S.; Hu, S. Selective Hydrogenation of Single Benzene Ring in Biphenyl Catalyzed by Skeletal Ni. *ChemCatChem* 2009, 1, 369–371.

(40) Titova, Y. Y.; Schmidt, F. K. Nanoscale Ziegler catalysts based on bis(acetylacetonate)nickel in the arene hydrogenation reactions. *Appl. Catal., A* 2017, 547, 105–114.

(41) Rekker, T.; Reesink, B. H.; Borninkhof, F. Process for the Production of Cyclohexane. U.S. Patent 5,856,603 A, 1999.

(42) Sanderson, J. R.; Renken, T. L.; McKinney, M. W. Manufacture of cyclohexane from benzene and a hydrogen source containing impurities. U.S. Patent 6,750,374 B2, 2004.

(43) Luo, W.; Shi, H.; Schachtl, E.; Gutiérrez, O. Y.; Lercher, J. A. Active Sites on Nickel-Promoted Transition-Metal Sulfides That Catalyze Hydrogenation of Aromatic Compounds. *Angew. Chem., Int. Ed.* 2018, 57, 14555–14559.

(44) Hu, S.-C.; Wang, L.-K.; Wu, J.-C. Process for the hydrogenation of benzene to cyclohexane. U.S. Patent 4,731,496 A, 1998.

(45) Stuhl, L. S.; Rakowski DuBois, M.; Hirsekorn, F. J.; Bleeke, J. R.; Stevens, A. E.; Muetterties, E. L. Catalytic homogeneous hydrogenation of arenes. 6. Reaction scope for the (.eta.3-2-propenyl)tris(trimethyl phosphite-P)cobalt catalyst. *J. Am. Chem. Soc.* 1978, 100, 2405–2410.

(46) Sapre, A. V.; Gates, B. C. Hydrogenation of aromatic hydrocarbons catalyzed by sulfided cobalt oxide-molybdenum oxide/.alpha.-aluminum oxide. Reactivities and reaction networks. *Ind. Eng. Chem. Process Des. Dev.* 1981, 20, 68–73.

(47) Ji, P.; Song, Y.; Drake, T.; Veroneau, S. S.; Lin, Z.; Pan, X.; Lin, W. Titanium(III)-Oxo Clusters in a Metal-Organic Framework

Support Single-Site Co(II)-Hydride Catalysts for Arene Hydrogenation. *J. Am. Chem. Soc.* 2018, 140, 433–440.

(48) Liu, X.; Xu, L.; Xu, G.; Jia, W.; Ma, Y.; Zhang, Y. Selective Hydrodeoxygenation of Lignin-Derived Phenols to Cyclohexanols or Cyclohexanes over Magnetic CoNx@NC Catalysts under Mild Conditions. *ACS Catal.* 2016, 6, 7611–7620.

(49) Nanotechnologies: Principles, Applications, Implications and Hands-On Activities; European Commission, European Union, 2012.

(50) Polshettiwar, V.; Asefa, T. Nanocatalysis: Synthesis and Applications; Wiley, 2013.

(51) Jagadeesh, R. V.; Surkus, A.-E.; Junge, H.; Pohl, M.-M.; Radnik, J.; Rabeah, J.; Huan, H.; Schunemann, V.; Bruckner, A.; Beller, M. Nanoscale Fe2O3-Based Catalysts for Selective Hydrogenation of Nitroarenes to Anilines. *Science* 2013, 342, 1073–1076.

(52) Jagadeesh, R. V.; Murugesan, K.; Alshammari, A. S.; Neumann, H.; Pohl, M.-M.; Radnik, J.; Beller, M. MOF-derived cobalt nanoparticles catalyze a general synthesis of amines. *Science* 2017, 358, 326–332.

(53) Corma, A.; Serna, P. Chemoselective Hydrogenation of Nitro Compounds with Supported Gold Catalysts. *Science* 2006, 313, 332–334.

(54) Sankar, M.; Dimitratos, N.; Miedziak, P. J.; Wells, P. P.; Kiely, C. J.; Hutchings, G. J. Designing bimetallic catalysts for a green and sustainable future. *Chem. Soc. Rev.* 2012, 41, 8099–8139.

(55) Torres Galvis, H. M.; Bitter, J. H.; Khare, C. B.; Ruitenbeek, M.; Dugulan, A. I.; de Jong, K. P. Supported Iron Nanoparticles as Catalysts for Sustainable Production of Lower Olefins. *Science* 2012, 335, 835–838.

(56) van Schrojenstein Lantman, E. M.; Deckert-Gaudig, T.; Mank, A. J. G.; Deckert, V.; Weckhuysen, B. M. Catalytic processes monitored at the nanoscale with tip-enhanced Raman spectroscopy. *Nat. Nanotechnol.* 2012, 7, 583.

(57) Yuan, Y.; Yan, N.; Dyson, P. J. Advances in the Rational Design of Rhodium Nanoparticle Catalysts: Control via Manipulation of the Nanoparticle Core and Stabilizer. *ACS Catal.* 2012, 2, 1057–1069.

(58) He, L.; Weniger, F.; Neumann, H.; Beller, M. Synthesis, Characterization, and Application of Metal Nanoparticles Supported on Nitrogen-Doped Carbon: Catalysis beyond Electrochemistry. *Angew. Chem., Int. Ed.* 2016, 55, 12582–12594.

(59) Kong, X.; Fang, Z.; Bao, X.; Wang, Z.; Mao, S.; Wang, Y. Efficient hydrogenation of stearic acid over carbon coated Ni Fe catalyst. *J. Catal.* 2018, 367, 139–149.

(60) Li, M.; Li, Y.; Jia, L.; Wang, Y. Tuning the selectivity of phenol hydrogenation on Pd/C with acid and basic media. *Catal. Commun.* 2018, 103, 88–91.

(61) Wei, Z.; Chen, Y.; Wang, J.; Su, D.; Tang, M.; Mao, S.; Wang, Y. Cobalt Encapsulated in N-Doped Graphene Layers: An Efficient and Stable Catalyst for Hydrogenation of Quinoline Compounds. *ACS Catal.* 2016, 6, 5816–5822.

(62) Wei, Z.; Wang, J.; Mao, S.; Su, D.; Jin, H.; Wang, Y.; Xu, F.; Li, H.; Wang, Y. In Situ-Generated Co0-Co3O4/N-Doped Carbon Nanotubes Hybrids as Efficient and Chemoselective Catalysts for Hydrogenation of Nitroarenes. *ACS Catal.* 2015, 5, 4783–4789.

(63) Pachfule, P.; Shinde, D.; Majumder, M.; Xu, Q. Fabrication of carbon nanorods and graphene nanoribbons from a metal-organic framework. *Nat. Chem.* 2016, 8, 718.

(64) Tang, J.; Yamauchi, Y. MOF morphologies in control. *Nat. Chem.* 2016, 8, 638.

(65) Dang, S.; Zhu, Q.-L.; Xu, Q. Nanomaterials derived from metal–organic frameworks. *Nat. Rev. Mater.* 2018, 3, 17075.

(66) Shen, K.; Chen, X.; Chen, J.; Li, Y. Development of MOF-Derived Carbon-Based Nanomaterials for Efficient Catalysis. *ACS Catal.* 2016, 6, 5887–5903.

(67) Lee, K. J.; Lee, J. H.; Jeoung, S.; Moon, H. R. Transformation of Metal-Organic Frameworks/Coordination Polymers into Functional Nanostructured Materials: Experimental Approaches Based on Mechanistic Insights. *Acc. Chem. Res.* 2017, 50, 2684–2692.

(68) Guan, B. Y.; Kushima, A.; Yu, L.; Li, S.; Li, J.; Lou, X. W. D. Coordination Polymers Derived General Synthesis of Multishelled

Mixed Metal-Oxide Particles for Hybrid Supercapacitors. *Adv. Mater.* 2017, 29, 1605902.

(69) Hu, M.; Reboul, J.; Furukawa, S.; Torad, N. L.; Ji, Q.; Srinivasu, P.; Ariga, K.; Kitagawa, S.; Yamauchi, Y. Direct Carbonization of Al-Based Porous Coordination Polymer for Synthesis of Nanoporous Carbon. *J. Am. Chem. Soc.* 2012, 134, 2864–2867.

(70) Morsali, A.; Hashemi, L. *Main Group Metal Coordination Polymers: Structures and Nanostructures*; Wiley, 2017.

(71) Foo, M. L.; Matsuda, R.; Kitagawa, S. Functional Hybrid Porous Coordination Polymers. *Chem. Mater.* 2014, 26, 310–322.

(72) Kitagawa, S.; Kitaura, R.; Noro, S.-i. Functional Porous Coordination Polymers. *Angew. Chem., Int. Ed.* 2004, 43, 2334–2375.

(73) Liu, B.; Zou, R.-Q.; Zhong, R.-Q.; Han, S.; Shioyama, H.; Yamada, T.; Maruta, G.; Takeda, S.; Xu, Q. Microporous coordination polymers of cobalt(II) and manganese(II) 2,6-naphthalenedicarboxylate: preparations, structures and gas sorptive and magnetic properties. *Microporous Mesoporous Mater.* 2008, 111, 470–477.

(74) Murugavel, R.; Krishnamurthy, D.; Sathiyendiran, M. Anionic metal-organic and cationic organic layer alternation in the coordination polymers [{M(BTEC)(OH2)4}-{C4H12N2}-4H2O]n (M = Co, Ni, and Zn; BTEC = 1,2,4,5-benzenetetracarboxylate). *J. Chem. Soc., Dalton Trans.* 2002, 34–39.

(75) Rase, H. F. *Handbook of Commercial Catalysts: Heterogeneous Catalysts*; CRC Press, 2016.

(76) http://processflowsheet.com/cyclohexane-production-by-benzene-hydrogenation/, (accessed December 27, 2012).

(77) Stalzer, M. M.; Nicholas, C. P.; Bhattacharyya, A.; Motta, A.; Delferro, M.; Marks, T. J. Single-Face/All-cis Arene Hydrogenation by a Supported Single-Site d0 Organozirconium Catalyst. *Angew. Chem., Int. Ed.* 2016, 55, 5263–5267.

(78) Mechelhoff, M.; Dreisbach, C.; Jentsch, J.-D.; Heuer, L.; Wasserscheid, P.; Rittsteiger, A. Process for the preparation of menthol. U.S. Patent 2014/0,066,665 A1, 2014.

(79) Preuster, P.; Papp, C.; Wasserscheid, P. Liquid Organic Hydrogen Carriers (LOHCs): Toward a Hydrogen-free Hydrogen Economy. *Acc. Chem. Res.* 2017, 50, 74–85.

(80) Markiewicz, M.; Zhang, Y. Q.; Bösmann, A.; Brückner, N.; Thöming, J.; Wasserscheid, P.; Stolte, S. Environmental and health impact assessment of Liquid Organic Hydrogen Carrier (LOHC) systems - challenges and preliminary results. *Energy Environ. Sci.* 2015, 8, 1035–1045.

(81) Brückner, N.; Obesser, K.; Bösmann, A.; Teichmann, D.; Arlt, W.; Dungs, J.; Wasserscheid, P. Evaluation of Industrially Applied Heat-Transfer Fluids as Liquid Organic Hydrogen Carrier Systems. *ChemSusChem* 2014, 7, 229–235.

(82) R. F., Egerton *Electron Energy-Loss Spectroscopy in the Electron Microscope*, 3rd ed.; Springer, 2009.

(83) Ernst, B.; Bensaddik, A.; Hilaire, L.; Chaumette, P.; Kiennemann, A. Study on a cobalt silica catalyst during reduction and Fischer-Tropsch reaction: In situ EXAFS compared to XPS and XRD. *Catal. Today* 1998, 39, 329–341.

(84) Okamoto, Y.; Nagata, K.; Adachi, T.; Imanaka, T.; Inamura, K.; Takyu, T. Preparation and characterization of highly dispersed cobalt oxide and sulfide catalysts supported on silica. *J. Phys. Chem.* 1991, 95, 310–319.

(85) Voß, M.; Borgmann, D.; Wedler, G. Characterization of Alumina, Silica, and Titania Supported Cobalt Catalysts. *J. Catal.* 2002, 212, 10–21.

(86) Wei, G.; Wainright, J. S.; Savinell, R. F. Catalytic activity for oxygen reduction reaction of catalysts consisting of carbon, nitrogen and cobalt. *J. New Mat. Electrochem. Systems* 2000, 3, 121–129.

(87) Miao, H.; Li, S.; Wang, Z.; Sun, S.; Kuang, M.; Liu, Z.; Yuan, J. Enhancing the pyridinic N content of Nitrogen-doped graphene and improving its catalytic activity for oxygen reduction reaction. *Int. J. Hydrogen Energy* 2017, 42, 28298–28308.

(88) Wu, Z.; Sugimoto, Y.; Kawashima, H. Formation of N2 from Pyrrolic and Pyridinic Nitrogen during Pyrolysis of Nitrogen-Containing Model Coals. *Energy Fuels* 2003, 17, 694–698.
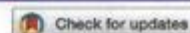
Check for updates

Reductive amination using cobalt-based nanoparticles for synthesis of amines

Kathiravan Murugesan, Vishwas G. Chandrashekhar, Thirusangumurugan Senthamarai, Rajenahally V. Jagadeesh[✉] and Matthias Beller[ORCID][✉]

Reductive aminations are an essential class of reactions widely applied for the preparation of different kinds of amines, as well as a number of pharmaceuticals and industrially relevant compounds. In such reactions, carbonyl compounds (aldehydes, ketones) react with ammonia or amines in the presence of a reducing agent and form corresponding amines. Common catalysts used for reductive aminations, especially for the synthesis of primary amines, are based on precious metals or Raney nickel. However, their drawbacks and limited applicability inspired us to look for alternative catalysts. The development of base-metal nanostructured catalysts is highly preferable and is crucial to the advancement of sustainable and cost-effective reductive amination processes. In this protocol, we describe the preparation of carbon-supported cobalt-based nanoparticles as efficient and practical catalysts for synthesis of different kinds of amines by reductive aminations. Template synthesis of a cobalt–triethylenediamine–terephthalic acid metal–organic framework on carbon and subsequent pyrolysis to remove the organic template resulted in the formation of supported single cobalt atoms and nanoparticles. Applying these catalysts, we have synthesized structurally diverse benzylic, aliphatic and heterocyclic primary, secondary and tertiary amines, including pharmaceutically relevant products, starting from inexpensive and easily accessible carbonyl compounds with ammonia, nitro compounds or amines and molecular hydrogen. To prepare this cobalt-based catalyst takes 26 h, and the reported catalytic reductive amination reactions can be carried out within 18–28 h.

Introduction

Among different kinds of chemicals, amines represent highly valuable compounds widely applied in many science areas, including chemistry, biology, medicine, materials and energy[1-7]. As an example, the majority of top-selling drugs contain nitrogen and/or amino groups, which constitute integral parts and play vital roles in their activities[3]. For the synthesis and functionalization of amines, catalytic reductive aminations using molecular hydrogen represent a resourceful method used in both academic laboratories and industry[8-26]. Common catalysts known for these reactions are based on precious metals[8-19] and Raney nickel[8,9,20]. However, for the advancement of cost-effective and selective reductive amination processes, the development of non-noble metal-based catalysts is preferable and continues to attract substantial interest. Compared to traditional homogeneous catalysts, heterogeneous catalysts offer advantages such as stability and recyclability. Among heterogeneous catalysts, supported nanoparticles[23-35], or single metal atoms[35-37] are of prime importance because of their low energy consumption and high activities and selectivities. In this regard, in recent years these materials have become the subject of increasing interest as catalysts for organic synthesis[6,23-39]. With respect to reductive aminations using molecular hydrogen, to our knowledge, only a few nanocatalysts have been developed[21-26]. Among these, carbon-supported Co_3O_4 nanoparticles surrounded by nitrogen-doped graphene layers, developed by our group, represent excellent catalysts for oxidation and hydrogenation reactions, as well as reductive amination[24]. These cobalt oxide nanoparticles are prepared by the immobilization of a cobalt–phenanthroline complex on carbon and subsequent pyrolysis at 800 °C under argon for 2 h. This cobalt oxide–based nanocatalyst worked well for the reductive amination of aldehydes and nitro compounds or amines to produce secondary/tertiary amines[24]. Unfortunately, this catalyst is not active for the synthesis of primary amines from carbonyl compounds and ammonia in presence of molecular hydrogen.
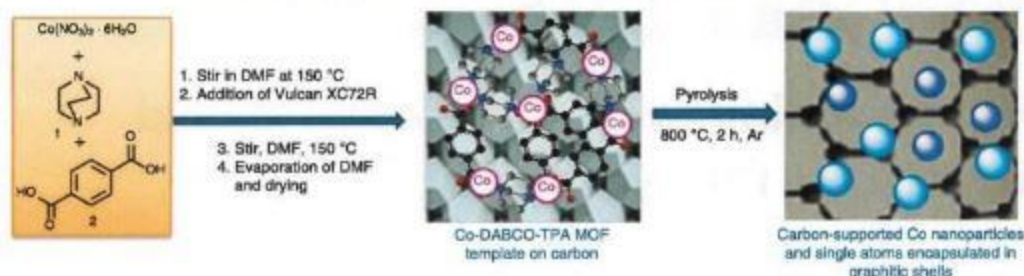
Fig. 1 | Preparation of carbon-supported single cobalt atoms and nanoparticles encapsulated within graphitic shells using a MOF template.

We recently developed a new type of carbon-supported cobalt nanoparticle and single atom–based catalysts[25]. The ordered arrangement of cobalt nanoparticles and single atoms is achieved by using a cobalt metal–organic framework (MOF) as a template on carbon and subsequent pyrolysis under an inert atmosphere[25]. The resulting cobalt nanoparticles were found to be general and selective catalysts for reductive aminations to prepare different kinds of amines[25].

Here, we describe the detailed procedure for the synthesis of these cobalt-based nanocatalysts and their application to obtain various amines of commercial and industrial importance. Notably, MOFs represent suitable precursors and self-scarifying templates for the preparation of nanomaterials under pyrolytic methods[6,25,39].

In a representative procedure, the most active material is prepared by immobilization of an in situ–generated cobalt–triethylenediamine (DABCO; **1**)–terephthalic acid (TPA; **2**) (Co-DABCO-TPA) MOF on carbon and subsequent pyrolysis of the templated material under argon atmosphere (Fig. 1)[25]. To identify a suitable MOF precursor, different MOFs, such as Co-DABCO-TPA, Co-DABCO and Co-TPA, were generated in situ and used for the preparation of catalytic materials. In particular, cobalt nitrate, DABCO and TPA in a molar ratio of 1:3:3 are mixed in *N,N*-dimethylformamide (DMF) and stirred at 150 °C to generate the MOF used in this procedure. After MOF formation, carbon is added (Vulcan XC72R) and the mixture is stirred again at 150 °C. Slow evaporation of the solvent (DMF) generates the desired template material (Co-DABCO-TPA@C). Pyrolysis at 800 °C leads to the formation of carbon-supported single cobalt atoms and nanoparticles (Co-DABCO-TPA@C-800). Under a similar procedure, other cobalt materials using Co-MOFs containing single linkers such as Co-DABCO and Co-TPA are also prepared.

The resulting materials are characterized using Cs-corrected scanning transmission electron microscopy (STEM), energy-dispersive X-ray spectroscopy (EDXS), electron energy loss spectroscopy (EELS), X-ray photoelectron spectroscopy (XPS), and X-ray powder diffraction (XRD) spectral analysis[25] (see Supplementary Figures for detailed characterizations). The most active material (Co-DABCO-TPA@C-800) is characterized by the formation of graphitic shells encapsulating metallic cobalt particles with sizes ranging from <5 to 30 nm (Fig. 2, Supplementary Figs. 1a and 2a). The EDXS (Supplementary Fig. 4a, left) shows mainly the presence of metallic Co particles within the carbon matrix. In addition to these small metallic particles, single Co atoms, visible as bright dots by high-resolution, high-angle annular dark-field (HR-HAADF) STEM, were also detected within so-called cloudy regions of short-range ordered carbon (Fig. 2, Supplementary Figs. 1a and 2a, right). Apart from these, a small quantity of oxidic cobalt (Co(II)) in the surface of core shell particles is also present. To obtain information on Co, C and N relations, the parallel mapping of EDXS for all elements and EELS (Supplementary Fig. 1b) are performed. Compared to EDXS, the EELS technique allows the detection of nitrogen species because, in the case of EDXS, the overlap of the C and N edges minimizes, allowing visualization of small amounts of N. These analyses identified the presence of nitrogen located in the vicinity of metallic Co particles and single Co atoms within short-range ordered carbon (Supplementary Fig. 1). The XRD analysis of the Co-DABCO-TPA@C-800 catalyst also showed predominately the presence of metallic Co particles, along with small quantity of cobalt oxide particles (Supplementary Fig. 7). XPS analysis showed two states of nitrogen. One is correlated to imine-like N known from pyridine (~98 eV) and the other, displaying at higher binding energy, corresponds to N bonded to Co (Supplementary Fig. 10a, right). These characterization data are summarized in Table 1.

Hereafter, we denote the most active catalyst, Co-DABCO-TPA@C-800 as Co/GS@C, where 'GS' stands for graphitic shells.

NATURE PROTOCOLS   **PROTOCOL**
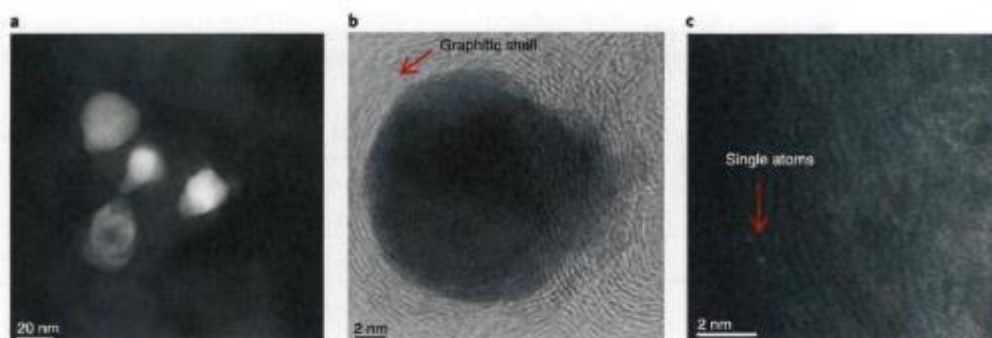
Fig. 2 | TEM images of Co/GS@C (Co-DABCO-TPA@C-800) catalyst. a, Distribution of cobalt nanoparticles. **b,** Graphitic shell encapsulated Co nanoparticles. **c,** Single cobalt atoms. Scale bars, 20 nm (**a**); 2 nm (**b,c**).

Table 1 | Characterization data for Co-DABCO-TPA@C-800 catalyst

Entry	Technique	Required analysis	Data found
2	STEM	Distribution, morphology, size and nature of nanoparticles	Graphitic shells encapsulated metallic cobalt particles with sizes from <5 nm to a maximum of 30 nm. Cobalt single atoms. Small quantity of cobalt oxide nanoparticles.
3	EDXS	Elemental detection and mapping	Metallic cobalt with small quantity of oxidic cobalt particles
4	EELS	Detection and distribution of nitrogen	Presence of nitrogen is detected and located in the vicinity of metallic Co particles and single Co atoms within short-range order carbon
5	XPS	Nature and states of nitrogen	XPS analysis showed two states of nitrogen. One is correlated with imine-like N known from pyridine (-398 eV) and the other, displaying at higher binding energy, corresponds to N bonded to Co
6	XRD	Different phases of cobalt	Predominate presence of metallic Co particles, along with small quantity of cobalt oxide particles

We tested commercial and prepared cobalt materials for the reductive amination of veratraldehyde (3,4-dimethoxybenzaldehyde; 3) to veratrylamine (3,4-dimethoxybenzylamine; 4) using ammonia and molecular hydrogen. In this benchmark reaction, the synthesis of the desired primary amine competes with the formation of unwanted secondary and tertiary amines/imines or alcohols. First, we tested commercial Raney nickel and Raney cobalt in the benchmark reaction and found that these two materials exhibited lower selectivity toward the formation of primary amine and as a results produced only 30–50% of veratrylamine (Table 2, entries 1-2). In these two cases, formation of the corresponding alcohol (45–64%) and secondary amine (2-3%) as side products was observed, which obviously lowered the selectivity toward the primary amine, a desired product in the present study. However, the cobalt materials prepared by the immobilization and pyrolysis of a Co-DABCO-TPA@C MOF on carbon (400–1,000 °C) exhibit significant activities (16–88% of 4; Table 2, entries 3–6).

Among these materials, the ones pyrolyzed at 800 °C showed maximum activity and produced veratrylamine in an 88% yield (Table 2, entry 3). Pyrolysis of cobalt–MOF's on carbon using cobalt nitrate with either DABCO (Co-DABCO@C-800) or TPA (Co-TPA@C-800) alone yielded less active catalysts (15–20% yields; Table 2, entries 7-8). We also tested our previously reported[24] cobalt oxide–based nanocatalyst (Co-phenanthroline@C-800), prepared by the pyrolysis of Co-phenanthroline complex on carbon, and found that this catalyst is not active enough for the reductive amination to produce the desired primary amines (Table 2, entry 9). As expected, homogeneous cobalt salts, different cobalt-based MOFs, and non-pyrolyzed materials were completely inactive (Table 2, entries 10–13).

The general applicability of the Co/GS@C catalyst for the reductive amination of carbonyl compounds to access all kinds of amines is shown in Figs. 3–8 [25]. A series of functionalized and

Table 2 | Activity of supported cobalt nanoparticles and commercial heterogeneous catalysts for the reductive amination of veratrylamine using ammonia and hydrogen
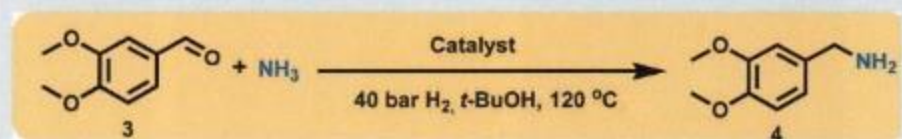
Entry	Catalyst	Yield of veratrylamine (%)
1	Raney nickel	50
2	Raney cobalt	30
3	Co-DABCO-TPA@C-800	88
4	Co-DABCO-TPA@C-400	16
5	Co-DABCO-TPA@C-600	75
6	Co-DABCO-TPA@C-1000	83
7	Co-DABCO@C-800	15
8	Co-TPA@C-800	20
9	Co-phenanthroline@C-800	1
10	$Co(NO_3)_2 \cdot 6H_2O$	1
11	Co-DABCO-TPA	1
12	Co-DABCO-TPA MOF	1
13	Co-DABCO-TPA@C	1

Reaction conditions: 0.5 mmol of 3,4-dimethoxybenzaldehyde, weight of catalyst corresponds to 3.5 mol% C, 5-7 bar NH_3, 40 bar H_2, 120 °C, 3 ml of t-BuOH, 15 h. Yields were determined by GC using n-hexadecane (100 µL) as standard. In the case of Raney nickel, 45% of corresponding alcohol and 2% of secondary amine were observed as side products. In the case of Raney cobalt, 64% of corresponding alcohol and 3% of secondary amine were observed as side products. The synthesis of Co-DABCO@C-800 and Co-DABCO-TPA MOF is described in Supplementary Method 2.

structurally diverse primary, secondary, and tertiary amines, including existing drug molecules, were prepared in good to excellent yields (**5–66**). Industrially relevant primary aliphatic amines were obtained from various aldehydes and ketones Fig. 3). Interestingly, this primary amine synthetic methodology can been applied for the introduction of an -NH_2 moiety in structurally complex and pharmaceutically applicable molecules, such as steroid derivatives, with high functional group tolerance (Fig. 4).

Next, various aldehydes were reacted directly with nitroarenes (products **37–44**) or amines (products **45–50**) in the presence of molecular hydrogen to obtain the corresponding secondary and tertiary amines (Fig. 5). For example, the alkylation of amino acid esters such as tyrosine methyl ester with different aldehydes proceeded smoothly in up to an 89% yield (products **47–49**), albeit racemization was observed. Under the present experimental reaction conditions, it is quite difficult to obtain retention of chirality without racemization in the case of reductive N-alkylation of amino acids. However, Fering et al. have shown the possibility of retention of chirality with single isomers in the case of N-alkylation of unprotected amino acids with alcohols by homogeneous Ru-catalyst[40]. By contrast, the reductive N-alkylation of (S)-(−)-α-methylbenzylamine and (R)-(+)-α-methylbenzylamine took place without racemization of the stereocenter (products **51–52**). Furthermore, we applied this cobalt catalyst for the preparation of N-methylamines (Fig. 6), which represent an important motif in numerous drugs (e.g., Oxycontin, Venlafaxine, Lexapro). Hence, different carbonyl compounds were reacted with aqueous N,N-dimethylamine (DMA) to yield products **53–57**. In addition, N-methyl amines were also prepared directly from nitro compounds or amines using aqueous formaldehyde as a methylation source (products **58–61**).

The synthetic applicability of this novel amination protocol is showcased by applying the catalyst system to the preparation of different existing drug molecules such as piribedil (**62**), buclizine (**63**), fenpropimorph (**64**), befuraline (**65**), and fipexide (**66**) in good to excellent yields (Fig. 7).

Reaction scale-up was demonstrated by performing the reductive amination of three substrates at the 5- to 20-g scale (Fig. 8). In all these cases, excellent yields were obtained (similar to those of the small-scale reactions (100–150 mg). In addition to excellent activity and selectivity, our Co/GS@C catalyst exhibits high stability and can be easily recycled six times without any reactivation (Table 3; Box 1).

NATURE PROTOCOLS   **PROTOCOL**
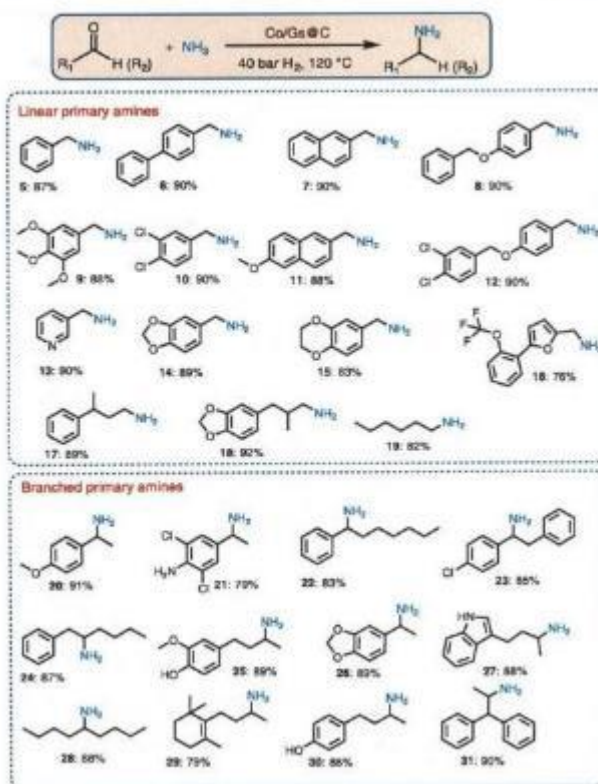
Fig. 3 | Co/GS@C-catalyzed reductive amination of aldehydes and ketones for the synthesis of linear and branched primary amines. Reaction conditions: 0.5 mmol of substrate, 25 mg of catalyst (3.5 mol% Co), 5–7 bar NH$_3$, 40 bar H$_2$, 3 mL t-BuOH, 120 °C, 15 h, with exceptions as follows. **20–30**: in THF (dry) solvent; **21, 22,31**: for 20 h; **23**: for 30 h with 35 mg of catalyst. **24**: for 24 h. Isolated yields reported unless otherwise indicated. Isolated as free amines and converted to hydrochloride salts for measurement of NMR and HRMS spectra.
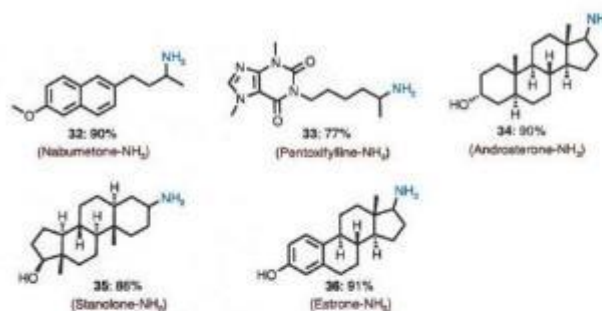
Fig. 4 | Co/GS@C-catalyzed amination of pharmaceuticals and steroid derivatives. Reaction conditions: 0.5 mmol of ketone, 25 mg of catalyst (3.5 mol% Co), 5–7 bar NH$_3$, 40 bar H$_2$, 3 mL of THF (dry), 120 °C, 15 h, with exceptions as follows. **33, 34**: for 24 h. Isolated yields reported unless otherwise indicated. Isolated as free amines and converted to hydrochloride salts for measuring NMR and HRMS.

Although this cobalt-based reductive amination protocol can be applied to the synthesis of different kinds of amines, it still displays limitations such as (i) poor reactivity of ketones with amines to produce branched secondary or tertiary amines and, (ii) racemization of N-alkylated products of amino acids without retention of chirality.

117
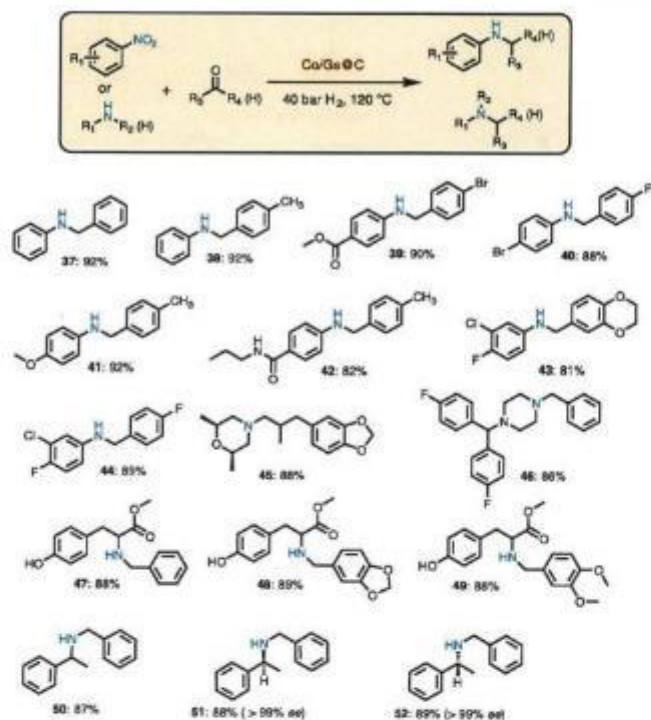
Fig. 5 | Co/GS@C-catalyzed synthesis of secondary and tertiary amines. Reaction conditions: 0.5 mmol of nitroarene, 0.75–1 mmol of aldehyde, 25 mg of catalyst (3.5 mol% Co), 20 mg of Amberlite IR-120, 3 mL of t-BuOH, 120 °C, 24 h, with exceptions as follows. **45–52:** 0.5 mmol of amine, 0.75 mmol of aldehyde. **46:** 30 mg of catalyst, 30 h. **50–52:** 10 mmol of amine, 15 mmol of benzaldehyde, 500 mg of catalyst (3.5 mol% Co), 400 mg of Amberlite IR-120, 15 mL of t-BuOH, 120 °C, 24 h. Isolated yields. ee, enantiomeric excess.
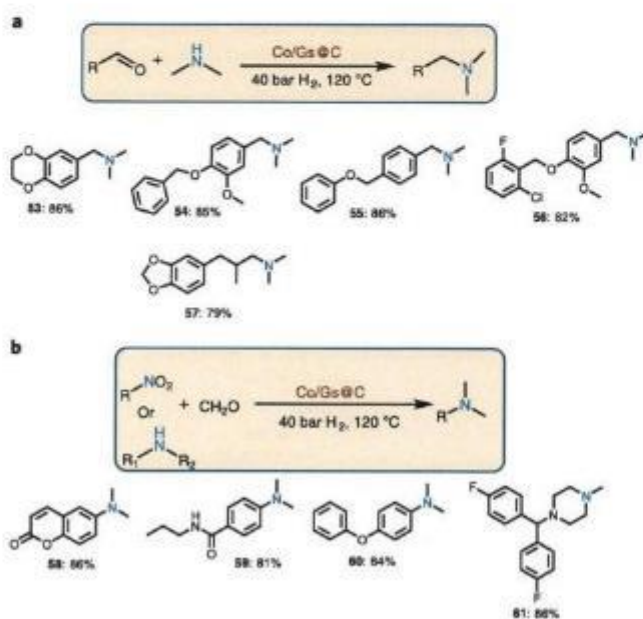
Fig. 6 | Co/Gs@C-catalyzed preparation of N-methylamines. a, Reactions of aldehydes with dimethylamine. Conditions: 0.5 mmol of aldehyde, 100 µL of aqueous dimethylamine (40 %), 25 mg of catalyst (3.5 mol% Co), 3 mL of t-BuOH, 120 °C, 24 h; isolated yields. **b,** Reactions of nitroarenes or amines with formaldehyde. Conditions: 0.5 mmol of nitroarene, 100–200 µL of aqueous formaldehyde (37%), 1:1 THF/H$_2$O (3 mL), with the following exception. **61:** 0.5 mmol of amine, 100–200 µL of aqueous formaldehyde (37%), 1:1 THF/H$_2$O (3 mL). Isolated yields.

NATURE PROTOCOLS   PROTOCOL
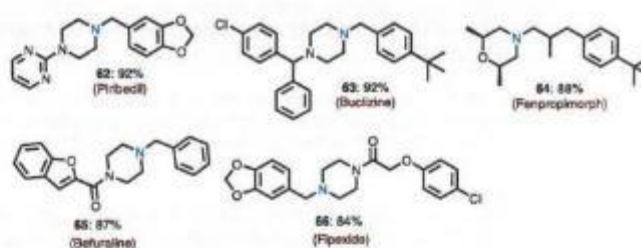
Fig. 7 | Preparation of drug molecules. Reaction conditions: 1 mmol of amine, 1.5 mmol of aldehyde, 50 mg of catalyst (3.5 mol% Co), 3 mL of t-BuOH, 120 °C, 24 h, with exceptions as follows. **65, 66:** 2 mmol of amine, 1 mmol of aldehyde; synthesis of amine followed by acylation with acid chlorides (see Supplementary Method 2 for detailed procedure). Isolated yields.
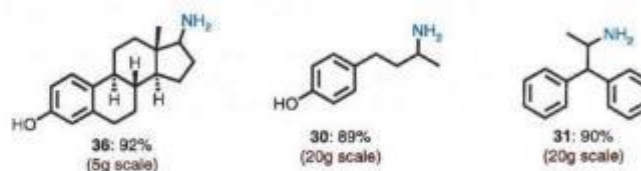
Fig. 8 | Reaction upscaling. Reaction conditions: 5–20 g of substrate, 25 mg of Co/Gs@C (3.5 mol% Co) for each 0.5 mmol of substrate, 5–7 bar NH_3, 40 bar H_2, 50–150 mL dry THF, 120 °C, 24 h. Isolated yields.

Table 3 | Recycling of Co/GS@C for the reductive amination of 4-(4-hydroxyphenyl)butan-2-one (67)
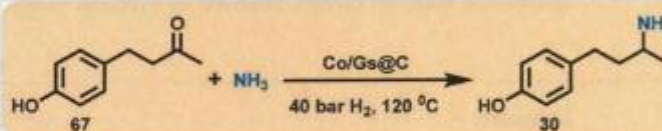
No. of runs	Yield of 4-(3-aminobutyl)phenol (%)
1	90
2	90
3	89
4	89
5	88
6	87
7	87

Reaction conditions: 5 mmol, 250 mg of catalyst (3.5 mol%), 5–7 bar NH_3, 40 bar H_2, 20 mL of dry THF, 120 °C, 15 h, isolated yields.

Experimental design
Catalyst preparation
The experimental procedure and setup reported below are applicable to the preparation of the catalyst on a 1- to 5-g scale. Following this experimental procedure, all the catalytic materials prepared exhibited similar activity and selectivity toward reductive amination reactions.

Characterization of catalysts
The catalytic materials have been systematically characterized using STEM, EDXS, EELS, XPS, and XRD spectral analysis.

Catalytic reactions
The described protocol was applied to reactions ranging from a 0.5-mmol to a 120-mmol scale. Similar yields were obtained in this range. The detailed experimental procedures to synthesize

Box 1 | Catalyst-recycling experiments with 4-(4-hydroxyphenyl)butan-2-one (Raspberry ketone)
● **Timing** 15 h

This reaction is performed to test and to demonstrate recycling and reusability of the catalyst. The catalyst can be recycled and reused up to six times without any substantial loss of catalytic activity or selectivity. In each step, after the reaction, the catalyst is separated (recycled) and reused without any reactivation (six times).

Procedure
1. Charge the Teflon or glass fitted 100-mL autoclave with a magnetic stir bar and 20 mL of THF solvent. Then add 821 mg of 4-(4-hydroxyphenyl)butan-2-one (5.0 mmol).
2. Weigh 250 mg (3.5 mol%) of the cobalt-based catalyst prepared in Step 8 of the main Procedure and add it to the autoclave.
3. Perform the reaction in an autoclave as described in Step 11A(iv-vi).
4. After completion of the reaction, let the autoclave cool to room temperature. Discharge the remaining ammonia and hydrogen and remove the reaction solution from the autoclave.
5. Transfer all of the reaction mixture to a centrifuge tube. Centrifuge the solution and separate the catalyst by decanting the supernatant.
▲ CRITICAL STEP Apply a centrifugation rate of 4,032g (6,000 r.p.m.) at room temperature (25 °C) for 5-10 min.
6. Wash the catalyst with an excess of ethyl acetate three times and dry the material in vacuo.
■ PAUSE POINT The dried catalyst can be stored for hours without further ado. Reuse it directly without further reactivation or purification for the next run.

the different amines given in Step 11A–E have been optimized (e.g., solvent, temperature, stirring time).

Different MOFs, such as Co-DABCO-TPA, Co-DABCO, and Co-TPA, were generated in situ under similar experimental procedures and have been used as precursors for the preparation of supported cobalt nanoparticles. The same procedure was applied to generate different MOFs and immobilize them on carbon, followed by pyrolysis to obtain cobalt nanoparticles.

Materials

Reagents
! CAUTION For the handling of reaction gases (hydrogen and ammonia), appropriate safety measures should be taken. Hydrogen is a flammable gas and hence it should be handled carefully. When filling the autoclave with hydrogen, care should be taken to avoid allowing the gas to leak out. Gaseous ammonia is corrosive and an irritant and can be fatal when inhaled. Check the material safety data sheets for hydrogen and ammonia before handling. The autoclaves should be handled carefully; hence, proper training is required. Convenient and pre-checked autoclaves should be used in order to avoid hydrogen leakage ▲ CRITICAL All solvents are used as received commercially without any purification.

- Cobalt(II) nitrate hexahydrate ($Co(NO_3)_2 \cdot 6H_2O$; Alfa Aesar, cat. no. 36418-100G)
- 1,4-Diazabicyclo[2.2.2]octane (DABCO; ReagentPlus, ≥99%; Sigma-Aldrich, cat. no. D27802-25G)
- Terephthalic acid (TPA, 98%; Sigma-Aldrich, cat. no.185361)
- Aqueous formaldehyde (37%, stabilizer with ~10% methanol; Sigma-Aldrich, cat. no. 252549)
- Aqueous dimethylamine solution (40 wt% in H_2O; Sigma-Aldrich, cat. no. 426458)
- Tetrahydrofuran (THF; 99.8%; stabilizer free; extra dry; Acros Organics, cat. no. 45070010)
- Methanol (MeOH; J.T. Baker, cat. no. 9070-01)
- Tertiary butanol (t-buOH, 99.8%; Acros Organics, cat. no. 390690025)
- N,N-Dimethylformamide (DMF, 99%; Sigma-Aldrich, cat. no. 348435000)
- Methanolic HCl (0.5 M HCl in methanol, Alfa Aesar, cat. no. H31570)
- Dioxane HCl (4 N HCl in dioxane; TCI Europe, cat. no. H1062)
- Vulcan XC72R carbon black (Cabot, cat. no. LOT-1584452)
- 3-Chloro-4-fluoronitrobenzene or 2-chloro-1-fluoro-4-nitrobenzene (98.0%; Sigma-Aldrich, cat. no. 233234)
- Ethyl acetate (Walther CMP, cat. no. WAL10521 5000)
- n-Hexane (Walther CMP, cat. no. BAK8669 9025)
- Hexadecane (ReagentPlus, 99%; Sigma-Aldrich, cat. no. H6703)
- Silica gel (high-purity grade, pore size 60 Å, 130–270 mesh, for column chromatography; Sigma-Aldrich, cat. no. 288608)
- Sodium sulfate (Na_2SO_4, ReagentPlus, ≥99.0%; Sigma-Aldrich, cat. no. S9627)

NATURE PROTOCOLS   **PROTOCOL**

- Deionized water
- Hydrogen (99.999%; Air Liquide)
- Argon
- Helium (He)
- Ammonia gas (99.999%; Linde)
- Dimethylsulfoxide (DMSO-d_6) (Sigma-Aldrich, cat. no. 151874)
- Deuterated methanol (CD$_3$OD) (Sigma-Aldrich, cat. no. 151947)
- Deuterated chloroform (CDCl$_3$) (Sigma-Aldrich, cat. no. 151823)
- Holey carbon-supported Cu grid (mesh 300)
- 3,4,5-Trimethoxybenzaldehyde (98.0%; Sigma-Aldrich, cat. no. T68403)
- 4-(4-Hydroxyphenyl)butan-2-one (>99.0%; TCI Europe, cat. no. H0604)
- 2-Chloro-1-fluoro-4-nitrobenzene (98.0%; Sigma-Aldrich, cat. no. 233234)
- 2,3-Dihydrobenzo[b][1,4]dioxine-6-carbaldehyde (98.0%; Sigma-Aldrich, cat. no. 264598)
- Amberlite IR-120 (Sigma-Aldrich, cat. no. 1.15966)
- 4-(Phenoxymethyl)benzaldehyde (Maybridge, cat. no. CC63704CB)
- 4-Nitro-N-propylbenzamide (98.0%; Sigma-Aldrich, cat. no. 394130)

Equipment
- Round-bottom (RB) flasks (50, 100 and 250, pear-shaped, NS 29/32; Fisher Scientific, cat. no. 10303511)
- Teflon-coated magnetic stir bars (19 × 41.3 mm; VWR, cat. no. 58949-210,)
- Pasteur pipettes (glass, 230 mm, with cotton stoppers;, Carl Roth, cat. no. E327.1)
- Filter funnel (Buchner, 30 mL, glass-fritted disk, porosity = fine; VWR, cat. no. 89426-722)
- Magnetic stir plate with heating functionality (temperature range 50–300 °C, stirring speed 100–1,250 r.p.m.; Heidolph, model no. MR 3001 K)
- Aluminum block
- Weighing balance
- Vacuum pump
- Mortar and pestle (polytetrafluoroethylene (PTFE) stir bar, cylindrical, 10 × 6 mm; Cowie, cat. no. 001.110.6)
- Rotary evaporator
- Crucible and lid (china, 65 mL, 60 mm; Carl Roth, cat. nos. L222.1 and L239.1)
- Crucible and lid (china, 11 mL, 35 mm; Carl Roth, cat. nos. L218.1 and L235.1)
- Oven (Neytech Qex)
- Autoclaves (100, 300 mL; Parr Instrument)
- Glass centrifuge tube
- TEM instrument (JEOL, model no. JEM-ARM200F) equipped with corrector (CEOS), energy-dispersive X-ray-spectrometer (JEOL, model no. JED-2300), and a dual-EELS system (Gatan, Enfinium ER model)
- Diffractometer equipped with a linear position-sensitive detector (PSD; Stoe, STADI P model)
- X-ray photoelectron spectrometer (Thermo Fisher Scientific, model no. VG ESCALAB 220i XL)
- Gas chromatograph (Agilent, model no. 6890N network) equipped with a mass selective detector (Agilent, model no. 5973 network) and a 30 m × 0.250 mm × 0.25-μm column (Agilent, model no. HP-5MS; cat. no. 19091S-433)
- Gas chromatograph (Agilent 6890 series) with a flame ionization detector (FID) and a 30 m × 0.320 mm × 0.25-μm column (Agilent, model no. HP-5; cat. no. 19091J-413)
- Spectrometers (Bruker, model nos. AV 300 and AV 400)
- High-resolution electrospray ionization mass spectrometry (ESI-HRMS) instrument (HPLC system; Agilent, model no. 1200) and an electrospray ionization–time of flight–MS (ESI-TOF-MS) system (Agilent, model no. 6210)
- Electron ionization mass spectrometry (EI-HRMS) instrument (mass spectrometer; Thermo Fisher Scientific, model no. MAT 95XP)
- Reflux condenser
- Needles
- Aluminum plate
- Silica gel (pore size 3 or 4)
- Silica gel column (length, 200 mm; inner diameter, 15 mm; volume, 35 mL)
- Silica gel column (length, 1,000 mm; inner diameter, 75 mm; volume, 200 mL)
- Beaker
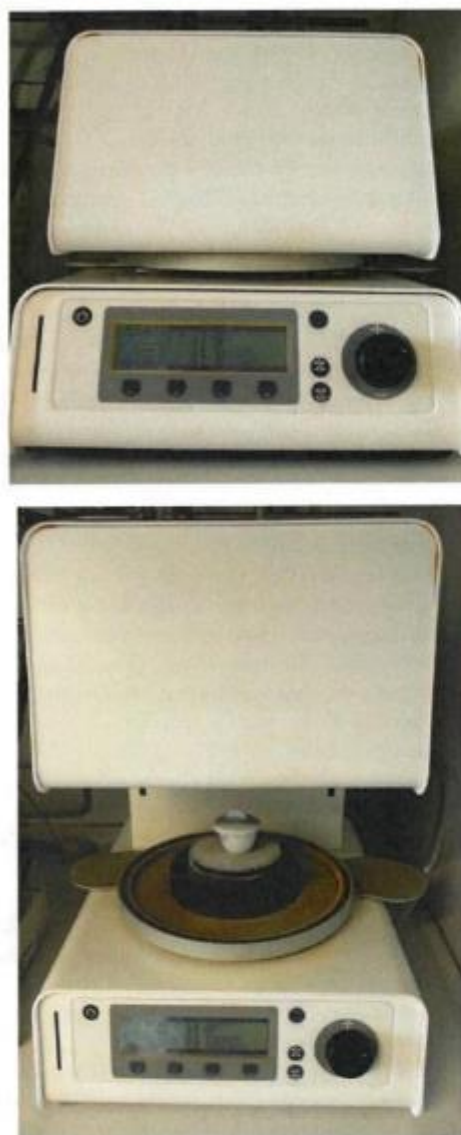
Fig. 9 | Heat treatment of the prepared Co-MOF@C material with a Neytech Qex oven.

Software
- WinX^{POW} (https://www.stoe.com/product/software-powder-xrd/)
- NMR-MestReNova (https://mestrelab.com/software/mnova/nmr/)

Equipment setup
Pyrolysis furnace (oven)
In our lab, a Neytech Qex oven is used to pyrolyze the material. The following temperature program is applied: conditions 25 °C/min, ~10 mL/min argon. The solid material to be pyrolyzed is transferred to a crucible and placed in the oven (Fig. 9). After placement of the crucible with lid, the chamber is closed and then the temperature of the oven is set to 100 °C. The air in the oven is evacuated by generating pre-vacuum for 5 min and then the chamber is flooded with argon for 60 s. The oven is heated again and evacuates another two times (three in total). The temperature of the oven is increased to 800 °C with constant argon flow and held at the same temperature (800 °C) for 2 h. After the completion of pyrolysis time, the oven is cooled to 100 °C and then the chamber is opened.

TEM

The TEM measurements are performed at 200 kV with an aberration-corrected instrument with a corrector. The microscope is equipped with an EDXS instrument and a dual-EELS system for chemical analysis. The aberration-corrected STEM imaging (HAADF and annular bright field (ABF)) is performed under the following conditions: HAADF and ABF imaging both are done with a spot size of approximately 0.1 nm, a convergence angle of 30–36° and collection semi-angles for HAADF and ABF of 90–170 mrad and 11–22 mrad, respectively. Dual EELS is done at a cathodoluminescence (CL) of 4 cm, an illumination semi-angle of 21.3 mrad and an entrance aperture semi-angle of 19.8 mrad.

XRD

XRD powder patterns are recorded on a Stoe STADI P diffractometer equipped with a linear PSD using Cu Kα radiation ($\lambda = 1.5406$ Å). Processing and assignment of the powder patterns is done using WinX^{POW} software (Stoe) and the Powder Diffraction File (PDF) database of the International Centre for Diffraction Data (ICDD).

XPS

XPS data are obtained with an X-ray photoelectron spectrometer with monochromatic Al Kα (1486.6 eV) radiation. The electron-binding energies (E_B) are obtained without charge compensation. For quantitative analysis, the peaks are deconvoluted with Gaussian–Lorentzian curves and the peak area is divided by a sensitivity factor obtained from the element-specific Scofield factor and the transmission function of the spectrometer.

Autoclaves for carrying out reductive amination reactions

All catalytic experiments are performed in either a 100- or 300-mL autoclave by placing it into a pre-heated aluminum block (Fig. 10). ▲ CRITICAL To avoid unspecific reactions, all catalytic reactions are performed in either glass vials, which were placed inside the autoclave, or Teflon/glass vessel-fitted autoclaves.

Gas chromatography–mass spectrometry

Perform gas chromatography–mass spectrometry (GC-MS; instrument coupled to both GC and MS instruments used for the analysis of organic compounds) analyses with column temperature limits of −60 °C to 325 °C and helium as carrier gas. A representative method for monitoring the reaction is shown in the table below.

Time (min)	Temperature (°C)	Temperature ramp
0–2	40	
2–11	250	21 °C/min
11–19	250	

Gas chromatography

Perform gas chromatography (GC) analysis on a GC system with an FID and a 30 m × 0.320 mm × 0.25-μm column, with column temperature limits of −60 °C to 325 °C and hydrogen as carrier gas. A representative method for monitoring the reaction is as shown in the table below.

Time (min)	Temperature (°C)	Temperature ramp
0–2	80	
2–10	160	10 °C/min
10–19	300	14 °C/min
19–24	300	

NMR spectral analysis

^{1}H, ^{13}C NMR data are recorded on spectrometers using DMSO-d$_6$, CD$_3$OD and CDCl$_3$ solvents. Temperature should be ~25 °C (unless stated otherwise). Chemical shift reference (shifts are given relative to tetramethylsilane) normal is 7.27 (^{1}H) and 77.0 (^{13}C) for CDCl$_3$; 3.32 (^{1}H) and 49.0 (^{13}C)
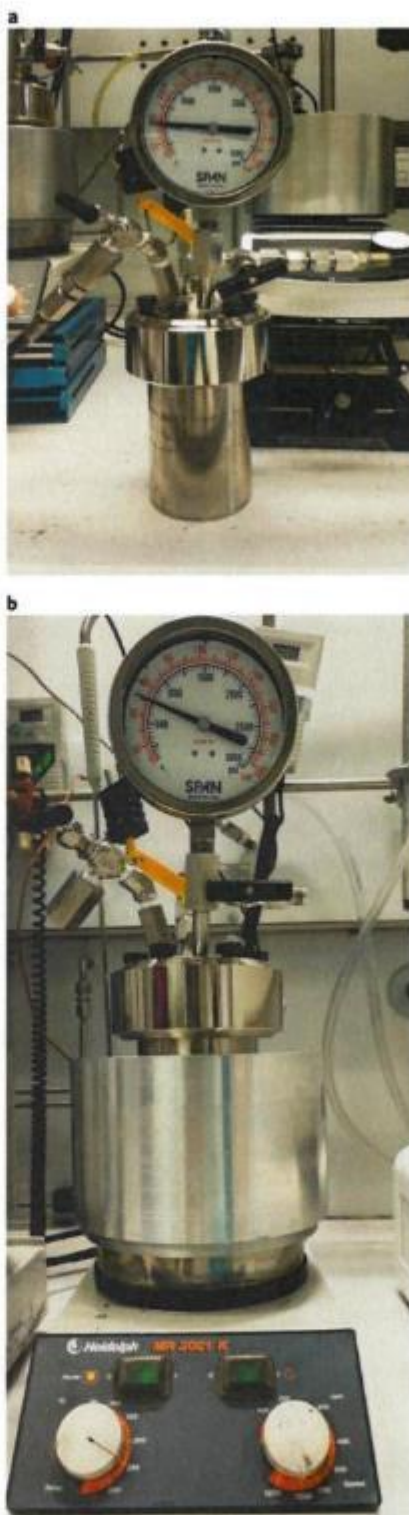
Fig. 10 | Equipment setup for reductive amination reactions. a, Pressurizing the autoclave. **b,** Autoclave placed into an aluminum block.

NATURE PROTOCOLS   **PROTOCOL**
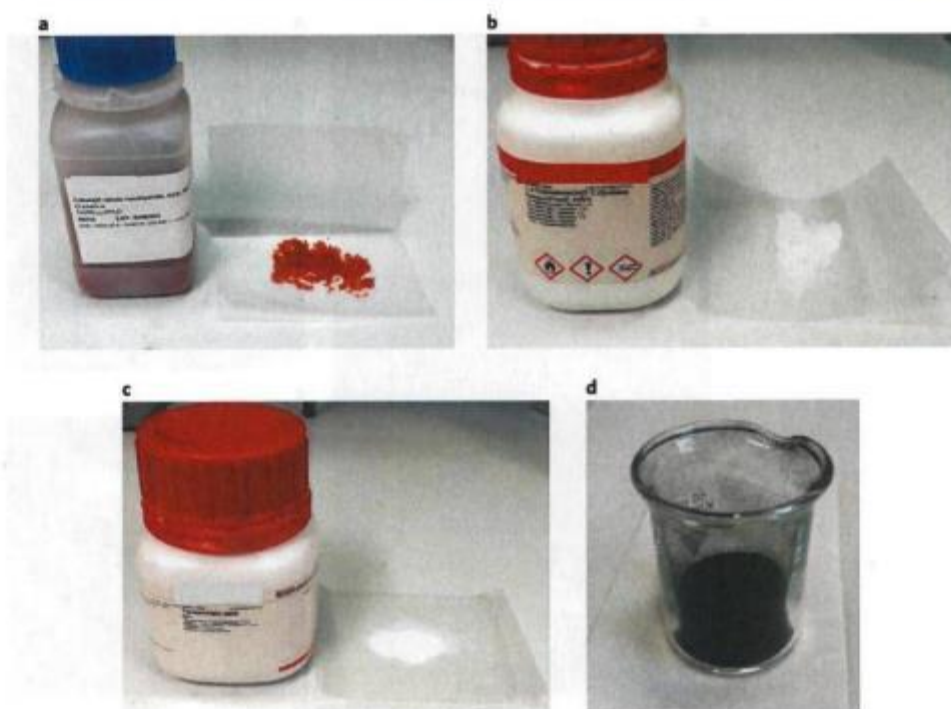
Fig. 11 | Starting materials for the preparation of Co/GS@C catalyst. a–d, Cobalt(II) nitrate hexahydrate (Co(NO₃)₂ 6H₂O; **a**); 1,4-diazabicyclo[2.2.2]octane (DABCO; **b**); TPA (**c**); Vulcan XC72R carbon powder (**d**).

for CD₃OD; 2.49 (¹H) and 39.5 (¹³C) for DMSO-d₆. NMR-MestReNova software is used to integrate the spectra.

HRMS spectral analysis
HRMS data were recorded on (i) an ESI-HRMS instrument and (ii) an EI-HRMS instrument, 70 eV.

Procedure

Catalyst preparation
▲ **CRITICAL** The catalyst preparation has been adapted for the different scales. All catalyst preparation steps (Steps 1–6) can be performed in air, except for the pyrolysis of the immobilized MOF on carbon (Step 8).

Wet impregnation of Vulcan XC72R carbon powder ● **Timing** 26 h
1 Calculate the appropriate weights of cobalt nitrate ((Co(NO₃)₂ · 6H₂O), DABCO, TPA and Vulcan XC72R carbon powder required for the preparation of 1 g, 3 g or 5 g of catalyst (see entries 1–3 in the table below; Figs. 11–15). See Fig. 11 for starting materials.

Entry	Co/Gs@C (g)	Co(NO₃)₂ · 6H₂O (g)	DABCO (g)	TPA (g)	Vulcan XC72R (g)	DMF (mL)
1	1	0.148	0.171	0.253	0.5	20
2	3	0.444	0.513	0.761	1.5	40
3	5	0.740	0.855	1.265	2.5	60

2 Use a 100-mL RB flask for a 5-g-scale catalyst preparation and charge with Co(NO₃)₂ · 6H₂O and DABCO. For small-scale reactions, use smaller flasks as appropriate (50 mL).
? TROUBLESHOOTING
3 Add the appropriate amount of DMF (20 mL). Stir the mixture for 2–3 min at room temperature (25 °C), which leads to a dark blue solution. Set the speed of stirring to ~750 r.p.m.
? TROUBLESHOOTING
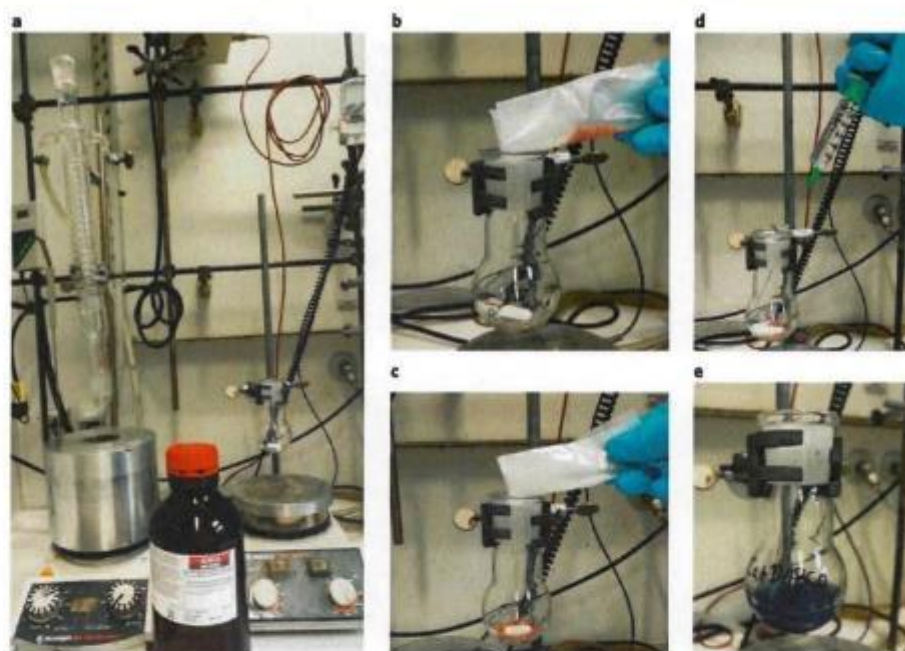
Fig. 12 | Addition of cobalt nitrate and DABCO in DMF. a–e, Reaction setup (**a**); addition of Cobalt(II) nitrate hexahydrate (Co(NO$_3$)$_2$ · 6H$_2$O; **b**); addition of 1,4-diazabicyclo[2.2.2]octane (DABCO) to cobalt(II) nitrate hexahydrate (**c**); addition of DMF to the mixture of cobalt(II) nitrate and DABCO (**d**); after 2–3 min of stirring the mixture of cobalt(II) nitrate and DABCO in DMF (**e**).

4　Add the solution of TPA in hot DMF (15 mL) to the dark blue solution obtained in Step 3. The dark blue solution should turn into a solution with a light-blue precipitate. Then place the RB flask containing the reaction mixture into an aluminum block preheated to 150 °C and stir the mixture for 20–30 min with a fixed reflux condenser. The color of the solution should change to the pale green of the Co-DABO-TPA MOF after 20 min. Keep the stirring speed at ~750 r.p.m.
? TROUBLESHOOTING

5　Slowly add the appropriate amount of Vulcan XC72R carbon black powder to the solution, followed by addition of DMF (10 mL), and stir the suspension at 150 °C for 4 h. Keep the stirring speed at ~750 r.p.m.
▲ **CRITICAL STEP** Vulcan XC72R carbon black is a fine powder and should be handled carefully while wearing protective clothes and with local exhaust ventilation. Note, the ratio of cobalt to linkers should be 1:3:3 (Co(NO$_3$)$_2$ · 6H$_2$O/DABCO/TPA). TPA dissolves only in hot DMF.

6　Remove the reflux condenser and allow the RB flask containing the reaction products to stand without stirring or closing for 20 h at 150 °C in order to slowly evaporate the DMF and to grow the Co-MOF template on the carbon.
▲ **CRITICAL STEP** After the evaporation of the solvent and ensuring that the material is completely dry, the material should be cooled to room temperature and ground to obtain a fine powder.

Heat treatment of the Co-MOF template on carbon ● **Timing 8 h**

7　Grind the dried material isolated in Step 6 into a fine powder and transfer it to a suitable crucible with a lid (Fig. 16).

8　Place the crucible in the chamber of the oven (Fig. 9) and pyrolyze the material at 800 °C for 2 h under an argon atmosphere (Equipment setup). The average percentage mass loss of the catalyst after pyrolysis was found to be ~50 %.
▲ **CRITICAL STEP** After the pyrolysis, the catalytic material should be cooled to room temperature in the closed chamber.
■ **PAUSE POINT** The obtained material can be stored for at least 4 months in closed glass vials at room temperature without taking any special precautions.

Fig. 13 | Preparation of TPA solution in DMF. a–e, Addition of TPA to the other RB flask (**a**); addition of DMF to TPA in RB flask (**b**); after addition of DMF to TPA at room temperature (**c**); placing the undissolved TPA in the aluminum block for heating at 150 °C for 5 min with stirring (**d**); TPA solution after 5 min of heating at 150 °C (**e**).

Catalyst characterization ● Timing variable

9   Characterize the material by STEM, EDXS, EELS, XPS, and XRD spectral analysis. Refer to the Materials section for setup of the TEM, XPS and XRD equipment. For TEM, deposit the samples on a holey carbon-supported Cu grid (mesh 300) without any pretreatment, and transfer it to the microscope.

10   Before using the material, check that the spectra are similar to those shown in the Supplementary Information (see also Table 1).

Amination reactions

11   The prepared catalyst can be used for reductive amination reactions (Fig. 17). Procedures for each reaction type are described in options A–E. Options A and B are used to prepare (3,4,5-trimethoxyphenyl)methanamine and 4-(3-aminobutyl)phenol, respectively. Option C is for reductive amination of nitro compounds and aldehydes, such as the synthesis of 3-chloro-*N*-((2,3-dihydrobenzo[b][1,4]dioxin-6-yl)methyl)-4-fluoroaniline. Options D and E are for the synthesis of tertiary amines. Option D is for reductive amination of carbonyl compounds and dimethyl amine to prepare, for example, *N,N*-dimethyl-1-(4-(phenoxymethyl)phenyl)methanamine. Option E is for reductive amination of nitro compounds with formaldehyde solution, for example, for the preparation of 4-(dimethylamino)-*N*-propylbenzamide.

(A) **Synthesis of (3,4,5-trimethoxyphenyl)methanamine hydrochloride ● Timing 15 h**

     (i)   Prepare the glass vial with a magnetic stir bar (Fig. 17a) and add 3 mL of *t*-buOH as solvent.

     (ii)   Add 98.1 mg of 3,4,5-trimethoxybenzaldehyde (0.5 mmol) to the prepared glass vial.

     (iii)   Weigh carefully 25 mg of the cobalt-based catalyst (3.5 mol%) prepared in Step 8 and add it to the reaction mixture. Fit the prepared vial with septum, cap and needle and place it in an aluminum plate inside a 300-mL autoclave (Fig. 17b).

PROTOCOL
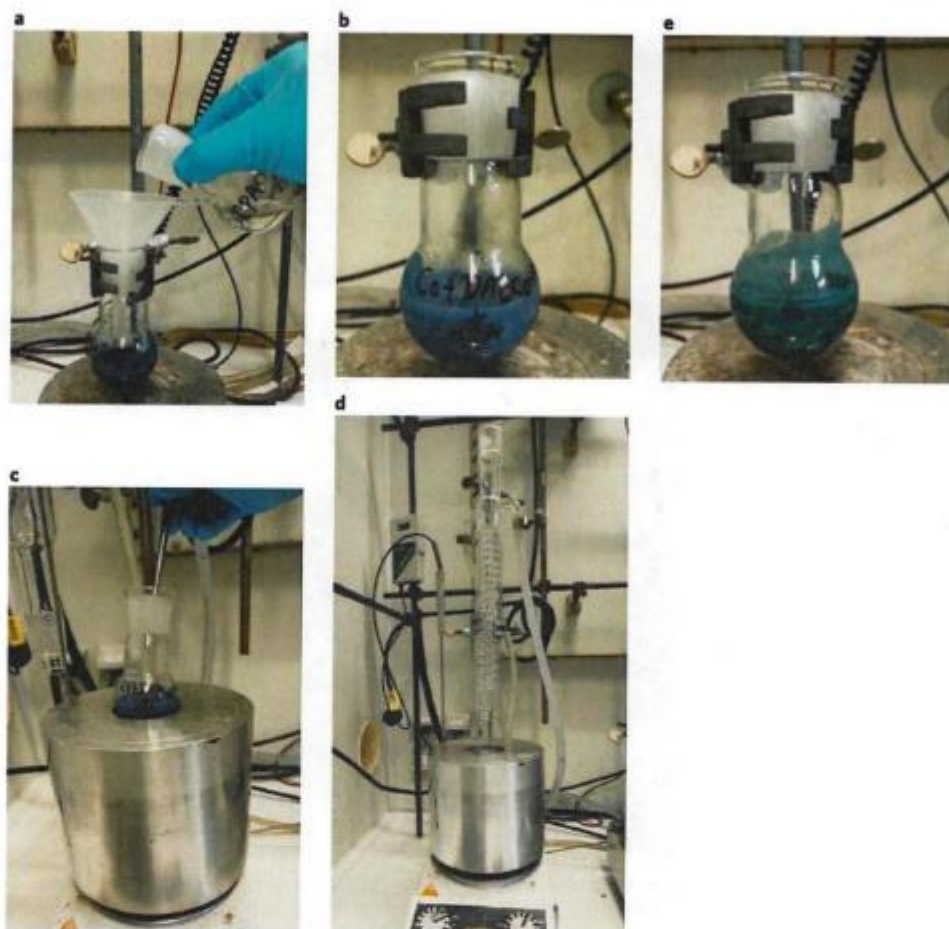
Fig. 14 | Preparation of Co-DABCO-TPA MOF. a–e, Addition of TPA solution to cobalt nitrate+DABCO mixture in DMF (**a**); color of the reaction mixture after addition of TPA solution to cobalt nitrate+DABCO mixture in DMF (**b**); placement of the reaction mixture in the aluminum block (**c**); fixation with reflux condenser and stirring at 150 °C (**d**); color of the reaction mixture after 30 min of stirring at 150 °C (**e**).

(iv) To evacuate the air, flush the autoclave with 40 bar hydrogen gas twice. Then, pressurize the autoclave with 5–7 bar ammonia gas and 40 bar hydrogen (Fig. 17b).

(v) Pre heat the aluminum block to 130 °C. Place the autoclave into the preheated aluminum block. Stir the reaction for 15 h, setting the speed of stirrer to 750 r.p.m. (Fig. 17b).

▲ **CRITICAL STEP** The temperature inside the autoclave and at the aluminum block might vary depending on the autoclave. To avoid this difference, the temperature of the aluminum block (heating system) should be verified and set to obtain the exact reaction temperature inside the autoclave. The temperature measured inside the autoclave is considered to be the reaction temperature. In our case, we observed 10 °C temperature differences between the aluminum block and inside the autoclave. For this reason, the temperature of the aluminum block is set to 130 °C (10 °C higher than the reaction temperature). When charging the autoclave with ammonia and hydrogen, ammonia should be pressurized first and then hydrogen.

(vi) After completion of the reaction, cool the autoclave to room temperature. Discharge the remaining hydrogen and ammonia and then remove the samples from the autoclave.

▲ **CRITICAL STEP** The reaction times differ between substrates (Fig. 3). Work up the sample using a Pasteur pipette with cotton stopper, filter off the catalyst from the reaction solution through a short plug of silica gel (~3 cm), and rinse it with 4 mL of ethyl acetate

(vii) For each reaction with a different kind of substrate (Fig. 3), monitor the progress of the reaction by GC-MS. To identify the desired product, take an aliquot (100 μl) of the filtrate and perform GC-MS as described in the 'Equipment setup' section.

Fig. 15 | Impregnation of Co-DABCO-TPA MOF on carbon. a-c, Addition of Vulcan XC72R carbon black support (**a**); after addition of Vulcan XC72R carbon powder support (**b**); after 20 h of drying by slow solvothermal process (**c**).

(viii) For quantitative analysis of products by GC, add hexadecane (100 μl) as a standard to the filtrate containing the reaction products. Take an aliquot (200 μl) of this filtrate for GC analysis with the calibrated method of the substrate and the product according to the instructions in the 'Equipment setup' section.

(ix) After completion of the reaction, cool the autoclave to room temperature. Discharge the remaining hydrogen and ammonia and then remove samples from the autoclave.

▲ CRITICAL STEP It should be noted that the reaction times differ between substrates (Fig. 3). Work up the sample using a Pasteur pipette with a cotton stopper, filter off the catalyst from the reaction solution through a short plug of silica gel (~3 cm) and rinse it with 4 mL of ethyl acetate.

(x) *Purification*. After completion of the autoclave reaction, remove the sample from the autoclave. Separate the catalyst from the solution using a 30-mL Buchner filter funnel with an embedded silica filter (pore size 3 or 4). Wash the catalyst along with the filter funnel, using ethyl acetate (3 × 5 mL).

(xi) Collect all the filtrate fractions and concentrate the solution under reduced pressure (at 240 mbar for 15 min, then further reduced to 10 mbar for 10 min), using a rotary evaporator at a temperature of 40 °C.

(xii) Purify the crude product by flash column chromatography. Use a silica gel column with the following size: length, 200 mm; inner diameter, 15 mm; and volume, 35 mL. As eluent, use a mixture of ethyl acetate and hexane (1:10 ethyl acetate/hexane progressively brought to 1:5 ethyl acetate/hexane).

(xiii) Collect the fractions of the pure product into a beaker, stir with anhydrous Na_2SO_4 for 5 min, and filter it off using a Buchner funnel.

(xiv) Remove the solvent from the filtrate under reduced pressure, using a rotary evaporator at a temperature of 40 °C, and dry the obtained product in vacuo.

(xv) Convert amines into their respective hydrochloride salts. To obtain the corresponding salts, add 1–2 mL of methanolic HCl or dioxane HCl (0.5 M HCl in methanol or 4 N HCl in dioxane) to the ether solution of the respective amine and stir the mixture at room temperature for 4–5 h. Then remove the solvent and dry the resulting hydrochloride salt of amine under vacuum.

PROTOCOL
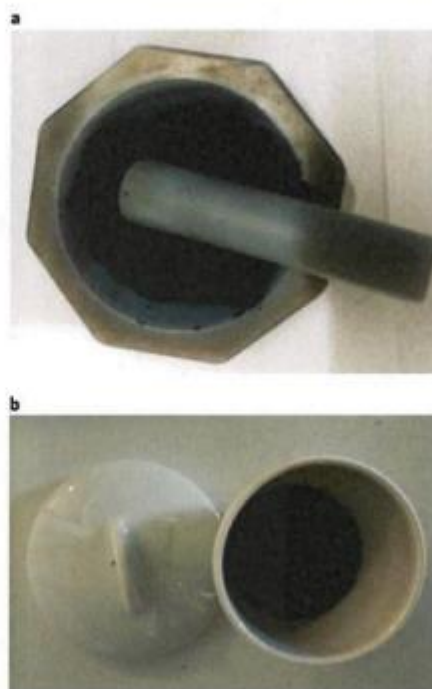
Fig. 16 | Grinding of the dried catalyst and pyrolysis. a,b, Grinding of the dried catalyst Co-DABCO-TPA solid material (**a**); used crucible with lid after pyrolysis (**b**).

(xvi) Analyze the structure and purity of the product by GC-MS, HRMS and NMR spectral analysis.
? TROUBLESHOOTING

(B) **Synthesis of 4-(3-aminobutyl)phenol hydrochloride** ● **Timing** 15 h
▲ **CRITICAL** The reaction described here is at a 0.5-mmol scale. This reaction can be scaled up to a 20-g scale. Refer to Box 2 for a detailed procedure for doing this.

(i) Prepare the glass vial with a magnetic stir bar (Fig. 17a) and add 3 mL of dry THF.
? TROUBLESHOOTING

(ii) Add 82.1 mg of 4-(4-hydroxyphenyl)butan-2-one (0.5 mmol) to the prepared glass vial.

(iii) Weigh carefully 25 mg of the cobalt-based catalyst (3.5 mol%) prepared in Step 8 and add it to the glass vial containing the reaction mixture. Fit the prepared vial with septum, cap and needle and place it into an aluminum plate inside a 300-mL autoclave (Fig. 17b).

(iv) Perform the reaction in an autoclave as described in Step 11A (iv–xiii) to obtain 4-(3-aminobutyl)phenol hydrochloride.

(v) Analyze the structure and purity of the product by GC, GC-MS, HRMS and NMR spectral analysis.
? TROUBLESHOOTING

(C) **Reductive amination of 2,3-dihydrobenzo[b][1,4]dioxine-6-carbaldehyde with 2-chloro-1-fluoro-4-nitrobenzene** ● **Timing** 24 h

(i) Place a magnetic stir bar in an 8-mL reaction vial and add 3 mL of t-buOH solvent (Fig. 17).

(ii) Add 87.7 mg of 2-chloro-1-fluoro-4-nitrobenzene (1.0 equiv.) and 82.1 mg of 2,3-dihydrobenzo[b][1,4]dioxine-6-carbaldehyde (1.5 equiv.) to the glass vial.

(iii) Add 25 mg of the cobalt-based catalyst (3.5 mol%) prepared in Step 8 and 20 mg of Amberlite IR-120 to the glass vial containing the reaction mixture.
? TROUBLESHOOTING

(iv) Flush the autoclave with hydrogen at 40 bar pressure twice and pressurize it with hydrogen to 40 bar.
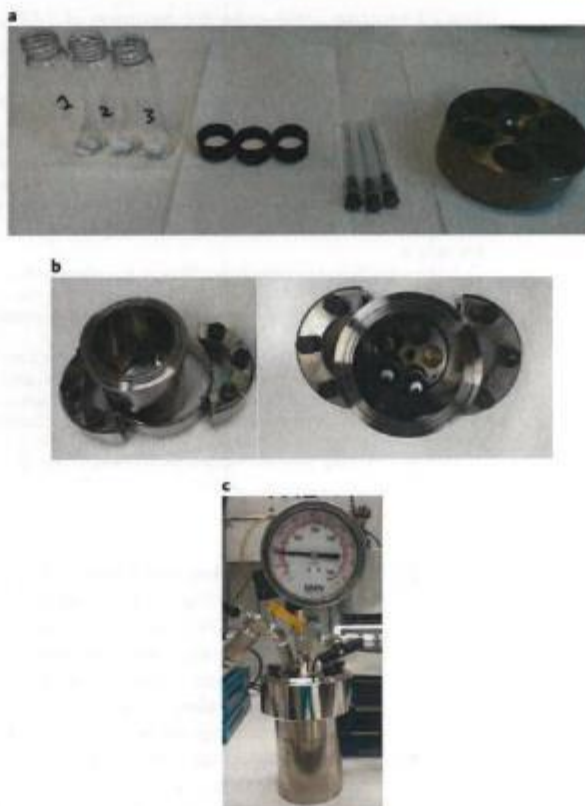
Fig. 17 | Glass reaction vials and autoclave setup. a–c, Glass vials with magnetic stir bars, caps with septa, needles and aluminum plate for placing vials (**a**); 300-mL autoclave (left) and autoclave with prepared reaction vials (right; **b**); pressurized autoclave (**c**).

(v) Place the autoclave into an aluminum block preheated to 130 °C and stir the reaction mixture for 24 h at 130 °C (Fig. 17a). Set the stirring rate to 650–700 r.p.m.

▲ **CRITICAL STEP** The temperature of the aluminum block (heating system) should be verified by a temperature sensor to obtain the required reaction temperature. While heating up the reaction system, a temperature gradient between the aluminum block and the reaction vial inside the autoclave occurs. Preheat the autoclave for 30 min in order to achieve the desired reaction temperature before starting to count the reaction time.

(vi) Implement Step 11A(vi–xii) to obtain the pure product of 3-chloro-N-((2,3-dihydrobenzo[b] [1,4]dioxin-6-yl)methyl)-4-fluoroaniline as an oil. For the chromatographic purification of the desired product, use a silica gel column with the following size: length, 200 mm; inner diameter, 15 mm; and volume, 35 mL. As eluent, use a mixture of ethyl acetate and hexane (100% hexane progressively brought to 1:1 ethyl acetate/hexane).

(vii) Analyze the structure and purity of the product by GCMS, HRMS and NMR spectral analysis.

(D) **Synthesis of N-methylamines: reaction between 4-(phenoxymethyl)benzaldehyde and dimethylamine ● Timing 24 h)**

(i) Place a magnetic stir bar in an 8-mL reaction vial and add 3 mL of t-buOH solvent (Fig. 17).

(ii) Add 100 μL of aqueous dimethylamine (40 wt% in H_2O) and 111.2 mg of 4-(phenoxymethyl) benzaldehyde to the glass vial.

(iii) Add 25 mg of the cobalt-based catalyst (3.5 mol%) prepared in Step 8 to the glass vial containing the reaction mixture.

(iv) Flush the autoclave with hydrogen at 40-bar pressure twice and pressurize it with hydrogen to 40 bar.

PROTOCOL   **NATURE PROTOCOLS**

Box 2 | Reaction scale-up for the synthesis of 4-(3-aminobutyl)phenol hydrochloride ● Timing 15 h

The reaction described in the Procedure is scaled up to 20 g. This scaled-up method generates 17.6 g of product (4-(3-aminobutyl)phenol) hydrochloride. In scaling up any of these reactions, the steps below need to be optimized.
For other upscaling reactions (5- to 20-g scale), the amounts of catalyst and solvent need to be altered. An amount of catalyst equivalent to 3.5 mol% and an amount of solvent equivalent to 10 mL for 1 g of substrate. Other parameters, such as reaction time, temperature, and pressure of hydrogen and ammonia, are applied in a manner similar to that used for small-scale reactions (0.5. mmol).

Procedure
1 Charge the Teflon or glass fitted 300-mL autoclave with a magnetic stir bar and 150 mL of THF solvent. Then add 20 g of 4-(4-hydroxyphenyl)butan-2-one (121.8 mmol).
2 Weigh 3.6 g (3.5 mol%) of the cobalt-based catalyst prepared in Step 8 of the main Procedure and add it to the autoclave.
3 Perform the reaction in an autoclave as described in Step 11A(iv–vi).
4 After completion of the reaction, let the autoclave cool to room temperature. Discharge the remaining ammonia and hydrogen and remove the reaction solution from the autoclave.
5 For purification, implement Step 11A(viii–xii). For purification, use a silica gel column with the following size: length, 1,000 mm; inner diameter, 75 mm; and volume, 200 mL. As eluent, use a mixture of ethyl acetate and hexane (1:10 ethyl acetate/hexane progressively brought to 1:5 ethyl acetate/hexane).

(v) Place the autoclave into an aluminum block preheated to 130 °C and stir the reaction mixture for 24 h at 130 °C (Fig. 17a). Set the stirring rate to 650–700 r.p.m.
▲ CRITICAL STEP The temperature of the aluminum block (heating system) should be verified by a temperature sensor to obtain the required reaction temperature. While heating up the reaction system, a temperature gradient between the aluminum block and the reaction vial inside the autoclave occurs. Preheat the autoclave for 30 min in order to achieve the desired reaction temperature before starting to count the reaction time.

(vi) Implement Step 11A(vi–xii) to obtain the pure product N,N-dimethyl-1-(4-(phenoxymethyl) phenyl)methanamine as a yellow gum. For the chromatographic purification of the desired product, use a silica gel column with the following size: length, 200 mm; inner diameter, 15 mm; and volume, 35 mL. As eluent, use a mixture of ethyl acetate and hexane (100% hexane progressively brought to 1:1 ethyl acetate/hexane).

(vii) Analyze the structure and purity of the product by GCMS, HRMS and NMR spectral analysis.

(E) **Synthesis of N-methylamines: reaction between 4-nitro-N-propylbenzamide and aqueous formaldehyde ● Timing 24 h**

(i) Charge an 8-mL glass vial with a magnetic stir bar and add 3 mL of a THF–H₂O (1:1) solvent mixture (Fig. 17).

(ii) Add 100 µL of aqueous formaldehyde (37% in water, stabilized with ~10% methanol), and 104.1 mg of 4-nitro-N-propylbenzamide to the glass vial.

(iii) Add 25 mg of the cobalt-based catalyst (3.5 mol%) prepared in Step 8 to the solution.

(iv) Flush the autoclave with hydrogen at 40-bar pressure twice and pressurize it with hydrogen to 40 bar.

(v) Place the autoclave into an aluminum block preheated to 130 °C and stir the reaction mixture for 24 h at 130 °C (Fig. 17a). Set the stirring rate to 650–700 r.p.m.
▲ CRITICAL STEP The temperature of the aluminum block (heating system) should be verified by a temperature sensor to obtain the required reaction temperature. While heating up the reaction system, a temperature gradient between the aluminum block and the reaction vial inside the autoclave occurs. Preheat the autoclave for 30 min in order to achieve the desired reaction temperature before starting to count the reaction time.

(vi) Implement Step 11A(vi–xii) to obtain the pure product 4-(dimethylamino)-N-propylbenzamide as brown solid. For the chromatographic purification of the desired product, use a silica gel column with the following size: length, 200 mm; inner diameter, 15 mm; and volume, 35 mL. As eluent, use a mixture of ethyl acetate and hexane (100% hexane progressively brought to 1:1 ethyl acetate/hexane).

(vii) Analyze the structure and purity of the product by GCMS, HRMS and NMR spectral analysis.

NATURE PROTOCOLS   **PROTOCOL**

Troubleshooting

Troubleshooting advice can be found in Table 4.

Table 4 | Troubleshooting table

Step	Problem	Possible reason	Solution
2–4	The catalytic activity is lower than expected	Dissolving of both linkers and cobalt nitrate together or dissolving of TPA and cobalt nitrate together.	DABCO and cobalt nitrate should be dissolved in DMF first. Next, TPA that has already been dissolved in DMF should be added.
11A(xvi), 11B(v)	NH₂ peak in ¹H NMR observed	It is possible that the NH₂ peak merged with the residual solvent–water peak in DMSO	Convert amines into HCl salts and measure NMR in DMSO
11B(i)	The yield of the product is lower than expected	If an old bottle of THF was used, water might be present in the THF	Use fresh and dry THF
11C(iii)	The yield of the product is lower than expected	Less effective formation of the secondary imine	The Amberlite IR-120 is needed as an additive to form the corresponding imine effectively

Timing

Catalyst preparation

Steps 1–6, wet impregnation of Vulcan XC72R black carbon powder: 26 h

Step 7 and 8, heat treatment of the adsorbed Co-DABCO-TPA MOF on carbon: 8 h

Steps 9 and 10, catalyst characterization: variable

Amination reactions

Step 11A, synthesis of (3,4,5-trimethoxyphenyl)methanamine hydrochloride: 15 h

Step 11B, synthesis of 4-(3-aminobutyl)phenol hydrochloride: 15 h

Step 11C, reductive amination of 2,3-dihydrobenzo[b][1,4]dioxine-6-carbaldehyde with 2-chloro-1-fluoro-4-nitrobenzene: 24 h

Step 11D, synthesis of *N*-methylamines: reaction between 4-(phenoxymethyl)benzaldehyde and dimethylamine: 24 h

Step 11E, synthesis of *N*-methylamines: reaction between 4-nitro-*N*-propylbenzamide and aqueous formaldehyde: 24 h

Box 1, catalyst-recycling experiments with 4-(4-hydroxyphenyl)butan-2-one: 15 h

Box 2, reaction scale-up for the synthesis of 4-(3-aminobutyl)phenol hydrochloride: 15 h

Anticipated results

Co-DABCO-TPA@C-800 catalyst

TEM analysis and data

Aberration-corrected STEM analysis of the most active material (Co-DABCO-TPA@C-800; Co/GS@C) shows the formation of mainly metallic cobalt particles with diameter ranging from <5 nm to 30 nm (Fig. 2 and Supplementary Fig. 1). The EDXS (Supplementary Fig. 1a, left) shows mainly the presence of metallic Co particles within the carbon matrix. Most of these particles are surrounded by a combination of some graphitic layers and short-range ordered graphitic shells (Supplementary Fig. 1a, middle). In addition, a smaller quantity of core–shell particles with cobalt oxide shells at metallic Co is also present (Supplementary Fig. 2a). In regions of short-range ordered carbon, we detected single Co atoms as bright dots in HAADF images (Supplementary Fig. 1a, right).

To get information on the cobalt–carbon–nitrogen relation, the parallel mapping of EDXS for all elements and EELS (Supplementary Fig. 1b) optimized for carbon, nitrogen and oxygen were performed. Because the nitrogen signal is superimposed on the carbon signal in EDXS, these maps were used only for the Co distribution. Figure 2b shows the maps of C, N and Co (left image) in the neighborhood of a metallic particle wrapped by graphitic carbon. The C–N overlay in the HAADF image (middle image) gives evidence that nitrogen is located not only in the graphitic shell on the Co particle but surprisingly also in short-range ordered carbon, which is not part of the graphitic shell and corresponds to features with single atoms shown in Supplementary Fig. 1a. Co traces are

detectable everywhere in the nitrogen-containing carbon at low concentrations. By contrast, the less active material, Co-DABCO@C-800, contained mainly hollow cobalt oxide (Co_3O_4) particles (Supplementary Fig. 2b). In addition to Co_3O_4, some Co–Co_3O_4 core–shell particles were also present. Although sub-nanometer Co structures were found in this material, no single Co atoms were detected. Similarly, Co-TPA@C-800 (Supplementary Fig. 2c) also contained mainly cobalt oxide (Co_3O_4) particles encapsulated within graphitic shells, along with a small quantity of metallic cobalt in Co–Co_3O_4 core–shell structures. No single Co atoms or sub-nanometer Co structures were detected in this material. Cobalt nitrate@C-800, which was completely inactive, contained hollow Co_3O_4 with short-range ordered carbon from the support in the vicinity (Supplementary Fig. 2d). To understand the formation mechanism of the active catalyst, materials pyrolyzed at lower temperatures were also characterized (Supplementary Fig. 3). In Co-DABCO-TPA@C-400, a minor amount of metallic cobalt was present in the core of cobalt–cobalt oxide core–shell structures, and no formation of graphitic shells was observed. Co-DABCO-TPA@C-600 contained more metallic cobalt, and incipient formation of graphitic shells enveloping the metallic Co was evident. Apparently, this structural process is critical to high activity and stability. For the most active Co-DABCO-TPA@C-800, single Co atoms within some of the graphitic structures were detected. In the case of Co-DABCO-TPA@C-1000, most of the Co was present in metallic crystallite morphology completely covered by graphitic structures. In all the active catalysts, cloudy regions of cobalt species in the 1- to 2-nm range were detected.

XRD analysis and data

The different phases of cobalt in both active and less active catalysts have been also confirmed by XRD data (Supplementary Figs. 7 and 8) that accorded with the TEM analysis.

XPS analysis and data

The nature and quantity of nitrogen in these materials were further explored by XPS (Supplementary Figs. 10 and 11). Surprisingly, the combination of the two linkers increased the quantity of nitrogen in the near-surface region compared to either linker alone (Supplementary Fig. 12). The N content in Co-DABCO-TPA@C-800 was three times higher than in Co-DABCO@C-800, whereas in Co-TPA@C-800, only traces of N were observed. In both Co-DABCO-TPA@C-800 and Co-DABCO@C-800, two N-states could be detected (Supplementary Fig. 10): one correlating with imine-like N known from pyridine (~398 eV)[41,42] and the other manifesting a higher binding energy, corresponding to N bonded to the metal. For the former sample a clear separation of the two peaks was observed due to the slightly higher binding energy. For Co-DABCO-TPA@C pyrolyzed at different temperatures, iminic N was observed, and the binding energy of the Co–N bond increased as pyrolysis temperature ascended to 800 °C (Supplementary Fig. 10). In comparison to all other samples, the observation of the two N states was unique to these active systems (Supplementary Fig. 11)[41,42]. It seems that for the optimal catalyst, the bonding between Co and N is most pronounced. In the material pyrolyzed at 1,000 °C, the formation of nitrides could be observed as well (Supplementary Fig. 11). In the un-pyrolyzed and 1,000 °C samples, the amount of Co in the near-surface region was too low for a reasonable peak fitting; for all other samples, the metal content was nearly the same.

(3,4,5-Trimethoxyphenyl)methanamine hydrochloride

Column chromatography on silica gel (method: 10% ethyl acetate/hexane—60% ethyl acetate/hexane; Fig. 15) yielded the free amine, which is further converted into the corresponding hydrochloride salt to obtain the title compound in solid form (88%, 173.5 mg). ^{1}H NMR (300 MHz, rt, DMSO-d_6) δ_H = 8.69 (br s, 3H, NH_2·HCl), 6.98 (s, 2H, 2x CH), 3.95 (s, 2H, CH_2), 3.78 (s, 6H, 2x OCH_3), 3.65 (s, 3H, OCH_3). ^{13}C NMR (75 MHz, rt, DMSO-d_6) δ_C = 153.25 (2x C), 137.72 (C), 130.12 (C), 107.07 (2x CH), 60.48(OCH_3), 56.50 (2x OCH_3), 42.86 (CH_2) p.p.m. HRMS (EI): calcd. for $C_{10}H_{15}O_3N_1$ [M]+ 197.1046; found 197.1042. White solid.

4-(3-Aminobutyl)phenol hydrochloride

Column chromatography on silica gel (method: 10% ethyl acetate/hexane—60% ethyl acetate/hexane; Fig. 18) yielded the free amine, which is further converted into the corresponding hydrochloride salt to get the title compound in solid form (89%, 146.8 mg). ^{1}H NMR (300 MHz, rt, DMSO-d_6) δ_H = 9.14 (br s, 1H, OH), 8.40 – 8.03 (br s, 3H, NH_2·HCl), 6.98 (d, J = 8.4 Hz, 2H, 2x CH),
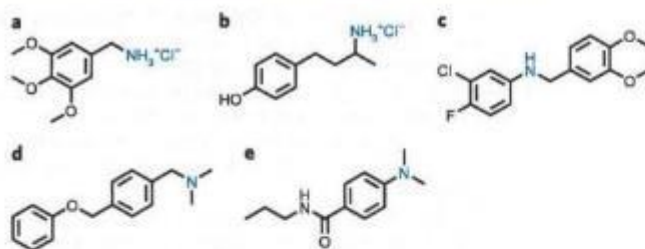
PROTOCOL

Fig. 18 | Structures of selected amines prepared in Step 11A–E. a–e, (3,4,5-trimethoxyphenyl)methanamine hydrochloride (Step 11A; **a**); 4-(3-aminobutyl)phenol hydrochloride (Step 11B; **b**); 3-chloro-N-((2,3-dihydrobenzo[b] [1,4]dioxin-6-yl)methyl)-4-fluoroaniline (Step 11C; **c**); N,N-dimethyl-1-(4-(phenoxymethyl)phenyl)methanamine (Step 11D; **d**); A4-(dimethylamino)-N-propylbenzamide (Step 11E; **e**).

6.71 (d, $J = 8.4$ Hz, 2H, 2x CH), 3.20 – 2.93 (m, 1H, CH), 2.68 – 2.35 (m, 2H, CH$_2$), 2.00 – 1.80 (m, 1H, CH), 1.77 – 1.56 (m, 1H, CH), 1.22 (d, $J = 6.5$ Hz, 3H, CH$_3$). ^{13}C NMR (75 MHz, rt, DMSO-d$_6$) $\delta_C = 155.52$ (C), 130.79 (C), 128.94 (2x CH), 115.14 (2x CH), 46.37 (CH), 36.10 (CH$_2$), 29.96 (CH$_2$), 17.94 (CH$_3$) p.p.m. Traces of dioxane solvent peaks were observed in NMR. HRMS (ESI-TOF, m/z): calcd. for C$_{10}$H$_{15}$NO [M+H]+ 166.1226; found 166.1226. Off white solid.

3-Chloro-N-((2,3-dihydrobenzo[b][1,4]dioxin-6-yl)methyl)-4-fluoroaniline

Column chromatography on silica gel (method: 0% ethyl acetate/hexane–40% ethyl acetate/hexane; Fig. 18) provided the title compound as colorless liquid (81%, 237.5 mg). ^{1}H NMR (300 MHz, rt, chloroform-d) $\delta_H = 6.79$ – 6.74 (m, 1H, CH), 6.71 – 6.68 (m, 1H, CH), 6.67 (d, $J = 0.4$ Hz, 1H, CH), 6.66 – 6.59 (m, 1H, CH), 6.42 (dd, $J = 6.1$, 2.9 Hz, 1H, CH), 6.24 (ddd, $J = 8.9$, 3.8, 2.9 Hz, 1H, CH), 4.05 (s, 4H, 2x CH$_2$), 3.95 (s, 2H, CH$_2$), 3.81 (br s, 1H, NH). ^{13}C NMR (75 MHz, rt, chloroform-d) $\delta_C = 150.90$ (d, $J = 237.3$ Hz, ipso C), 145.14 (d, $J = 2.1$ Hz, C), 143.73 (C), 142.94 (C), 131.99 (C), 120.99 (d, $J = 18.4$ Hz, C), 120.44 (CH), 117.49 (CH), 116.83 (d, $J = 21.9$ Hz, CH), 116.34 (CH), 113.76 (d, $J = 0.7$ Hz, CH), 112.08 (d, $J = 6.3$ Hz, CH), 64.40 (OCH$_2$), 64.35 (OCH$_2$), 47.99 (CH$_2$) p.p.m. HRMS (ESI-TOF, m/z): calcd. for C$_{15}$H$_{11}$ClFNO$_2$ [M+H]+ 292.0535; found 292.0529. Colorless liquid.

N,N-Dimethyl-1-(4-(phenoxymethyl)phenyl)methanamine

Column chromatography on silica gel (method: 10% ethyl acetate/hexane–50% ethyl acetate/hexane; Fig. 18) yielded the title compound in liquid form (86%, 207.7 mg). ^{1}H NMR (300 MHz, rt, chloroform-d) $\delta_H = 7.39$ – 7.19 (m, 5H, 5x CH), 7.13 (d, $J = 8.6$ Hz, 2H, 2x CH), 6.84 (d, $J = 8.6$ Hz, 2H, 2x CH), 4.94 (s, 2H, CH$_2$), 3.29 (s, 2H, CH$_2$), 2.14 (s, 6H, 2x CH$_3$). ^{13}C NMR (75 MHz, rt, chloroform-d) $\delta_C = 158.10$ (C), 137.11 (C), 130.75 (C), 130.45 (2x CH), 128.62 (2x CH), 127.98 (2x CH), 127.54 (CH), 114.65 (2x CH), 70.04 (CH$_2$), 63.62 (CH$_2$), 45.12 (2x CH$_2$) p.p.m. HRMS (EI): calcd. for C$_{16}$H$_{19}$O1N1 [M]+ 241.1461; found 241.1463. Yellow gum.

4-(Dimethylamino)-N-propylbenzamide

Column chromatography on silica gel (method: 10% ethyl acetate/hexane–70% ethyl acetate/hexane; Fig. 18) yielded the title compound in solid form (81%, 167.3 mg). ^{1}H NMR (300 MHz, rt, chloroform-d) $\delta_H = 7.61$ (d, $J = 8.9$ Hz, 2H, 2x CH), 6.57 (d, $J = 8.9$ Hz, 2H, 2x CH), 6.15 (br s, 1H, NH), 3.45 – 3.20 (m, 2H, CH$_2$), 2.92 (s, 6H, 2x CH$_3$), 1.73 – 1.40 (m, 2H, CH$_2$), 0.88 (t, $J = 7.4$ Hz, 3H, CH$_3$). ^{13}C NMR (75 MHz, rt, chloroform-d) $\delta_C = 167.49$ (CO), 152.32 (C), 128.33 (2x CH), 121.66 (C), 111.07 (2x CH), 41.59 (CH$_2$), 40.17 (2x CH$_3$), 23.13 (CH$_2$), 11.53 (CH$_3$) p.p.m. HRMS (EI): calcd. for C$_{12}$H$_{18}$O1N$_2$ [M]+ 206.1413; found 206.1415. Brown solid.

Reporting Summary

Further information on research design is available in the Nature Research Reporting Summary linked to this article.

References

1. Lawrence, S. A. *Amines: Synthesis, Properties and Applications* (Cambridge University Press, 2004).
2. Ricci, A. *Amino Group Chemistry: From Synthesis to the Life Sciences* (Wiley-VCH, 2008).

3. Smith, D. T., Delost, M. D., Qureshi, H. & Njarðarson, J. T. Top 200 pharmaceutical products by retail sales in 2016. https://njardarson.lab.arizona.edu/sites/njardarson.lab.arizona.edu/files/2016Top200Pharmaceutica lRetailSalesPosterLowResV3_0.pdf (2017).

4. Roughley, S. D. & Jordan, A. M. The medicinal chemist's toolbox: an analysis of reactions used in the pursuit of drug candidates. *J. Med. Chem.* **54**, 3451–3479 (2011).

5. Dewick, P. M. *Medicinal Natural Products: A Biosynthetic Approach* 3rd edn (John Wiley & Sons, 2008).

6. Yan, T., Feringa, B. L. & Barta, K. Direct N-alkylation of unprotected amino acids with alcohols. *Sci. Adv.* **3**, eaao6494 (2017).

7. Froidevaux, V., Negrell, C., Caillol, S., Pascault, J.-P. & Boutevin, B. Biobased amines: from synthesis to polymers; present and future. *Chem. Rev.* **116**, 14181–14224 (2016).

8. Gomez, S. A., Peters, J. A. & Maschmeyer, T. The reductive amination of aldehydes and ketones and the hydrogenation of nitriles: mechanistic aspects and selectivity control. *Adv. Synth. Catal.* **344**, 1037–1057 (2002).

9. Alinezhad, H., Yavari, H. & Salehian, F. Recent advances in reductive amination catalysis and its applications. *Curr. Org. Chem.* **19**, 1021–1049 (2015).

10. Wakchaure, V. N., Zhou, J., Hoffmann, S. & List, B. Catalytic asymmetric reductive amination of α-branched ketones. *Angew. Chem. Int. Ed.* **49**, 4612–4614 (2010).

11. Gallardo-Donaire, J. et al. Direct asymmetric ruthenium-catalyzed reductive amination of alkyl-aryl ketones with ammonia and hydrogen. *J. Am. Chem. Soc.* **140**, 355–361 (2018).

12. Kadyrov, R. & Riermeier, T. H. Highly enantioselective hydrogen-transfer reductive amination: catalytic asymmetric synthesis of primary amines. *Angew. Chem. Int. Ed.* **42**, 5472–5474 (2003).

13. Tax, X. et al. Asymmetric synthesis of chiral primary amines by ruthenium catalyzed direct reductive amination of alkyl aryl ketones with ammonium salts and molecular H₂. *J. Am. Chem. Soc.* **140**, 2024–2027 (2018).

14. Chusov, D. & List, B. Reductive amination without an external hydrogen source. *Angew. Chem. Int. Ed.* **53**, 5199–5201 (2014).

15. Ogo, S., Uehara, K., Abura, T. & Fukuzumi, S. pH-Dependent chemoselective synthesis of α-amino acids. Reductive amination of α-keto acids with ammonia catalyzed by acid-stable iridium hydride complexes in water. *J. Am. Chm. Soc.* **126**, 3020–3021 (2004).

16. Nakamura, Y., Kon, K., Touchy, A. S., Shimizu, K.-i & Ueda, W. Selective synthesis of primary amines by reductive amination of ketones with ammonia over supported Pt catalysts. *ChemCatChem* **7**, 921–924 (2015).

17. Gross, T., Seayad, A. M., Ahmad, M. & Beller, M. Synthesis of primary amines: first homogeneously catalyzed reductive amination with ammonia. *Org. Lett.* **4**, 2055–2058 (2002).

18. Gallardo-Donaire, J., Ernst, M., Trapp, O. & Schaub, T. Direct synthesis of primary amines via ruthenium-catalysed amination of ketones with ammonia and hydrogen. *Adv. Synth. Catal.* **358**, 358–363 (2016).

19. Liang, G. et al. Production of primary amines by reductive amination of biomass derived aldehydes/ketones. *Angew. Chem. Int. Ed.* **56**, 3050–3054 (2017).

20. Wang, Z. Mignonac reaction. in *Comprehensive Organic Name Reactions and Reagents* (John Wiley & Sons, 2010).

21. Mao, F. et al. Heterogeneous cobalt catalysts for reductive amination with H₂: general synthesis of secondary and tertiary amines. *RSC Adv.* **6**, 94068–94073 (2016).

22. Santoro, F., Psaro, R., Ravasio, N. & Zaccheria, F. Reductive amination of ketones or amination of alcohols over heterogeneous Cu catalysts: Matching the catalyst support with the N-alkylating agent. *ChemCatChem* **4**, 1249–1254 (2012).

23. Jagadeesh, R. V. et al. Hydrogenation using iron oxide–based nanocatalysts for the synthesis of amines. *Nat. Protoc.* **10**, 548–557 (2015).

24. Jagadeesh, R. V. et al. Cobalt-based nanocatalysts for green oxidation and hydrogenation processes. *Nat. Protoc.* **10**, 916–926 (2015).

25. Jagadeesh, R. V. et al. MOF-derived cobalt nanoparticles catalyze a general synthesis of amines. *Science* **358**, 326–332 (2017).

26. Hahn, G., Kunnas, P., de Jonge, N. & Kempe, R. General synthesis of primary amines via reductive amination employing a reusable nickel catalyst. *Nat. Catal.* **2**, 71–77 (2019).

27. Filipponi, L. & Sutherland, D.S. *Nanotechnologies: Principles, Applications, Implications and Hands-on Activities* (European Commission, European Union, 2012).

28. Polshettiwar, V. & Asefa, T. *Nanocatalysis: Synthesis and Applications* (John Wiley & Sons, 2013).

29. Sankar, M. et al. Designing bimetallic catalysts for a green and sustainable future. *Chem. Soc. Rev.* **41**, 8099–8139 (2012).

30. Manoj., B. G. et al. Core-shell nanoparticles: synthesis and applications in catalysis and electrocatalysis. *Chem. Soc. Rev.* **44**, 7540–7590 (2015).

31. Munnik, P., de Jong, P. E. & de Jong, K. P. Recent developments in the synthesis of supported catalysts. *Chem. Rev.* **115**, 6687–6718 (2015).

32. Tao, F. *Metal Nanoparticles for Catalysis: Advances and Applications* (Royal Society of Chemistry, 2014).

33. van Schrojenstein Lantman, E. M., Deckert-Gaudig, T., Mank, A. J. G., Deckert, V. & Weckhuysen, B. M. Catalytic processes monitored at the nanoscale with tip-enhanced Raman spectroscopy. *Nat. Nanotechnol.* **7**, 583–586 (2012).

ARTICLE

Catalytic reductive aminations using molecular hydrogen for synthesis of different kinds of amines

Kathiravan Murugesan,[a]† Thirusangumurugan Senthamarai,[a]† Vishwas G. Chandrashekhar,[a]† Kishore Natte, [a, b] Paul C. J. Kamer,[a] Matthias Beller*[a] and Rajenahally V. Jagadeesh*[a]

Reductive aminations constitute an important class of reactions widely applied in research laboratories and industries for the synthesis and functionalization of amines. In particular, catalytic reductive aminations using molecular hydrogen are highly valued and essential for the cost-effective and sustainable production of different kinds of amines. These reactions couple easily accessible carbonyl compounds (aldehydes or ketones) with ammonia, amines or nitro compounds in presence of suitable catalysts and hydrogen that enable the preparation of linear and branched primary, secondary and tertiary amines including N-methylamines and molecules related to life science applications. In general, amines represent valuable fine and bulk chemicals, which serve as key precursors and central intermediates for the synthesis of advanced chemicals, life science molecules, dyes and polymers. Noteworthy, amine functionalities are presented in large number of pharmaceuticals, agrochemicals and biomolecules, and play vital roles in the function of these active compounds. In general, reductive aminations are challenging processes, especially for the syntheses of primary amines, which often are non-selective and suffer from over-alkylation and reduction of carbonyl compounds to the corresponding alcohols. Hence, the development of suitable catalysts to achieve these reactions in highly efficient and selective manner is crucial and continues to be important and attracts scientific interest. In this regard, both homogeneous and heterogeneous catalysts have successfully been developed for these reactions to access various amines. Although number of articles has been published on catalytic reductive aminations, there is a lack of in-depth reviews on this topic. Hence, there is a need of comprehensive review on catalytic reductive aminations to discuss in detail about potential catalysts used and applicability of this methodology for the preparation of different kinds of amines, which are of commercial, industrial and medicinal importance. Consequently, in this review we broadly discuss the development of different transitions metal catalysts for reductive aminations and their applications in the synthesis of functionalized and structurally diverse benzylic, heterocyclic and aliphatic primary, secondary and tertiary amines as well as N- methylamines and more complex drug targets. In addition, mechanisms of reductive aminations including selective formation of desired amine-products as well as possible side reactions are discussed. This review aims at the scientific communities working in the area of organic synthesis, catalysis, medicinal and biological chemistry.

1. Introduction

Amines represent highly privileged chemicals extensively applied in different science areas such as chemistry, biology, medicine, energy, materials and environment (Fig. 1).[1-33] These important compounds serve both as fine and bulk chemicals as well as key precursors and central intermediates for the synthesis of advanced chemicals, pharmaceuticals, biomolecules, agrochemicals and polymers.[1-6] Notably, amine functionalities are presented in majority of drugs and biomolecules, and hence they constitute as integral parts of these life science molecules (Figure 2).[1-6] As an example, >80% of the top

200 selling drugs of 2018 contained amine and/or nitrogen moieties, which play significant roles in their activities.[3] Moreover, amines are involved in the creation of proteins, enzymes, nucleic acids and hormones in living beings (Fig. 2).[1-6] For the synthesis and functionalization of amines, catalytic reductive aminations represent convenient and common methodologies widely applied in both research laboratories and industries.[7-33]

In this amination process, carbonyl compounds such as ketones and aldehydes react with ammonia or amines using suitable catalysts in presence of molecular hydrogen or stoichiometric reducing agents.[7-16] Regarding potential reducing agents, molecular hydrogen is highly preferred because this regent is abundant, inexpensive, and atom-economical well as produces only water as the by-product.[34, 35] Hence, catalytic hydrogenations provide an important synthetic tool box in

7. Curriculum Vitae

Thirusangumurugan Senthamarai ganapathy

Leibniz Institute for Catalysis (LIKAT) in University of Rostock,

Room No: 2.129, Albert-Einstein-Str. 29a,

18059 Rostock, Germany.

Mobile: +49 1749360381

E-mail: thirusangumurugan.senthamarai@catalysis.de

        thirusangu007@gmail.com

Date of birth: 05 feb 1986

Place of birth: Thenpothai, India

Nationality: Indian

Education

2008-2010	Master of science in chemistry (70.5%, 1st class), Sri Paramakalyani college of Arts and Science, Tirunelveli, India.
2005-2008	Bachelor of science in chemistry (66.9%, 1st class), Sri Paramakalyani college of Arts and Science, Tirunelveli, India.
2002-2004	Higher secondary in science (75.8%, 1st class), S.M.S.S Govt. boys' school, Tirunelveli, India.

Research Experience

02/2017-present	PhD Scholar Leibniz Institute for Catalysis (LIKAT) in University of Rostock, **Thesis title**: Sustainable synthesis of amines using molecularly defined and nanoparticles-based catalysts **Supervisors**: Prof. Matthias beller and Dr. Jagadeeesh Rajanahally
06/2010-01/2017	Associate Scientist, Drug Discovery, Syngene International, Bangalore, India. -**Supervisors**: Dr. Jeyaprakash Narayanan and Murugan Nagarajan. Project trainee in Sri Paramakalyani Chemistry Research Lab, Alwarkurichi.
06/2008-05/2010	**Thesis title**: Effect of Pumice, Embilica and Ocimum Extract on Brass in Acid Medium **Supervisor**: Dr. Selvaraj

Publications

- Simple ruthenium-catalyzed reductive amination enables the synthesis of a broad range of primary amines Senthamarai, Thirusangumurugan; Murugesan, Kathiravan; Schneidewind, Jocob   Kalevaru, Narayana V.; Baumann, Wolfgang; Neumann, Helfried; Kamer, Paul C. J.; Beller, Matthias*; Jagadeesh, Rajenahally V*, *Nature Communications*, **2018**, *9*, 4123.

- Ultra-small cobalt nanoparticles from molecularly-defined Co-salen complexes for catalytic synthesis of amines, Senthamarai, Thirusangumurugan; Chandrashekhar, Vishwas G.; Gawande, Manoj B.; Narayana Kalevaru, V.; Zbořil, Radek; Kamer, Paul C. J.; Rajenahally V. Jagadeesh* and Matthias Beller*, *Chemical Science*, **2020**, *11*, 2973–2981.

- Expedient Synthesis of N-Methyl- and N-alkylamines by reductive amination using reusable cobalt oxide nanoparticles, Senthamarai, Thirusangumurugan; Murugesan, Kathiravan; Natte, kishore; Kalevaru, Narayana V.; Neumann, Helfried; Kamer, Paul C.J.; Jagadeesh, Rajenahally V, *ChemCatChem*, **2018**, 10, 1235-1240. (with front cover picture).

- Ligand controlled design of monodisperse cobalt nanoparticles as reusable catalysts for benign synthesis of nitriles, amides, aldehydes and acids, Thirusangumurugan Senthamarai, Ahmad S. Alshammari, Manzar Sohail, Paul C. J. Kamer, Rajenahally V. Jagadeesh* and Matthias Beller * (Manusript on progress).

- Catalytic Reductive Aminations Using Molecular Hydrogen for the Synthesis of Different Kinds of Amines, Murugesan, Kathiravan[$]; Senthamarai, Thirusangumurugan[$]; Chandrashekhar, Vishwas G[$].; Natte, Kishore; Beller, Matthias*; Jagadeesh, Rajenahally V*. *Chemical Society Review*, **2020** (revised) ($-1st, 2nd and 3rd authors equally contributed and co-first authors)

- Stable and Reusable Nanoscale Fe_2O_3-catalyzed Aerobic Oxidation Process for the Selective Synthesis of Nitriles and Primary Amides, Murugesan, Kathiravan; Senthamarai, Thirusangumurugan; Sohail, Manzar; Sharif, Muhammad; Kalevaru, Narayana V.; Jagadeesh, Rajenahally V*. *Green Chemistry*, **2018**, *20*, 266-273.

- Cobalt-based Nanoparticles Prepared from MOF-carbon Templates as Efficient Hydrogenation Catalysts, Murugesan, Kathiravan; Senthamarai, Thirusangumurugan; Sohail, Manzar   Alshammari, Ahmad S.;   Pohl, Marga-Martina; Beller, Matthias*; Jagadeesh, Rajenahally V*. *Chemical Science*, **2018**, *9*, 8553-8560

- Cobalt-nanoparticles Catalyzed Efficient and Selective Hydrogenation of Aromatic Hydrocarbons, Murugesan, Kathiravan; Senthamarai, Thirusangumurugan; Alshammari, Ahmad S.; Altamimi, Rashid M.; Kreyenschulte, Carsten; Pohl, Marga-Martina; Lund, Henrik; Rajenahally V. Jagadeesh* and Matthias Beller* *ACS Catalysis*, **2019**, *9*, 8581−8591

- Reductive amination using cobalt-based nanoparticles for synthesis of amines, Kathiravan Murugesan, Vishwas G. Chandrashekhar, Thirusangumurugan Senthamarai, Rajenahally V. Jagadeesh* and Matthias Beller* *Nature Protocols*, **2020**, https://doi.org/10.1038/s41596-019-0258-z.

Conference:

- Poster presentation at **Hanse Chemistry Symposium 2019** (Rostock, Germany, 8th-
  9th may 2019), and poster entitled "Tuning the size of cobalt nanoparticles by the nature of ligand for improving catalytic performance"

- Poster presentation at **28th International Conference on Organometallic Chemistry** (ICOMC-2018, Florence, Italy, 15th-20th July 2018), and poster entitled
  "Homogeneous ruthenium-catalyzed efficient synthesis of primary amines from carbonyl compounds and ammonia using molecular hydrogen"

- Poster presentation at **Second International Symposium on Synthesis and Catalysis** (ISySyCat2017, Evora, Portugal, 5th-8th September 2017), and poster
  entitled "Reductive N-methylation of Amines and Amino Acids using Nanoscale Co3O4-based Catalysts"

Awards:

- PhD fellowship by Leibniz-Institut für Katalyse, Rostock, Germany (Feb 2017)
- Best performer of the group for continuously 3 times (2014-2016)

Research Interest

- Catalysis and organic synthesis, Homogeneous and heterogeneous catalysis, Photocatalysis,
  Organocatalysis,C-H activations, Amination and redox reactions, Hydrogen borrowing reactions.

Research Skills:

- Organic synthesis, homogeneous and heterogeneous catalysis
- Skilled in operation of analytical instruments: GC, GC-MS, HPLC, LC-MS, BET
- Skills with MS Office, ChemOffice, SciFinder, Reaxys

Language Skills:

- Tamil (mother language), English (fluent), Kanada (Spoken), German (basic)

References:

- Prof. Dr. Matthias Beller, Director, Lebeniz-Institute for Catalysis. Rostock, Germany.
  Tel: +49 (381)1281-113; *email*: matthias.beller@catalysis.de

- Dr. Jagadeesh Rajenahally, Group Leader, Synergy between Homogeneous and Heterogeneous Catalysis, Lebeniz-Institute for Catalysis. Rostock, Germany.
  Tel: +49(381)1281-210; *email*: jagadeesh.rajenahally@catalysis.de

- Prof. Dr. Paul C. J. Kamer, Head of the department, Bioinspired Homo- & Heterogeneous catalysis, Leibniz Institute for Catalysis, Rostock, Germany.
  Tel: +49(381)1281-158; *email*: Paul.Kamer@catalysis.de

Annex 1

Declaration of the doctoral candidate according to § 4 (1) letters g and h of the doctoral degree regulations of the Faculty of Mathematics and Natural Sciences of the University of Rostock

Name

Senthamarai, Thirusangumurugan

....

(Name, First name)

Albert-Einstein-Str. 29a, 18059, Rostock

Address...

(Street, Postal code, Place of Residence)

I intend to elaborate a dissertation on the topic

Sustainable synthesis of amines using molecularly defined and nanoparticles-based catalysts

....

at the Faculty of Mathematics and Natural Sciences at the University of Rostock.

My supervisor is Mr/Ms

Prof. Dr. Matthias Beller

....
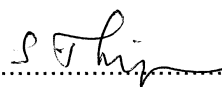
I, herewith, declare the following:

1. The opportunity for this PhD project was not communicated to me commercially. In particular I have not engaged any organization that for money seeks supervisors for the drawing up of dissertations or that performs entirely or partially on my behalf the duties incumbent upon me regarding the examinations.

2. I hereby declare under oath that I have completed the work submitted here independently and have composed it without outside assistance. Furthermore, I have not used anything other than the resources and sources stated and where I have taken sections from these works in terms of content or text, I have identified this appropriately.

19.05.2020/ Rostock

.... this ....

(Date/Place)   (Signature)